Predicting the Past of Dried Blood Spots: Time Since Deposition and Toxicology

Thesis submitted for the degree of

Doctor of Philosophy

at the University of Leicester, United Kingdom

By

Thalassa Sandra Eliza Valkenburg (MSc, MSc)

Department of Chemistry, University of Leicester

2019

Declaration

I hereby certify that this material which I now submit for assessment on the program of study leading to the award of Doctor of Philosophy is original unless stated otherwise within the text or by references. I also certify that the thesis has been written by me and that the help I have received in the preparation of the thesis including the research work has been acknowledged.

Signed

Date
21 March 2019

The research leading to the findings presented in this thesis has received funding from the European Union Seventh Framework Programme (FP7/2007-2013) under grant agreement no 607930.

Predicting the Past of Dried Blood Spots: Time Since Deposition and Toxicology

by Thalassa Sandra Eliza Valkenburg

Abstract

Blood is among the most frequently encountered evidence types at crime scenes and establishing the time since deposition (TSD) of bloodstains can be critical in certain cases. A method to establish the TSD of bloodstains is not routinely applied yet, because of because of age estimation inaccuracies caused by environmental conditions, influence of the substrate, inter-person variation and sample quantity. A bottom-up proteomics approach in combination with nano-liquid chromatography hyphenated to tandem mass spectrometry with electrospray ionisation and surface acoustic wave nebulisation coupled to mass spectrometry was used to assess the molecular profile of dried blood spots (DBS) aged up to 8 days. A major reduction in the workflow time of DBS analysis was achieved by the application of a novel developed microfluidic immobilised-enzyme reactor for the digestion of DBS proteins. A model was developed to predict the TSD of DBS from its molecular composition and is currently able to classify aged from non-aged DBS samples.

The analysis of toxicology from micro-volumes of blood would also be beneficial in a variety of forensic scenarios. The collection of DBS onto cards or the collection of micro-volumes of blood onto the novel volumetric absorptive microsampling (VAMS) device would allow simple, quick and non-invasive sampling in situations where the volume of blood is limited or repetitive sampling is needed. No medical trained personnel are needed, there is no location restriction, samples can be stored at room temperature and samples can be transported by regular post. Methods were developed for the quantification of two drugs of abuse, salbutamol and pseudoephedrine, from blood sampled onto VAMS devices including from the blood of healthy volunteers collected after administration with either one of the drugs.

Acknowledgements

Firstly, I would like to thank my first supervisor Prof. Paul Monks for his continuous support throughout my PhD studies. I can't remember a single idea or request he didn't approve of and he encouraged me to broaden my field of expertise by attending conferences and with experimental work. I would also like to thank my second supervisor Dr. Hitesh Pandya for helping me structuring my work plans and brainstorming about experiments. The coffee meetings helped me getting me through the probation review period.

I would also like to thank the many members of the Atmospheric Chemistry research group that made my time in the office enjoyable. Many thanks go to Dr. Rebecca Cordell for training me on the instruments, helping me with my many questions even by text after out-of-office hours, for proof-reading my thesis, for the fresh coffee in the morning as a reward for 'early' starts and for being my main volunteer to practise my acquired phlebotomy skills on. Many thanks have to go to Jonathon Brooks for always being there as a friend and colleague, inside and outside the university. He was the rock that kept me going during failing experiments, data analysis struggles and difficult collaborations. I've got many amazing memories from our trips to Amsterdam, Verona, Newcastle and Manchester. Thanks are also due to Dr. Saleh Ouheda for supporting each other with writing-up in the out-of-office hours and for the nuts to keep on going, to Dr. Robert Blake for the daily work encouragements in Dutch/Afrikaans, to Dr. Rik Panchal for helping me understanding the PTR experiments, to Dr. Mike Wilde for his help with the GCxGC experiments, to Dr. Roberto Sommariva for the help with R, to Dr. Lloyd Hollis for exchanging chemistry puns every now and then, to Dr. Sarkawt Hama for reducing the noise level in the office at times, to Jasmine Wareham for the chats in the office, to Luke Bryant for sharing his statistical knowledge and helping me with data explorations, to Toraia Takteek for bringing some more biological experiments and discussions into the group and to Marios Panagi for the laughter and magical tricks in the office.

There are some more students and graduates of the Department of Chemistry I also have to thank. Georgie for the countless happy-hours we've been to and the crazy things we have done to make Leicester a nice place. Alexandra, Javier, Todd, Shannon, Tom, Marian, Stellios, Joanna, Julie, Mariana and Stephen for the Friday evening beers and pub talks at our local pub. Will, Simran, Vicky, Neringa, James and Beth for having a daily 'social' meetup.

I would also like to thank Prof. Lisa Smith for offering me this incredible opportunity in the first place. The INTREPID Forensics programme she coordinated has given me all the opportunities and resources for my PhD studies, but also for my professional development by the many trainings, summer schools and other events the programme offered. Many thanks also for bringing me into contact with many people of your network and for the catch-ups over coffee. I also have to thank the programme administrator Tom Horton for going beyond his duties in helping me getting started, relocating from abroad, handling my many expense forms, dealing with my many questions and even looking into some of my excel datasheets while he moved abroad temporarily. He has become a friend and finishing my project would have been a lot more difficult without him. Many thanks also have to go to the other INTREPID Forensics fellows. It was nice to be part of a group to have lunches with at the start, to share research interests with, to explore Leicester and to 'complain' about how lucky we were with the opportunities. Annelies for sorting out the English life style together, finding a normal bike to buy, having sweet pancakes for dinner, having chocolate sprinkles on sandwiches and travelling together to conferences and the summer school in Switzerland. Alex and Francisco for letting me campervan with you for a week after the conference in New Zealand. It was nice to hit the road together and have many laughs and daily garlic breads. Sophia for the collaboration, for showing me around in Greece and for sorting out induction things. Maurits for having some Dutch time. Marwan, Silke, Etienne and Jessica for their stimulating discussions during lectures.

A few other members of the Department of Criminology also have to be thanked; Alex Murphy for taking over Tom his duties while he was away, Dr. John Bond for the lectures and forensic brainstorming meetings, Audrey for arranging the many order payments

and shipments and Wilma for organising my packages. A big thank you also goes to Lisa-Linn, who I initially met through the forensic science society and who has made my time in Leicester more enjoyable. She has become a great friend who has already moved back to the Netherlands after her master studies, but we are still meeting up for holidays, drinks and other events and I'm sure many more activities will be planned.

Many thanks also have go to the people I met during my secondment at the University of Amsterdam. First of all, thanks go to my supervisor Prof. Garry Corthals for offering me a place within his research group and giving me the freedom to set up the various experiments that have become part of this thesis. Special thanks go to Petra Jansen for her continuous support with the experiments and data analyses, to Dr. Irena Dapic and Dr. Bert Wouters for letting me test your developed IMER with DBS, to Dr. Alina Astefanei and Bas Groothuis for exploring the application of SAWN to DBS and to the other people I shared an office with and gave me a warm welcome; Michelle, Petra, Stan, and later Pascal, Gino and Dorina. I will miss the Friday 'borrels' where collaborations and friendships started. Marvin, Marta, Mo and Peter have not been mentioned yet, but definitely have to be thanked for making my secondment great.

I also feel privileged to have met some great people during the various trips I've made for my studies. Stuart James and Anna Cox for teaching me the basic bloodspatter pattern analysis skills during their exciting course in Florida. Martin Eversdijk and René Gelderman for turning my basic bloodspatter pattern analysis skills into more advanced skills during their course in the Netherlands, while we initially met at a conference in New Zealand. Beitze and Rachelle for ploughing through the daily exam questions together at the MSBM summer school in Croatia and for enjoying some cocktails in the limited spare time.

Then there are some people in and around Leicester that I have to thank for making my life outside the university great. Seb, Sylvia, Doug, Rami, Rachel and Ant for going to gigs and festivals, going out on the boat and having lots of fun. Seb and Sylvia in special for going on camping trips, kayaking from your back garden, visiting me abroad during my secondment and having me as a bridesmaid at your wedding. Noortje, who I knew from

the Netherlands but came to Leicester for a minor, for exploring Leicester. Tom and Becca for familiarising me with car booth sales, tobogganing and bingo, and Tom later for introducing me to the English culture from Sunday carvery and chicken nugget sharer boxes, through English television and lots of slang to things such as strawpedos. Oriol, Irena an Eva for refreshing my Spanish and exploring Leicester both as internationals.

There also many people in the Netherlands that have to be thanked for their ongoing support from a distance, for keeping in touch, giving me a place to stay and for visiting me in Leicester. Nienke and Thomas for their enormous hospitality, their visit in Leicester and unlimited support. It didn't matter at what time I arrived at your place, for how long I stayed, at what time I left or until what time I slept in. Thijs, Daniel and Toke for visiting me not once but twice in Leicester, for finding the time and place to meet up at other places such as in Copenhagen and for renting a car together in England to drive on the 'wrong' side of the road. Also a special thanks to Daniel and Toke for the very lengthy stay at your apartments. Thanja for being the first to visit me, providing nice breakfasts and dinners when I was staying over and for sharing your own PhD experiences. Tim and Flemming for being the ultimate winners of friends visits to Leicester. One wonders if they came for the English ales and pies or to catch up. Just kidding guys, many thanks for the many beers we've had, games we've played and sightseeing we've done. Suzan for visiting me in Leicester twice and letting me take care of your house when you were on holidays, plus thanks for the lovely catch-ups over tea. Mette for coming over for my birthday and many thanks to you and your flatmates for hosting me so often and having a laugh, dance, drink or actually normally all three at the same time. Bardo, Anniek, Amanda, Conrad, Iris and Els for visiting me in Leicester and treating ourselves to English breakfasts, pies, muffins, ciders and scones. Tanja and Jasper for letting me stay at your house even when you were not there and for the catch-ups when I was over. Ivo and Simone for catching up when I was back home and Ivo for indulging us in the English culture during a bank holiday weekend. Ilva for meeting up somewhere random in the Netherlands and for giving me a place to stay after a night out or day of chilling. Pepijn, Willem and Daniel for organising a writing-up weekend at a holiday park, I was surprised with the amount of work I actually got done. Thanks for the fun and productive time away at a nice Dutch island. Dominique and Carina for a

‘terrasje pakken’ when I was around. Mireille, who also moved to England, for our meet-ups in Manchester, Leicester, Leiden and other places. Thanks for writing-up together for a week and for becoming a good friend.

Lastly, I would like to thank my family for their unwavering support (and my apologies for moving away so far from home and using my entire fourth year for writing up before moving back). Many thanks to my sister Marinka for visiting me five times. For exploring Leicester and its surroundings as well as the culture together, for making a big road trip through the US to have some time off study and for celebrate my birthday twice in style. I’m not sure if my birthday in Vegas or my 30th birthday wins the contest. Also thanks to my other sister Wytske and her family for coming over with the six of you in one car. I’m blessed that I was part of the wedding proposal your (now) husband had prepared for your visit here. Also thanks to my brother Rinze and his family for making the journey to Leicester. I’m happy I could show you around where I lived and studied. Lastly, many thanks to my parents for driving over five times, helping me move part of my belongings, having the other part stored at your place, for trying to read my publications, for being the main readers of my INTREPID blog, for sending postcards with encouragements and congratulations and for always welcoming me back with lots of love during the holiday times.

Contents

List of Tables

List of Figures

List of Abbreviations

AAR	aspartic acid racemisation
AFM	atomic force microscopy
AM	ante-mortem
APCI	atmospheric pressure chemical ionisation
APTDCI	atmospheric pressure thermal desorption chemical ionisation
ATR	attenuated total reflection
CE	capillary electrophoresis
CID	collision-induced dissociation
Cl	clearance
C_{max}	maximum concentration
COC	cyclic-olefin-copolymer
CV	coefficient of variation
DART	direct analysis in real time
DBS	dried blood spot
DESI	desorption electrospray ionisation
DFS	dried fluid spot
DIA	data independent acquisition
DPS	dried plasma spot
DSS	dried serum spot
DUID	driving under the influence of drugs
DUS	dried urine spot
DWT	discrete wavelet transform
EB	exhaled breath
EDTA	ethylenediaminetetraacetic acid
ELISA	enzyme-linked immunosorbent assay
emPAI	exponentially modified protein abundance index
EPR	electron paramagnetic resonance
ESI	electrospray ionisation
FDR	false discovery rate
FIA	flow injection analysis
FID	flame ionisation detection
FTIR	Fourier transform infrared
GC	gas chromatography
GCxGC	two dimensional gas chromatography
GRAVY	grand average of hydropathy
HAP	high abundance protein
Hb	haemoglobin
HbO_2	oxygenated haemoglobin
HC	hemichrome
HCT	haematocrit
HESI	heated electrospray ionisation
HPLC	high pressure liquid chromatography
HUPO	Human Proteome Organization
ICP	inductively coupled plasma

IDA	information dependent acquisition
IMER	immobilised-enzyme reactor
IR	infrared
LA	laser ablation
LAP	low abundant protein
LC	liquid chromatography
LDTD	laser diode thermal desorption
LLOQ	lower limit of quantification
LMJ	liquid microinjection
LOD	limit of detection
LOO	leave-one-out
m/z	mass to charge
MALDI	matrix assisted laser desorption ionisation
MARS	multi-affinity removal system
Met-Hb	met-haemoglobin
MS	mass spectrometry
MS/MS	tandem mass spectrometry
MW	molecular weight
NPS	novel psychoactive substances
NSAF	normalised spectral abundance factor
OF	oral fluid
PAI	protein abundance index
PC	principal component
PCA	principal component analysis
PCR	polymerase chain reaction
pI	isoelectric point
PM	post-mortem
PPD	proteome plasma database
PTR	proton transfer reactor
qMS	quadrupole mass spectrometry
RBC	red blood cell
RFE	recursive feature elimination
RSD	relative standard deviation
S/N	signal to noise
SAF	spectral abundance factor
SAWN	surface acoustic wave nebulisation
SCAP	sample card and prep
sd	standard deviation
SEM	scanning electron microscopy
SIFT	selected ion flow tube
SLE	solid liquid extraction
SPE	solid-phase extraction
SPME	solid-phase microextraction
SSP	surface sampling probe
SSSP	sealing surface sampling probe
SVM	support vector machine
SWATH	sequential window acquisition of all theoretical (mass spectra)

$T_{½}$	half-life
TIC	total ion current
T_{max}	time of maximum concentration
ToF	time-of-flight
TSD	time since deposition
UV	ultraviolet
VAMS	volumetric absorptive microsampling
VIS	visible
VOC	volatile organic compound
WADA	World Anti-Doping Agency

1 Introduction

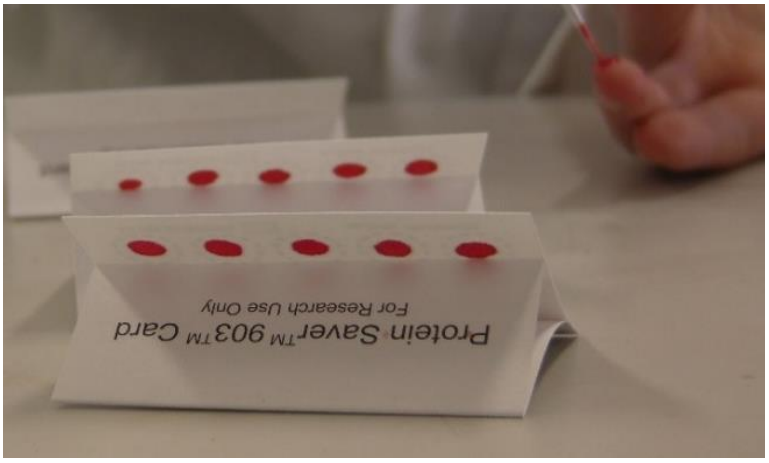

Micro-volumes of blood collected as dried blood spots (DBS) onto cards

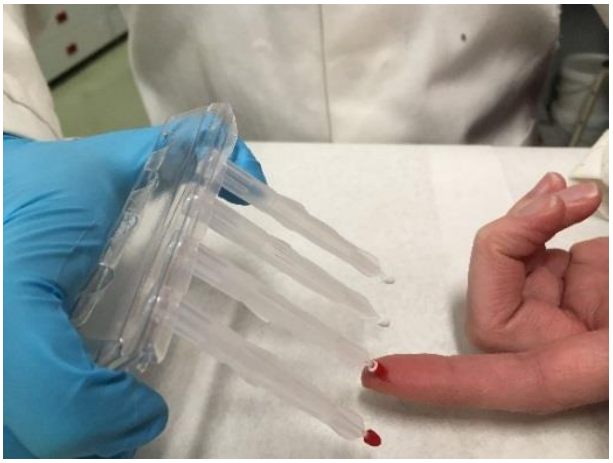

and by volumetric absorptive microsampling (VAMS) using Mitra™ devices

1.1 Blood

Biological fluids are among the most frequently encountered evidence types at crime scenes [1]. The most common are blood, semen and oral fluid, but others such as urine, vaginal fluid and sweat can also be of importance and biological sample types such as hair, skin cells and nails can also aid forensic investigations [2]. Detection and identification of biological trace evidence is the first step in investigations followed by the recovery of DNA to identify who could have been involved in the crime and by the reconstruction of events. In the case of blood traces or available blood samples, intelligence can additionally be retrieved such as for toxicology purposes and the search of human remains. Also, the classification of blood into groups known as the ABO system has been used to obtain intelligence for application to casework samples [3]. Estimating the time since deposition (TSD) of blood and other biological traces is not routinely used, but could be helpful for reconstructions and the verification of statements. The use of micro-volumes of blood to determine TSD and toxicology are the topics of this thesis. This chapter provides context to the experiments through the introduction of dried blood spots (DBS) and the applications of micro-volume blood sampling plus the properties of blood in general that are important for research and a range of applications.

The average human adult has approximately 5 litres of blood consisting of plasma which suspends the red blood cells (RBCs or erythrocytes), white blood cells (leukocytes) and platelets (thrombocytes) as well as electrolytes, proteins, lipids, carbohydrates and minerals [4]. Serum is similar to plasma and can be obtained by removal of the blood cells and clotting proteins. Blood collected from living humans, termed ante-mortem (AM) blood, differs considerably from blood obtained post-mortem (PM) from deceased people. The water content of PM blood shows a wide variation, ranging from 60% to 90%, and PM blood can be clotted, partially clotted, partly fluid, haemolysed, putrefied or inhomogeneous depending on the state of haemolysis and pH [5]. Furthermore, a PM versus AM metabolic analysis performed using rat blood showed increased concentrations of metabolites for the 96-hour timespan tested [6] and toxicological analysis from PM blood comes with difficulties in interpretation [7]. Formation of new substances and degradation of analytes may occur

as well as inhomogeneous distribution of analytes throughout the body. Lastly, RBCs could still be identified in an ancient human PM blood sample, but degradation of the cells was observed [8].

Clotting and drying will start immediately whenever a person loses blood, accompanied by visible changes of the resulting bloodstain. The colour changes from red to brown over time, for which a colour chart has already been published by Tomellini over a century ago [9]. The kinetics underlying the colour change are now known and represented in Figure 1.1. The morphological changes for a drying blood droplet on glass at ambient conditions have been characterised in five stages [10]. Within 36 minutes, the droplet from a healthy volunteer changed as follows, 1) RBCs moved out of the centre of the spot and formed a receding desiccation line, 2) crystallisation occurred at the edge of the spot and propagated inwards with continued desiccation from the edge towards the inside of the drop, 3) the first cracks appeared as the drop was almost fully desiccated and the central part of the spot became lighter red, 4) the central part of the drop desiccated and produced smaller plaques whereas circular drying spots were observed at the edge, 5) the plaques moved slightly until total desiccation was established. It has to be noted that treated whole blood (addition of anti-coagulant, storage in a fridge up to 6 days and removal of the main coagulation protein fibrinogen) was used for the above described experiment, but the study gives an indication of the changes. Environmental conditions, the quantity of blood and substrate all affect the drying and further ageing of bloodstains.

Aside from the visible changes upon drying of bloodstains, there is some knowledge about the underlying physical and biochemistry changes related to drying and further ageing. Light microscopy [11, 12] and scanning electron microscopy [13, 14] showed that RBCs were dehydrated but preserved in bloodstains, even in ancient stains. A decrease in the elasticity, cell volume and adhesive force of RBCs was shown by atomic force microscopy [15, 16]. Changes in volatile organic compound (VOC) composition [17, 18] as well as a degradation of RNA [19, 20] and beta-haemoglobin coding DNA [21] are also known to occur. As for blood protein levels, decomposition of globulins and albumin [22], denaturation of creatine kinase and alanine transaminase [23], a decrease in alkaline phosphatase level [24] as well as in catalase and peroxidase levels [25] have been reported. Haemoglobin (Hb) is the most investigated protein with

respect to bloodstain ageing. Hb functions as an oxygen carrier within the human body and changes have been studied with a variety of techniques. An increase in abundance of one of the Hb derivatives has been reported [26], as well as an increase in met-haemoglobin (met-Hb) and hemichrome (HC) [27, 28] which is linked to a decrease in oxygenated haemoglobin (HbO_2). The reaction kinetics of Hb inside and outside of the body have been visualised by Bremmer et al. (Figure 1.1). A small part of the HbO_2 auto-oxidises into met-Hb, which can reduce back to normal Hb by a reductase protein. However, Hb will completely saturate outside the body and denature to the irreversible HC derivative. Both HbO_2 and met-Hb are prevented from reduction to Hb outside a body, because of a decreased bioavailability of the necessary reductase protein. The entire oxidation kinetics are known to be the major contributor for the colour change of bloodstains. Less is known about the degradation of other proteins and components in bloodstains.

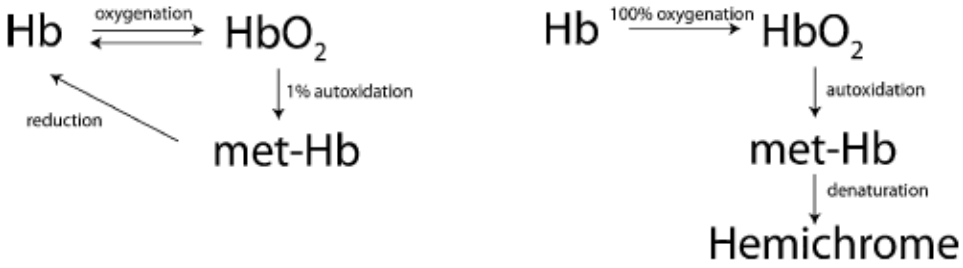

Figure 1.1. Simplified reaction kinetics of haemoglobin inside a body (left) and within bloodstains (right), *Hb=haemoglobin* [29].

Lastly, blood can be drawn from veins, arteries and capillaries. Within the body, >90% of Hb in arterial blood and >70% of Hb in venous blood are kept saturated with oxygen via oxygen transport from the lungs [29]. Capillary blood is a mixture of arterial and venous blood with the addition of interstitial and intracellular fluids [30]. Small volumes of capillary blood are generally used to create DBS, which were produced for many experiments in this thesis.

1.2 Dried blood spot technique

The introduction of DBS dates back to 1913, when Bang demonstrated its usefulness for glucose monitoring [31]. Exactly half a century after the first described DBS application, Guthrie and Susi demonstrated the applicability of DBS for screening phenylketonuria in neonates [32]. This reference is cited in most publications about DBS and can be marked as the start of widely adopted DBS applications. Today, DBS are still routinely collected onto cards and used for research and screening applications.

To create a DBS, capillary blood is usually collected by pricking a finger (or heel in case of neonates) and spotting onto a card. Opportunistic venous blood collection in clinical settings and the collection of venous blood for research purposes sometimes also take place to create spots. Initially non-fixed micro-volumes of blood were spotted after which sub-circles of the spots were used, but nowadays accurate volumes of ≤20 µL are also commonly spotted and the entire spot used. The use of larger volumes up to 100 µL has been reported as well [33-37]. Micro-volume blood sampling from laboratory animals is carried out by inserting a fine needle into the tail, paw or ear and using a glass capillary tube to transfer the drop that has formed at the tip of the sampling needle or sample site to a blood spot collection card [38].

After collection, a drying time of 3-4 hours is recommended for neonatal screening [39]. Research demonstrated that the drying process is complete within 90 minutes under controlled ambient laboratory conditions with a relative humidity less than 60%, but a drying time of 2 hours has been recommended as DBS continues to dry upon packaging with a desiccant [40, 41]. The majority of research studies use a drying time between 2-3 hours in the dark with ambient laboratory conditions. After drying, the samples can be stored and/or shipped. The impact of environmental conditions experienced during storage and transport of DBS has been investigated extensively by GlaxoSmithKline [40, 42]. DBS stored on Whatman 903 and FTA cards did not show visible signs of deterioration when stored at elevated conditions whereas the integrity was compromised when stored on FTA Elute cards [40]. The effect for different analytes should always be assessed per study and further method validation criteria were implemented by including stability tests at elevated temperatures for 48 hours in parallel with tests at the defined ambient temperature for the likely storage period of

the study samples. Temperature and humidity will also be recorded during on-site storage and during transport using validated data loggers [42]. For biomarker samples, minimising temperature and humidity is essential as the majority of 34 markers of inborn disorders in DBS samples showed severe degradation within a week of storage at 37 °C and high-humidity [43].

The first step in processing the samples for analysis is the punching of the spots from the cards. When sub-punches are being taken, generally between 3.0-6.35 mm in diameter [44], varying sample volumes can occur because of varying haematocrit (HCT) levels between people. HCT reflects the level of RBCs in blood and ranges between 28%-67% in the majority of the population [45]. The higher the HCT, the more viscous the blood which results in less spreading on most types of DBS cards [46]. A sub-punch from a DBS with high HCT will thus contain more blood compared to a sub-punch from a DBS with low HCT. Although moderate variations in HCT have been shown to not significantly influence the recovery of some analytes tested [45, 47-49], the difference in actual volume collected between a sub-punch with a low versus a high HCT can be as high as 35% for 3 mm punches [45, 50] and 47% for 6 mm punches [39]. For larger HCT differences, the recovery of some analytes is shown to be significantly different but not linearly correlated such as for HCT and blood volume [45, 51]. In addition, it was found that the location of the punch also influences bioanalytical results as nonhomogeneous distribution of compounds across spots has been observed [46, 52, 53]. Therefore, spotting an accurate volume of blood and using the entire spot is an alternative to the use of sub-punches [54]. Another approach would be to correct for HCT effects, either by predicting the HCT via potassium measurement on a routine clinical chemistry analyser [55] or by using single-wavelength reflectance spectroscopy [56].

Extraction of analytes from DBS is usually performed with a mixture of aqueous and organic solvents [57]. In some cases, the addition of an extraction solvent is enough and in other cases the temperature needs to be increased or energy added to improve recovery. It is common practice to add an internal standard to the extraction solution as it is often impractical to add an internal standard to blood prior to spotting it onto a card. However, in that way matrix effects will not be compensated for. The internal standard could be spotted directly onto the DBS or directly onto the card prior to the spotting of blood, but the spreading of internal standards can be irregular and the

stability of the internal standard is questionable when pre-treating cards for implementation in certain scenarios. A last alternative would be to spot the DBS and internal standard on two different cards and merge them together in the extraction solution. The DBS consortium of the European Bioanalytical Forum investigated the different ways of introducing the internal standard to DBS samples and concluded that the best way of addition has to be decided per case [58]. Finally, additional pre-treatment steps are sometimes needed such as sample clean-up, chemical treatment, dilution, concentration, derivatisation, enzymatic digestion and/or separation before the samples are ready for analysis which is generally by mass spectrometry (MS) [57].

Aside from DBS, other types of dried fluid spots (DFS) have later been introduced. Dried plasma spots (DPS) can either be created after venous blood collection and subsequent separation of plasma [59] or by using special filter paper that filters the plasma from blood cells onto a second layer [60-62]. Dried serum spots (DSS) have been compared to its fluid equivalent [63] and dried urine spots (DUS) have been assessed for detection of analytes [64-66]. The use of dried synovial fluid spots has even been explored using synovial fluid from pigs as a non-blood matrix [67].

1.3 Applications using micro-volumes of blood

DBS are routinely used for medical purposes, with the main application being a genetic screening of millions of neonates each year [68]. Over 500 laboratories in 78 countries screen more than 50 disorders and analytes [69]. Other medical DBS applications are therapeutic drug monitoring [70-74] and epidemiological surveys [75, 76], suitable for sample collection from neonates, children and adults. Also, the use of DBS for implementation in forensic toxicology cases using PM samples [77] and in forensic related scenarios such as traffic controls for driving under the influence of drugs (DUID) [37, 78, 79], nightclub's medical room admission testing [80], doping analyses [81-84] and even inspection of environmental pollution [44] has been assessed. Furthermore, a similar application is the toxicological screening of small blood samples and bloodstains in forensic casework [85]. The aspects of using micro-volumes of blood for toxicological analyses are described in more depth in section 1.3.2.

Research using DBS has increased exponentially since 2000 [86]. Medical research mainly includes pharmacokinetic studies [87, 88], toxicokinetic studies [89] and biomarker studies [90, 91]. The use of DBS in pre-clinical pharmacokinetic and toxicokinetic studies has been recommended and applied as the preferred approach for assessing small molecule drug candidates which have previously passed bioanalytical validation [87]. Also, pharmaceutical companies are making efforts to use DBS for drug discovery and testing phases including studies with animals and home-based sampling. Lastly, copious research has been carried out to determine the age of small bloodstains (section 1.3.1).

1.3.1 Bloodstain age explorations

Police forces are sometimes confronted with the question when certain events have taken place and establishing the TSD of bloodstains would be helpful in certain cases [28, 92, 93]. Since the beginning of the 20th century researchers have tried to determine the TSD of bloodstains by targeting various blood components with different techniques. The first attempts were based on the investigation of colour changes [9], haemoglobin changes [25, 94] and solubility in water [95]. The latest methods mainly include various types of spectroscopy and spectrometry. An overview of studies and techniques is presented in Table 1.1. None of the approaches are routinely applied in forensic casework, because of the age estimation inaccuracies caused by environmental conditions, influence of the substrate, inter-person variation and sample quantity [96].

Table 1.1. Overview of techniques used to investigate the age of bloodstains, *NS=not specified*.

Technique	Bloodstain target	Time range tested	Reference (study, year)
Aspartic acid racemisation (AAR)	d–l-aspartic acid ratio	Up to 20 years	[97] Arany et al., 2011
Atomic force microscopy (AFM)	Elasticity, cell volume, adhesive force and surface area of red blood cells	Up to 157 days	[98] Chen et al., 2006 [15] Strasser et al., 2007 [16] Wu et al., 2009

Table 1.1. *Continued.*

Technique	Bloodstain target	Time range tested	Reference (study, year)
Attenuated total reflection (ATR) Fourier transform infrared (FTIR) spectroscopy	Absorbance measurements	Upon drying (~40 min) and up to 18 months	[99] McCutcheon, 2010 [100] Orphanou, 2015 [101] Zhang et al., 2016
Bioaffinity assay	Creatine kinase and alanine transaminase	Up to 5 days	[23] Agudelo et al., 2015
Biocatalytic assay	Concentration of alkaline phosphatase	Up to 2 days	[24] Agudelo et al., 2016
Colour chart	Colour change on linen	Up to 1 year	[9] Tomellini, 1907
Digital image analysis	Level of magenta in digital images of smart phone cameras	Up to 6 months	[102] Thanakiatkrai et al., 2013
Electron paramagnetic resonance (EPR) spectroscopy	Electro spin resonance signal of ferric high and low spin, ferric non-haem and free radical species	Up to 698 days	[103] Miki et al., 1987 [104] Sakurai et al., 1989 [105] Fujita et al., 2005
Entomological analysis	Identification of fauna on a bloodstained shirt	Case sample, less than a month old	[92] Nuorteva, 1974
Enzyme-linked immunosorbent assay (ELISA)	Melatonin and cortisol quantity (circadian rhythm)	24 hour profile	[106] Ackermann et al., 2010
Guaiacum-based assay	Catalase and peroxidase activity of Hb	Up to 22 year old samples	[25] Schwarz, 1937
High pressure liquid chromatography (HPLC)	Peak area ratio of Hb derivatives and other proteins	Up to 1 year	[107, 108] Inoue et al., 1991-1992 [26] Kumagai, 1993 [109] Andrasko, 1997
Hyperspectral imaging	Fraction of Hb derivatives from reflectance spectra	Up to 200 days	[28] Edelman et al., 2012 [110] Li et al., 2013

Table 1.1. *Continued.*

Technique	Bloodstain target	Time range tested	Reference (study, year)
Immunoelectrophoresis	Protein ratios	Up to 1 year	[22] Rajamannar, 1977
Infrared (IR) spectroscopy	Detection of IR peak changes due to proteins, water and lipids	Up to 1 month	[111] Botonjic-Sehic et al., 2009 [112] Edelman et al., 2012
Oxygen electrodes	Measurement of oxygen	Up to 10 days	[27] Matsuoka et al., 1995
Photometry	Solubility in water	Up to 10 hours of irradiation	[95] Schwarzacher, 1930 [113] Rauschke, 1951
Polymerase chain reaction (PCR)	Quantification of RNA and DNA	Up to 15 years	[19] Bauer et al., 2003 [20, 114] Anderson et al., 2005-2011 [21] Morta, 2012 [115] Alrowaithi et al., 2014
Raman spectroscopy	Scattering peaks	Upon drying (~60 min)	[116] Boyd et al., 2011
Reflectance spectroscopy	Fractions of three Hb derivatives	Up to 60 days	[29] Bremmer et al., 2011 [117] Li et al., 2011 [118] Sun et al., 2017
Silver chloride electrode	Diffusion of chloride ions	NS	[119] Fiori, 1962
Solid-phase microextraction (SPME) – gas chromatography - mass spectrometry (GC-MS)	VOC profile	Up to 6 weeks	[120] Forbes et al., 2014
Solid-phase microextraction (SPME) – two-dimensional gas chromatography – time-of-flight mass spectrometry (GCxGC-ToF-MS)	VOC profile	Up to 1 year	[18] Rust et al., 2016 [17] Chilcote et al., 2018

Table 1.1. *Continued.*

Technique	Bloodstain target	Time range tested	Reference (study, year)
Spectrofluorometry	Fluorescence lifetime of fluorophores	Up to 2.5 months	[93] Guo et al., 2012 [121] Shine et al., 2017
Spectro-photometry	Quantification of absorption bands	Up to 8 year old samples	[122] Patterson, 1960 [123] Kleihauer et al., 1967 [124] Kind et al., 1972 [125] Köhler et al., 1977 [126] Blazek et al., 1982 [127] Bergmann et al., 2017
Spectroscopy	Hb spectra	NS	[94] Leers, 1910
Ultraviolet (UV) photometry	Activity ratio of enzymes	Up to 12 weeks	[128] Tsutsumi et al., 1983
Ultraviolet visible (UV-VIS) spectrophotometry	Shifting of Hb Soret band	Up to 1 month	[129] Hanson et al., 2010

The various studies outlined in Table 1.1 focus mainly on spectral changes of Hb and a few other compounds, but fundamental knowledge about intrinsic changes of ageing bloodstains is scarce. An alternative approach has been taken by Forbes et al., who focused on changes of VOCs demonstrating changes in chemical composition as bloodstains age [17, 18, 120]. The aim of the VOC studies is somewhat different compared to the other blood ageing studies as profiles of aged blood were studied in order to improve training aids for blood-detection dogs and the associated aim of locating missing people instead of determining the TSD of bloodstains. Agudelo et al. went one step further by combining the estimation of TSD with estimating the age of its originator [24]. A differentiation between young and old donors could be made for bloodstains up to 2 days after deposition by measuring levels of alkaline phosphatase using a biocatalytic assay.

In this thesis, nano-liquid chromatography hyphenated to tandem mass spectrometry with electrospray ionisation (nano-LC-ESI-MS/MS) was used to investigate DBS ageing by studying the abundance of peptides and proteins over time. Aside from

obtaining a fundamental understanding of blood ageing based on proteomics, there was the potential of introducing a new method for determining the TSD of bloodstains.

1.3.2 Dried blood spots for toxicological analyses

Drug screening plays an important part in both clinical and forensic toxicological settings, for example sport doping testing has been performed systematically since 1968 [130]. Gas chromatography hyphenated to mass spectrometry (GC-MS) has been the gold standard for toxicological analyses and doping screening for decades, but in recent years LC-MS has become a powerful alternative [131]. Wagner et al. have published an extensive review about DBS analysis with an overview of many suitable MS techniques developed to date [57], split in off-line and integrated workflows (Figure 1.2).

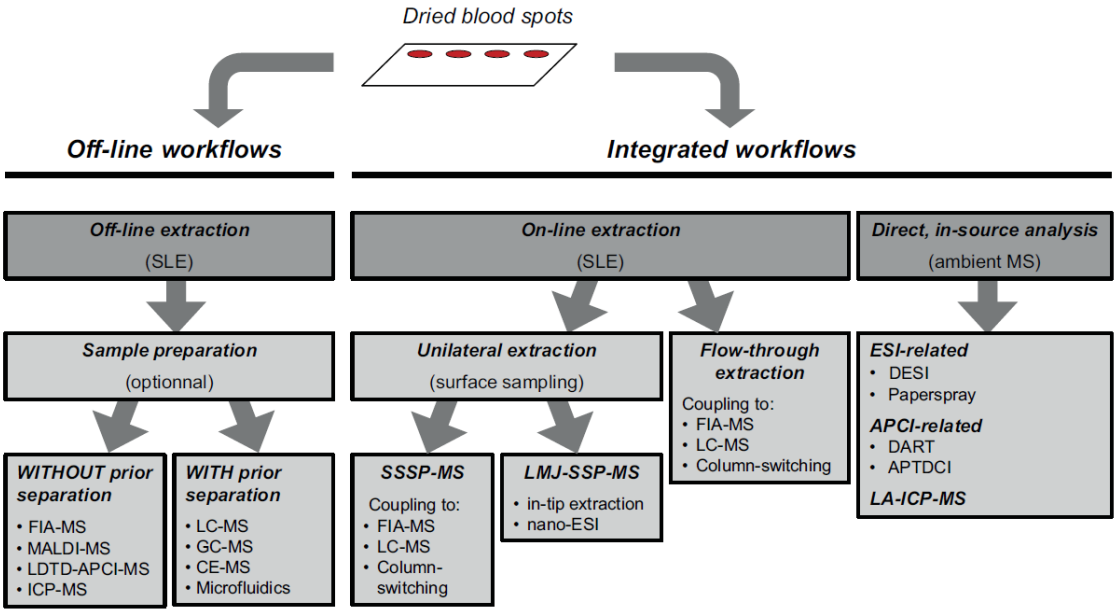

Figure 1.2. MS workflows for DBS analysis [57]. *SLE=solid liquid extraction, see list of abbreviations at the start of the thesis for full names of other techniques.*

The off-line workflows outlined in the left panel of Figure 1.2 encompass the aforementioned GC-MS and LC-MS options plus others with [132-134] and without [135, 136] prior separation. The instrumentation used in the off-line workflows generally has high resolution and sensitivity. However, sample preparation is needed prior to most analyses and can be time-consuming, thereby limiting high throughput analyses. To automate DBS analyses, a system consisting of an automated DBS puncher with 96-well-

microplate has been introduced to process up to 96 samples in approximately 2.5 hours [137]. The extraction of analytes from blood on cards is complex in both off-line and integrated workflows, but the introduction of on-line extraction techniques reduced sample treatment and without the need for punching spots out of cards (middle panel of Figure 1.2). Commercially available systems emerged from CAMAG, Spark Holland, Prolab and Advion [138] and are based on unilateral extraction and flow-through extraction. Unilateral extraction systems consist of a sealing surface sampling probe (SSSP) [139, 140], including one with a thin-layer chromatography MS interface [141], or a liquid microinjection surface sampling probe (LMJ-SSP) [140]. Flow-through extraction and desorption systems were developed later [142, 143] including a novel developed desorption cell for direct analysis using LC-MS [144]. Simultaneously, the analysis of DBS by application of ambient MS techniques was studied as visualised in the right panel of Figure 1.2. Ambient MS entirely evades extraction by direct ionisation of samples in the atmosphere external to the MS. For example, desorption electrospray ionisation (DESI), direct analysis in real time (DART) and paperspray analysis allow DBS to be directly analysed from cards [145-147].

The various techniques for analysis of DBS target the different classes of drugs. Overviews are given for therapeutic drugs [148], small molecules [74], a range of analytes [39, 91] and drugs of abuse [44, 149]. Methods have also arisen that are able to screen for multiple drugs, such as those published for novel psychoactive substances (NPS) [150] and other recreational drugs [77, 79].

In this thesis, conventional GC-MS and LC-MS/MS with heated electrospray ionisation (LC-HESI-MS/MS) were used to quantify salbutamol and pseudoephedrine respectively from blood collected with a new micro-volume sampling device. Methods were developed, validated and tested with healthy volunteer studies for the two drugs of abuse.

1.4 Considerations for blood sampling

1.4.1 Dried blood spots versus conventional blood samples

Plasma and serum are usually preferred over liquid whole blood samples, because of the delicacy of RBCs present in whole blood. However, the introduction of DBS offers numerous advantages over all forms of liquid blood. To start with the ease of capillary blood collection over venepuncture, the collection is simple and can be performed by non-specialised personnel. This has the additional advantage that collection is not restricted to hospitals and/or medical centres where trained personnel is present and can even be performed by patients themselves at home [71, 72, 151]. The collection of DBS is found to be less invasive than other types of blood collection and patients have expressed a strong preference of capillary blood collection over venous blood collection because of reduced pain and shorter collection time [72, 73, 151, 152]. The use of DBS in paediatric and animal studies specifically offers a solution where blood collection is usually restricted because of ethical issues and technical challenges as a result of a low total blood volume [47]. For comparison, up to 3 mL blood is usually collected in human studies by conventional sampling and volumes of 100-200 µL in animal studies [87, 153].

DBS also offer a solution for animal welfare and the 3R goal in animal research; replacement, refinement and reduction [38]. Less stress is caused to animals, because the animals don't need to be warmed prior to sampling and finer needles can be used. Also, fewer animals are needed for studies as serial sampling from a smaller number of animals is possible. In addition, DBS analysis could improve data quality as conventional blood collection leads to the necessity of using multiple animals to cover several time points. Pooling data from different animals together has led to more scatter, which could lower the quality of data [89].

DBS have the advantage that they can be shipped by regular post without the need of special containers and conditions required for shipping liquid blood samples. DBS shipping costs and consumables needed for DBS collection are also lower compared to costs associated with venous blood sample collection and shipment [154, 155]. In addition, DBS are not subject to dangerous good regulations [156] as they were found to pose low exposure risks of potentially infectious hazards [76, 157, 158]. Furthermore, many exogenous and endogenous compounds have been reported to be stable in DBS

stored at room temperatures for relative long periods [33, 87, 159-162] and even improved when stored cooled [163, 164]. Degradation of drugs in blood normally occurs as a result of hydrolysis, but hydrolysis of analytes in dried blood on cards is minimised. Moreover, enhanced stability of opiates, cocainics and amphetamines has been reported in DBS compared to liquid whole blood samples [33, 79, 160]. In the case of less stable analytes, measures such as modifying sample pH, chemical or temperature treatment can be applied to improve stability. Lastly, risks associated with the use and disposal of needles and syringes needed for conventional blood sampling are also not an issue for the collection of DBS.

The use of PM blood to create DBS has been explored and found suitable for analyte screening [165] and metabolic screening [166], but to date no study has directly compared bioanalytical results of conventional PM blood samples with DBS created from PM blood. The creation of DBS from PM blood might be a suitable alternative to conventional PM blood analysis as blood is difficult to collect PM due to its changed composition [5]. In addition, many analytes in liquid PM blood stored at different conditions showed instability [7].

Although capillary blood differs from venous blood in terms of endogenous analyte composition [30, 167, 168], similar bioanalytical results were reported when comparing DBS created from capillary blood with DBS created from venous blood after distribution equilibrium of the exogenous analytes has been reached [88] and in spiked samples [169]. Similar results were also reported for the detection of exogenous analytes in DBS and liquid venous blood samples [37, 71-73, 79], with the exception of zopiclone which was prone to degradation [36]. This also applies when comparing DBS with liquid plasma samples [81, 169, 170] and DBS are sometimes even preferred over plasma samples depending on the blood to plasma ratio of analytes [171]. Similarly, comparable [172] or even improved [173] bioanalytical results have been obtained when comparing DBS with liquid whole blood samples from rodents.

On the other hand, comparison of small-molecule profiles between venous and capillary blood revealed differences. Most of the observed differences were attributed to chemicals involved in cleaning of the skin for capillary blood collection, but they could also be attributed to endogenous human blood compounds [174] as proteomic differences are known to exist between serum and plasma [175]. Many studies have,

however, focussed on just one endogenous protein and have found comparable results for DBS and venous samples [176]. Furthermore, Chambers et al. compared proteins in liquid whole blood, serum and plasma with their DFS equivalents and showed both similar numbers and identities of proteins and peptides for each fluid type [63]. Also, no deviating results have been reported for the detection of insulin-like growth factor-1, between DBS created from human blood and DBS from animal blood [169].

Aside from all the advantages DBS collection has over conventional blood collection and the comparable, or even improved, analytical results and stability for DBS samples, sensitivity of analyses and ion suppression effects can pose a challenge. As the majority of existing blood analysis protocols are based on plasma and serum samples, method redevelopment and validation for DBS samples requires considerable time and effort.

1.4.2 Developments in micro-volume blood collection

Various types of blood spot cards are available for different applications, with the main difference being with or without chemical treatment. All blood spot cards are composed of pure cellulose and the chemically treated cards are impregnated with chemicals to lyse cells, inactivate pathogens and denature proteins. The main effect of chemical treatment on DBS appearance is the spreading of blood. Mei et al. have reviewed the use of cards for collection and analysis of DBS and the quality and performance of the different cards are evaluated by various international regulatory agencies and quality assurance programs [39]. No variation in quantitative bioanalytical results was observed for six analytes tested on different cards [177], with the exception of biases introduced by HCT effects and taking sub-punches as explained in section 1.2 [45]. Furthermore, the use of non-specific papers for DBS analysis has also been reported [57] as well as modification of the commercially available cards to improve analyte stability [178].

The traditional analysis of DBS from cards has some drawbacks. Most importantly, by using sub-punches the recovery of analytes is inconsistent as a result of uncertain volumes and associated HCT effects [45, 46, 50-53]. Sub-punching also leads to human biological waste and care should be taken to minimise carry-over by punching through the spots. Therefore, adaptations to conventional DBS collection and sample

preparation were introduced. The collection of blood into a capillary tube containing anti-coagulant and subsequent spotting onto the card using a suction bulb was one of the first advances in pharmacokinetic studies to facilitate an even spreading of blood and accurate blood volume [47]. Alternatively, the use of a pipet for fixed volumes or using the entire spot instead of sub-punches also avoids the issues [54]. In addition, a microfluidic-based sampling system enabling fixed blood volume sample collection onto cards [160, 179] and a disposable chip for fixed volume collection [180] have been introduced. To improve the punching of DBS from cards, cards with perforated circles [181] and pre-cut disks [182] have been developed together with devices that hold pre-cuts disks and collect excessive blood by capillary force from the spotting tubes [183, 184]. Furthermore, numerous automated card punching systems have become commercially available [185] including one that also automates sample preparation [137]. Automated blood collection samplers have also been introduced to facilitate micro-volume blood sampling from animals [186, 187], including the automatic spotting of DBS [186].

Alternative approaches to the DBS technique are also being developed, such as the Mitra™ microsampling device which is a device based on patent-pending volumetric absorptive microsampling (VAMS) technology [153, 188]. In short, the tip of the device saturates in a few seconds by wicking and an additional two seconds of contact with blood is recommended to fully saturate the tip. VAMS devices with an average blood wicking volume of 10.1 µL have been used for experiments in this thesis (Figure 1.3).

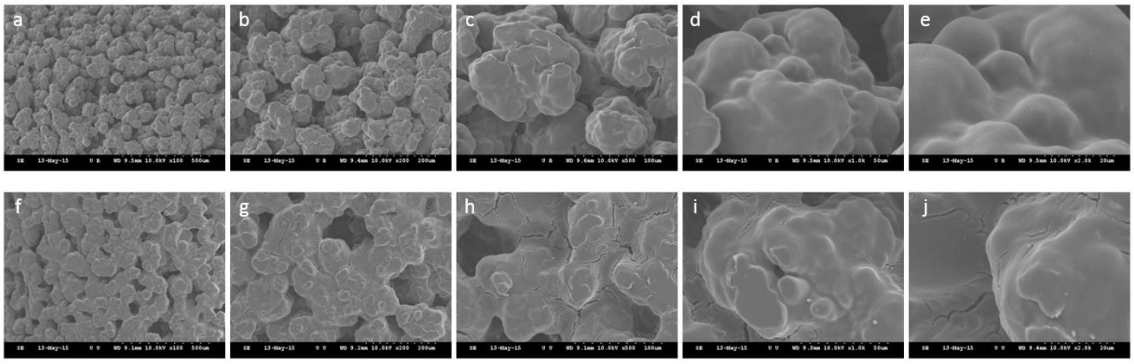

Figure 1.3. Scanning electron microscopy (SEM) images of a Mitra™ microsampling tip without (top row) and with human blood collected (bottom row) and dried for 1 day. Magnification increases from left to right (100x, 200x, 500x, 1000x, 2000x). Samplers were sputter coated with gold and images were taken with a Hitachi S3000H SEM with an accelerating voltage of 10 kV (based on the RBC analysis in a previous study [14]).

The use of VAMS in research has been increasing since its introduction in 2014, with 58 publications at the time of submitting this thesis [189]. It is an easy to handle device, facilitating the accurate collection of a fixed micro-volume of blood without the need of additional equipment and with a convenient holder for drying, storing and shipping. In the future, the application of VAMS to sample bloodstain traces at crime scenes could be interesting for forensic investigations. Therefore, research to explore the possibilities of sampling both wet and dried blood from various surfaces is desired.

1.4.3 Influence of anticoagulant

Anticoagulants are used to prevent clotting of blood, thus keeping it fluid for testing. The most used anticoagulants are ethylenediaminetetraacetic acid (EDTA), sodium citrate and heparin. EDTA and citrate seize calcium ions needed for clotting [190]. Heparin works by inhibiting the formation of thrombin which is needed for clotting, but it also binds to other proteins [191]. It is assumed that anticoagulants do not affect the physical characteristics of blood such as its viscosity [192]. Blood cells and Hb were found to be stable for up to 72 hours in blood with the addition of anticoagulants, but this did not apply to platelets. Side-effects such as leukocyte clumping with immunoglobulin antibodies, plasma dilution and protein binding are known to interfere with proteomics analyses [190]. Low-mass protein profiles changes have also been reported after the addition of anticoagulant to blood samples [193], but no significant effect on the chemical profile of both fresh and aged blood has been reported after the addition of anticoagulants [120]. Most studies that have investigated bloodstain ageing used blood with anti-coagulants to prevent clotting, but the influence of anticoagulants on the ageing of bloodstains and on the presented TSD approaches has not been investigated [96]. Using anticoagulated blood for experiments is not a realistic simulation of bloodstains at crime scenes in the first place, but it is especially important and recommended not to use treated blood for blood(stain) ageing studies. Lastly, similar bioanalytical results have been demonstrated for blood collected using VAMS devices with and without anti-coagulant pre-treatment [153] and the effects of analyte detection between DBS and blood collected with anti-coagulants is also similar as explained in section 1.4.1.

1.5 Blood versus other biological sample types

This entire introduction chapter has focussed on blood, DBS and bloodstains, but other biological sample types can also be encountered at crime scenes and/or collected from individuals. Most of those sample types can be used to retrieve DNA for identification, to reconstruct what happened and to retrieve intelligence information such as toxicology. For toxicology, each sample type is suitable for a different time window and application. Oral fluid (OF), exhaled breath (EB) and hair are other novel alternative matrices for sample collection. Thevis et al. have reviewed the intrusiveness, invasiveness and duration of collection of those alternative matrices together with available sample volume, analyte stability performance, tamper resistance, costs and analysis performances [194]. Using a combination of matrices seems the way forward for doping analyses, but further research and development regarding sampling and analysis was recommended.

OF has become common for a variety of applications such as traffic controls for DUID and scenarios where the detection of recent drug intake is desired [195]. The collection of samples is easy, regarded both low intrusive and invasive, quick and can be performed at any location. Stability of analytes is moderate and samples can be stored and shipped easily. However, OF testing also has some disadvantages. The volume of fluid available can be limited, especially after intake of certain drugs, and questions have been raised about the correlation to blood concentrations. Furthermore, false negative and highly variable bioanalytical results have been reported such as those possibly caused by mouth washing and other contamination and adulteration issues [195].

EB has been studied as a novel matrix for drug testing, especially for screening of recent drug intake. Alcohol breath tests are performed routinely at traffic controls for DUID and Beck et al. have studied the detectability of other drugs such as amphetamines with promising results [196-199]. EB collection is easy and quick, can be at any location and is regarded both low intrusive and invasive. The sensitivity of detection is higher or similar for some drugs of abuse compared to conventional urine and blood samples, but lower for others. Breath samples have been collected in parallel with micro-volume blood samples for one experiment in this thesis to study the pharmacodynamic profile after the intake of a drugs of abuse.

Hair specimens are also easy and quick to collect, store and ship. The collection is regarded both low intrusive and invasive with high analyte stability. Hair analysis is interesting for the detection of drugs after chronic use and/or continuing investigations with wider time frames. The suitability for detecting and quantifying a single drug administration is limited as well as the availability of untargeted methods for the detection of multiple analytes [131].

Urine has been the preferred biological sample type for many toxicological analyses and for sport doping testing [200]. Sample collection can be non-invasive, quick and resulting in a large sample volume, but it can also be intrusive, with a long waiting time and low sample volume. Multiple collections in a short time frame can be problematic and advanced storage and shipping conditions are needed. Both excreted compounds and their metabolites are concentrated in urine, which is beneficial for analyses but analyte stability is only moderate. Unlike blood samples, urine is not suitable for providing temporal information and generally has a limited correlation with pharmacological effects [131].

Lastly, organs and PM samples are routinely used for toxicological screening. Furthermore, other biological sample types such as semen, vaginal fluid, nails and skin cells can also be found at crime scenes, but are generally not used for toxicological analyses.

In conclusion, DBS is the sample type of interest for both the toxicology and ageing part of this thesis because blood traces are frequently encountered at crime scenes and DBS offers many advantages for collection and analyses. The window of detection for DBS toxicological analyses is intermediate between OF and EB on one hand and urine and hair on the other hand. Estimating the TSD using any of the biological sample types including DBS is not possible yet.

1.6 Summary of introduction and thesis study aims

Advances have been made in estimating the TSD of bloodstains with different techniques, some suitable for bloodstains deposited recently and others for the longer-term. However, the accuracy of estimations generally decreases with increasing TSD. Environmental influences, substrate, bloodstain quantity and inter-person variation add to the inaccuracy of the estimations. Therefore no age estimation technique is being routinely applied in casework. In addition, some studies have started investigating the underlying physical changes of ageing bloodstains, mainly focussed on Hb changes.

Many advantages have been outlined for using DBS as an alternative matrix to conventional blood samples and other biological sample types for toxicological screening. Initially, instrumentation limited the ability to measure analytes in micro-volume blood samples, but improvements in sensitivity as well as automated sample preparation, on-line extraction and direct analysis have resolved some of the challenges. High throughput toxicological analysis of DBS samples is possible, but as of yet not common practice. Bioanalytical procedures have to be adapted and new methods for interpreting results have to be introduced before this can occur.

The hypothesis tested in this thesis was if micro-volume samples of blood can be used to enhance the current forensic practice of blood analysis. To evaluate the TSD of blood it was investigated if a molecular profile of DBS ages could be established using nano-LC-ESI-MS/MS and for toxicology purposes it was investigated if VAMS technology could confer advantages for the detection and quantification of two selected drugs of abuse from micro-volume blood samples.

The ageing experiments were performed as a secondment at the University of Amsterdam (Amsterdam, the Netherlands). Chapter 2 describes the collection of DBS samples from multiple volunteers together with the ageing procedure, extraction of blood proteins from cards, overnight digestion, analysis of peptides using nano-LC-ESI-MS/MS and protein quantification approaches. To speed up the DBS workflow, an immobilised microfluidic enzyme reactor (IMER) was developed and tested as outlined in Chapter 3. To reduce acquisition time, the application of the novel technique surface acoustic wave nebulisation (SAWN) followed by MS was tested as explained in Chapter 4. For the toxicology experiments, micro-volume blood samples were collected using

VAMS at the University of Leicester (Leicester, United Kingdom). Chapter 5 presents the development of a GC-MS method for salbutamol quantification using micro-volume blood samples followed by partial validation and application to samples of healthy volunteers after administration with the drug of abuse. The collection of EB samples in parallel with blood samples collected onto VAMS devices of healthy volunteers dosed with pseudoephedrine hydrochloride is described in Chapter 6. The blood samples were analysed by the Center for Preventive Doping Research (Cologne, Germany) using LC-HESI-MS/MS. The breath analyses were performed in-house using proton transfer reactor time-of-flight mass spectrometry (PTR-ToF-MS) and two dimensional gas chromatography with flame ionisation and quadrupole mass spectrometric detection (GCxGC-FID/qMS). Chapter 7 concludes this thesis and outlines future perspectives.

2 Proteomics approach for the evaluation of dried blood spot age

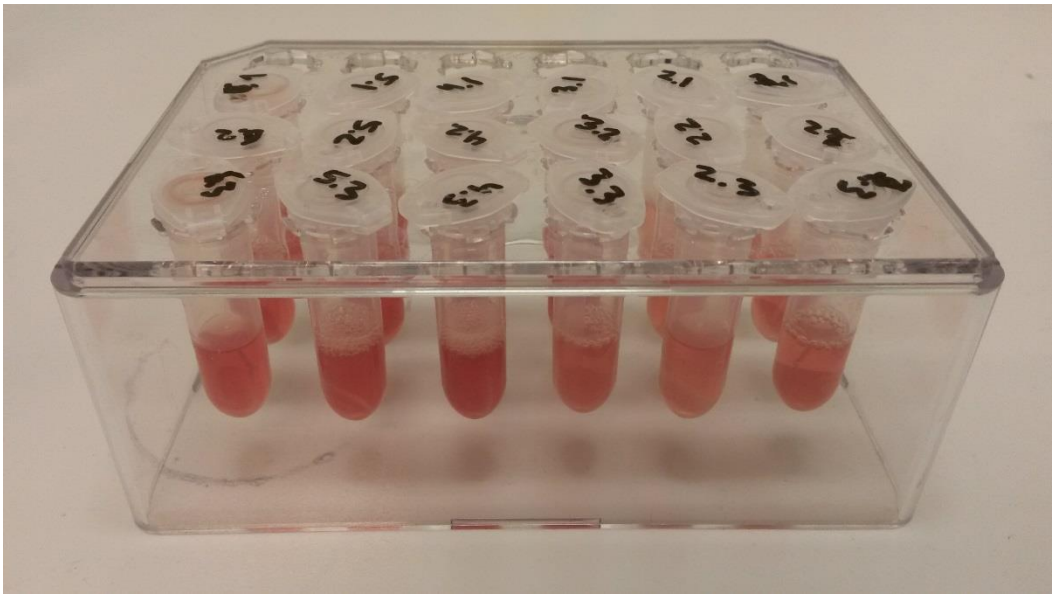

Extracted dried blood spots

This study took place as a secondment at the University of Amsterdam (Amsterdam, the Netherlands). A special thanks goes to Prof. Garry L. Corthals for his supervision, to Katarzyna Szykula for sharing in-house data of trials prior to this study and to Petra J. Jansen for her experimental assistance (University of Amsterdam, Van 't Hoff Institute for Molecular Sciences). Dr. Andrew Bottrill (University of Leicester, Department of Molecular and Cell Biology) and Winfried Roseboom (University of Amsterdam, Swammerdam Institute for Life Sciences) are gratefully acknowledged for helping with the data conversion and searches. Dr. Yassene Mohammed (Leids Universitair Medisch Centrum, Center for Proteomics and Metabolomics) is gratefully acknowledged for helping with the protein cluster analyses.

2.1 Introduction

In 2005, the Human Proteome Organization (HUPO) started to develop a plasma proteome database (PPD; http://www.plasmaproteomedatabase.org/) which currently contains 10,546 proteins that have been detected in serum and/or plasma [201]. A plethora of instruments and techniques is available that can be used to detect and quantify those proteins. Chromatography in-line with mass spectrometry (MS) is the most commonly used combination of analytical techniques. In addition, a variety of sample preparation methods are available which can lead to a broad range of proteins identifications. As few as 59 proteins were detected by a non-targeted approach using whole plasma and trypsin digestion [202] and as many as 4600 proteins were identified per sample by a non-targeted approach using plasma depleted of high abundance proteins (HAPs) and trypsin digestion [203]. The main application for studying proteins in blood is its potential to identify and quantify biomarkers of diseases [204, 205]. The determination of relative and/or absolute concentrations of blood proteins has the potential to monitor disease onset and progression. Although most studies use liquid plasma or serum, a small number have started to explore the use of dried blood spots (DBS) [162, 176, 206], including by volumetric absorptive microsampling [207]. Chambers et al. compared the detection of proteins from liquid whole blood, serum and plasma with their dried fluid spot equivalents and showed both similar numbers and identities of proteins for each fluid type [63].

The time since deposition (TSD) of blood has not been the topic of proteomics studies. Attempts with a plethora of other techniques to determine the TSD of blood are extensive (outlined in Chapter 1, Table 1.1), but fundamental knowledge about the intrinsic changes of ageing bloodstains remains scarce and no accurate method to determine the TSD is available yet. Therefore, the aim of this study was to evaluate the molecular profile of DBS ageing using nano-liquid chromatography hyphenated to tandem mass spectrometry with electrospray ionisation (nano-LC-ESI-MS/MS). Whereas biomarker studies focus on proteins that remain stable over time, protein abundances that change quantitatively over time would be of interest for forensic scenarios in which the age of bloodstains is of relevance.

Top-down proteomics has demonstrated success in the characterisation of intact proteins and their post-translational modifications, however limitations such as difficult protein ionisation make proteomics research mainly driven by bottom-up analysis [208]. In bottom-up analysis, a peptide mixture is formed by enzymatically digesting proteins. When the analysis is applied to a mixture of proteins it is called “shotgun proteomics”. Trypsin was chosen here to digest proteins of DBS aged for up to 8 days. An extra set of DBS was aged for 398 days and also analysed. Database searches were performed to identify proteins based on detected peptides. Different label-free quantitative proteomics approaches were explored to determine changes in the abundance of spectra, detected peptides and identified proteins.

2.2 Experimental design

2.2.1 Chemicals and materials

Ammonium bicarbonate (NH_4HCO_3, BioUltra, ≥ 99.5%), dithiothreitol (DTT, ≥ 99.0%), Empore C18 solid-phase extraction cartridges (SPE cartridges, 4 mm/1mL), iodoacetamide (IAA, ≥ 99%), sodium deoxycholate (SDC, BioXtra, ≥ 98%), trifluoroacetic acid (TFA, ≥ 99%), tris(2-carboxyethyl)phosphine hydrochloride solution (TCEP, 0.5 M, pH7), trypsin (European Pharmacopoeia (EP) reference standard) and Whatman Human ID Bloodstain Cards BFC 180 were purchased from Sigma-Aldrich (Zwijndrecht, the Netherlands). Acetonitrile (ACN, LC-MS grade), formic acid (FA, ULC/MS – SFC-CC grade, 99%) and water (ULC/MS – CC/SFC) were purchased from Biosolve (Valkenswaard, the Netherlands). Contact-activated lancets were purchased from Becton Dickinson (Breda, the Netherlands).

2.2.2 Dried blood spot collection

Capillary blood was collected from the fingertips of 7 healthy donors (4 males, 3 females) using contact-activated lancets at the University of Amsterdam (Amsterdam, the Netherlands). The first drop of blood was wiped away and 30 aliquots of 10 µL of blood were spotted directly onto Whatman bloodstain cards. Sets of triplicate spots per donor were left to dry for 2 hours in freely circulating air in the dark at room temperature. The remainder of the spots were left to age for up to 8 days. Each day, 3

spots per donor were cut out and placed into 2 mL Eppendorf tubes. In addition, a set of triplicate spots from 6 donors were aged for 398 days. One of those donors donated blood twice in order to study intra-person variability and batch effects. The seventh donor donated blood at the second instance only.

2.2.3 Sample preparation

The method used for the preparation of samples was adapted from the method developed by Chambers et al. [209]. For the extraction of blood and its proteins from the cards, 800 µL of 25 mM NH_4HCO_3 was added and samples were vortexed for 5 minutes at 1400 rpm. After collection, drying and extraction of the blood from the cards, a pre-treatment was carried out before starting overnight in-solution protein digestion. First, proteins were denatured by adding 100 µL of 10% SDC and 10 µL of 0.5 M TCEP followed by incubation for 1 hour at 60 °C. Next, 52 µL of 200 mM IAA was added and the samples were alkylated for 1 hour in the dark at room temperature. To consume any remaining IAA, 55.4 µL of 200 mM DTT was added, followed by incubation for 30 minutes at 37 °C. For digestion, 3.5 µL of trypsin (1000 mg/L) was added and samples were incubated at 37 °C for 16 hours. To precipitate SDC, 40 µL of 2% FA was added to the digests the next day. Digests were centrifuged at 4000×*g* for 20 minutes and their supernatant was desalted using Empore C18 SPE cartridges, evaporated to dryness and stored at -20 °C until analysis.

2.2.4 IDA nano-LC-ESI-MS/MS analysis of digested proteins from DBS

Digested DBS samples were reconstituted in 100 µL water of which 5 µL per sample was loaded in a randomised order onto an Eksigent trap column (nano LC trap set, ChromXP C18, 120 Å, 350 µm i.d.). Desalting was performed at 2 µL/min for 10 minutes with 3% ACN and 0.1% TFA. Peptides were then separated on an in-house packed analytical column (Magic C18 resin, 100 Å pore size, 5 µm particles, 75 µm i.d., 100 mm column length) at 300 nL/min and eluted using a 94 minute long gradient composed of solvent A (0.1% FA in H_2O) and solvent B (0.1% FA in ACN). The 94 minute gradient ran from 5% to 45% B (0–90 min), 45% to 90% B (90–92 min) and was kept at 90% B (92-94 min). Re-equilibrations of the columns followed with solvent A during sample injection and

loading. Different gradients were tested previously [210], but the number of spectra, peptides and protein identifications were found to be highest with this gradient as published by Chambers et al. [63]. A blank injection with loading buffer (5 µL of 3% ACN + 0.1% TFA in H_2O) was performed following each first and second DBS sample using a shortened 30 minute gradient and a calibration test was performed after each third DBS sample. The shortened gradient ran from 5% to 100% B (0-20 min), was kept at 100% B (20-25 min), decreased from 100% to 5% B (25-29 min) and was kept at 5% B (29-30 min). The calibration tests were based on β-galactosidase digest injections using a 45 minute gradient which ran from 5% to 35% B (1-16 min), 35% to 80% B (16-18 min), was kept at 80% B (18-24 min), decreased from 80% to 5% B (24-25 min) and was kept at 5% B (25-45 min). Eluted peptides were analysed using an Eksigent Ekspert nanoLC 425 system (Sciex, Singapore) coupled to a nano-ESI installed on a TripleToF 5600+ mass spectrometer (Sciex, Singapore) and spectra were acquired in high-sensitivity mode by information dependent acquisition (IDA). Time-of-flight MS (ToF-MS) scans were performed in the mass range *m*/*z* 400–1250 Da and the top 30 precursor ions with charge states from +2 to +4, exceeding a threshold of 100 cps, were selected for MS/MS analysis. Product-ion spectra were formed using collision-induced dissociation (CID) in rolling-collision-energy mode and collected across the mass scan range *m/z* 100–2000 Da. Both the nanoLC and TripleTOF 5600+ instruments were operated using Analyst 1.7 (Sciex, Singapore).

2.2.5 Assay evaluation

One sample was selected to be measured 10 times by IDA nano-LC-ESI-MS/MS analysis to assess instrument performance and method repeatability. Digested DBS samples from 6 donors were pooled per DBS age (6 * 3 biological replicates) as well as all 144 samples (6 donors * 3 biological replicates * 8 days) to assess data analysis performance. The biological triplicates of one of the donors were pooled per DBS age to evaluate the effects on protein identification and quantification. Recovery of proteins from DBS was investigated by analysis of capillary blood samples spotted into Eppendorf tubes instead of onto cards and aged for 0, 3 and 10 days. Matrix effects were studied by analysis of blank card punches without blood that underwent the same sample treatment. Intra-

person variation and batch effect were assessed by analysis of DBS collected at two different points in time from one donor.

2.2.6 DIA SWATH-MS/MS analysis of digested proteins from DBS

Sequential window acquisition of all theoretical (SWATH) mass spectra was performed on a selection of 8 DBS samples, aged for up to 8 days from the same donor. The little known technique of SWATH-MS was introduced in 2012 as a new technique combining data independent acquisition (DIA) with targeted data extraction [211]. Briefly, all precursor ions within a selected mass to charge ratio (*m/z*) range are fragmented and product ion spectra are acquired of all fragments. The full precursor *m/z* range is divided in smaller precursor windows, the swathes, which are scanned rapid and repeatedly in a consecutive order. The resulting dataset can be analysed by creation and comparison to a library based on similar measurements performed with the same instrument in IDA mode. 0.5 µL of indexed retention time standard was added to 25 µL digested DBS sample (reconstituted in water) and each sample was measured 3 times. Similar to the IDA nano-LC-ESI-MS/MS analyses (section 2.2.4), 5 µL of sample was loaded onto the trap column and desalted for 10 minutes. Peptides were then separated on the analytical column with the same 94 minute gradient from 5% to 45% B (0–90 min), 45% to 90% B (90–92 min) and kept at 90% B (92-94 min). Spectra were acquired in SWATH mode by DIA, with 200 variable windows and an accumulation time of 96 milliseconds. Product-ion spectra were formed using CID in rolling-collision-energy mode and collected across the mass scan range *m/z* 400–1250 Da. Analyst 1.7 (Sciex, Singapore) was used for data acquisition.

2.2.7 Protein identifications by ProteinPilot software

Proteins were identified using ProteinPilot 5.0 (Sciex, Singapore) with the identification threshold set at 1% false discovery rate (FDR). Searches were performed against the Uniprot human database (www.uniprot.org). Trypsin was selected as the digestion enzyme and iodoacetamide as the alkylation reagent. Pooled searches were performed in an identical way.

2.2.8 Protein quantifications by spectral counting using Scaffold software

Data files obtained with Analyst 1.7 (Sciex, Singapore) were first converted to vendor independent format files (mzmL) using the MSConvertGUI tool of the Trans-Proteomic Pipeline 5.0.0 and then to ThermoScientific format files using the mzXML2Search tool [212]. Proteome Discoverer 1.4.1.14 + Daemon (ThermoScientific, Waltham, MA, US) was used to perform a spectral library search with Mascot against the Uniprot human database (www.uniprot.org). Trypsin was selected as the digestion enzyme, oxidation as dynamic modification, carbamidomethyl as static modification and the tolerance was set at 10 ppm with 0.05 Da. A second spectral library search was performed with X!Tandem using Scaffold Q+S 4.8.4 (Portland, OR, US). The identification threshold was set at 1% FDR for both proteins and peptides and the minimum number of peptides for protein identification was set at 2. Both the exponentially modified protein abundance index (emPAI) and normalised spectral abundance factor (NSAF) build-in label-free spectral counting methods of the Scaffold viewer 4.0 software (Portland, Oregon, US) were used to estimate the abundance of identified proteins. The non-quantitative build-in options percentage coverage, percentage of total spectra, peptide count and spectrum count were also assessed to investigate changes in the spectra, detection of peptides and identified proteins of DBS aged for up to 8 days. Finally, changes in average total ion current (TIC) values were explored.

2.2.9 Precursor intensities evaluation using Mascot Distiller software

As spectral counting methods were not found reliable for the quantification of low abundant proteins (LAPs), Mascot Distiller 2.7.0.0 (Matrix Science, London, UK) was used to estimate average precursor intensities with the aim of detecting changes in DBS related to TSD. Searches were performed with Mascot Server 2.6.2 (Matrix Science, London, UK) against the contaminants and Swissprot human database from the Uniprot consortium (www.uniprot.org). The label-free quantification method of the Mascot distiller toolbox was used to obtain relative peptide and protein intensities. Raw data files were processed as a single project per donor, consisting of 3 biological replicate files for each of the 8 days. Default settings for SciexAnalyst files were used, trypsin was selected as the digestion enzyme, 2 missed cleavages were allowed,

carbamidomethylation of cysteine was selected as fixed modification and oxidation of methionine as variable modification. The peptide mass tolerance was set at 50 ppm and the peptide fragment mass tolerance at 0.06 Da. The significance threshold was set at 0.05, the minimum number of peptides was set at 2 and the elution time delta was set at 500 seconds. Triplicate samples of day 0 were set as reference for each donor and protein intensities were weighed against the triplicates of the other DBS ages. In addition, relative peptide intensities of the triplet of samples per DBS age were averaged for each donor. Those averages were then normalised by dividing them by the total of relative peptide intensities over all ages for that peptide per donor. Normalised relative peptide intensities were then averaged per protein per DBS age for each donor. Relative protein intensities per age were scaled by standardisation and protein cluster analysis was performed with R studio 1.0.143 (64 bits, R version 3.4.4, Vienna, Austria) to explore trends over time for each donor. The number of clusters was set to 9 and time profiles per protein per donor were also produced for further inspection.

2.2.10 SWATH-MS data analysis

SWATH 2.0 (Sciex, Singapore), Spectronaut 10 (Biognosys, Schlieren, Switzerland) and Skyline (MacCoss lab, Seattle, WA, US) were used to explore protein quantity trends over time. Searches were attempted against a DBS database created from the IDA analyses (section 2.2.4) as well as against the pan human SWATH library (Sciex, Singapore).

2.3 Results and discussion

2.3.1 Assay evaluation

A selected DBS sample was run 10 times using IDA nano-LC-ESI-MS/MS. Spectra, peptides and proteins identifications (global, 1% FDR) obtained with ProteinPilot were compared for the technical replicates. On average, 5529 ±233 spectra were obtained with an excellent relative precision of 95.8% for instrument performance. Furthermore, 1997 ±67 peptides and 120 ±13 proteins were identified on average, consistent with a decent method repeatability of 89.1%-96.6%. The same sample was also measured on an additional day which resulted again in a similar performance and repeatability.

Table 2.1 shows that more peptides and proteins were identified (global, 1% FDR) by analysing samples individually and pooling the data per DBS age post nano-LC-ESI-MS/MS analysis compared to the analysis of samples pooled per age and measured as pool by nano-LC-ESI-MS/MS with the exception of DBS aged for 2 days. The same applies to the samples of all donors and ages pooled prior to nano-LC-ESI-MS/MS analysis compared to the data of individual samples pooled post nano-LC-ESI-MS/MS analysis (224 proteins and 2828 peptides versus 289 proteins and 7993 peptides identified respectively). The pooled samples of biological triplicates per age for one of the donors resulted in a similar number of detected peptides as the average of the biological samples measured individually (maximum of 5% difference for the different ages). However, the differences for spectra and protein identifications were much larger (with maximum differences of 42% and 23% respectively for the different ages). Also, differences between biological replicates were observed to be large (with maxima of 28%, 38%, 36% for spectra, peptide and protein identifications respectively).

Table 2.1. Comparison of identified proteins and peptides between samples pooled prior to nano-LC-ESI-MS/MS analysis (1 data file per DBS age) and data pooled post nano-LC-ESI-MS/MS analysis (24 data files per DBS age). The number of spectra is also shown. Identifications were performed at 1% FDR, global. *ID=identification.*

	Protein ID yield	Protein ID yield	Peptide ID yield	Peptide ID yield	Spectra ID yield	Spectra ID yield
	Pooled sample	Pooled data	Pooled sample	Pooled data	Pooled sample	Pooled data
TSD: 0 days	171	248	2292	4721	8246	121045
TSD: 1 day	213	228	2561	5541	6786	132001
TSD: 2 days	242	221	2932	5151	7416	134296
TSD: 3 days	235	251	2993	5322	8758	127756
TSD: 4 days	236	270	2832	5007	9143	136673
TSD: 6 days	228	244	2646	5319	8224	134385
TSD: 7 days	234	234	2751	4820	8190	136449
TSD: 8 days	223	289	2535	4488	8199	112685
All 8 ages	224	289	2828	7993	7673	1038630

An explanation of the lower yields for the samples pooled prior to analysis by nano-LC-ESI-MS/MS could be ion suppression owing to the complexity of the samples. All samples were therefore analysed individually by nano-LC-ESI-MS/MS. Moreover, it is

contradictive to pool DBS samples because one of the motives to work with DBS is because of its micro-volume.

Considerably more proteins were identified from the samples spotted into Eppendorf tubes compared to DBS proteins extracted from cards (for example, an average of 164 versus 133 for samples aged for 3 days). However, all experiments in this study were designed and performed with DBS on cards as this is a common matrix in DBS research. It would be interesting to test other matrices in future research, e.g. forensically relevant substrates. The cards did not cause interference, but a few HAPs were detected in the card samples without blood. To reduce carry-over of HAPs, blanks and calibrations were run between DBS samples.

Low variation was found when comparing the averages per DBS age between the first and second batch of samples (with maximum differences of 16% for spectra and 10% for both peptides and proteins for the different ages). However, intra-person variation was found to be higher (with up to 39%, 12% and 28% for the average number of spectra, peptides and protein identifications respectively for the different ages). This is consistent with the large variation found for biological replicates as discussed earlier. On the other hand, reasonable inter-person variation was found for the different ages (with maximum average differences of 12.5%, 12.2%, and 13.5% for spectra, peptide and protein identifications respectively).

Additionally, the extraction of proteins from DBS that were aged for over a year (398 days) was visibly different from the extraction of more recently spotted DBS (aged for up to 8 days). The 398 days aged DBS were brown and the NH_4HCO_3 extraction solvent did not noticeably change colour after the standard 5 minute extraction at 1400 rpm, in contrast to the more bright red coloured spots and extraction mixture of DBS aged for up to 8 days (Chapter 2 front page). The biological triplicates of DBS aged for 398 days were therefore split and treated differently. One spot per donor was subjected to the standard sample treatment with the 5 minute extraction at 1400 rpm (section 2.2.3). Another spot was also subjected to the standard sample treatment with the exception that the actual punched DBS was left in the pre-treatment solution until digestion. The last spot was left in the extraction solvent for 24 hours prior to continuation with the standard sample treatment. Figure 2.1 shows that most peptides

and proteins were identified by leaving the spots in the sample pre-treatment solution until digestion.

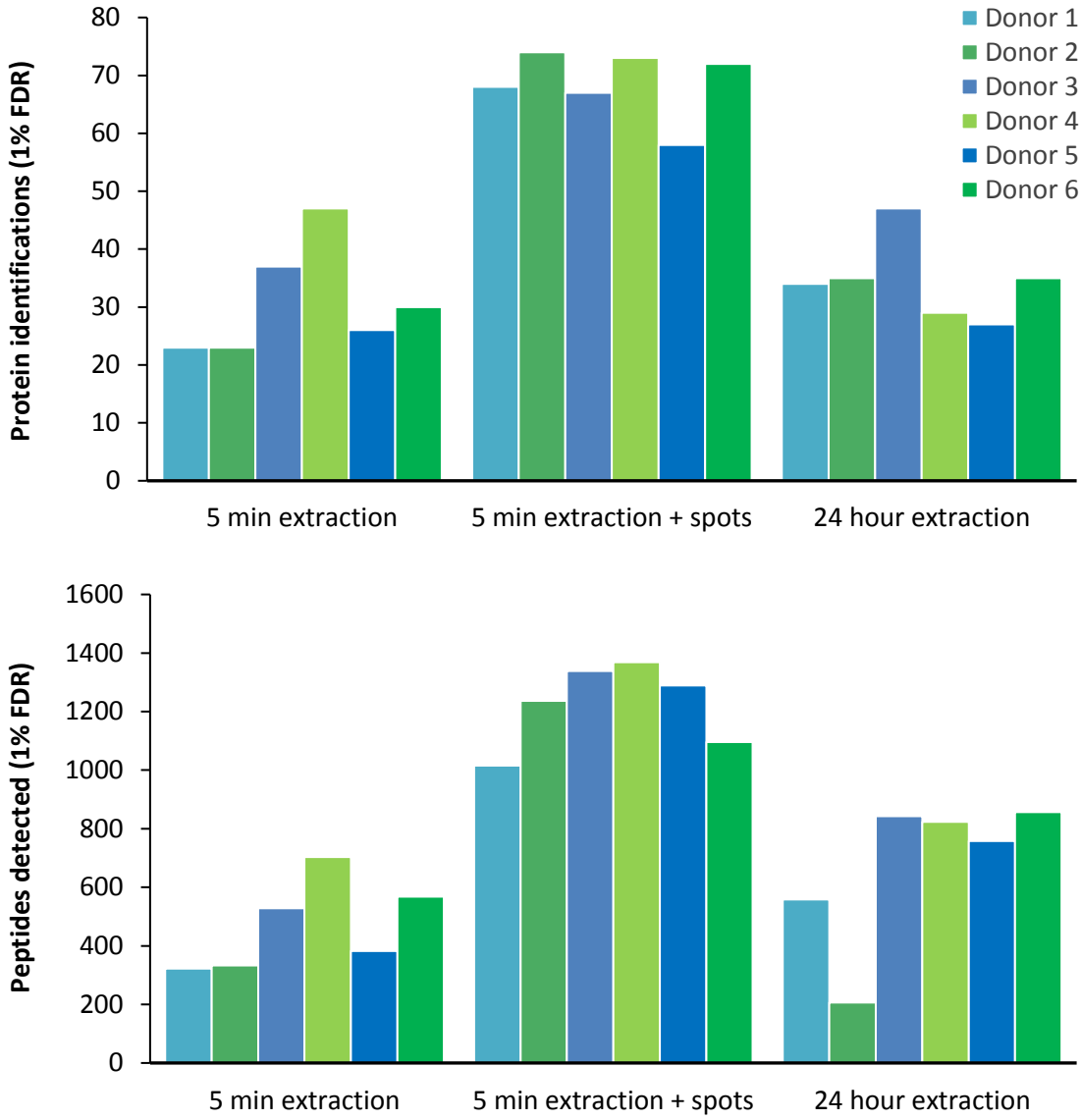

Figure 2.1. Effect of three methods on the extraction of proteins from DBS aged on cards for 398 days. The number of proteins identified (top) and peptides detected (bottom) is shown. Each plot shows from left to right; the results after standard extraction with NH_4HCO_3 for 5 minutes at 1400 rpm, standard extraction without removal of DBS from the extraction solvent until digestion, extended extraction for 24 hours.

As all DBS samples of this study were subjected to the standard 5 minute extraction with removal of the spots, the results of the DBS aged for 398 days cannot be compared accurately to the results of the DBS aged for up to 8 days. Roughly, the number of peptides and proteins identified from the DBS aged for 398 days was half compared to

DBS aged for up to 8 days when using the optimised extraction method of leaving the spots in the pre-treatment solution until digestion for the 398 days aged DBS. The detected peptides as well as the acquired spectra were found particularly low for donor 2, but this did not influence the number of proteins identified. The reason for this increased percentage of identified spectra and low number of detected peptides remains unknown. For future experiments, it is recommended to use an optimised sample treatment procedure by not removing the DBS from the sample pre-treatment solution until digestion.

2.3.2 Protein identifications

Blood comprises of 22 HAPs which make up 99% of the total protein abundance in plasma [201]. All HAPs, including the well-known albumin, immunoglobulins and haptoglobin, were also identified from DBS in this study. The dynamic range of plasma protein abundance is greater than ten orders of magnitude, which makes the detection of LAPs difficult [213]. Compared to the 10,546 proteins listed in the PPD, the maximum number of proteins identified from a single DBS in this study is 206 (global, 1% FDR). In total between 88-206 proteins and 929-2595 peptides were identified from 2946-10015 spectra per DBS sample (global, 1% FDR). Figure 2.2 shows the number of proteins identified by ProteinPilot for DBS aged for up to 8 days of one of the donors. For most donors, the number of proteins, peptides and spectra is lower for DBS extracted and digested at the day of collection (day 0) compared to DBS aged for at least a day. However, no distinct upwards or downwards trend was observed for the number of spectra, peptides or proteins identified over time for any of the donors nor for the pools of samples per DBS age.

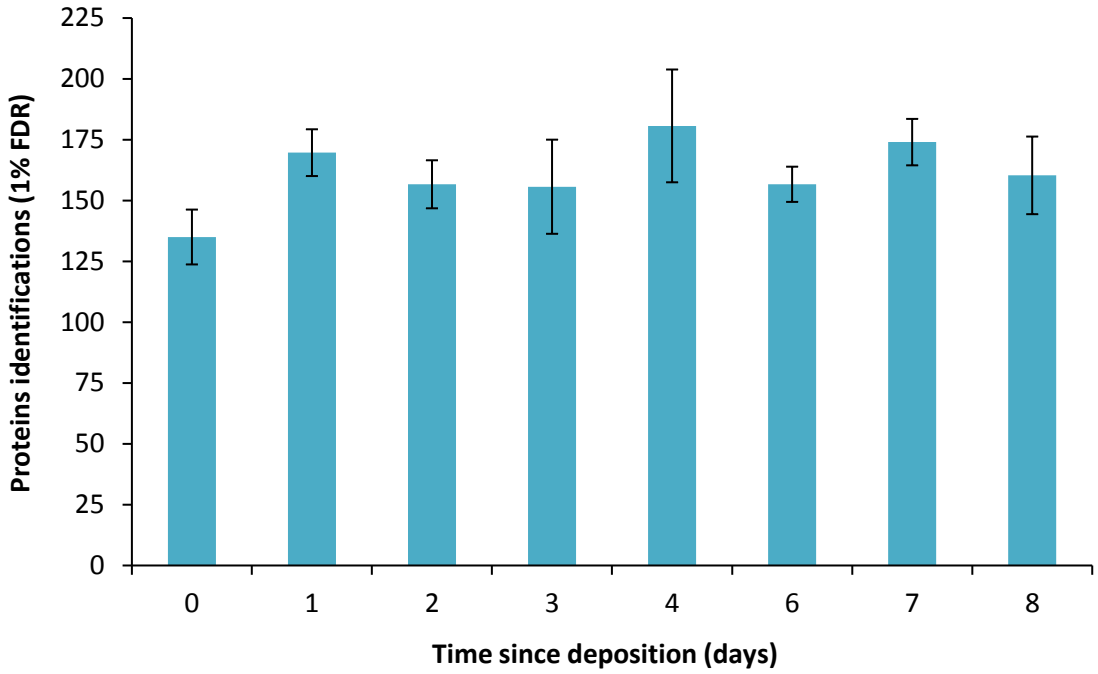

Figure 2.2. Number of identified proteins by ProteinPilot (global, 1% FDR) from DBS samples (n=3) aged for up to 8 days for one of the donors (number 4).

To get an indication if the abundance of certain proteins or peptides changes with increasing TSD, the identities of proteins detected for just 1 age and for more than 1 age were investigated. When comparing protein identifications (95% probability, minimum number of peptides set at 2) of pooled data from DBS not aged (0 days) with the pooled data of the other ages, 8 of the 221 proteins identified were found unique for day 0 and up to 13 unique protein identifications for the other ages (Table 2.2). In total, 380 unique proteins were identified with less than half (176) detected at all DBS ages. Upon inclusion of the 398 aged DBS pooled data, 393 unique proteins were identified with only 77 proteins detected at all ages and 99 for day 0 to day 8. The 13 unique protein identifications for pooled data of 398 days aged DBS comprised of 11 keratin proteins (K1C10, K1C13, K1C14, K1C16, K1C17, K2C4, K2C5, K2C6A, K2C6C, K2C73 and K22E), collagen alpha chain (CO3A1) and an immunoglobulin (IGHG1). Keratins are known as skin proteins [214], thus these might not be indicative for detecting changes related to DBS ageing. The unique proteins identified per DBS age up to 8 days of ageing could give an indication about protein changes related to DBS ageing, but could also be attributed to the low sample number.

Table 2.2. Unique proteins identified for data pooled per DBS age using ProteinPilot (95% probability, minimum number of peptides set at 2). *ID=identification*.

	TSD: 0 days	TSD: 1 day	TSD: 2 days	TSD: 3 days	TSD: 4 days	TSD: 6 days	TSD: 7 days	TSD: 8 days
Total protein ID yield	221	273	252	272	269	270	286	281
Unique protein ID yield	8	9	6	13	3	10	7	8
Unique protein names	DYSF IGHA2 LV310 LV743 LV743 RHOA T10IP TPM2	CO5 DEF1 DEF3 EPB42 HBE HV349 KV224 PRPS1 UCHL3	ACTA ACTC ACTH ACTS GMPR1 RPIA	ADDB APOF IGD IGHD LV316 LV327 MYL6P RS7 TBB2A TBB2B TBB3 TBB5 TCPB	PLSL S10A9 TNG2	BIEA ENOG IMB1 INPP KV229 KVD26 KVD29 OTU1 TBB1 UBP15	BPL1 CO7 K1C9 K2C6B KV113 KVD13 PHP14	AL9A1 CAN1 DPOLQ IGE KCY KV106 PUR6 PUR9

The relative low number of proteins identified for all DBS ages can be explained by the proteins detected for more than one age but not for every age. The various combinations of sub-overlaps could also reveal interesting trends such as proteins either less or more accessible for digestion upon multiple days of ageing. The number of unique proteins sub-overlapping a couple of ages is as low as the number of unique protein identifications for individual ages (up to 7 and 13 unique identifications respectively), which can be attributed to low sample number again. However, 22 proteins were identified for the sub-overlap of DBS ages between ≥1 and ≤8 days and 4 proteins (LDHA, IGKC, SPTB1 and A1AG2) were identified for the sub-overlap of all ages from 1 up to 398 days. Both these findings could indicate that these proteins were more denatured from the day after deposition onwards, thus more accessible for digestion. It also supports the lower yield for DBS proteins detected at the day of deposition as visualised in Figure 2.1, Table 2.1 and Table 2.2. The lower number of unique proteins for the sub-overlap of DBS aged for 398 days compared to DBS aged for up to 8 days only can be explained by the limited number of proteins recovered from the DBS aged for 398 days. To determine abundance changes of proteins over time, the next section

will not take unique identified proteins into account but will solely focus on the overlapping proteins identified for all ages.

2.3.3 Protein quantifications by spectral counting

The DBS spectra obtained with Analyst 1.7 by nano-LC-ESI-MS/MS were loaded in Scaffold Q+S 4.8.4. Multiple methods have been developed to quantify and compare protein abundances in label-free bottom-up proteomics, Blein-Nicolas and Zivy published an extensive review split up in spectral counting methods and methods that make use of extracted ion currents [215]. Both emPAI and NSAF were used as label-free spectral counting methods of the Scaffold viewer 4.0 to estimate the abundance of identified proteins that were detected for all DBS ages per donor. Percentage coverage, percentage of total spectra, peptide count, spectrum count as well as TIC values were also assessed to investigate changes in the spectra, detection of peptides and identified proteins of DBS aged for up to 8 days.

The protein abundance index (PAI) is defined as the number of identified peptides ($N_{observed}$) divided by the number of theoretically observable tryptic peptides ($N_{observable}$) for each protein (Equation 2.1) [216]. This index was later converted to its exponential form minus 1 (emPAI) (Equation 2.2) [217].

Equation 2.1

$$PAI = \frac{Nobserved}{Nobservable}$$

Equation 2.2

$$emPAI = 10^{PAI} - 1$$

Extremely high values were found for some HAPs; albumin (2667-3169), haemoglobin subunit alpha (2131-2618), haemoglobin subunit beta (1727-1907), apolipoprotein A-I (47-187), apolipoprotein A-II (35-98), transferrin (8-11) and alpha1-antitrypsin (4-13), with the ranges indicating the variation between the donors. High emPAI values were also found for some other proteins; carbonic anhydrase (5-90), peroxiredoxin-2 (9-24), flavin reductase (3-13), apolipoprotein CI (3-13), alpha-synuclein (6-12) and superoxide

dismutase (3-11). An increase in emPAI values for every donor was found for both a HAP (alpha1-antitrypsin) and LAPs (antithrombin-III, glyceraldehyde-3-phosphate dehydrogenase, hemopexin, peptidyl-prolyl cis-trans isomerase A, peroxiredoxin-1, -2 and -6, protein S100-A4, transthyretin and vitamin-D binding protein) of DBS aged for 8 days compared to the day of deposition. Decreased emPAI values were found for albumin (HAP), apolipoprotein C-III and clusterin. However, no distinct upwards or downwards trend was observed with increasing TSD for any of the proteins as visualised in Figure 2.3 for a selected donor. Additionally, ratios of emPAI values were evaluated as Inoue et al. showed that the ratio of α-chain to haem decreases after deposition when plotted on a logarithmic scale [108]. However, emPAI ratios in this study did not result in the discovery of a distinct upwards or downwards trend for any of the protein combinations with increasing TSD.

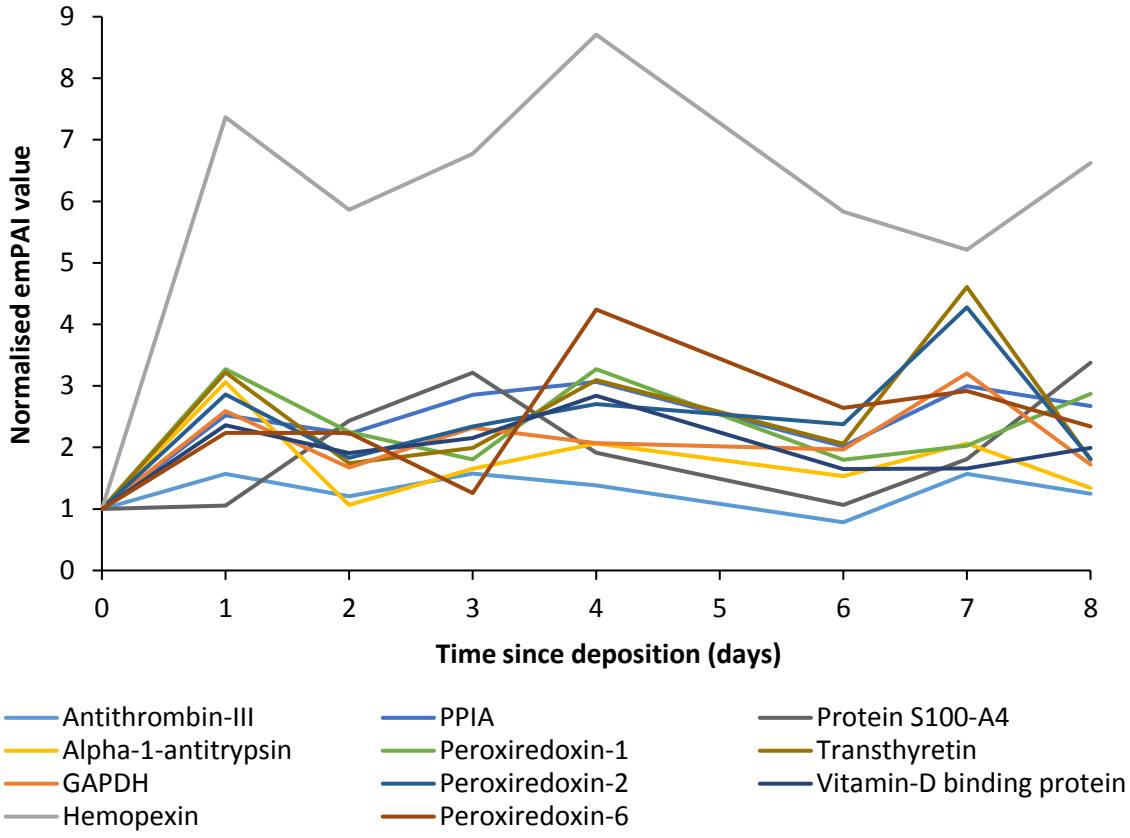

Figure 2.3. Abundance changes of DBS proteins based on emPAI values normalised to the day of deposition for one of the donors (number 4). An increase of emPAI values was detected for DBS aged for up to 8 days compared to the day of deposition, however no distinct upwards trend was detected.

Studies comparing different methods of quantifications showed that emPAI is the least accurate method and NSAF has found to be more precise [218-220]. Unfortunately, similar results were obtained using the build-in option of Scaffold viewer for the estimation of protein abundance based on NSAF compared to emPAI. The NSAF method has been introduced to compare the abundance of individual proteins in multiple independent samples and is typically applied to quantify the expression changes in various complexes [221], such as the multiple complex DBS samples in this study. The spectral abundance factor (SAF) is defined as the number of spectra (SpC) identifying a protein divided by the protein length (L) (Equation 2.3). The normalised SAF (NSAF) is calculated by normalising SAF over the total sum of SpC/L in a given analysis (Equation 2.4) [222].

Equation 2.3

$$SAF = \frac{SpC}{L}$$

Equation 2.4

$$NSAF = \frac{SAF}{\sum \mathrm{SAF}}$$

An increase in NSAF values for every donor was found for both HAPs (alpha1-antitrypsin and apolipoprotein A-I) and LAPs (carbonic anhydrase 1 and 2, hemopexin, peptidyl-prolyl cis-trans isomerase A, peroxiredoxin-1, -2 and -6 and triosephosphate isomerase) of DBS aged for 8 days compared to the day of deposition. Decreased NSAF values were found for apolipoprotein A-IV and haemoglobin subunit alpha (HAP). A distinct upwards or downwards related to the ageing of DBS was absent however.

Discrepancies in protein changes over time were found between donors. For approximately half of the proteins, an increase in emPAI values was found with increasing TSD for some of the donors whereas a decrease was found for the other donors. The same was found for NSAF values and also up to 1/3 of the proteins showed a contrary trend between emPAI and NSAF changes over time. This could be due to the fact that NSAF overestimates LAPs by overcorrecting for protein length [218, 223]. More

of such discrepancies have been found in other studies as summarised by Blein-Nicolas and Zivy [215].

The non-quantitative build-in options percentage coverage, percentage of total spectra, spectrum count and peptide count were also assessed for one of the donors to investigate changes in the spectra, detection of peptides and identified DBS proteins of different ages. Again, neither of these options showed a distinct upwards nor downwards trend related to the ageing of DBS. Figure 2.4 visualises the absolute percentage coverage of detected peptides for the proteins of one of the donors (number 1).

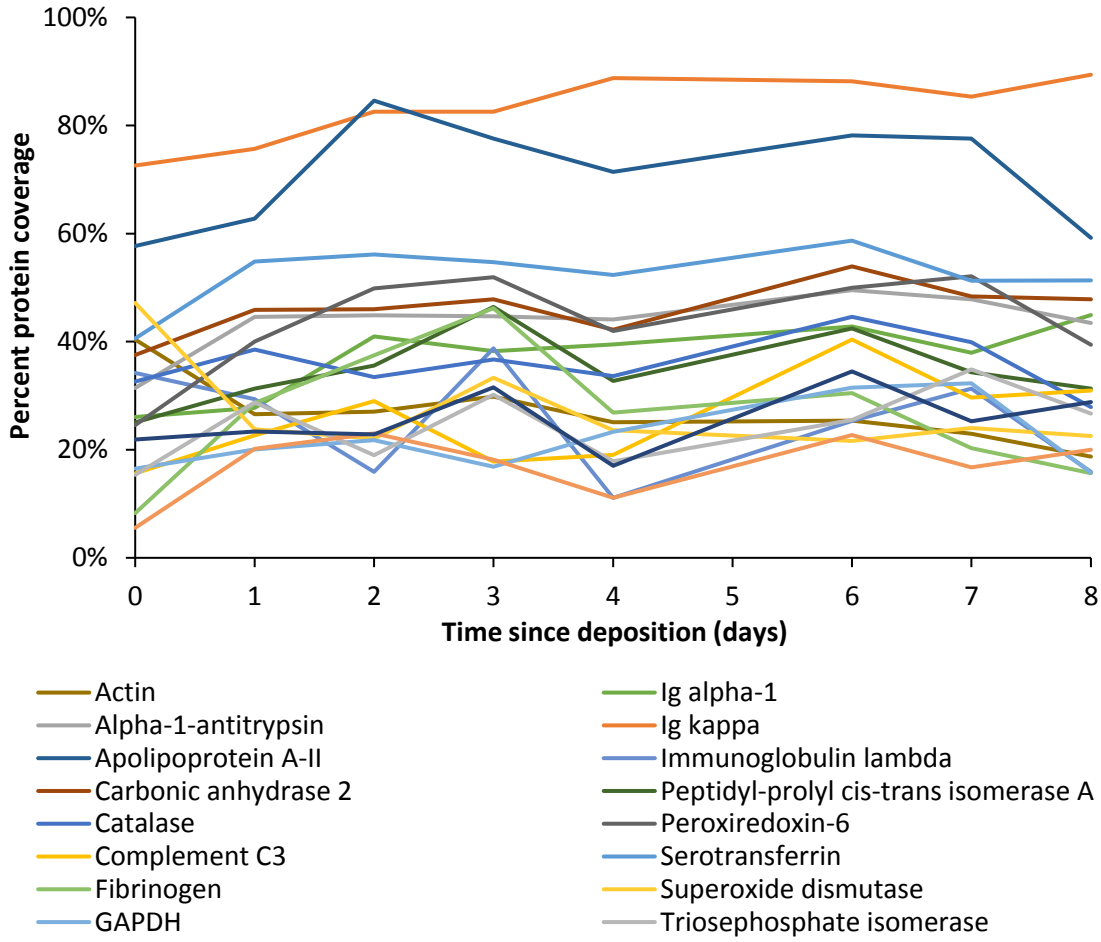

Figure 2.4. Changes in absolute percentage coverage of identified proteins from DBS aged for up to 8 days for one of the donors (number 1). Proteins with >15% changes were selected for visualisation, however no distinct upwards trend was detected for any of the identified proteins.

The coverage varied enormously (4%-100%) for the different identified proteins. The highest coverages were found for the HAPs, mainly the haemoglobin subunit alpha and

beta (94%-100%) and albumin (83%-86%). The largest differences in coverage for the different DBS ages was found for fibrinogen (8%-46%). The percentages of total spectra for identified proteins per DBS sample were much lower, with >1% only observed for the HAPs albumin and the haemoglobin subunits. The exclusive unique spectrum and peptide count also reflected the large variation in coverages, with only approximately 50% of the proteins per sample identified by >10 spectra and >10 peptides respectively.

Finally, average TIC values were explored, but again a distinct upwards or downwards trend related to the ageing of DBS was absent. The average TIC values ranged between 729-4566 for the different identified proteins in the DBS samples of the donor and could give a first indication about changes related to intensity as TIC represents the summed intensity across the entire range of masses detected. A more extensive investigation estimating average precursor intensities with the aim of detecting a trend related to the TSD of DBS is discussed next.

2.3.4 Precursor intensity evaluation

As the spectral counting methods mainly apply to HAPs, Mascot Distiller 2.7.0.0 was used to estimate average precursor intensities for all detected peptides with the aim of detecting changes in DBS related to TSD. Protein cluster analysis was performed with the normalised relative peptide intensities of DBS aged for up to 8 days, however no distinct upwards or downwards trend could be observed with increasing TSD for any of the protein clusters and neither for the individual proteins inspected. Figure 2.5 shows the 9 clusters for one of the donors (number 6), which has similarities with the clusters of the other donors. The first cluster shows increased intensities for DBS both aged for 4 and 7 days, which matched a cluster of donor 4. A single increase in intensity was seen for some of the DBS proteins aged for 6 days as shown by the second cluster of donor 6, which also matched a cluster of donor 4. The third and eighth cluster show increased intensity for DBS proteins at the day of deposition compared to DBS aged for up to 8 days. The y-axis scaling of those clusters also shows that the intensity of DBS proteins at the day of deposition was high compared to the other clusters. Similar clustering was found for donor 1, 2 and 4. Many physical and biochemical changes are known to occur upon drying of blood as discussed in Chapter 1, therefore the high intensities detected

at the day of deposition compared to the DBS aged for up to 8 days could be expected. However, the reason for the non-linear trend of increased intensities with increasing TSD remains a question. The fourth cluster shows increased intensity for DBS aged for 7 days similar to three clusters of donor 6 and of clusters of the other donors except donor 3. Donor 1, 2 and 3 all have a similar cluster as the sixth cluster of donor 6 with a sharp increase in intensity starting in DBS aged for 7 days and a further increase in DBS aged for 8 days. Donor 2 and 3 even have multiple clusters with such an increase starting from day 7 onwards. It would be interesting to examine older DBS to evaluate if a distinctive upwards or downwards trend could be observed with increasing TSD. Lastly, the seventh and ninth clusters of donor 6 show consecutive increases and decreases in intensities over time. This trend of clustering is seen multiple times for all donors, however this is however not useful for TSD predictions.

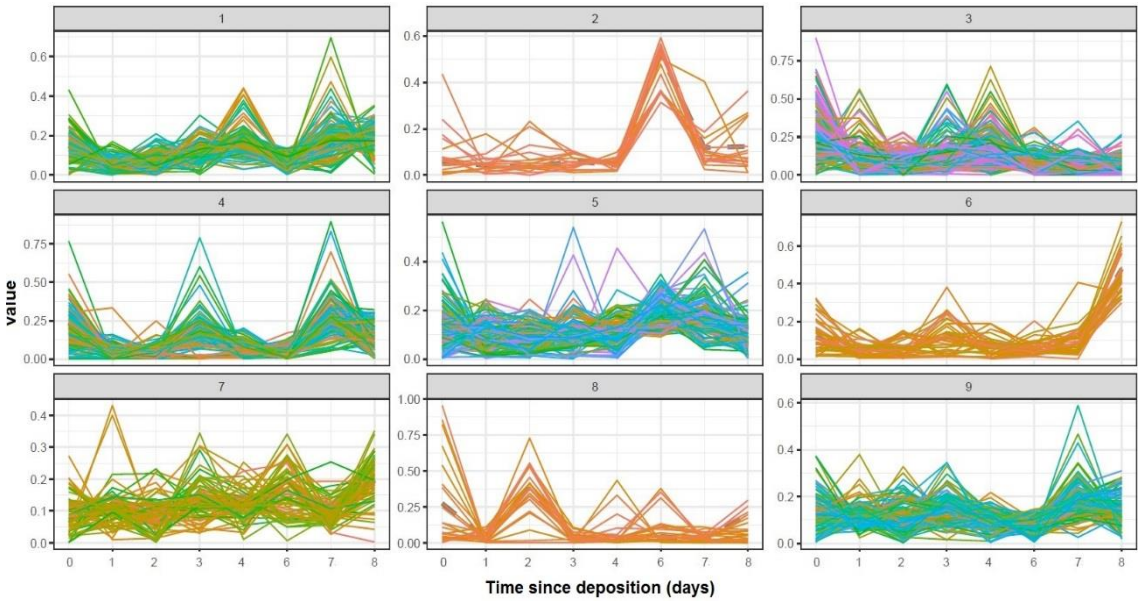

Figure 2.5. Protein clusters based on normalised relative peptide intensities of DBS aged for up to 8 days from one of the donors (number 6). The number of clusters was set to 9 with each cluster showing a different trend in time.

2.3.5 SWATH-MS analysis

DIA SWATH-MS analyses were performed to complement the IDA nano-LC-ESI-MS/MS analyses of digested proteins from DBS aged for up to 8 days. However, further method optimisation is needed as no quantitative data could be obtained with the current approach. Longer accumulation times and DBS library settings have to be assessed.

2.4 Concluding remarks and future perspectives

A bottom-up proteomics approach was used to digest DBS proteins and the resulting peptides were analysed using nano-LC-ESI-MS/MS. Instrument performance and method repeatability were found to be good (89.1%-96.6%). Up to 2595 peptides and 206 proteins were identified from a single DBS. A total of 8 unique identified proteins was found in the pooled data of DBS samples aged for 0 days and up to 13 for DBS aged for up to 8 days. The extraction of proteins from DBS aged for 398 days posed difficulties, but 13 unique proteins were identified in those samples compared to DBS aged for up to 8 days. This indicated that there is a potential to detect short-term and longer-term biomarkers to estimate the TSD of DBS.

No distinct upwards or downwards trends related to the ageing of DBS was found based on the number of spectra, peptides or proteins identified over time for any of the donors or for the pools of samples per DBS age. Neither were distinct upwards or downwards trends related to the ageing of DBS found by using various label-free methods for the quantification of proteins from the spectral data. Individual emPAI values, ratios of emPAI values and NSAF values did not result in the discovery of a distinct upwards or downwards trend for any of the identified proteins with increasing TSD. A non-quantitative investigation by percentage protein coverage, percentage of total spectra, spectrum count, peptide count and TIC values was performed for one of the donors to investigate changes in the spectra, detection of peptides and identified DBS proteins of different ages. Again, these options did not show a distinct upwards nor downwards trend related to DBS ageing either. The cluster analyses based on estimated precursor intensities showed various trends for identified proteins of DBS aged for up to 8 days, however no distinct upwards or downwards trend was observed which could be used to predict the TSD of DBS.

The spectral counting approaches mainly resulted in the quantification of HAPs. It would be interesting to either enrich LAPs from DBS or to deplete HAPs as no useful profile has been unravelled to determine the TSD of DBS. The HAPs could have masked interesting changes of LAPs using the spectral counting approaches and the precursor intensity approach might not have been suitable to detect changes in LAPs if HAPs were bound to or interacted with the LAPs. Rassi et al. systematically reviewed liquid-phase

based separation systems for depletion, prefractionation and enrichment of proteins in biological fluids and matrices for in-depth proteomics analyses. The first review covered more than 90 papers published between 2000-2008 [224], 98 papers published between 2008-2011 were additionally reviewed a few years later [225], the next update covered an additional 77 papers published between 2011-2014 [226] and the latest update from 2017 added more than 70 papers [227]. To highlight a few developments, the most abundant protein albumin has been depleted by many methods such as affinity antibodies, salt precipitation and size exclusion [228], but albumin has also been subjected to enrichment procedures [229]. The first methods were only targeted to one abundant protein and had low sensitivity and co-depletion due to protein carrier effects, but more recently a couple of commercial kits have become available to remove multiple HAPs from samples. The kits are based on antibody- and ligand-based affinity methods and have been applied in proteomics studies [226, 230]. A study comparing six available kits showed an increase of proteins being detected compared to non-depleted samples [231].

For future research, a small pilot study was performed with a multi-affinity removal system (MARS) from Agilent Technologies UK Ltd (Stockport, UK). The MARS which was used can deplete 14 HAPs making up 94% of protein mass [232]. A total of 107 and 137 proteins were identified for two donors tested, compared to the 88-206 proteins detected in DBS samples without HAP depletion (section 2.3.2). An interesting additional observation was that the number of identified proteins increased (from 99 to 138 for one donor and from 85 to 132 for the other donor) by using the MARS buffer instead of conventional NH_4HCO_3 solvent (section 2.3.2) for the extraction of DBS without HAP depletion. The number of detected peptides remained similar with 1806 versus 1823 peptides for one donor and 1667 versus 1771 peptides for the other donor.

Chambers et al. investigated the stability of 169 peptides corresponding to 97 proteins in DBS on cards and found the stability to be >95% after 2 days at -20 °C, 4 °C, room temperature and 37 °C [162]. The percentage of stable peptides was between 81%-84% after 7 days, between 72%-80% after 16 days, between 72%-76% after 29 days, between 65%-72% after 77 days and between 52%-66% after 154 days across the different temperatures. In this thesis, differences were also found for proteins and peptides over time. However, no linear trend was detected that is suitable to predict

the TSD of DBS. Chambers et al. used stable isotope-labelled standard peptides in their study for quantification, which is a recommendation for future studies investigating protein changes in bloodstains as the label-free quantification approaches in this thesis were rendered not suitable.

Finally, the spotting of blood onto other surfaces would also be interesting in future studies for both a forensic perspective as well as the potential to reduce the stability of DBS proteins. By depletion of HAPs or enrichment of LAPs from DBS, the use of peptide markers and by exploring other matrices for the deposition of micro-volumes of blood, a molecular profile of DBS age could be established. This profile would increase the understanding of proteomic changes underlying the ageing of bloodstains and could lead to a method for predicting the TSD of bloodstains.

3 Speeding up digestion of proteins from dried blood spots

Immobilised-enzyme reactor consisting of an aluminium holder with NanoPort connections (left) and microfluidic channel (right).

This Chapter is based on B. Wouters, I. Dapic, T.S.E. Valkenburg, S. Wouters, L. Niezen, S. Eeltink, G.L. Corthals, P.J. Schoenmakers, A cyclic-olefin-copolymer microfluidic immobilised enzyme reactor for rapid digestion of proteins from dried blood spots, Journal of Chromatography A, 1491 (2017) 36-42 [233].

Statement of originality: B.W. developed the reactor of which I.D. tested its performance with protein standards. T.S.E. Valkenburg tested the application of dried blood spots, which is presented in this thesis. S.W., L.N. and S.E. helped with the design of the reactor. G.L.C. and P.J.S. proof-read the manuscript and supervised the study.

This study took place during a secondment at the University of Amsterdam (Amsterdam, the Netherlands). Special thanks go to Prof. Ron Peters (University of Amsterdam and DSM Coating Resins, Waalwijk) and Dr. Wim Genuit (Shell Technology Centre Amsterdam) for their contributions during scientific discussions. Prof. Gert Desmet (Free University of Brussels, Department of Chemical Engineering) is gratefully acknowledged for use of the micromilling facility. Petra J. Jansen (University of Amsterdam, Van 't Hoff Institute for Molecular Sciences) is gratefully acknowledged for her experimental assistance. Further support of this work by a grant of the Netherlands Organization for Scientific Research (NWO) in the framework of the Programmatic Technology Area PTA-COAST3 of the Fund New Chemical Innovations (project C.2322.0291) is gratefully acknowledged.

3.1 Introduction

Mass spectrometry (MS) has become an indispensable tool for large-scale proteome analysis. In almost all workflows, proteins are extracted from their environment by a sample specific procedure. After this they are often denatured before performing a reduction and/or alkylation step, which is immediately followed by enzymatic digestion that leads to a complex peptide mixture. The entire process typically takes up to 24 hours. Following digestion, the peptide mixture is commonly separated by liquid chromatography (LC) and analysed by MS or tandem mass spectrometry (MS/MS) [234]. Enzymatic digestion of proteins is a critically important step in sample preparation prior to MS analysis. It is usually performed in solution by mixing a proteolytic enzyme e.g. trypsin, Lys-C or chymotrypsin with proteins in a specific ratio, typically between 1:100 and 1:20 [235]. The digestion is conventionally carried out overnight, and as such remains a bottleneck for high-throughput analysis [208, 236, 237]. Numerous protocols have been reported to accelerate digestion, including the use of elevated temperatures and pressures, microwave and infrared irradiation, ultrasound, microspin columns, and solvent-facilitated digestion. These methods may significantly reduce digestion times to a range of several hours to 30 seconds [238-240], yet 18 hours remains the most commonly used digestion duration. However, these methods still suffer from disadvantages such as the inability to reuse (costly) enzymes and challenges or incompatibility with automated or in-line LC-MS workflows [241].

Immobilised-enzyme reactors (IMERs) offer a principle that is fundamentally different from in-solution digestion and subsequently lead to several advantageous characteristics. First, enzymes are immobilised in a confined space, allowing much higher enzyme-to-protein ratios owing to the prevention of auto-digestion [242]. Secondly, shorter diffusion distances lead to shorter digestion times in the order of minutes to seconds [243, 244]. Finally, the immobilised enzymes are typically more stable than free enzymes [245]. Enzymes can be immobilised through matrix entrapment and/or encapsulation, adsorption through hydrogen bonds, hydrophobic interactions, ionic bonds, or by covalent bonding. The surface of an open microfluidic channel can be used as a substrate for enzyme immobilisation [246, 247]. However, this approach offers a very small surface-to-volume ratio. Therefore, immobilisation on

membranes [248, 249], particles [250] or porous monolithic structures [251, 252] is typically preferred.

In this study, a cyclic-olefin-copolymer (COC) microfluidic reactor containing trypsin immobilised on a polymer monolithic material was constructed. COC was chosen owing to its low material costs, compatibility with mass replication methods, chemical resistance to a wide range of solvents and chemicals, and good transparency in both the ultraviolet and visible-light regions [253]. The IMER was tested for the rapid offline digestion of both singular protein standards and a complex protein mixture obtained from dried blood spots (DBS). The effect of a range of IMER residence times and protein concentrations on protein-sequence coverage, number of identified proteins and number of missed cleavages was assessed for singular proteins of varying molecular weight from 11 to 240 kDa. The effect of omitting workflow steps and decreasing conventional digestion time on the number and type of identified proteins was assessed for DBS analysis using the developed IMER. As speed is a key issue in many settings including forensic scenarios, the use of an IMER may offer a solution for shortening forensic proteomic analyses such as for the DBS ageing study presented in Chapter 2.

3.2 Experimental design

3.2.1 Chemicals and materials

Acetonitrile (ACN, LC-MS grade), formic acid (FA, ULC/MS - SFC-CC grade, 99%) and water (ULC/MS - CC/SFC) were purchased from Biosolve (Valkenswaard, the Netherlands). Albumin from bovine serum (BSA, ≥ 96%), albumin from chicken egg white (OVA, ≥ 98%), aluminium oxide (Al_2O_3), ammonium bicarbonate (NH_4HCO_3, BioUltra, ≥ 99.5%), 4,4’ bis(diethylamino) benzophenone (DEBP, > 99%), t-butanol (American Chemical Society reagent, ≥ 99%), 1,4-butanediol (ReagentPlus quality, ≥ 99%), butyl methacrylate (BMA, 99%), calcium chloride dihydrate ($CaCl_2$, American Chemical Society reagent, ≥ 99%), α-casein from bovine milk (CAS, ≥ 70%), catalase from bovine liver (CAT), cytochrome C from equine heart (CYC, ≥ 95%), 2,2-dimethoxy-2-phenylacetophenone (DMPA, 99%), dithiothreitol (DTT, ≥ 99.0%), Empore C18 solid-phase extraction cartridges (SPE cartridges, 4 mm/1mL), ethanolamine (> 98%), ethylene glycol diacrylate (EDA, 90%, technical grade), ethylene glycol dimethacrylate

(EDMA), iodoacetamide (IAA, ≥ 99%), methanol, methyl methacrylate (MMA, 99%), myoglobin from equine heart (MYG, ≥ 90%), poly(ethylene glycol) methacrylate (PEGMA, number-average molar mass M_n 500 g/mole), 1-propanol (≥ 99.8%), sodium deoxycholate (SDC, BioXtra, ≥ 98%), transferrin from human serum (THS), trifluoroacetic acid (TFA, ≥ 99%), tris(2-carboxyethyl)phosphine hydrochloride solution (TCEP, 0.5 M, pH7), tris(hydroxymethyl)aminomethane hydrochloride (Tris-HCl), trypsin (European Pharmacopoeia (EP) reference standard) and Whatman Human ID Bloodstain Cards BFC 180 were purchased from Sigma-Aldrich (Zwijndrecht, the Netherlands). BMA and EDMA were passed over activated basic alumina to remove hydroquinone inhibitors. Other monomers were used as received. Contact-activated lancets were purchased from Becton Dickinson (Breda, the Netherlands). Hydrochloric acid (HCl, 37% in water) was purchased from Acros Organics (Geel, Belgium). Sodium hydroxide (NaOH, American Chemical Society reagent, ≥ 97.0%) was purchased from Merck (Hohenbrunn, Germany). TOPAS cyclic-olefin-copolymer substrate material (grade 8007) was purchased from Kunststoff-Zentrum Leipzig (Leipzig, Germany). 2-Vinyl-4,4-dimethylazlactone was purchased from Pure Chemistry Scientific (Watertown, MA, US). Water was purified in-house using an Arium 611 UV water-purification system (Sartorius, Göttingen, Germany).

3.2.2 Assembling of a microfluidic immobilised-enzyme reactor

Channel layouts for the microfluidic reactor were designed in AutoCAD (Autodesk, San Rafael, CA, US) and machined using a computer-controlled micromilling robot (Datron M7 Compact, Mühltal, Germany). Ball-nose end mills were used to machine semi-circular channels in each of the two COC layers. Subsequently, the layers were cleaned with 2-propanol followed by solvent-vapour-assisted bonding to seal the channels. During the bonding process, the top layer was positioned above a reservoir of cyclohexane and exposed to solvent vapour for 5.5 minutes. After aligning the two layers, they were pressed together for 10 minutes by applying 2.5 kN of force. The applied procedure was based on a previous study [254]. Finally, holders were manufactured in-house, consisting of two aluminium plates bolted together with

controlled torque, connecting the reactor with flat-bottom NanoPort connections (Upchurch Scientific, Oak Harbor, WA, US) for 360 µm o.d. capillary fused-silica tubing.

A multi-step enzyme-immobilisation procedure was adapted from Logan et al. [255]. First, for surface modification of COC and *in-situ* polymerisation the empty microfluidic channel was flushed with acetone and dried with a flow of nitrogen gas. A mixture of DEBP, EDA and MMA (0.1, 49.95, and 49.95%, by weight, respectively) was introduced into the channel which was then exposed to 365-nm UV light for 4 minutes (XL-1500 UV Crosslinker, Distrilab, Leusden, the Netherlands). The reactor was again flushed with acetone and dried with a flow of nitrogen gas. A homogeneously stirred and degassed polymerisation mixture of BMA (24% by weight), EDMA (16%), 1,4-butanediol (32%), 1-propanol (28%) and DMPA (10 mg per gram of monomers) was then introduced into the reactor and exposed to UV irradiation (365 nm, 10 min), yielding the polymer monolithic material. Subsequently, the reactor was flushed with methanol (overnight, 10 µL/min).

Second, for the photografting of PEGMA and 2-vinyl-4,4-dimethylazlactone a 5% solution by weight of DEBP in methanol was pumped through the reactor (30 min, 0.5 µL/min) using a syringe pump (KDS 210 model, KD scientific, Zoeterwoude, the Netherlands), followed by UV irradiation (365 nm, 2 min) and a washing step with methanol (20 min, 0.5 µL/min). Subsequently, a solution of 0.1 M PEGMA in water was pumped through the reactor (30 min, 0.5 µL/min). The reactor was then irradiated (365 nm, 2 min) and flushed with water (overnight, 0.5 µL/min). A solution of 2-vinyl-4,4-dimethylazlactone was photografted on the polymer substrate by flushing the reactor with a mixture (15% by weight) and DEBP solution (0.22%) in 75:25 (% by weight) t-butanol/water solution, exposing the reactor to UV irradiation (365 nm, 5 min) and flushing with acetone (1h, 0.5 µL/min).

Third, trypsin was immobilised on the polymer monolithic material by flushing a 2000 mg/L trypsin solution in 50 mM Tris HCl containing 20 mM $CaCl_2$ (pH = 8) through the reactor (2 h, 0.5 µL/min), followed by 1 M ethanolamine (1 h, 0.5 µL/min) to quench unreacted azlactone groups and finally a 50 mM Tris HCl, 20 mM $CaCl_2$, (pH = 8.0) buffer solution (1 h, 1.0 µL/min). The reactor was stored at 4°C until further use.

3.2.3 Sample preparations

Stock protein solutions (1000 mg/L) of proteins (α-S1 casein, bovine serum albumin, catalase, cytochrome c, myoglobin, ovalbumin and transferrin) were prepared in 50 mM Tris-HCl containing 20 mM $CaCl_2$ (pH = 8.0) for IMER-facilitated digestion and with the addition of 6 M urea for in-solution digestions. A range of concentrations was obtained by subsequent dilution. Prior to in-solution digestion, 5 µL of DTT (200 mM in 25 mM NH_4HCO_3) was added to 300 µL of protein solution and samples were reduced for 1 hour at 37 °C. Samples were then alkylated with 20 µL of IAA (200 mM in 25 mM NH_4HCO_3) for 1 hour in the dark at room temperature and subsequently an additional 20 µL of DTT was added. Samples were diluted with 50 mM Tris HCl containing 20 mM $CaCl_2$ to bring the urea concentration below 1 M.

DBS were created by the collection of capillary blood from the fingertip of a healthy male donor using a contact-activated lancet at the University of Amsterdam (Amsterdam, the Netherlands). The first drop of blood was wiped away and 10 µL of blood was spotted directly in triplicate onto a bloodstain card. Blood spots were left to dry for 2 hours in freely circulating air in the dark at room temperature, cut out and placed into 2 mL Eppendorf tubes. The method for the preparation of samples is adapted from the method developed by Chambers et al. [209]. For the extraction of blood and its proteins from the cards, 800 µL of 25 mM NH_4HCO_3 was added and samples were vortexed for 5 minutes at 1400 rpm. Some of the DBS samples received a pre-treatment prior to digestion. First, proteins were denatured by adding 100 µL of 10% SDC and 10 µL of 0.5 M TCEP followed by incubation for 1 hour at 60 °C. Next, 52 µL of 200 mM IAA was added and the samples were alkylated for 1 hour in the dark at room temperature. To consume any remaining IAA, 55.4 µL of 200 mM DTT was added, followed by incubation for 30 minutes at 37 °C. Adjusted volumes were added when working with aliquots of the extracted DBS protein solution. Figure 3.1 shows how DBS were aliquoted to study the effects of pre-treatment on digestion performance.

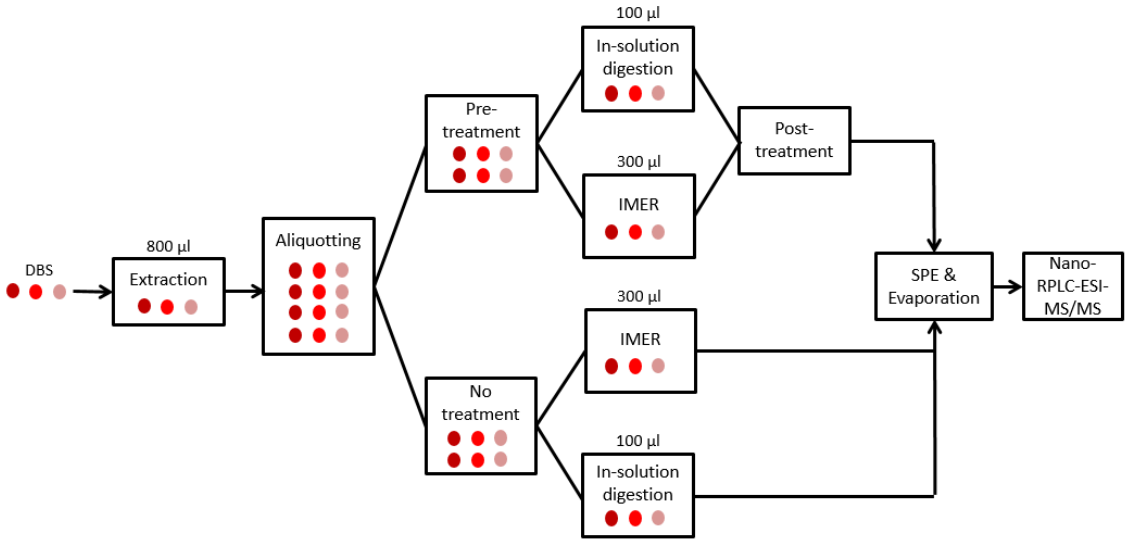

Figure 3.1. After extraction of DBS and its proteins from cards, each of the triplicate DBS (visualised with the three different shades of red) was aliquoted and prepared as shown.

Samples that were pre-treated received a post-treatment after digestion by addition of 40 µL of 2% FA to precipitate SDC, followed by centrifugation at 4000x*g* for 20 minutes and collection of supernatant for desalting using Empore C18 SPE cartridges, also according to the method of Chambers et al. [209].

3.2.4 IMER-facilitated digestion

Protein solutions were introduced into the reactor using a syringe pump at set flow rates, allowing to control the residence time in the IMER. Digested samples were collected after discarding the first two reactor volumes. After each digestion, the reactor was flushed with 15 reactor volumes of 50 mM Tris HCl containing 20 mM $CaCl_2$ (pH = 8.0) buffer solution.

3.2.5 In-solution digestion

To compare the performance of IMER-facilitated digestion to conventional digestion, in-solution digestions were performed with similar or aliquots of the samples that underwent IMER-facilitated digestion. Trypsin was added to the singular protein standards with an enzyme-to-protein ratio of 1:30. Samples were incubated at 37 °C for 18 hours and 45 µL of 5% TFA was added next to stop digestion. For digestion of DBS

proteins, 3.5 µL of trypsin (1000 mg/L) was added and samples were incubated at 37 °C for 18 hours.

3.2.6 Nano-LC-ESI-MS/MS analysis

Digested DBS samples were evaporated to dryness, stored at -20 °C and reconstituted in water prior to nano-liquid chromatography - electrospray ionisation - tandem mass spectrometry (nano-LC-ESI-MS/MS) analysis. Samples were loaded onto an Eksigent trap column (nano LC trap set, ChromXP C18, 120 Å, 350 µm i.d.) and desalted at 2 µL/min for 10 minutes with 3% ACN and 0.1% TFA. After desalting, peptides were separated on an in-house packed analytical column (Magic C18 resin, 100 Å pore size, 5 µm particles, 75 µm i.d., 100 mm column length) at 300 nL/min. Peptides were eluted using a 60 minutes long gradient composed of solvent A (0.1% FA in H_2O) and solvent B (0.1% FA in ACN). The 60 minutes gradient ran from 5% to 40% B (0-45 min), 40% to 100% B (45-50 min), 100% B (50-59 min), and 100% to 5% B (59-60 min). A selected digested DBS sample was eluted with the elongated gradient of 94 minutes presented in Chapter 2, which ran from 5% to 45% B (0–90 min), 45% to 90% B (90–92 min) and was kept at 90% B (92-94 min). To minimize carryover, a 14 minute washing step was applied at the end of the chromatographic methods, which ran from 40% to 100% B (1-5 min) and was kept at 100% B (6-14 min). Re-equilibrations of the columns followed with solvent A during sample injection and loading. Eluted peptides were analysed using an Eksigent Ekspert nanoLC 425 system (Sciex, Singapore) coupled to a nano-ESI interface installed on a TripleToF 5600+ MS (Sciex, Singapore) and spectra were acquired in information dependent acquisition (IDA) and high sensitivity mode. Time-of-flight MS (ToF-MS) scans were performed in the mass range *m/z* 400-1250 Da and the top 30 precursor ions with charge states from +2 to +4, exceeding a threshold of 100 cps, were selected for MS/MS analysis. Product-ion spectra were formed using collision-induced dissociation in rolling-collision-energy mode and collected across the mass scan range *m/z* 100-1800 Da. Both the nanoLC and TripleToF 5600+ instruments were operated using Analyst 1.7 (Sciex, Singapore).

3.2.7 Data analysis

Proteins were identified by ProteinPilot 5.0 (Sciex, Singapore) using identification at 1% false-discovery rate (FDR). Results for protein standards were obtained by searching against the Uniprot sprot database (www.uniprot.org), DBS results were searched against Uniprot human database. For IMER-digested samples, trypsin was chosen as a digestion enzyme without prior cysteine alkylation. For in-solution digestion, trypsin was also selected as the digestion enzyme and iodoacetamide as the alkylation reagent. Both molecular weights (MW) and isoelectric points (pI) were retrieved using the Expasy website tool [256] and the grand average of hydropathy (GRAVY) indices were calculated using the GRAVY calculator [257].

3.3 Results

3.3.1 Prototyping of the microfluidic IMER

The developed microfluidic device consisted of microchannel with a 300 µm diameter circular cross-section and a channel length of 60 millimetres. Assuming a complete conversion of monomers to polymer, the porosity of the polymer-monolithic support in the microchannel was approximately 60% and the interstitial volume of the reactor was 2.8 µL.

3.3.2 Evaluation of IMER-facilitated digestion of protein standards

To evaluate IMER-facilitated digestion offline, α-S1 casein digestion was performed at room temperature with varying protein concentrations (1, 5, 10, 25, 50, 75, and 100 mg/L) using an IMER residence time of 59 seconds. No denaturation or protein pre-treatment was used prior to IMER-facilitated digestion. Figure 3.2 shows the relation between α-casein protein concentration and α-S1 casein sequence coverage and the number of identified peptides for both IMER-facilitated and in-solution digestion. Generally, IMER-facilitated digestion resulted in a higher sequence coverage compared to overnight in-solution digestion. For α-S1 casein concentrations higher than 25 mg/L, IMER-digested samples resulted in sequence coverages of 75-80%, while in-solution digested samples resulted in sequence coverages of 72-76%. For α-casein concentrations lower than 25 mg/L, in-solution digestion resulted in a low number of

identified peptides and sequence coverage, which might be attributed to insufficient sensitivity or a matrix-related effect. Overall, an increase in α-S1 casein concentration resulted in a higher number of identified peptides both for IMER-facilitated and in-solution digestion.

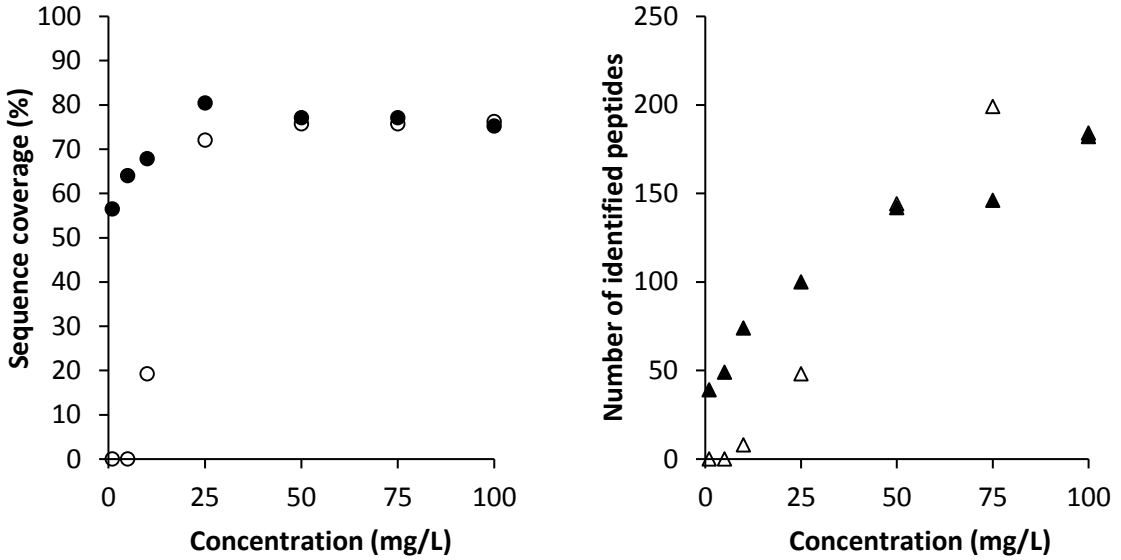

Figure 3.2. Sequence coverage (left) and number of identified peptides (right) obtained for different α-S1 casein concentrations using IMER-facilitated (solid symbols) or in-solution (open symbols) digestion. IMER-facilitated digestion was performed without pre-treatment for 59 seconds at room temperature. In-solution digestion was performed after protein pre-treatment, for 18 hours at 37 °C.

The efficiency of the IMER was assessed for digestion of 100 mg/L α-S1 casein with varying residence times; 39, 47, 59, 78, 117, 167 and 293 seconds. The shortest residence time of 39 seconds resulted in 81% sequence coverage for α-S1 casein with 196 assigned peptides. In comparison, overnight in-solution digestion resulted in a sequence coverage of 76% and 182 identified peptides. Pressure limitations of the syringe pump (KDS 210, KD Scientific Inc, 107 bar), syringe (1 mL Model 1001 TLL SYR, Hamilton, 14 bar), and connection between the syringe and the capillary tubing leading to the reactor (PEEK Luer Adapter 10-32 Female to Female Luer, 3 bar) limited the flow rate to 5 µL/min thereby preventing a decrease in IMER residence time below 39 seconds. Increasing the IMER residence time above 293 seconds did not result in an increased sequence coverage or a higher number of identified peptides.

In order to assess the repeatability of IMER-facilitated digestions, the same digestion was performed 9 times using the same reactor. For α-S1 casein with a concentration of 100 mg/L and an IMER residence time of 59 seconds, the average sequence coverage was 84% with a relative standard deviation (RSD) of 6%. In comparison, the average of 9 in-solution digestions resulted in a sequence coverage of 78% with a RSD of 4%. The average number of identified peptides after IMER-facilitated digestion was 195 (with a RSD of 15%) compared to 193 (with a RSD of 12%) for the average of 9 in-solution digestions. The number of peptides resulting from missed cleavage sites was 24% of the total number of identified peptides for both the average of 9 IMER-facilitated digestion (with a RSD of 15%) and in-solution digestion (with a RSD of 6%) repeats. Also, similar performances of the IMER for the digestion of α-S1 casein were observed after a week. Therefore, three IMERs were created and each used for one week at a time during this study. The batch-to-batch reproducibility for α-S1 casein was found to be 79% (with a RSD of 2.6%) for sequence coverage and 175 (with a RSD of 4.6%) for the number of identified peptides. Long-term tests have to be performed in future studies.

Finally, IMER-facilitated digestion was compared to overnight in-solution digestion for proteins with different MW; cytochrome c (11.7 kDa), myoglobin (17 kDa), α-S1 casein (23 kDa), ovalbumin (42.8 kDa), bovine serum albumin (66.5 kDa), transferrin (75.2 kDa), and catalase (240 kDa), as shown in Figure 3.3. The proteins were digested in the IMER at room temperature for 293 seconds and no protein pre-treatment was performed. IMER performance in terms of sequence coverage was slightly better than in-solution digestion for the proteins with a lower MW (cytochrome c, myoglobin, α-S1 casein and ovalbumin). Sequence coverages for IMER-facilitated digestions were lower than in-solution digestion for proteins with a higher MW (55% versus 95% for bovine serum albumin, 56% versus 78% for transferrin and 75 versus 88% for catalase). Both the size and the higher number of disulphide bridges in these proteins may be shielding cleavage sites from the digestion enzyme as no reduction and/or alkylation was performed prior to digestion.

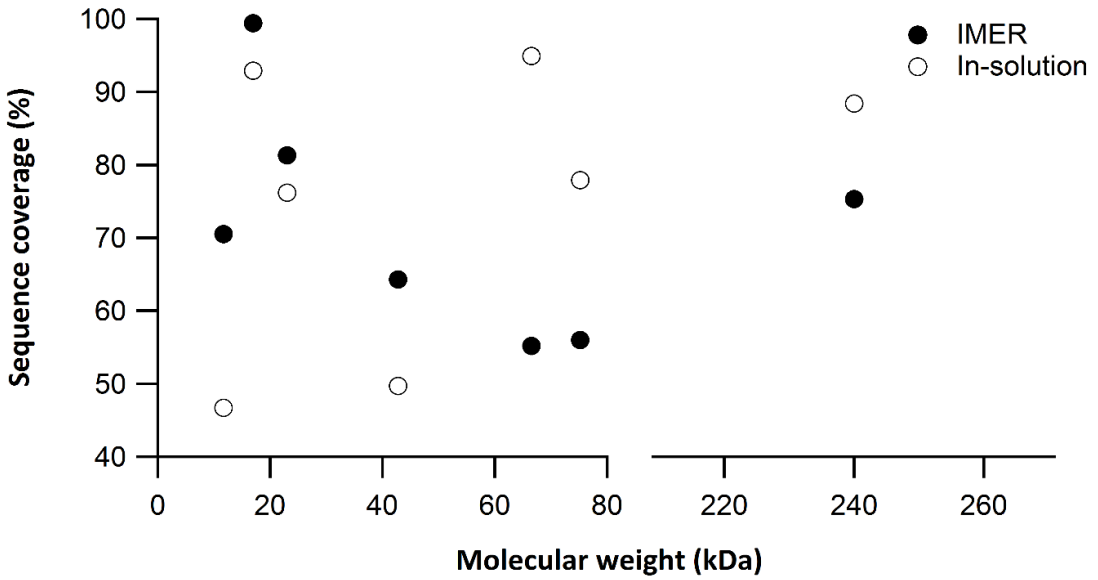

Figure 3.3. Sequence coverage obtained for proteins (100 mg/L) with different weights digested using IMER (solid circles) or in-solution (open circles). Sequence coverage was slightly better with IMER for proteins in the lower MW range, cytochrome c (11.7 kDa), myoglobin (17 kDa), α-S1 casein (23 kDa) and ovalbumin (42.8 kDa), but lower than in-solution digestion for proteins in the higher MW range, bovine serum albumin (66.5 kDa), transferrin (75.2 kDa) and catalase (240 kDa). IMER-facilitated digestion was performed without pre-treatment for 59 seconds at room temperature. In-solution digestion was performed after protein pre-treatment, for 18 hours at 37 °C.

All data underlying the Figures, the IMER repeatability data and further data concerning missed cleavages can be found in the Supplementary data appendix of Wouters et al. [233].

3.3.3 Application of the IMER to digest proteins from DBS

Although similar sequence coverage and number of identified peptides were observed for IMER-facilitated digestion of α-S1 casein with the shortest residence time compared to longer residence times, a longer residence time of 5.6 minutes was used for the digestion of DBS proteins as DBS comprises of a complex mixture of proteins and lower sequence coverage was observed for singular protein standards with higher MW. The effect of pre-treatment steps (denaturation, alkylation, reduction) prior to digestion was investigated. Table 3.1 shows that the number of identified proteins was higher for in-solution digestion with pre-treatment compared to almost zero for samples without sample pre-treatment, whereas IMER-facilitated digestion without sample pre-treatment resulted in a higher number of identified proteins. IMER-facilitated digestion

of singular protein standards was performed without pre-treatment, because pre-treatment chemicals negatively impact the activity of the immobilised enzymes (and prevent repeated use of the IMER) which was supported by these DBS results. The same 60 minutes nano-LC-ESI-MS/MS gradient was used for both the analysis of digested singular protein standards and for the analysis of digested DBS proteins, However, when using the 94 minutes nano-LC-ESI-MS/MS gradient of Chapter 2 for the analysis of a DBS sample digested with the IMER without pre-treatment, a higher number of identified proteins was found compared to the 60 minutes gradient used for this study (147 versus 111 respectively). However, this does not influence the results presented here regarding the effect of pre-treatment and IMER performance.

Table 3.1. Effect of sample pre-treatment (denaturation, alkylation, reduction) on the number of identified proteins from DBS samples using IMER-facilitated digestion and in-solution digestion (n=3, aliquoted as shown in Figure 3.1).

	DBS #1	DBS #2	DBS #3	Average
In-solution digestion with pre-treatment	110	122	124	119
IMER-facilitated digestion with pre-treatment	50	34	31	38
In-solution digestion without pre-treatment	3	3	4	4
IMER-facilitated digestion without pre-treatment	114	107	93	107

The identified proteins for the in-solution digestion with pre-treatment and IMER without pre-treatment were compared in terms of MW, pI and GRAVY index. Figure 3.4 shows that the identified proteins displayed a similar MW distribution. The majority of the proteins was distributed in the region of 10-20 kDa, followed by proteins in the region of 20-60 kDa. The similarity in distribution of proteins with higher MW is worth mentioning as a lower sequence coverage was found for singular protein standards with a higher MW (66.5, 75.2 and 240 kDa) digested with IMER compared to in-solution.

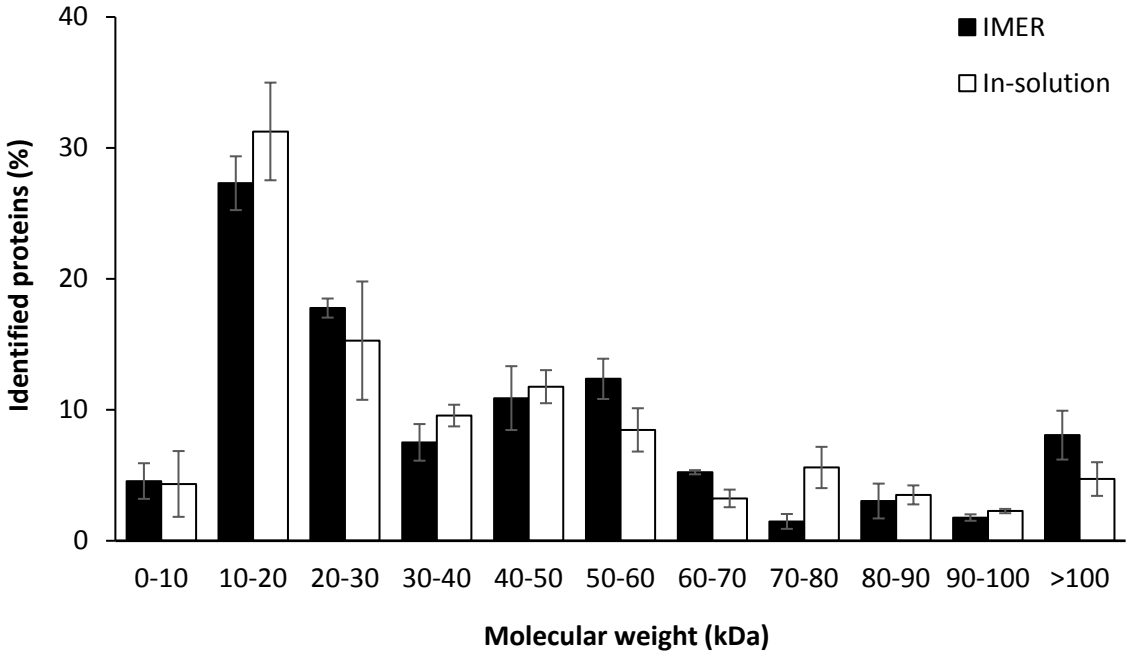

Figure 3.4. Molecular weight distribution of identified proteins from DBS extracts (n=3). IMER-facilitated digestions were without pre-treatment and in-solution digestions with pre-treatment.

A similar distribution was also found for the pI of identified proteins extracted from DBS and digested with IMER without pre-treatment and in-solution with pre-treatment as shown in Figure 3.5.

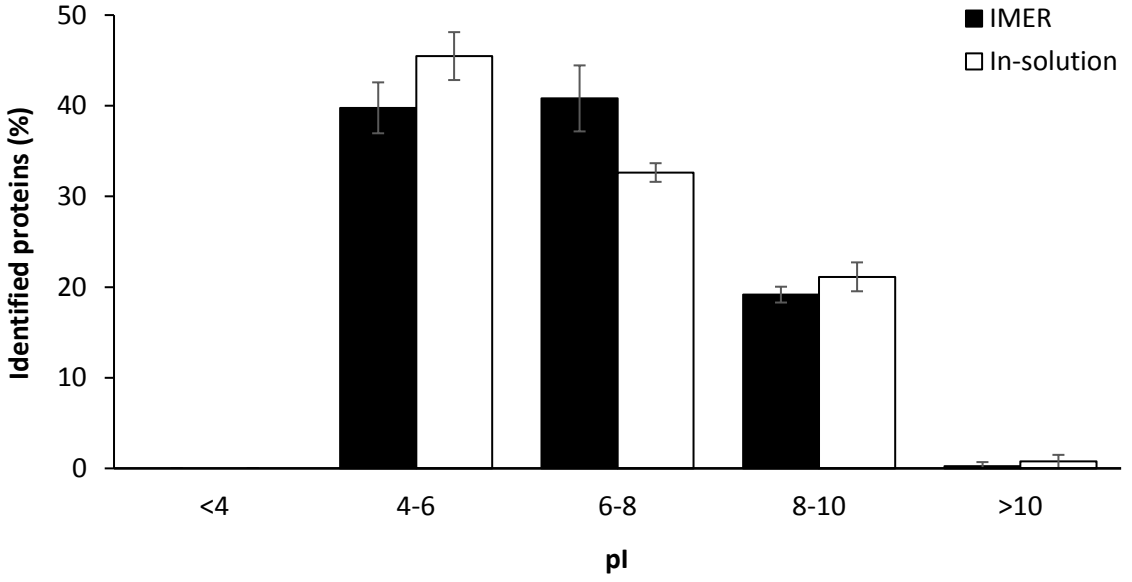

Figure 3.5. pI distribution of identified proteins from DBS extracts (n=3). IMER-facilitated digestions were without pre-treatment in-solution digestions with pre-treatment.

In terms of the GRAVY index where positive and negative scores are associated with hydrophobic and hydrophilic properties respectively, most of identified proteins for both digestion methods had hydrophilic GRAVY indices (Figure 3.6).

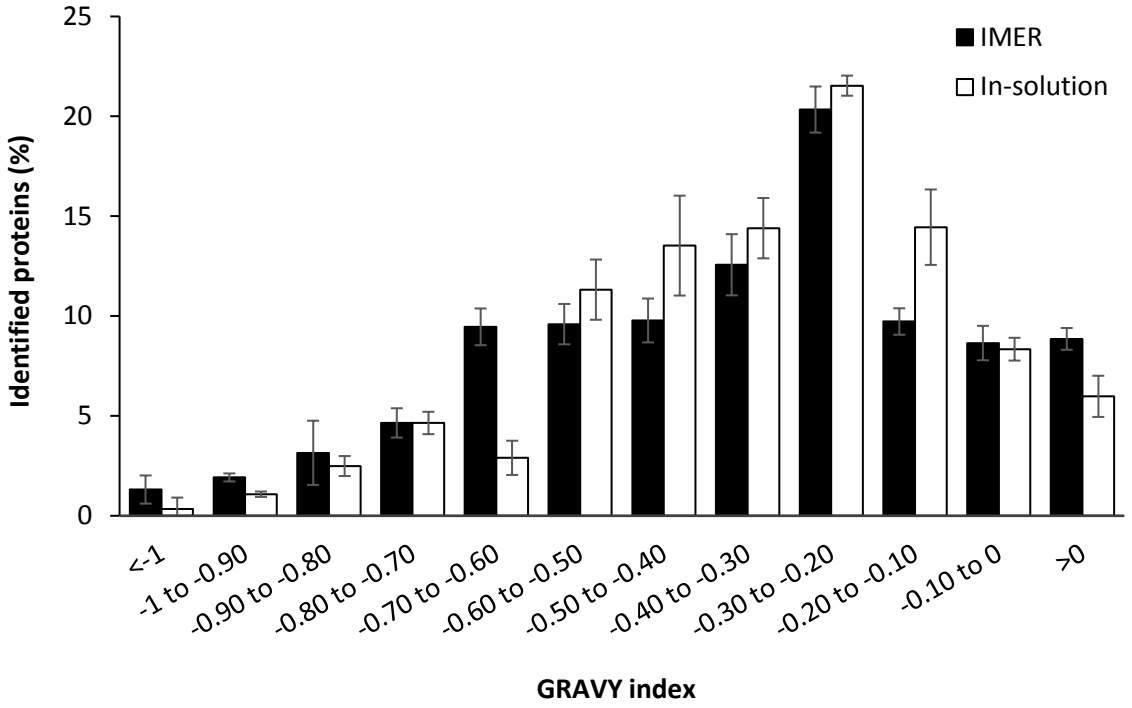

Figure 3.6. GRAVY indices of identified proteins from DBS extracts (n=3). IMER-facilitated digestions were without pre-treatment and in-solution with pre-treatment.

The majority of proteins were found to be in the region of -0.3 to -0.2 hydrophilicity (22% and 20% for in-solution and IMER-facilitated digestion respectively). A smaller percentage of identified proteins had GRAVY indices >0, which might be associated with their presence in a polar matrix e.g. blood. The similarity in GRAVY indices of identified proteins for both digestion methods indicates that unwanted adsorption of proteins to the inner surface of the IMER did not play a significant role.

The reusability of the IMER is one of its major advantages compared to in-solution digestion. An associated advantage is that sample pre-treatment steps have to be omitted, which lead to a shorter overall DBS workflow time from 22.5 hours for a workflow with in-solution digestion to 4 hours for a workflow with IMER-facilitated digestion. The reduction in digestion time itself was the main contributing factor for reducing the total workflow time by a factor 6, as digestion time was reduced from 18 hours to 5.6 minutes when using the IMER instead of in-solution digestion. Figure 3.7

visualises the duration of all necessary steps for both the IMER and in-solution workflow to digest and analyse DBS.

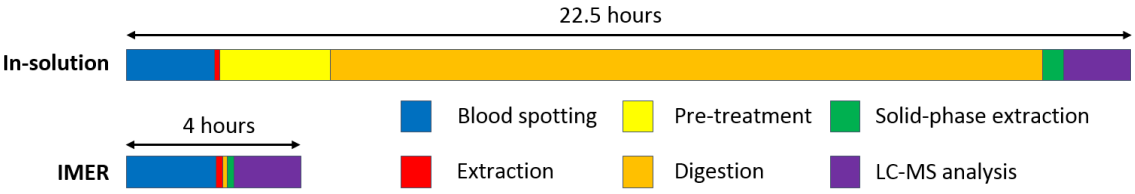

Figure 3.7. Comparison of the duration of a traditional workflow for DBS analysis by in-solution digestion (top) with the novel IMER-facilitated workflow (bottom) that omits the pre-treatment steps and reduces total analysis time to 4 hours.

3.4 Concluding remarks and future perspectives

A COC microfluidic reactor was created containing trypsin immobilised on a polymer monolithic substrate. The IMER was tested for the rapid offline digestion of both singular protein standards and the application to DBS proteins. No denaturation or protein pre-treatment was used prior to IMER-facilitated digestion of singular proteins. IMER-facilitated digestion of the model protein α-casein resulted in a higher sequence coverage compared to overnight in-solution digestion and a higher concentration of α-casein resulted in a higher number of identified peptides. Use of the IMER reduced the digestion time drastically compared to in-solution digestion, by more than three orders of magnitude from 18 hours to below 39 seconds for singular proteins and to 5.6 minutes for DBS. A comparable number of protein identifications for DBS was achieved with similar distributions in terms of MW, pI and hydrophilic character for IMER-facilitated digestion and in-solution digestion workflows. The fact that the IMER can be reused is one of its major advantages compared to in-solution digestion. An associated advantage is that sample pre-treatment steps have to be omitted, which lead to a reduction in overall DBS workflow time from 22.5 hours to 4 hours compared to a workflow based on in-solution digestion.

As speed is a key issue in many settings including forensic scenarios, the use of an IMER can offer a solution for shortening forensic proteomic analyses such as for the DBS ageing study presented in Chapter 2. For future applications, the implementation of flow-through immobilised-enzyme reactors in-line in a LC-MS workflow will be investigated for high-throughput sample analysis.

4 Rapid acquisition for the assessment of dried blood spot age

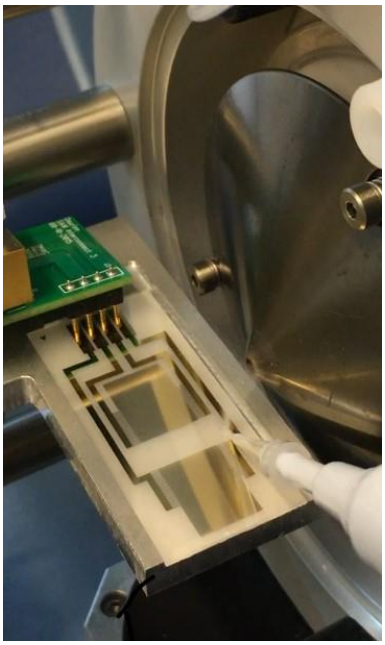

Nebulisation of a digested dried blood spot sample onto a SAWN-chip positioned directly in front of a mass spectrometer orifice

---

This study took place during a secondment at the University of Amsterdam (Amsterdam, the Netherlands). A special thanks goes to Prof. Garry L. Corthals for his supervision, to Dr. Alina Astefanei for the SAWN-MS training and help with data acquisition and to Petra J. Jansen for her for her experimental assistance (University of Amsterdam, Van 't Hoff Institute for Molecular Sciences). Bas F. Groothuis (University of Groningen, Department of Pharmacy) is gratefully acknowledged for exploring the data pre-processing possibilities during his MSc internship at the Van 't Hoff Institute for Molecular Sciences institute at the University of Amsterdam (Amsterdam, the Netherlands)

4.1 Introduction

Mass spectrometry (MS) ionisation techniques range from the more traditional hard ionisation methods such as electron ionisation to the newer softer ionisation methods such as atmospheric pressure chemical ionisation. In recent years, over 30 ambient ionisation methods have been developed allowing direct analysis of samples in real time, with desorption electrospray ionisation and direct analysis in real time being the first introduced [258-261]. Ambient ionisation techniques are based on the ionisation of samples in the atmosphere external to the mass spectrometer. Limited sample preparation is needed, low sample volumes are required, analysis times are short and the setup is simple without capillaries or other advanced mechanisms before MS analysis. These conditions are beneficial for forensic purposes, therefore ambient ionisation techniques have been tested for a variety of forensic applications including the analysis of inks and document authenticity, explosives, toxicological compounds and fingerprints [262].

In this study, the application of surface acoustic wave nebulisation (SAWN) [263] coupled to MS was explored to study the molecular profile of dried blood spots (DBS) aged for up to 8 days. Similar to other ambient ionisation techniques, the SAWN-MS setup is simple with the positioning of a chip directly in front of the mass spectrometer orifice, the acquisition time is short and both limited sample preparation and a low sample volume are required. Upon the application of a micro-volume sample onto a SAWN-chip, its interdigitated electrodes transduce acoustic waves on the surface towards the liquid sample droplet Figure 4.1. The waves refract upon reaching the droplet and fluid streaming starts within the sample droplet. Nebulisation occurs when the energy of the incoming surface acoustic wave is sufficient. Specifically, the acoustic energy causes the droplet to increase its wetting of the surface and internal oscillation. When the inertia of the droplet becomes too high, liquid fractionation causes emission of small droplets [264].

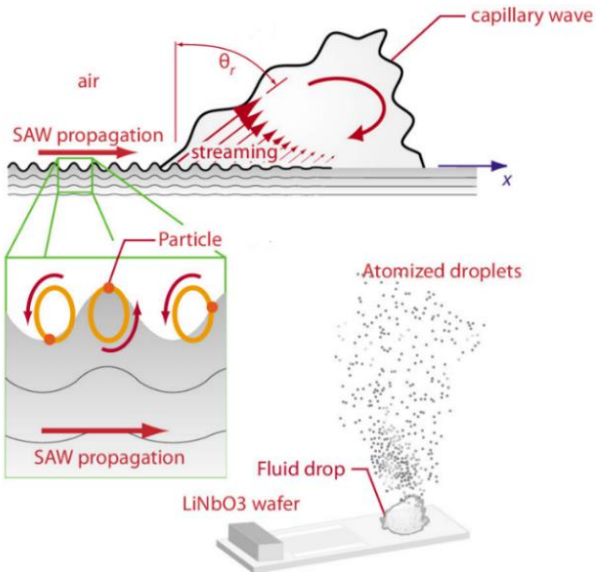

Figure 4.1. Visual representation of surface acoustic wave nebulisation (SAWN) [264].

SAWN-MS has already been incorporated into research, twice related to the subject of this study. Heron et al. used SAWN-MS for the production and detection of multiply charged peptide precursor ions [265]. The SAWN-MS spectra generated did not show interference in the low *m/z* range which is generally seen with another common ambient ionisation technique called matrix assisted laser desorption ionisation. A charge state distribution shift to higher *m/z* ratios was observed when comparing results to an identical sample analysed by the ambient ionisation technique called electrospray ionisation (ESI). Ho et al. detected drugs in human whole blood and plasma in conjunction with a paper-based sample delivery system [266]. The MS results for plasma and whole blood were similar, ascribed to the paper filtering contaminants and retaining blood cells. The focus of the current research is a combination of the two studies; blood that has been subjected to protein digestion. Extracted and digested DBS samples were evaluated to study the molecular profile of DBS aged for up to 8 days, linked to its time since deposition (TSD). Fundamental knowledge about the intrinsic changes of ageing bloodstains is scarce and no accurate method to determine the TSD is available yet. A plethora of techniques has been explored to determine the TSD of blood (outlined in Chapter 1, Table 1.1), however no proteomics approach has been tried apart from the work presented in Chapter 2. Therefore, the digested DBS samples of Chapter 2 analysed by nano-liquid chromatography hyphenated to tandem mass spectrometry with electrospray ionisation (nanoRPLC-ESI-MS/MS) were also analysed

by SAWN-MS as an alternative approach. SAWN has been reported to provide softer ionisation than ESI for sample introduction into the MS [267]. In addition, SAWN-MS reduces acquisition time from hours to only a few minutes compared to nanoRPLC-ESI-MS/MS analyses. To further reduce the entire workflow time, DBS samples with reduced sample treatment (non-digested) were measured by SAWN-MS as well. Variation in the molecular profile of DBS was explored by principal component analysis (PCA) and a support vector machine (SVM) model was developed for predicting the TSD of DBS.

4.2 Experimental design

4.2.1 Chemicals and materials

Ammonium bicarbonate (NH_4HCO_3, BioUltra, ≥ 99.5%), dithiothreitol (DTT, ≥ 99.0%), Empore C18 solid-phase extraction cartridges (SPE cartridges, 4 mm/1mL), iodoacetamide (IAA, ≥ 99%), sodium deoxycholate (SDC, BioXtra, ≥ 98%), trifluoroacetic acid (TFA, ≥ 99%), tris(2-carboxyethyl)phosphine hydrochloride solution (TCEP, 0.5 M, pH7), trypsin (European Pharmacopoeia (EP) reference standard) and Whatman Human ID Bloodstain Cards BFC 180 were purchased from Sigma-Aldrich (Zwijndrecht, the Netherlands). Acetonitrile (ACN, LC-MS grade), formic acid (FA, ULC/MS - SFC-CC grade, 99%) and water (ULC/MS - CC/SFC) were purchased from Biosolve (Valkenswaard, the Netherlands). Contact-activated lancets were purchased from Becton Dickinson (Breda, the Netherlands). Lithium niobate ($LiNbO_3$) chips were purchased from Deurion (Seattle, WA, US).

4.2.2 Sample preparation

DBS were collected, extracted, pre-processed, digested, post-processed and stored as described in Chapter 2. In summary, capillary blood was collected from the fingertips of 7 healthy donors using contact-activated lancets. The first drop of blood was wiped away and 30 aliquots of 10 µL of blood were spotted directly onto bloodstain cards. A set of triplicate spots per donor was left to dry for 2 hours in freely circulating air in the dark at room temperature. The remainder of the spots were left to age for up to 8 days. Each day three spots per donor were cut out and placed into 2 mL Eppendorf tubes. In addition, for each donor three spots were aged for 398 days but these posed extraction

difficulties. For extraction of blood and its proteins from cards, 800 µL of 25 mM NH_4HCO_3 was added and samples were vortexed for 5 minutes at 1400 rpm. After collection, drying and extraction of the blood from the cards, a pre-treatment was carried out before starting overnight in-solution protein digestion. First, proteins were denatured by adding 100 µL of 10% SDC and 10 µL of 0.5 M TCEP followed by incubation for 1 hour at 60 °C. Next, 52 µL of 200 mM IAA was added and the samples were alkylated for 1 hour in the dark at room temperature. To consume any remaining IAA, 55.4 µL of 200 mM DTT was added, followed by incubation for 30 minutes at 37 °C. For digestion 3.5 µL of trypsin (1000 mg/L) was added and samples were incubated at 37 °C for 16 hours. 40 µL of 2% FA was added to the digests to precipitate SDC. Digests were centrifuged at 4000×*g* for 20 minutes and supernatant was desalted using Empore C18 SPE cartridges. Samples were reconstituted in 100 µL water prior to LC-ESI-MS/MS analysis and afterwards stored for up to 1 year at -20 °C. For SAWN-MS analysis, 3 technical replicates per sample were created by further diluting the samples in water (1:1 v/v). A total volume of 24 µL was prepared to be applied to the SAWN chip. Different dilution volumes and dilution mixtures (70% of 0.1% FA in H_2O and 30% of 0.1% FA in ACN) were tested during method development in order to mimic the nano-LC-ESI-MS/MS conditions of Chapter 2. Signal intensities were found to be optimal after dilution of the sample with an equal volume of water.

4.2.3 SAWN-MS analysis of digested DBS proteins

All experiments were conducted with a TripleToF 5600+ mass spectrometer (Sciex, Singapore) after removal of the ESI source. The ESI source was replaced with the SAWN device (Deurion, Seattle, WA, USA), consisting of a controller, Android tablet with SAWN software and chip holder (Figure 4.2). Samples were loaded onto a lithium niobate ($LiNbO_3$) chip, which was placed directly in front of the mass spectrometer orifice. Approximately 1 µL of sample aliquots were spotted continuously for 2 minutes. SAWN was regulated by application of power to the chip's electrodes (40-70% ~ 3-5W) in continuous mode. Water was applied in between sample measurements similar to the acquisition of samples, but with a reduced acquisition time of 30 seconds in order to clean the chip.

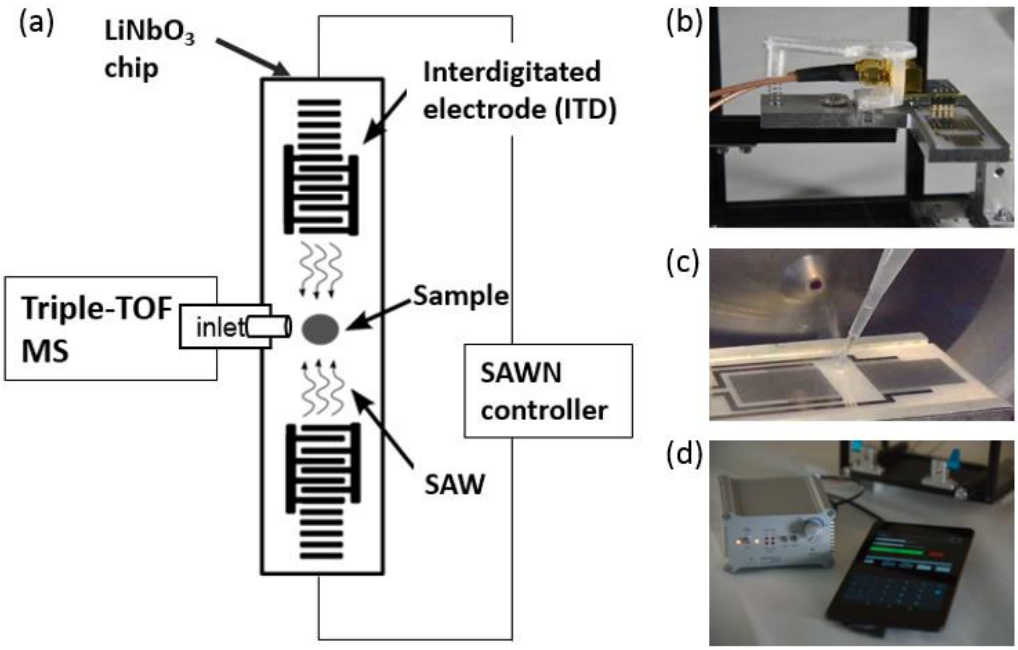

Figure 4.2. Schematic diagram of a (a) SAWN device connected to a mass spectrometer, and photos of the (b) chip holder, (c) chip and (d) SAWN controller with Android tablet [268].

Mass spectra (*m/z* 400-1250) were acquired in positive ionisation mode using multichannel acquisition. This *m/z* range was selected to mimic the range of the nano-LC-ESI-MS/MS conditions of Chapter 2. For the non-digested samples, spectra from *m/z* 400-2000 were acquired as larger molecules were expected. Different combinations of accumulation time and duration were tested, but signal intensities were found to be best for a duration of 2 minutes in combination with an accumulation time of 3 seconds. Analyst 1.7 (Sciex, Singapore) was used to acquire data and to fix the following settings; interface heater temperature at 150 °C, inlet and outlet gas pressures at 0 psi and curtain gas pressure at 10 psi.

4.2.4 Assay evaluation

Digested DBS samples from all donors (6 * 3 biological replicates) were pooled together per DBS age and measured in duplicate to obtain age references. Similarly, all 144 digested DBS samples (6 donors * 3 biological replicates * 8 days) were pooled together and measured in triplicate to obtain an overall reference. The biological triplicates of one of the donors were pooled per DBS age for a selection of two days as part of method development. To investigate matrix effects, blank card punches without blood that

underwent the same sample treatment were measured as well as capillary blood that was spotted into Eppendorf tubes instead of onto bloodstain cards and aged for a selection of 3 days. Additionally, a selection of samples of two donors from a second batch of DBS created at another point in time (Chapter 2) was measured to test the model developed for the prediction of DBS age. Finally, a DBS sample stored prior to digestion was analysed to assess the molecular profile of non-digested DBS. The non-digested DBS sample underwent extraction from cards, denaturation, alkylation and reduction before storage for approximately 1 year at -20 °C. This sample was measured ten times to also assess method repeatability.

4.2.5 Statistical approaches to establish a molecular profile of DBS age

PeakView 2.0 (Sciex, Singapore) was used for basic data analysis such as overlaying *m/z* spectra. Exploratory and advanced data analyses were performed with R studio 1.0.136 (64 bits, R version 3.4.2, Vienna, Austria), using various packages; MALDIquant, MALDIquantForeign, wmtsa, stringr, PROcess, prcacma, ggplot2, purr, foreach, doParallel, dplyr, caret, pca3D and ggpubr. Data pre-processing possibilities were explored by S.F. Groothuis during his MSc internship [269]. Outlier MS spectra were first removed by calculating the average intensity of data points and using third lowest quantiles from boxplots. Noise removal was then performed using discrete wavelet transform (DWT) with a universal threshold calculated using median absolute deviation and binning within 0.1 Da [270]. Peak detection was performed using a local maxima approach and the data was cleaned by removing peaks which were present in less than 10% of the samples [271]. Detection and removal of outlier peaks was performed using Cook's distance with a threshold set at 3 times the median [272]. Exploratory analysis was performed using PCA. Subsequently, important feature selection was performed using recursive feature elimination (RFE) combined with a bagged tree model [273, 274]. Finally, a SVM model was developed by separating the data into a training set containing 75% of the data and a test set containing 25% of the data. The training set was subjected to 20-fold cross validation repeated 10 times followed by evaluation using the test set.

4.3 Results

4.3.1 Pre-processing of DBS spectra

To retain as much signal as possible, DWT was chosen using a Coiflet wavelet as this wavelet resembles the peak shapes observed in the SAWN-MS spectra [270]. DWT is a so called hard thresholding method and was chosen over smoothing filters as the signal to noise ratio of the spectra was found to be low. DWT could also have been used for peak detection, but this appeared to be too time-consuming for this DBS dataset. Therefore, a local maxima approach was chosen which resulted in the detection of 21182 peaks in total [271]. This number is an overrepresentation of peaks useful for investigating the molecular profile of DBS as many peaks appeared in a few spectra only. A peak clean-up was performed by discarding peaks that were present in <10% of the spectra, thereby reducing the number of peaks from 211182 to 484. This percentage was chosen to have a theoretical representation of at least 1 DBS age or 1 donor. If the <10% threshold would be increased to cover more samples, the resulting number of peaks would decrease drastically (e.g. with a threshold of 100% only 4 peaks would remain). Besides peak clean-up, outliers were removed using Cook's distance with the threshold set at three times the median Cook's distance [272] on sets of 9 replicates (3 technical replicates of each of the biological triplicates). A spectrum was discarded if 25% of its peaks were marked as outliers, which resulted in removal of ±33% of the spectra. Figure 4.3 shows the effect of all pre-processing steps on the amount of SAWN-MS data available for investigating the molecular profile of DBS aged for up to 8 days. Prior to each consecutive step, the remaining peaks were normalised using auto-scaling [275]. In this way, all peaks were given a standard deviation of 1 to provide similar weight to both high and low intensity peaks.

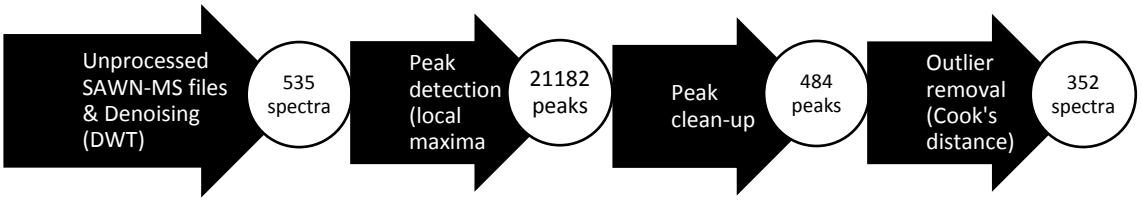

Figure 4.3. SAWN-MS data pre-processing steps to select DBS spectra for feature selection.

4.3.2 SAWN-MS method performance

Three technical replicates were created of each DBS sample measured using nanoRPLC-ESI-MS/MS (Chapter 2) to compensate for fluctuating nebulisation and fragmentation performance between SAWN measurements. Air movement was experienced around the SAWN setup during sample measurements, which led to differences in sample plumes entering the MS orifice and was reflected in the obtained spectra. Maximum intensities were observed around 1000 counts, but also as low as just above the level of noise. The broad range of intensities observed, especially the low intensities, resulted in high median relative standard deviations (RSD) for replicate samples. The RSD of both technical and biological replicates was just below 50% for most peaks. As was expected, the distribution of RSD values for the biological replicates was higher than that of the technical replicates. This effect was minimally and could be caused by the individual sample pre-treatments. The median RSD value of the non-digested DBS sample measured 10 times was 34%. The non-digested DBS sample was not representative for the DBS dataset of this study, but indicated that the presented RSD values for the technical and biological replicates could be an underrepresentation. Multiple measurements of the same digested DBS sample are desired to investigate those RSD values and thus method performance more in-depth. Method performance could potentially increase with increased accumulation time and duration. However, those parameters as well as the dilution factor of the samples were only explored minimally. To investigate if the intensity could be increased, the samples of three biological digested DBS replicates were pooled together and measured in triplicate. However, similar intensities were observed as can be seen in Figure 4.4 for both the overlaid spectra of pooled samples and for the individual samples. The same was observed for pooling all digested DBS samples from the donors together per DBS age compared to the measurements of the individual samples. However, this could also be an effect of ion suppression as was also suggested for the lower number of identifications obtained for the samples pooled prior to analysis by nano-LC-ESI/MS/MS presented in Chapter 2.

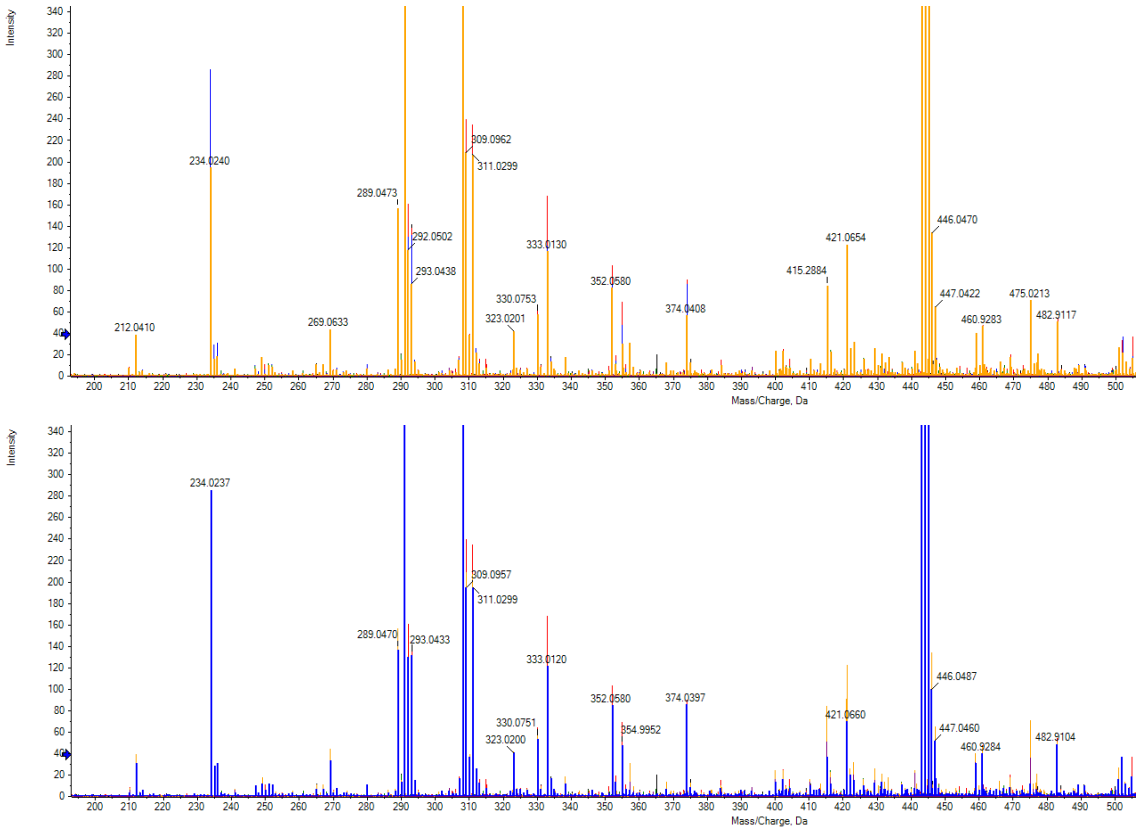

Figure 4.4. DBS spectra obtained with SAWN-MS, showing *m/z* 200-500 and the intensity limit set to 340 for better visualisation. Similar intensities were observed for pooling three biological replicate digested DBS samples together (top) and the individual biological replicates (bottom).

4.3.3 PCA exploration of DBS data acquired by SAWN-MS

The low intensity and high RSD values observed must be taken into account for the DBS data exploration. PCA was performed on the pre-processed DBS data by reconstructing the dataset against mathematically constructed orthogonal principal components [276]. The principal components serve as reflections of the variation that exists in a dataset and allow for rapid identification of clusters of data that are interesting for further examination.

PCA exploration showed only little clustering of donors, whereas all donors that participated in this study were healthy and were expected to have a similar molecular blood profile. Figure 4.5 shows a PCA plot for not aged DBS (day 0) with principal component (PC) 1 having a substantial variance of 41.6%. Variance between biological replicates of donors was observed, whereas clusters of technical replicates per donor can be seen. Intra-person variance was observed for the donor who donated blood at two different instances one year apart from each other (Figure 4.6). It was not expected

to see such a large intra-person variance (76.6% for PC1). When comparing the MS spectra, different peaks were detected between samples aged for the same amount of days with the exception of not aged DBS (day 0).

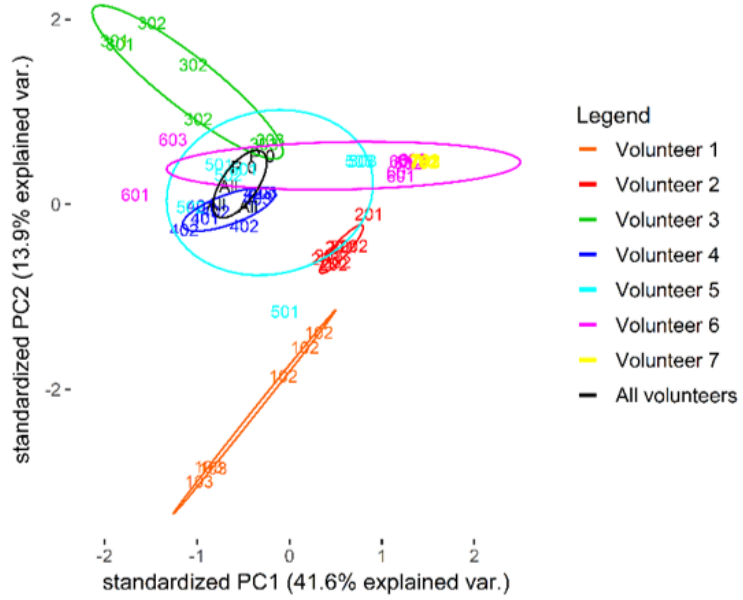

Figure 4.5. PCA plot showing inter-person variance for SAWN-MS analysis of DBS extracted and digested at the day of spotting (2 hours of drying). The first digit represents the donor (1-7, visualised with the different colours), the second digit the DBS age (here 0 days) and the third digit the biological replicate (1-3, each consisting of 3 technical replicates). In addition 'P0' in black represents all not aged DBS samples (day 0) from all donors pooled together.

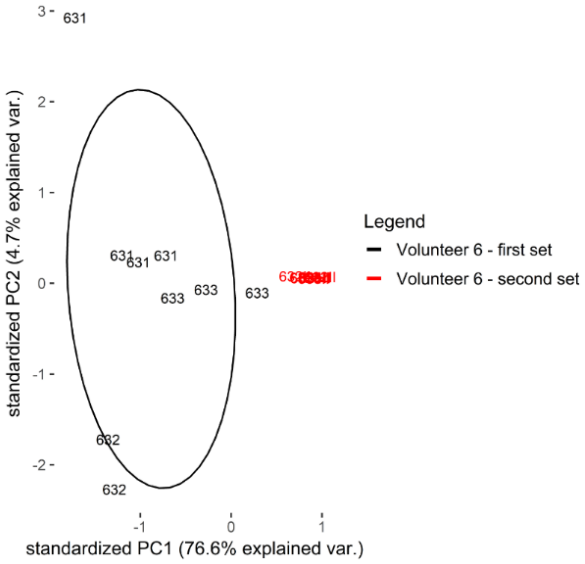

Figure 4.6. PCA plot showing the intra-person variance for the SAWN-MS analysis of DBS aged for 3 days. Numbering is the same as for Figure 4.5 with the first digit representing the donor (here 6), and the second digit the DBS age (here 3 days). The two colours visualise the two different days of collection.

Variance between donors was probably detected as a result of different metabolism, lifestyle, age and other individual factors. Therefore, all samples of the donors were also pooled together per DBS age to explore the molecular profile of DBS aged for up to 8 days. In addition, samples from all donors and all DBS ages were pooled together to serve as a reference. Both the PCA exploration of the samples pooled per DBS age prior to SAWN-MS analyses and all individually measured DBS samples are shown in Figure 4.7. Clustering was observed for all days, however the pooled samples of the day of spotting (day 0) clustered apart from the other samples pooled per day.

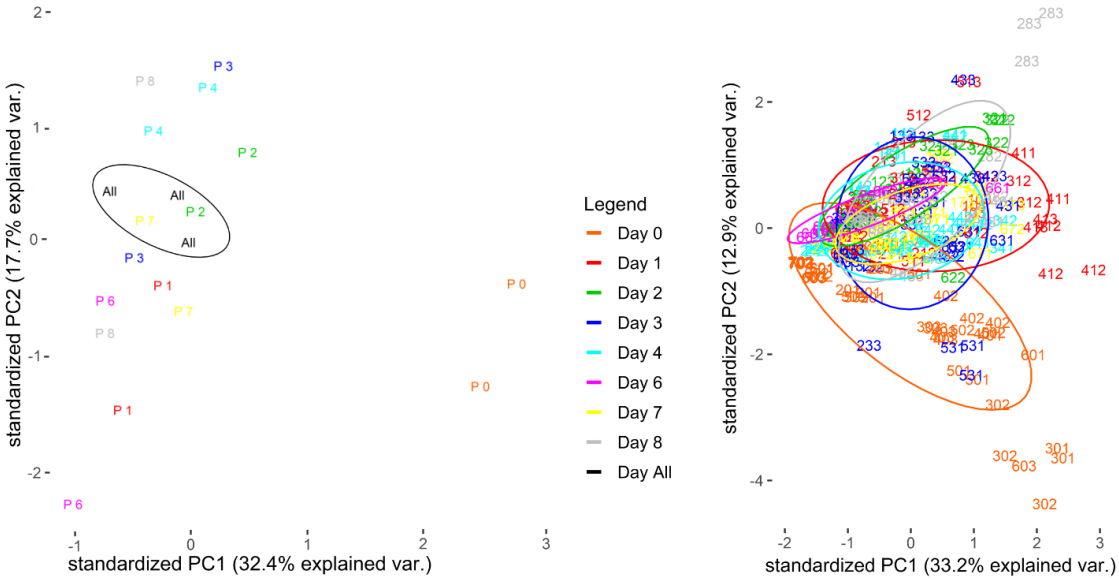

Figure 4.7. PCA plot of samples from all donors pooled per DBS age prior to SAWN-MS acquisition (left) and the DBS samples from all donors measured individually (right). The pooled samples from the day of spotting (P0) were separated from the pooled samples aged for up to 8 days (P1-P8). 'All' represents the samples from all days and donors pooled together. Numbering is the same as for Figure 4.5 with the colours additionally visualing the DBS ages.

A clear separation was observed between DBS extracted and digested at the day of spotting (day 0) and DBS aged for up to 8 days for 2 out of the 6 donors when exploring the molecular profile of aged DBS by PCA (Figure 4.8). Clustering of DBS ages was observed for the other donors, with PC1 variances between 21.1%-43.8% and PC2 variances between 10.2%-20.3%. These variances were potentially caused by the high RSD values outlined in the previous paragraph. A batch effect became apparent upon exploring the molecular profile of DBS by analysis of samples collected from 2 donors at a second point in time. This finding supports the intra-person variance observation

shown in Figure 4.6. Clustering with the other DBS ages was observed again upon inclusion of the DBS samples aged for 398 days (1 replicate per donor).

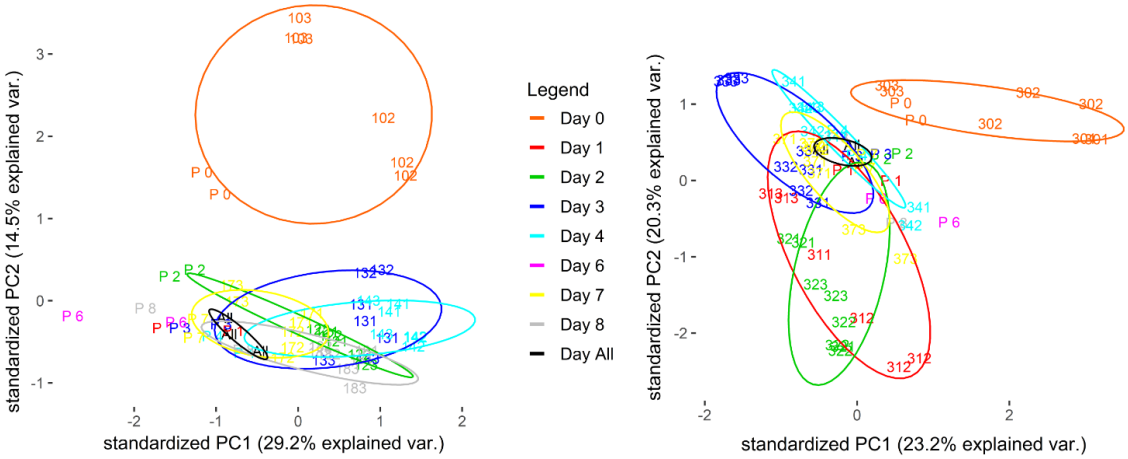

Figure 4.8. PCA plots of DBS samples aged for up to 8 days and analysed by SAWN-MS for 2 of the 6 donors. Numbering is the same as for Figure 4.7 with the first number representing the donor (left 1, right 3).

4.3.4 Development of a SVM model for DBS age classification

As exploratory PCA analyses did not reveal variation related to the TSD of DBS, feature selection was chosen to further explore the molecular profile of DBS aged for up to 8 days. RFE was applied as feature selection method, because all resulting peaks from the data pre-processing can be provided to a classifier algorithm to evaluate which combination of features is most important [274]. To increase the output, a bagged tree model was used instead of a single classifier [273]. Bagging is the combination of multiple weak classifiers to form one strong model, which resulted in approximately 75 features important for classifying the age of DBS. However, the importance of each feature turned out to be low. The feature of most importance was found to be *m/z* 555.10 with a relative importance of just below 25%. Another 12 important features with relative importance between 10%-20% were found (Figure 4.9). All features were detected as singly charged molecules with relatively low intensities (<5%) and large RSDs (45%-91%). The features of *m/z* 555.10 and 556.11 were highly correlated (r=0.945), which may be due to isotopes. Except for the features of *m/z* 555.10, 556.11, 745.39, 409.16 and 490.97, the other 8 features were also found in card samples without DBS. This indicated interference of the card matrix on the DBS measurements as the features

were not detected in the blood samples spotted directly in Eppendorf tubes instead of onto cards. However, none of the features were observed in the non-digested DBS samples which were also extracted from DBS cards. Not detecting the features of *m/z* 555.10 and 556.11 could be expected as those might be peptide features, but the absence of the other features was unexpected. Therefore, the 8 other most important features might still be important markers related to the TSD of DBS.

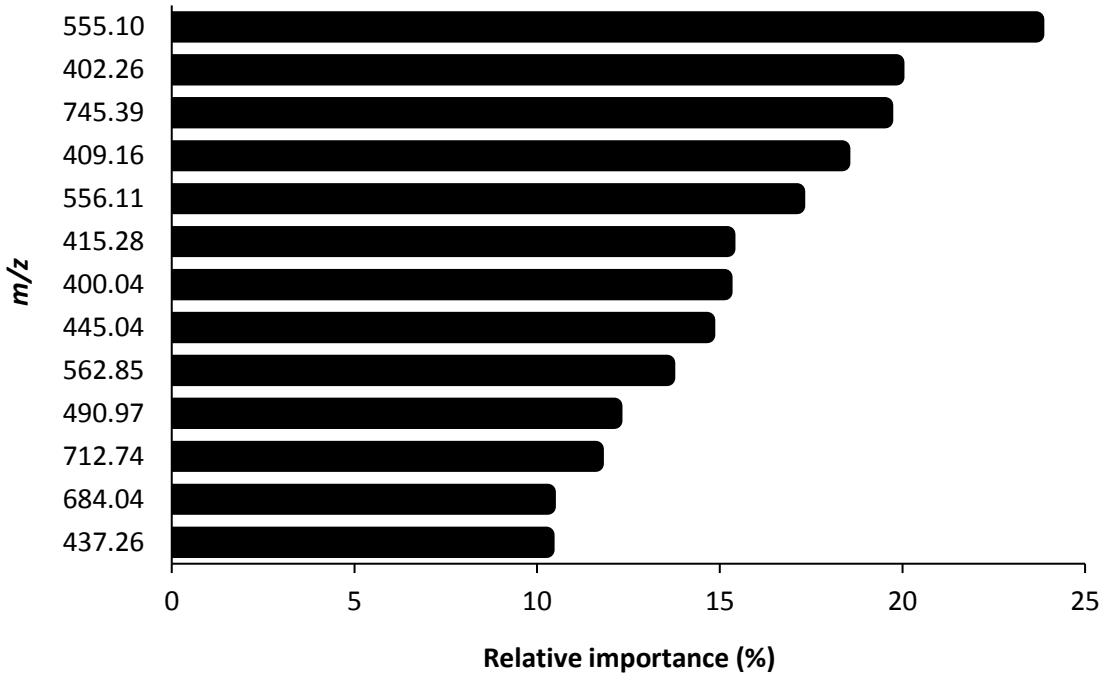

Figure 4.9. Results of feature selection for the classification of DBS age, with 13 out of 75 important features having a relative importance >10%.

The 13 most important features were selected to develop a SVM model for the prediction of DBS age. SVM is a machine learning technique that starts by classifying and mapping related variables using a support vector [277]. Potential clusters within clusters can also be identified, which might be the case for the DBS dataset. To develop the SVM model, the DBS dataset was split into a main training set (75% of the data) and a test set (25% of the data). Different kernels were tested (linear, radial and polynomial) and a linear kernel was selected for the SVM model as the highest accuracy, lowest number of false positives and highest number of true positives was found based on the DBS dataset [278]. A 20-fold cross validation was repeated 10 times by creating 10 combinations of 19 training sets and a test set from the main training set (containing 75% of the data). This resulted in a SVM model with an average overall accuracy of

46.4% for the classification of DBS age. This could be a result of the low classification accuracy for DBS aged >0 days as can be seen in Figure 4.10, with no prediction at all for DBS aged for 6 days using the developed SVM model.

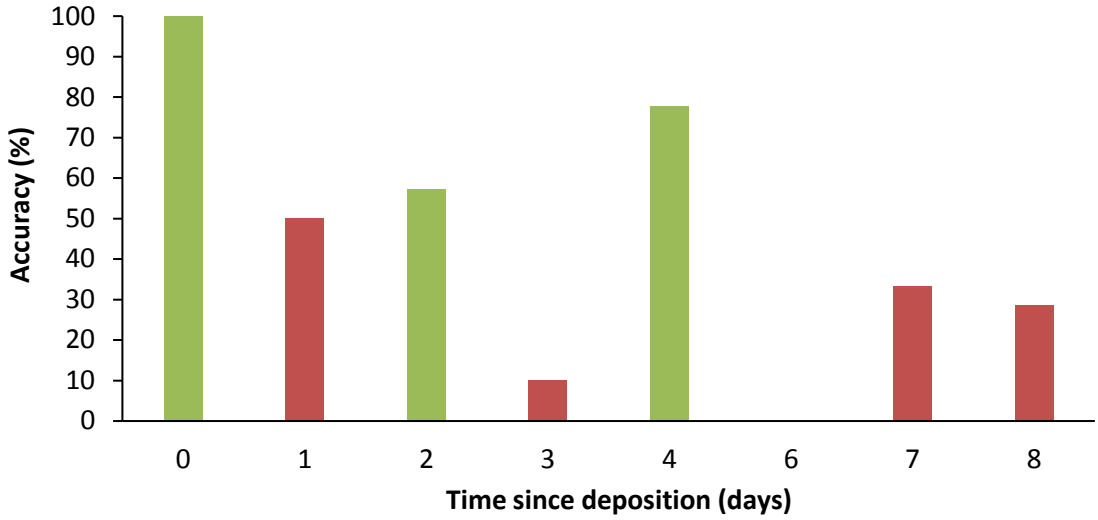

Figure 4.10. Classification results of DBS aged for up to 8 days using the developed multiclass linear SVM model. Accuracies >50% are shown in green and ≤50% in red.

A 100% accuracy was obtained for day 0 predictions upon application of the main test set (containing 25% of the data) to the model, however an accuracy of 50.8% was obtained overall. In addition, the number of false positive predictions for day 0 was high (42.8%). Considering that the PCA analyses also showed clustering of all days with the potential exception of DBS not aged (day 0), a binary classification model seemed a more suitable choice than the developed multiclass classification model. Hence, a 'day 0' versus 'all other days' approach was explored for DBS age classification. A SVM model with radial kernel [279], trained with the same cross validation as the linear model, showed the highest accuracy for binary classification on the DBS dataset. Using the optimised radial SVM model, a 78% drop of false positive classifications was observed for DBS samples not aged (day 0). Figure 4.11 shows the classification results for DBS age and percentage of true and false positives using the binary approach. Results were slightly better for the binary classification of DBS aged >0 days (any other day) compared to DBS not aged (day 0), which is most likely the result of the lower total number of not aged DBS samples compared to all other DBS aged for up to 8 days taken together. The two features of *m/z* 549.00 and 555.10 were observed to separate not aged DBS

samples (day 0) from the DBS samples aged for at least a day. The feature of *m/z* 555.10 could represent a triply charged molecule as a potential isotope peak at *m/z* 555.30 was observed. Whereas the feature of *m/z* 555.10 was found to be an important feature, the feature of *m/z* 549.00 was not included in the list of most important selected features shown in Figure 4.9.

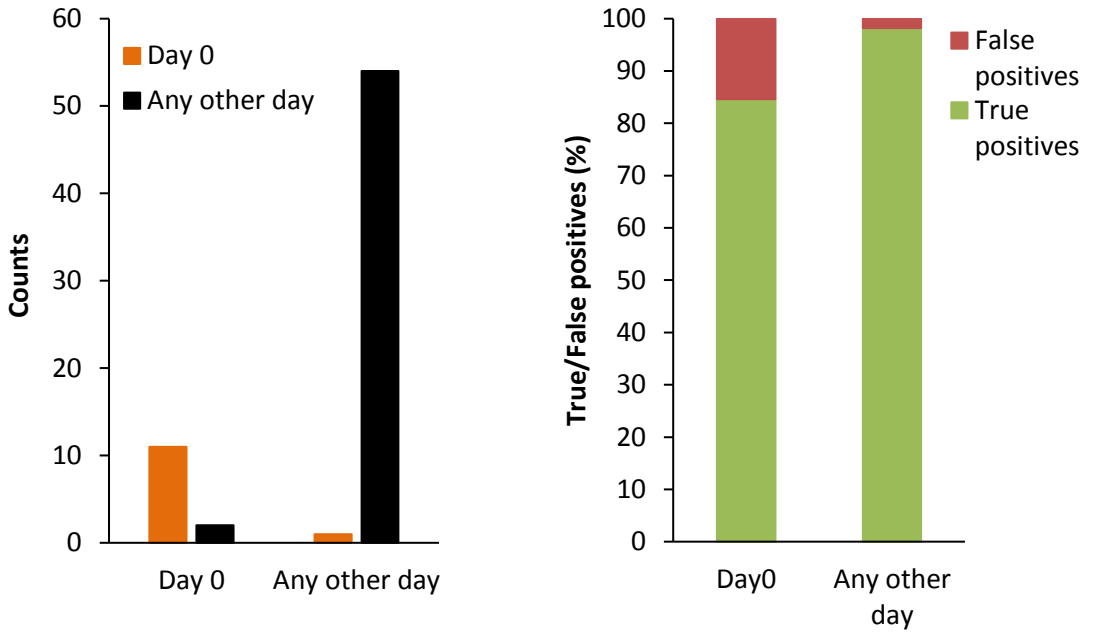

Figure 4.11. Radial SVM results for the binary classification of DBS age (left) and the associated true and false positives (right).

An overview of the developed and tested radial SVM model for the binary classification of DBS age is shown in Figure 4.12. The overall accuracy of the model was found to be 98.2%. Upon application of the main test set (containing 25% of the data) to the model for the prediction of DBS age a high accuracy of 95.6% was obtained. The prediction accuracy after leave-one-out (LOO) cross-validation was also high (92.1%). However, this is an inflated result as DBS age could be predicted perfectly for leaving 2 of the donors out but up to 60% misclassifications were observed when leaving out any of the other 4 donors. In order to further validate the model, a new batch of DBS samples was applied to the model. However, the age of DBS from the new batch could not be predicted with the developed model which could be the result of the possible batch effect discussed for the findings of Figure 4.6.

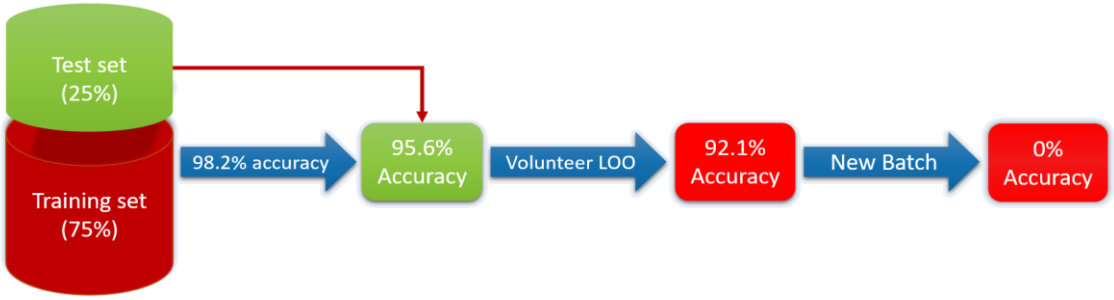

Figure 4.12. Radial SVM model accuracy for the binary prediction of DBS age (day 0 versus day 1-8). *LOO=Leave-One-Out.*

4.3.5 SAWN-MS versus nano-LC-ESI-MS/MS for DBS analysis

The main thing to note when comparing the nano-LC-ESI-MS/MS measurements outlined in Chapter 2 with the SAWN-MS measurements presented here is that the acquisition time was greatly reduced from 94 minutes to 2 minutes per DBS sample. Measurements with SAWN-MS are simple and quick, however at present more labour intensive than the nano-LC-ESI-MS/MS measurements which can be performed by an autosampler. For both techniques a low sample volume is required and for SAWN-MS less sample pre-treatment is potentially required if the acquisition appears suitable for non-digested DBS samples. Preliminary results of non-digested DBS measured by SAWN-MS showed a decreased RSD (median RSD of 34%) for method precision compared to the measurement of digested DBS samples (RSD ±50%). Table 4.1 gives a comparison between SAWN-MS and nano-LC-ESI-MS/MS for the analysis of DBS.

Table 4.1. Comparison between SAWN-MS and nano-LC-ESI-MS/MS for the analysis of DBS.

	SAWN-MS	nano-LC-ESI-MS/MS
Acquisition time	2 minutes	94 minutes
Sample application	Manual	Autosampler
Sample volume	24 µL (12 µL + 12 µL H_2O)	5 µL
Method precision	±50%	96%
Data pre-processing	Needed	Not needed
Data analysis	Peak detection	Protein identification

4.4 Concluding remarks and future perspectives

The application of SAWN-MS for the analysis of DBS samples was explored to assess a molecular profile of DBS aged for up to 8 days. Method acquisition precision for the analysis of DBS samples was low, with RSDs of ±50%. The dataset needed to be pre-treated for the analyses by denoising, peak detection, peak clean-up and outlier removal, which resulted in the removal of ±33% of the initial spectra. PCA showed that DBS aged between 1 and 8 days could be separated from the DBS samples not aged (day 0) for 2 of the donors and when pooling the samples of all donors per DBS age pre-acquisition. RFE was applied to evaluate which features, or combination thereof, were most important to classify DBS age. A total of 13 features were found with a relative importance ranging between 10%-20%. SVM models were developed for the prediction of DBS age. First, a multiclass prediction model was developed which showed a 100% accuracy for the classification of DBS not aged (day 0). However, the number of false positives was high and the classification accuracy for all other days was low with an overall accuracy of 50.8%. Therefore, a binary class model was adopted with a 98.2% accuracy for classifying DBS age as either day 0 or any other day. However, the SVM was unable to predict age from new batches of DBS.

It would be interesting to measure more non-digested samples to see if the entire workflow time for the prediction of DBS age by SAWN-MS analysis can be reduced. However, method development would be needed first to decrease variation. It would be useful to spike the samples with an internal standard in future experiments to be able to quantify molecular changes, as was also recommended for the nano-LC-ESI-MS/MS study of Chapter 2. The addition of an internal standard would also be useful to develop an optimised, possibly multiclass, model for the prediction of the TSD of DBS. In general, adjusting the experimental setup of the SAWN-MS, especially the application of samples onto the chip, would have a positive impact on the measurements. Improvements such as a wind barrier for the MS interface are being developed.

In conclusion, the application of SAWN-MS for the analysis of DBS samples provided limited insight into the molecular profile of DBS aged for up to 8 days. SAWN-MS is a novel technique with potential for analysing a plethora of sample types quickly, but it may not be compatible with the analysis of DBS for assessing its TSD.

5 Quantification of salbutamol using micro-volume blood samples

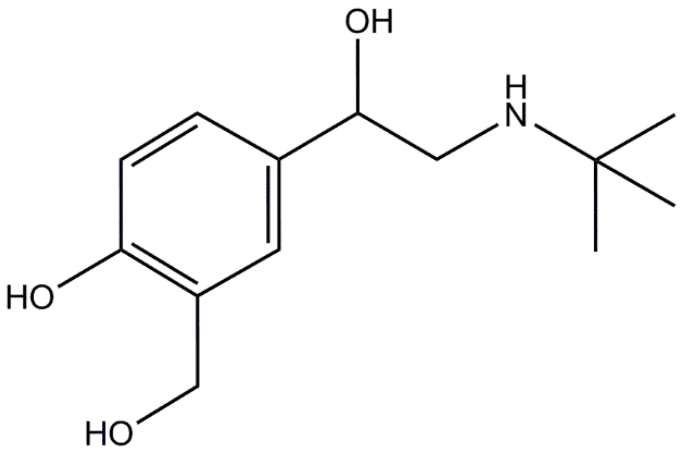

Salbutamol (MW 239.30 g/mol)

Chapter based on R.L. Cordell, T.S.E. Valkenburg, H.C. Pandya, D.B. Hawcutt, M.G. Semple, P.S. Monks, Quantitation of salbutamol using micro-volume blood sampling – applications to exacerbations of pediatric asthma, Journal of Asthma, (2017) 1-9 [280].

Statement of originality: R.L.C. developed the GC-MS method. T.S.E. Valkenburg tested the method with VAMS technique and subjected it to validation as is presented in this thesis.. D.B.H. and M.G.S. assisted the healthy volunteer study and proof-read the manuscript. H.C.P. and P.S.M. supervised the study.

A special thanks goes to Dr. J.B. Rudge from Neoteryx LLC, who kindly provided the VAMS devices for the study.

5.1 Introduction

Salbutamol is one of the many drugs for which analytical assays have been developed ($C_{13}H_{21}NO_3$, 2-(tert-butylamino)-1-[4-hydroxy-3-(hydroxymethyl)phenyl]ethanol). Salbutamol is also known as albuterol and sold under different brand names such as Ventolin (Figure 5.1).

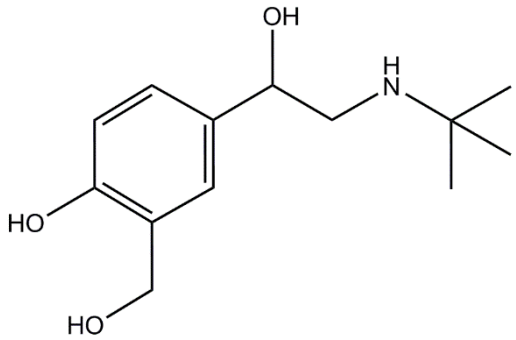

Figure 5.1. Chemical structure of salbutamol (MW 239.30 g/mol).

Salbutamol is a β_2-adreno-receptor agonist mainly used as a bronchodilation medicine for relieving the symptoms of asthma, including exercise-induced asthma [281]. Administration is primarily by inhalation and orally, but intravenous treatments are common in severe acute asthma attacks [282, 283]. In addition to its therapeutic effects, salbutamol has been reported to improve nitrogen retention, reduce body fat and promote muscle growth [284]. Therefore, salbutamol has also been administered as a drug of abuse, for example to alter meat yield and to improve performance of both horses and athletes [285-287].

The World Anti-Doping Agency (WADA) does approve the use of salbutamol in competitions by asthmatic athletes, therefore asthmatic athletes need to obtain a therapeutic use exemption that states their lung function is compromised. WADA monitors salbutamol use of athletes both in- and out-of-competition by urine analysis [288]. The maximum therapeutic dose set by WADA is 1600 µg by inhalation over 24 hours and oral administration is not allowed. The presence of >1000 ng/mL salbutamol in urine is presumed not to be intended therapeutic use [289] and has been exceeded in several big sport events such as the Olympic Games [290, 291]. The administration of multiple doses by inhalation throughout the day is however a weakness of this limit as

this has been demonstrated not to exceed WADA urine concentrations [292, 293]. Therefore, serious concern has been raised over the misuse of salbutamol.

The half-life of salbutamol varies from 3 to 7 hours and its elimination occurs generally through urinary excretion [294]. Detecting and quantifying analytes from urine brings disadvantages with it as outlined in Chapter 1. In short, collection can be invasive for privacy and it is not easy to carry out (multiple times or at certain times) during competitions. Advanced shipping and storage conditions need to be taken into account too. Blood samples could be an alternative, but for venous sampling trained medical personnel is needed. Venous blood collection is invasive and advanced transport and storage requirements need to be taken into account again. Dried blood spots (DBS) would be a valuable alternative as the collection is simple, quick, less invasive and cost saving. DBS can be transported by regular post and stored at room temperature. Additional advantages of using DBS would be that multiple samples can be collected easily due to its reduced sample volume and for many analytes enhanced stability has been demonstrated compared to venous blood and/or urine samples. A number of assays have been developed for the measurement of salbutamol in urine and blood, including one for DBS [82]. An overview of studies detecting and quantifying salbutamol in human biological fluids is outlined in Table 5.1.

Table 5.1. Studies determining salbutamol with a variety of analytical techniques, biological fluid types and sample volumes, sorted by year of publication. *IV= intravenous, NA=Not applicable, NS=not specified NT=Not tested, PM=post-mortem.*

Technique	Blood volume, fluid type	Additional sample types	Application to volunteers	Administration to volunteers, dose and route	Reference (study, year)
GC-MS	2 mL plasma	No	4 NS	4 mg orally or 200 µg by IV	[295] Martin et al., 1976
GC-MS	Plasma, volume NS	No	14 asthmatic patients	16 mg slow release orally	[296] Fairfax et al., 1980, based on [295]
GC-MS	1 mL serum	No	1 case of overdose	NA	[297] Leferink et al., 1982

Table 5.1. *Continued.*

Technique	Blood volume, fluid type	Additional sample types	Application to volunteers	Administration to volunteers, dose and route	Reference (study, year)
HPLC	1 mL plasma	No	1 healthy volunteer	8 mg orally	[298] Oosterhuis and van Boxtel, 1982
HPLC	1 mL plasma	No	>1 non-asthmatic patients	1.9 mg by IV, 4 mg orally 4-hourly	[299] Hutchings et al., 1983
GC-MS	2 mL plasma	No	12 healthy volunteers	4 mg orally	[300] Powell et al., 1984
HPLC	0.5 mL serum	No	2 healthy volunteers	2 mg orally	[301] Tan and Soldin, 1984
HPTLC, GC-MS	2 mL plasma	Urine	3 volunteers	4 mg orally and up to 500 µg intramuscularly	[302] Colthup et al., 1985
GC-MS	Serum, volume NS	No	36 pregnant patients, 8 non-pregnant volunteers	4 mg orally repetitively, IV - dose NS	[303] Haukkamaa et al., 1985, based on [295]
HPLC	1 mL plasma	No	1 healthy volunteer	4 mg orally	[304] Miller and Greenblatt, 1986
HPLC	1 mL plasma	Urine	10 healthy volunteers	4 mg orally, up to 1600 µg orally	[305] Morgan et al., 1986, based on [299]
HPLC	0.5 mL serum	No	16 healthy volunteers	4 mg orally, 1.5 mg by IV	[306] Goldstein et al., 1987, based on [301]
RPLC	1 mL serum	No	2 healthy volunteers	8 mg orally	[307] Emm et al., 1988
HPLC	1 mL plasma	No	15 asthmatic volunteers	4 mg and 8 mg orally	[308] Lipworth et al., 1989, based on [299]
Immuno-affinity, HPLC	1 mL plasma	No	1 healthy volunteer	4 mg orally	[309] Ong et al., 1989

Table 5.1. *Continued.*

Technique	Blood volume, fluid type	Additional sample types	Application to volunteers	Administration to volunteers, dose and route	Reference (study, year)
HPLC	1 mL plasma	No	1 healthy and 1 asthmatic volunteer	4 mg and 8 mg orally	[310] Bland et al., 1990
HPLC	NT	Urine	10 healthy volunteers	4 mg orally, 400 µg by inhalation	[311] Hindle and Chrystyn, 1992
HPTLC	2 mL serum	No	20 asthmatic volunteers	8 mg slow release orally	[312] Le Roux et al., 1992, based on [302]
RPLC	1 mL plasma	No	Hospital patients, number NS	Up to 3.6 mg by inhalation	[313] Gupta et al., 1994
HPLC	3 mL plasma	Urine	7 healthy volunteers	4 mg oral and 1.6 mg IV, 8 mg rectal	[314, 315] Boulton and Fawcett, 1995-1996, based on [310]
HPLC	1 mL serum	No	9 hospital patients, 10 healthy volunteers	Up to 1 mg by inhalation	[316] Duarte et al., 1996
GC-MS	1 mL PM blood	No	24 cases of asthmatic deaths	NA	[317] Couper and Drummer, 1996
GC-MS	1 mL plasma	No	1 healthy volunteer	360 µg by inhalation	[318] Logsdon et al., 1997
ELISA	NT	Urine	147 athletes	NA	[319] Ventura et al., 1998
GC-MS	1 mL plasma	No	10 healthy volunteers	180 µg by inhalation	[320] Anderson et al., 1998
GC-MS	PM blood, 1 gram	Urine	12 forensic cases with asthmatics	NA	[321] Black and Hansson, 1999
HPLC	1 mL plasma	Urine	22 healthy volunteers	Up to 800 µg by inhalation, 4 mg orally	[322] Schmekel et al., 1999, based on [315]

Table 5.1. *Continued.*

Technique	Blood volume, fluid type	Additional sample types	Application to volunteers	Administration to volunteers, dose and route	Reference (study, year)
GC-MS	500 µL plasma	Urine	12 healthy volunteers	8 mg orally	[284, 323] Saleh et al., 2000
GC-MS	NT	Urine	15 asthmatic and 17 non-asthmatic swimmers	20 mg orally and up to 1600 µg by inhalation	[324, 325] Berges et al., 1999-2000
GC-MS	NT	Urine	1 asthmatic volunteer	NS	[326] Damasceno et al., 2002
GC-MS	NT	Urine	1 healthy volunteer	2 mg orally	[327] Forsdahl, 2004
HPLC	1 mL plasma	Urine	10 healthy volunteers	Multiple doses over 4 days, by inhalation, orally and sub-cutaneous	[292] Pichon et al., 2006, based on [325]
LC-MS	NT	Urine	37 non-asthmatic cyclists and triathletes	Placebo, 200 µg, 400 µg and 800 µg by inhalation	[328] Sporer et al., 2007
Square wave voltammetry, GC-MS	4 mL plasma	Urine	Asthma patients, number NS	10 mg orally, inhalation - dose NS	[294] Goyal et al., 2007
LC-MS	NT	Urine	8 healthy volunteers	200 µg, 400 µg and 800 µg by inhalation	[288] Sporer et al., 2008
LC-MS	3-5 mL serum	Urine	10 asthma patients	800 µg by inhalation 4 mg orally	[329] Elers et al., 2009
HPLC	1 mL plasma	No	46 children with acute asthma	3 doses of 50 µg/kg by inhalation and 150 µg/kg by nebulisation	[330] Rotta et al., 2010, based on [299]

Table 5.1. *Continued.*

Technique	Blood volume, fluid type	Additional sample types	Application to volunteers	Administration to volunteers, dose and route	Reference (study, year)
HPLC	NT	Urine	10 asthmatic and 10 healthy volunteers	400 µg repetitively by inhalation	[293] Elers et al., 2011
GC-QqQ-MS	NT	Urine	No	NA	[331] Van Eenoo et al., 2011
GC-FID, GC-MS	NT	Solutions	No	NA	[332] Caban et al., 2011
LC-MS/MS	200 µL plasma	Urine	1 healthy volunteer	2.5 mg by nebulisation	[333] Sidler-Moix et al., 2011
LC-MS/MS	NT	Urine	No	NA	[334] Lee et al., 2011
GC-QqQ-MS	NT	Urine	No	NA	[335] Brabanter et al., 2012, based on [331]
HPLC	3-5 mL serum	Urine	8 asthmatic athletes, 10 non-asthmatic volunteers	800 µg by inhalation, 8 mg orally	[336] Elers et al., 2012
UHPLC	20 µL DBS	No	No	NA	[82] Thomas et al., 2012
LC-MS/MS	NT	Urine	9 healthy endurance athletes	8 mg orally	[337] Hostrup et al., 2014

As can be seen in Table 5.1, many assays have been developed to determine salbutamol in biological fluids. High-performance liquid chromatography (HPLC) and gas chromatography mass spectrometry (GC-MS) being the most used techniques for the development of the assays. Many studies focussed on or included urine as this is the current biological fluid used for sport doping testing. Two studies have developed

methods for the detection of salbutamol in post-mortem (PM) blood. The studies that involved blood (including serum or plasma), required several millilitres for their analyses. To the best of my knowledge, the use of a micro-volume of blood for the detection and quantification of salbutamol has only been studied by Thomas et al. [82]. They used HPLC however, which comes with the disadvantages of extensive sample preparation and specialist equipment. Therefore, the aim of this study was to develop a simple, fast, quantitative assay for the measurement of salbutamol in micro-volume blood samples using GC-MS. Thereby further reducing the volume of blood needed for analysis, from 20 µL used for the existing UHPLC assay to 10 µL used in this study. This further reduction can be important for the application to (forensic) toxicology cases including those with PM blood, cases where repeated sampling is needed such as sport doping testing, but also in paediatric clinical cases where the quantity of blood is a limiting factor [280, 338]. Two sampling techniques were assessed to determine their suitability for use in the quantification of therapeutic and toxic levels of blood salbutamol. The first being conventional DBS collection onto cards using a fixed volume of blood. The second the use of a volumetric absorptive micro-sampling (VAMS) device to ease sample collection [153, 188]. The developed assay has been subjected to partial bioanalytical validation using VAMS based on the guidelines of the US Food and Drug Administration [339]. Salbutamol dosed volunteer blood samples were collected by authentic capillary sampling to further assess the suitability of the VAMS technique for the quantification of blood salbutamol concentrations. Although many studies have included the application of their developed method to measure salbutamol from volunteer samples, this is the first time using VAMS and by using a lower volume of blood compared to the study of Thomas et al. that used DBS previously.

5.2 Experimental design

5.2.1 Chemicals and materials

Acetonitrile (ACN), N,O-Bis(trimethylsilyl)trifluoroacetamide (BSTFA) with 1% trimethylchlorosilane (TMCS), ethyl acetate (EA), methanol (MeOH) and salbutamol were purchased from Sigma Aldrich (Poole, UK). K_3-EDTA tubes (S-Monovette) were purchased from Sarstedt (Leicester, UK). Safety lancets were purchased from Medscope

(Cirencester, UK). (+)-Salbutamol-d3 (3-hydroxymethyl-d2; α-d1) was purchased from Qmx Laboratories (Thaxted, UK). Whatman 903 Protein Saver blood cards were purchased from Fisher (Loughborough, UK). VAMS devices (brand name Mitra™) were kindly donated by Dr. J.B. (Neoteryx LCC, Coventry, UK).

5.2.2 Preparation of micro-volume blood samples with salbutamol

In order to prepare spiked samples for assay evaluation, a stock solution of 5 mg/mL salbutamol in methanol was prepared which was then diluted to produce solutions in the range 720 ng/mL - 24 µg/mL. 5 µL aliquots of salbutamol at appropriate concentration in methanol were added to venous blood collected from one donor in 1.2 mL K_3-EDTA tubes and agitated gently to ensure even distribution. For the production of the DBS, 10 µL blood samples were spotted onto DBS cards using an auto-pipette. VAMS samples were collected by holding the tip just below the surface of the blood in the tube and allowing the blood to wick up into the tip until the tip was completely coloured. The VAMS devices used for this study had a calculated average blood wicking volume of 10.1 µL as specified on the certificate of performance. A standard drying time of 2-3 hours for both DBS and VAMS was used in freely-circulating air in the dark at room temperature directly followed by further sample preparation and analysis.

5.2.3 Extraction and derivatisation method

Each fully excised DBS or detached VAMS tip was placed in a GC vial before the addition of 300 µL of solvent and sonication for 15 minutes. DBS extractions were carried out using methanol whereas the relative extraction efficiencies of methanol, ethyl acetate and acetonitrile were investigated during method development for VAMS. The resultant solvent was placed into 300 µL insert GC vials with 180 pg d3-salbutamol internal standard (3 µL of 60 ng/mL in methanol) and dried by unheated centrifugal evaporation for 45 minutes for DBS samples and 60 minutes for VAMS samples. Samples were re-suspended in 25 µL of BSTFA/1% TMCS by vortexing shortly and 15 minutes sonication before derivatisation at 60 ^{o}C for 30 minutes.

5.2.4 GC-MS analysis

GC-MS analysis was carried out using an Agilent 7890A GC and 5975C MS with CTC-PAL autosampler (Agilent Technologies, Wokingham, UK). A DB-5MS capillary column (l = 30 m, I.D. = 0.25 mm, dF = 0.25 µm, Agilent Technologies, Wokingham, UK) was used for the analysis. The GC conditions were optimised as follows: the column starting temperature was 150 ^{o}C, which was raised to 250 ^{o}C at 10 ^{o}C/min, then increased to 300 ^{o}C at 50 ^{o}C/min where it was held for 4 minutes, giving a sample runtime of 15 minutes. The inlet temperature was maintained at 280 ^{o}C and the septum purged at 5 mL/min. The GC was operated in splitless mode with 1 mL/min column flowrate using helium as a carrier gas. 2 µL of sample was injected and a blank methanol injection was performed following each extract using a shortened runtime of 5 minutes: the column temperature was 200 ^{o}C which was then increased at 50 ^{o}C/min to 300 ^{o}C where it was held for 3 minutes, making the total analysis time per sample 20 minutes.

The mass spectrometer was operated in single ion monitoring mode with the following ions monitored: salbutamol *m/z* **369** and 86, and d3-salbutamol *m/z* **372**, with ions indicated in bold used for quantification. A dwell time of 200 ms was used for each ion. The transfer line to the mass spectrometer was heated to 280^{o}C, the source temperature was maintained at 230 ^{o}C and the quadrupole at 150 ^{o}C.

5.2.5 Setup of calibration lines

For calibration, DBS were prepared by spotting 10 µL of salbutamol spiked whole blood at concentrations of 5, 7.5, 10, 15, 20, 50 and 100 ng/mL onto Whatman 903 Protein Saver blood cards. Three replicates per concentration were produced in this manner and two additional replicates were carried out at the concentrations of 5, 20 and 100 ng/mL for the calculation of assay accuracy and precision.

VAMS samples were prepared by wicking of 10.1 µL of salbutamol spiked whole blood at concentrations of 5, 7.5, 10, 15, 20, 50 and 100 ng/mL. Three calibration lines were produced in this manner on separate days to assess inter-day variation. Two additional replicates were carried out at the concentrations of 5, 20 and 100 ng/mL for the calculation of assay accuracy and precision.

For analysis of dried blood samples, d3-salbutamol internal standard was added after extraction with methanol, followed by evaporation to dryness and derivatisation as described in section 5.2.3. For both sampling methods, precision was determined for the three calibration concentrations using the relative standard deviation (RSD) of the analyte peak area ratioed to the internal standard peak area and accuracy by the deviation at the measured concentration from the calibration determined true value (also internal standard ratioed). Recovery was determined by reference of the extracted dried blood sample spiked with salbutamol to its reference salbutamol solution in methanol (5, 20 and 100 ng/mL). For preparation of the reference solutions, 10 µL of salbutamol at 5, 20 and 100 ng/mL in methanol and 180 pg d3-salbutamol internal standard (3 µL of 60 ng/mL in methanol) were placed in insert GC vials, evaporated to dryness and derivatised. Five replicates for each concentration were carried out.

5.2.6 Assessment of drying time and storage stability

The effect of drying time was assessed for the blood samples spiked with salbutamol and collected both as DBS and onto VAMS devices in triplicate for three concentrations (5, 20 and 100 ng/mL) by leaving them at room temperature (20 °C) in the dark for 2 hours and stored for up to 96 hours.

The storage stability of the blood samples spiked with salbutamol collected onto VAMS devices was further assessed by storage in triplicate at room temperature (20 ^{o}C), in the fridge (4 ^{o}C), freezer (-20 ^{o}C) and oven (approximately 30 ^{o}C) for up to 5 months. The samples were stored in polystyrene bags with desiccants before sample processing.

Post-preparative stability was also examined by storage of triplicate derivatised samples in capped GC insert vials for up to 72 hours at room temperature, in the fridge and in the freezer.

5.2.7 Volunteer sample preparation

Three healthy adult male volunteers were administered 1 mg of salbutamol via a 100 µg per dose inhaler and spacer device. This dose was chosen to be in the mid-therapeutic range to be representative of doses administered by athletes for therapeutic use. Blood samples were collected pre-dosing and then similarly at 5, 10, 15, 30, 45, 90 and 120

minutes post salbutamol administration in triplicate. Peripheral capillary blood was collected from fingertips using a safety lancet and collected straight onto VAMS devices. Samples were then left to dry for at least 2 hours before sealing in a polystyrene bag with desiccant. For analysis, d3-salbutamol internal standard was added after extraction with methanol, followed by evaporation to dryness and derivatisation as described in section 5.2.3. Ethical approval was through the University of Leicester - Ethical Application Ref: hp28-3885.

5.3 Results

5.3.1 GC-MS analysis - DBS versus VAMS

GC separation was able to obtain good chromatographic resolution of salbutamol from other blood constituents. By reducing the sample clean-up to the bare minimum, sample throughput can be maximised but this also led to more interfering peaks in the resultant chromatograms (Figure 5.2). Both the main Figure 5.2 and its insert show that the salbutamol peak around the retention time of interest (8.05 minutes) is well separated from the majority of the noise. The profile of the VAMS samples (black curve) showed less interference than the DBS samples (red curve), which reduced the build-up of contaminants on the GC column. The insert in Figure 5.2 further presents the signal to noise (S/N) ratio for the chromatograms shown. For DBS, the average lower limit of quantitation (LLOQ) was determined to be 7.5 ng/mL (S/N 10:1, meeting accuracy and precision limits of $\leq$20%) and the limit of detection (LOD) to be 5 ng/mL (S/N > 5:1). For VAMS samples, the average LLOQ was determined to be 5 ng/mL (S/N 10:1, meeting accuracy and precision limits of $\leq$20%)) and the LOD to be 3 ng/mL (S/N > 3:1). VAMS offered improved S/N owing to lower interference levels, but more importantly offers simpler and easier blood collection. Method development was therefore focussed on VAMS as the blood collection method.

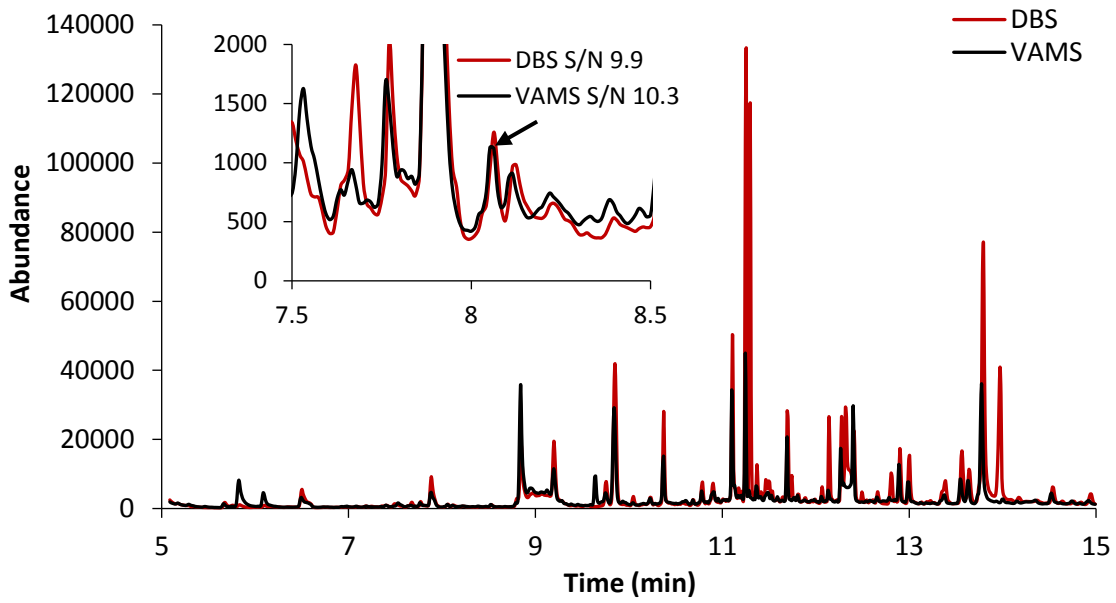

Figure 5.2. GC-MS analysis of blood spiked with 5 ng/mL salbutamol (LOD for DBS and LLOQ for VAMS), collected as DBS and onto VAMS devices. The insert shows the S/N ratio at the retention time of interest (8.05 minutes, indicated by the black arrow).

5.3.2 Optimisation of extraction and derivatisation

The small sample volume used for DBS/VAMS offers major advantages in terms of sample collection, but also poses a serious problem in obtaining sufficient sensitivity for quantitative analysis. Efficient sample recovery and in the case of GC-MS analysis, derivatisation, is therefore vital for assays. Derivatisation of salbutamol is a necessary step for its analysis by GC-MS to improve its volatility and chromatographic performance. Formation of a single derivative is preferable to obtain maximal sensitivity and specificity. Caban et al. investigated in some detail a variety of derivatisation techniques for the analysis of a mixture of β-blockers and β-agonists (including salbutamol) and found that trimethylsilylation (to produce salbutamol tri-*O*-TMS) was the most effective for derivatising the target compounds [332]. The use of MSTFA or BSTFA often in combination with the catalyst TMCS to produce a single analyte product with high conversion efficiency was found to be a good choice for salbutamol analysis [326, 327, 340]. For this study keeping the total derivatisation volume low was crucial to obtain maximal sensitivity, so a volume of 25 µL of 99% BSTFA + 1% TMCS was used for sample re-suspension/derivatisation post methanol extraction and evaporation to dryness.

Solvents employed for DBS extraction are commonly organic solvents such as methanol and acetonitrile and have been investigated previously [77, 200]. A limited number of studies, however, have looked at extracting analytes from VAMS devices. Three potential solvents were investigated here; methanol, acetonitrile and ethyl acetate. Figure 5.3 shows that the most favourable recoveries were achieved using methanol as the extraction solvent in this study, which has also been used successfully in previous studies using VAMS [188, 341]. Therefore, methanol was selected for both the salbutamol extractions from DBS onto cards and from the VAMS devices using a volume of 300 µL.

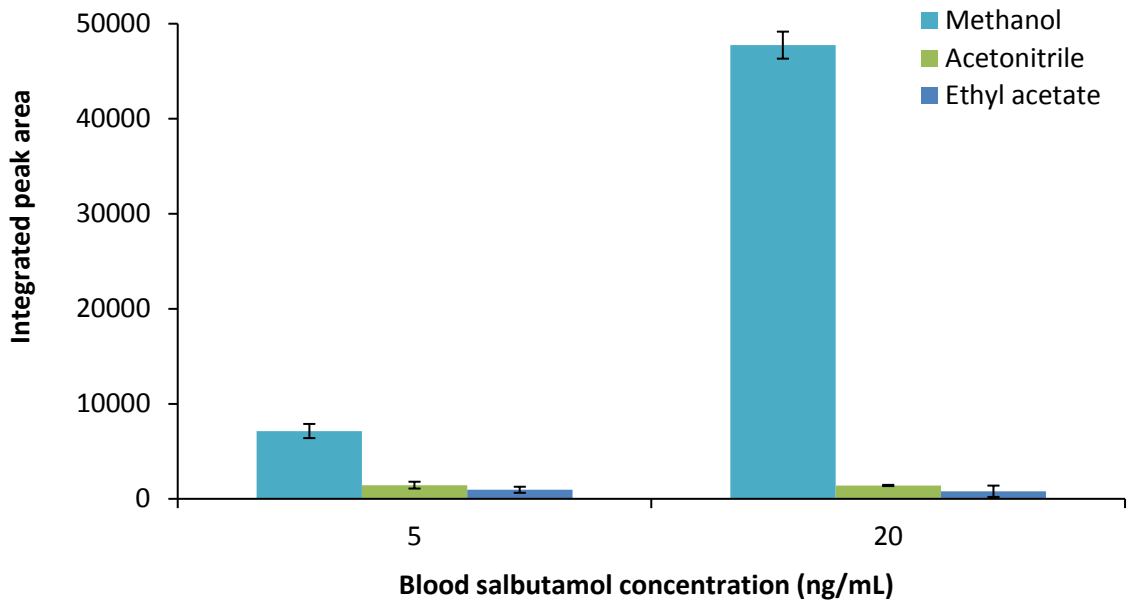

Figure 5.3. Effect of extraction solvent on the recovery of salbutamol collected onto VAMS devices (n=3).

5.3.3 Calibrations and assay evaluation

To assess the reliability of the method, precision, accuracy and recovery were tested at three salbutamol concentrations spread across the calibration range (5, 20 and 100 ng/mL) in blood. Linearity of the calibrations was proven by backward calculations. A short assessment of the assay using DBS was carried out, whereas the use of VAMS devices was subjected to a more comprehensive method appraisal based on the bioanalytical validation guidelines of the US Food and Drug Administration [339, 342, 343], specifically to the first version set out in 2001.

For DBS, the precision and accuracy fell within 15% (within 20% for the LLOQ) for all three concentrations (Table 5.2).

Table 5.2. Intra-day precision, accuracy and recovery of the GC-MS method determined for DBS created with salbutamol spiked blood.

		Intra-day	
Blood salbutamol concentration (ng/mL)	Precision (RSD %)	Accuracy (%)	Recovery (%) and CV
5 (LOD)	4.5	118	78.9 (±11.1)
20	9.0	104	80.5 (±4.3)
100	4.1	100	99.8 (±6.2)

The relatively simple extraction procedure gave an average extraction efficiency of 86% across the calibration range. A relatively wide calibration range (5-100 ng/mL) was used with 7 concentrations in order to allow for the different blood levels predicted for athletes during competitions (Figure 5.4). High concentrations were also included for possible other applications such as children dosed with high levels of salbutamol during asthma attacks [280] or toxicology cases such as those outlined in Table 5.1 with salbutamol levels detected up to 1690 ng/mL.

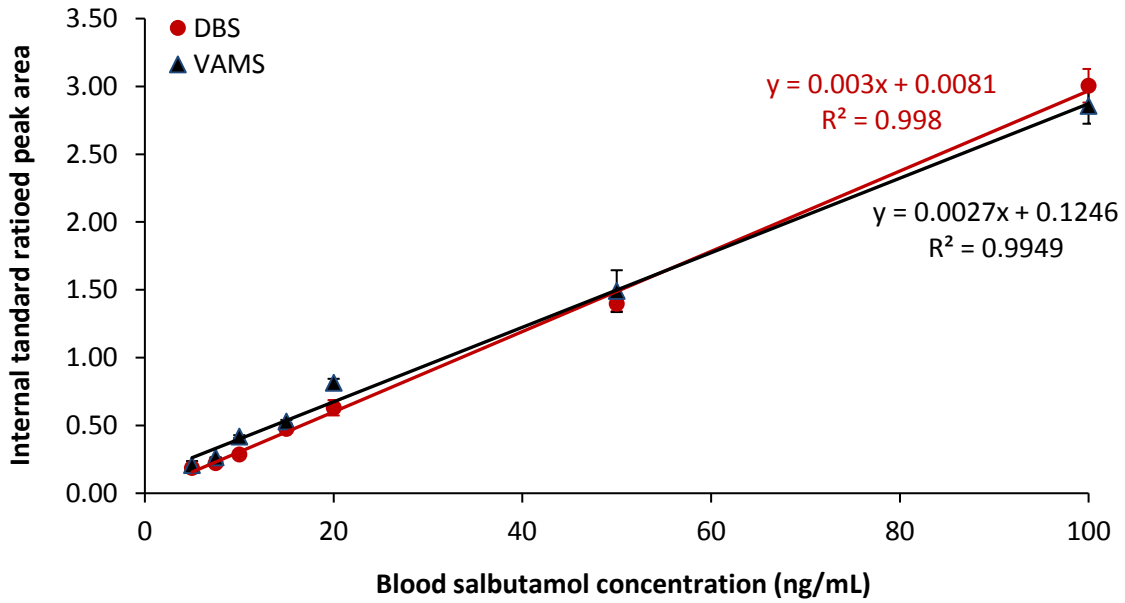

Figure 5.4. Sensitivity and linearity of the GC-MS method for analysis of salbutamol spiked blood collected as DBS and onto VAMS devices (n=3, except for the concentrations used to determine accuracy, precision and recovery where n=5 was used).

The basic evaluation of the assay using DBS demonstrated the potential for the application to the reliable quantification of salbutamol from micro-volumes of blood. However, owing to the inherent advantages of the VAMS technique this was investigated more thoroughly. Both inter- and intra-day calibrations were assessed for the assay using VAMS (Table 5.3). Precision and accuracy were tested independently on three occasions and all fell within acceptable limits (≤15%, or ≤20% at LLOQ). The reproducibility over multiple analysis days was demonstrated with an inter-day precision of <20% at the LLOQ and <15% for the mid and high concentrations tested. Again, the wide concentration range was chosen for calibration to cover sub-therapeutic levels (up to 5 ng/mL), the beginning of the therapeutic range (5-20 ng/mL), into the toxic range which can begin as low as 30 ng/mL in adults with a putative lethal level of 160 ng/mL [344].

Table 5.3. Intra-day precision and accuracy as well as inter-day precision and recovery of the GC-MS method determined for salbutamol spiked blood samples collected onto VAMS devices.

	Intra-day (n=5)						Inter-day (n=3)	
Blood salbutamol concentration (ng/mL)	Precision (RSD %)			Accuracy (%)			Precision (RSD %)	Recovery (%) and CV
5 (LLOQ)	6.5	2.9	5.5	106.9	114.9	106.2	9.0	62.7 (±11.9)
20	6.8	8.5	9.7	103.7	102.8	87.3	1.2	59.4 (±0.7)
100	7.8	4.5	6.4	100.4	103.1	98.7	5.3	80.9 (±4.5)

5.3.4 Effect of drying time and storage stability

Although not often considered in the past as an important factor in DBS method validation, evidence is emerging that drying time can have a significant effect on the recovery of analytes from DBS [345]. Figure 5.5 shows that in this study there was indeed some variation in the recovery of salbutamol from DBS by varying the drying time. The recovery was stable until 6 hours of drying after which a significant decrease in recovery was observed for the salbutamol concentrations of 5 and 20 ng/mL. However, the samples spiked with 100 ng/mL salbutamol only showed a significant decrease after 12 hours of drying.

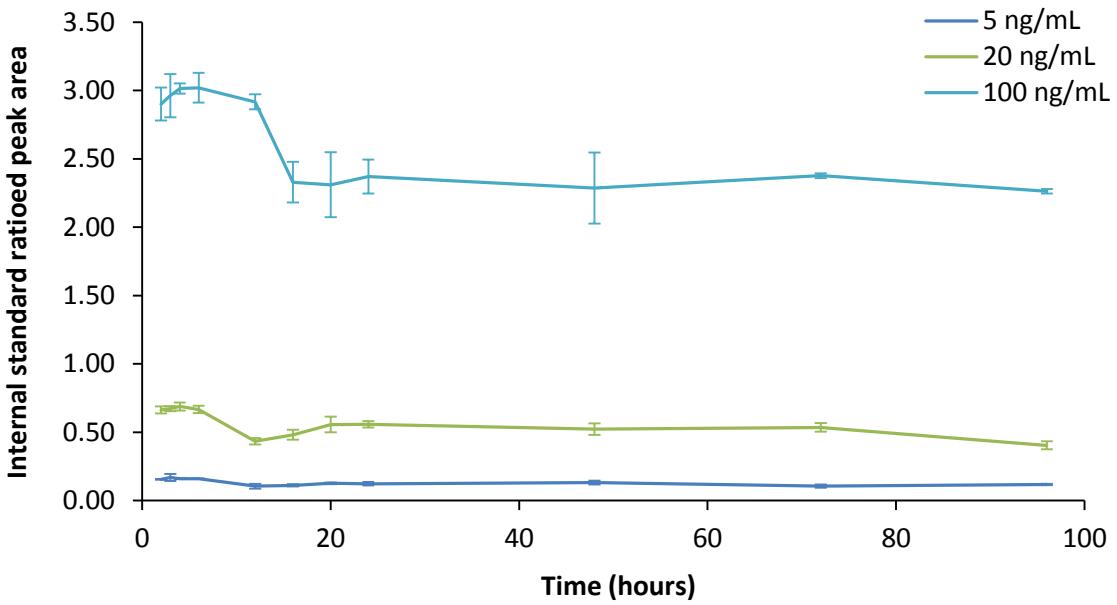

Figure 5.5. Effect of drying time on recovered salbutamol (mean±sd) from DBS (n=3).

Blood spiked with 5 ng/mL salbutamol collected onto VAMS devices showed a significant decrease in stability after only 4 hours of drying. For samples spiked with 20 ng/mL and 100 ng/mL salbutamol, a slightly increased stability compared to DBS was found with a significant decrease only occurring after 20 hours of drying. Figure 5.6 and Figure 5.7 show the effect of drying time on recovered salbutamol spiked in blood and collected by VAMS.

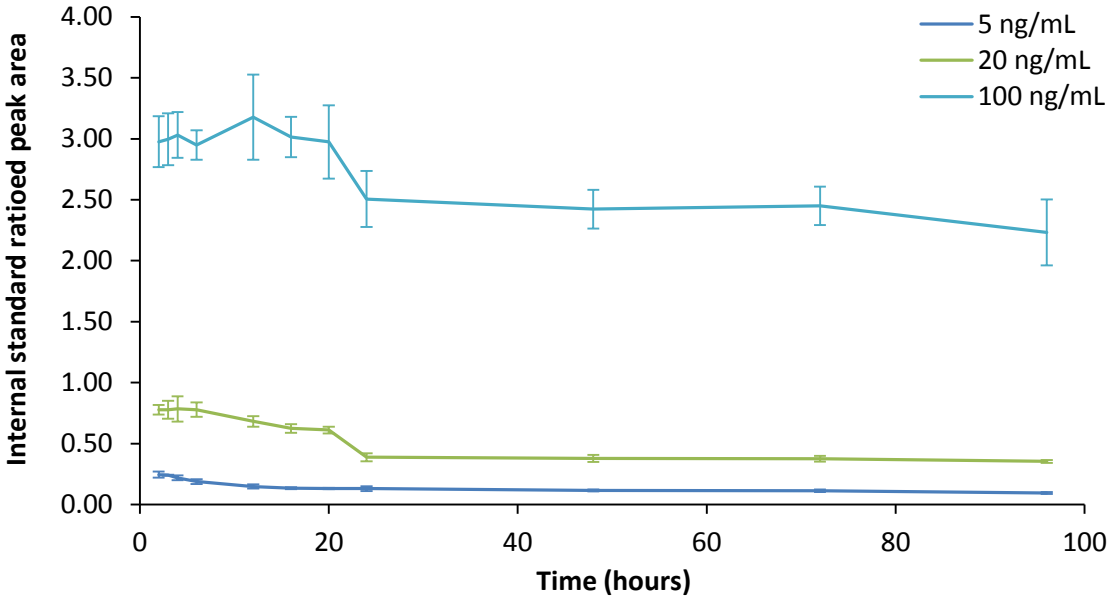

Figure 5.6. Effect of drying time on recovered salbutamol (mean±sd) from blood collected onto VAMS devices (n=3).

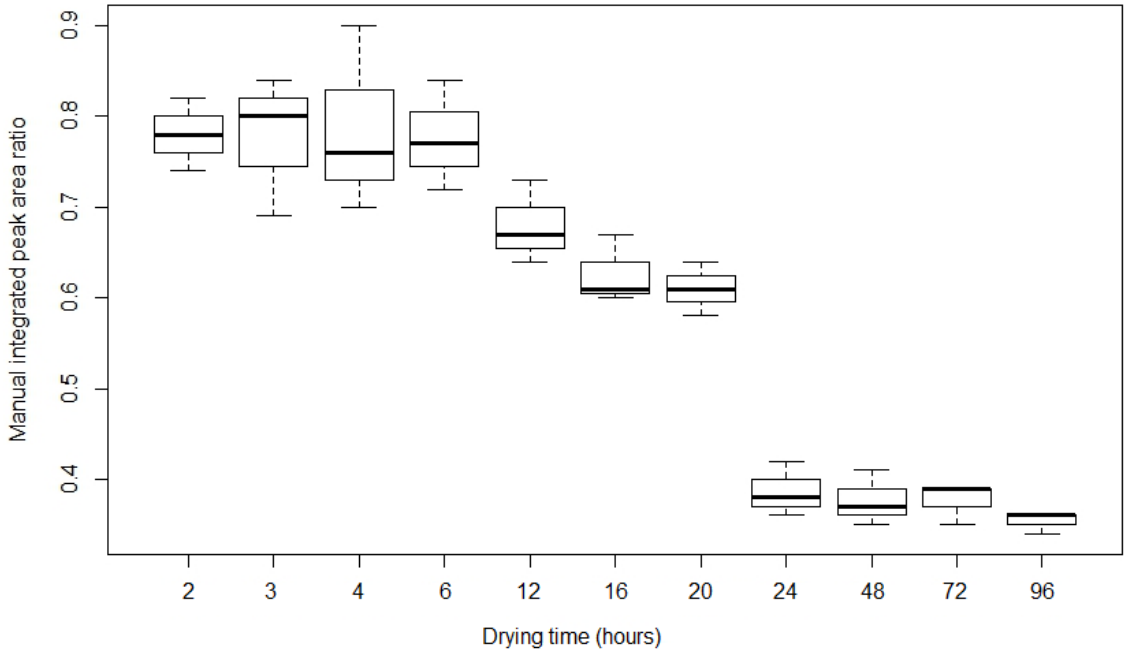

Figure 5.7. Effect of drying time on recovered salbutamol (mean±sd) from blood spiked with 20 ng/mL salbutamol and collected onto VAMS devices (n=3).

These data demonstrated that drying time is an important factor to control in designing DBS/VAMS assays in the future and for the implementation of the assay presented here. To ensure a constant recovery, drying time should be kept constant. Or alternatively as recommended by Koster et al. exceeding a minimum drying time in order to stabilise the samples and analyte recovery, e.g. 24 hours for the six immunosuppressants tested in their study [345]. The samples prepared for calibration experiments in this study were all dried for 2-3 hours to ensure a constant recovery. The samples from the healthy volunteers were dried minimally for 24 hours, representative for scenarios such as doping testing at sport events.

In order to ensure the integrity of the samples collected onto VAMS devices, spiked blood samples were stored for up to 145 days in a range of temperatures from -20 ^{o}C to 30 ^{o}C. The baseline immediate recovery achieved for the 20 ng/mL salbutamol spiked blood samples was 59% as shown in Table 5.3. Table 5.4 shows similar recoveries for the long-term stored samples. For all temperatures tested a similar recovery was found up to 145 days.

Table 5.4. Recovery of 20 ng/mL salbutamol from spiked blood collected onto VAMS devices after long-term pre-extraction storage (n=3).

	Recovery % and CV for pre-extraction storage		
Storage conditions	30 days	75 days	145 days
Freezer (-20°C)	57.0 (±4.0)	55.1 (±3.7)	53.1 (±6.4)
Fridge (4°C)	61.1 (±4.4)	63.5 (±2.6)	67.2 (±6.6)
Room temperature (21°C)	50.3 (±0.9)	59.7 (±8.6)	65.1 (±6.1)
Oven (30°C)	41.5 (±0.3)	57.7 (±5.5)	51.0 (±7.9)

Post-preparative recovery was also good for the 3-day time span tested, with similar recoveries for the different temporarily post-preparative storage conditions tested as shown in Table 5.5.

Table 5.5. Recovery of 20 ng/mL salbutamol from spiked blood collected onto VAMS devices after post-extraction storage (n=3).

	Recovery % and CV for post-extraction storage		
Storage conditions	1 day	2 days	3 days
Freezer (-20°C)	68.9 (±5.9)	66.7 (±9.6)	67.2 (±7.2)
Fridge (4°C)	69.4 (±6.3)	77.3 (±10.0)	86.6 (±5.9)
Room temperature (21°C)	57.0 (±7.2)	59.5 (±2.0)	67.5 (±4.9)

5.3.5 Volunteer samples

Salbutamol concentrations were successfully measured from capillary blood collected onto VAMS devices from three healthy volunteers administered with salbutamol. The dose used was chosen to be in the mid-therapeutic range for adults to test the suitability of the method for sport doping testing. The profiles in Figure 5.8 shows that the maximum concentration (C_{max}) of salbutamol was detected in samples taken between 10-20 minutes (T_{max}). C_{max} ranged from 7.3 ng/mL to 23 ng/mL and blood salbutamol levels up to 2 hours post administration could still be detected and quantified. Two samples were being classified as above the therapeutic range (>20 ng/mL), but below the toxic range (<30 ng/mL). The other samples fell within the therapeutic range or at least above LOD (grey area of Figure 5.8).

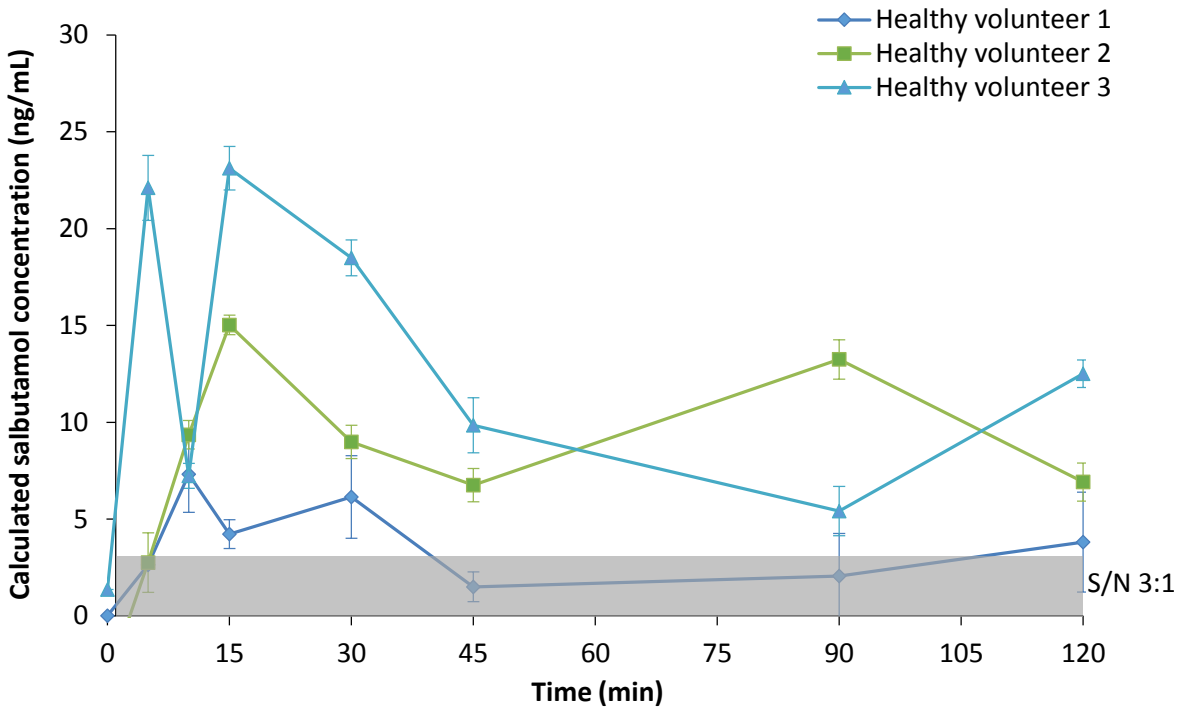

Figure 5.8. Analysis of capillary blood samples collected in triplicate onto VAMS devices from three healthy male volunteers dosed with 1 mg of salbutamol by inhalation. Samples were spiked with 180 pg of internal standard, then extracted with methanol, dried and derivatised (n=3). The grey area shows estimations of salbutamol concentrations below the method's LOD (3 ng/mL) for blood samples collected onto VAMS devices.

The salbutamol levels detected for volunteer 1 were comparable to those measured by several studies when considering that the dose administered here was 1 mg [316, 318, 320]. The salbutamol levels detected for volunteer 2 and 3 were up to 2.8 times as high as measured by previous studies using DBS instead of VAMS [316, 318, 320]. A study by Elers et al. showed that 8 mg of salbutamol administered orally resulted in serum levels of 18.77 ng/mL, but much lower levels (C_{max} of 1.75 ng/mL with a T_{max} at 1 hour) for the volunteer samples after administering similar salbutamol doses by inhalation [329]. Low levels of salbutamol in blood after inhalation (C_{max} of 2 ng/mL with a T_{max} between 25 and 50 minutes) have also been observed in the study of Schmekel et al. [322]. The profile of the blood salbutamol concentration observed was similar as reported previously [316, 318, 320], with a sharp initial spiking in concentration (10-15 minutes) followed by a rapid decrease which tails off leaving elevated salbutamol levels several hours post administration.

Whereas venous blood was used for the method development and assessment experiments, capillary blood was used for the measurements of healthy volunteers after

administration of salbutamol. Venous blood was chosen for the method development and assessments experiments owing to the quantity of blood needed for those experiments. Previous work has demonstrated that there is no significant difference between whole blood and capillary samples for a selection of forensically relevant analytes [36]. As salbutamol partitions 1:1 in blood to plasma, similar results were expected leading to no implications for sport doping testing using capillary blood [305, 346].

The volunteer study showed that the developed method would allow frequent sampling for the application in sport doping testing or other cases. The low invasiveness of the sampling technique and the very small blood volumes required makes the assay particularly suitable for application to monitor the relationship between administered doses and blood concentrations of salbutamol in- and out-of-competition.

5.4 Concluding remarks and future perspectives

The quantification of salbutamol from conventional DBS collected onto cards using a fixed volume of blood was compared to blood samples collected with the novel VAMS device to ease sample collection. A GC-MS method was developed for the quantification of salbutamol and the GC-MS chromatograms showed less interference for blood samples collected onto VAMS devices than for DBS. Better LLOQ, LOD and S/N were also found for salbutamol spiked blood samples collected onto VAMS devices compared to DBS samples. The method met accuracy and precision limits for both DBS and VAMS samples according to the bioanalytical validation guidelines of the US Food and Drug Administration.

This was the first time that VAMS was used with a GC-MS method for the quantification of salbutamol levels from micro-volume blood samples. Volumes of 10 µL capillary blood were collected, which is a reduction compared to the 20 µL DBS samples spiked with salbutamol and analysed by UHPLC previously. The sensitivity of the developed GC-MS method was sufficient to allow its application for the measurement of blood salbutamol levels for up to 2 hours post administration of 1 mg of salbutamol to three healthy volunteers. The developed method would be applicable to monitor blood salbutamol concentrations in athletes where reduced invasiveness sampling and

a low sample volume are preferable. The method also facilitates frequent blood sampling in order to quantify salbutamol blood concentrations both in- and out-of-competition. As the pharmacokinetics of blood could change with exercise, it would be interesting to change the design of future studies by having the volunteers exercise instead of sampling them while passively sitting still during the experiment.

6 Pseudoephedrine testing by volumetric absorptive micro-sampling of blood and breath sampling

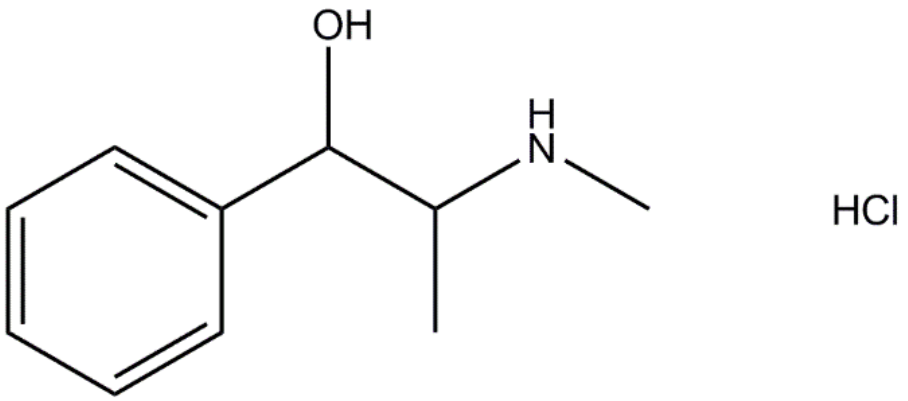

Pseudoephedrine hydrochloride (MW 166.12 g/mol)

A special thanks goes to Sophia Mirmigkou (University of Leicester, INTREPID Forensics and Department of Chemistry) for designing the breath study and carrying out the breath sampling. Dr. Michael Wilde and Luke Bryant are gratefully acknowledged for their help with the breath data analyses (University of Leicester, Department of Chemistry). Prof. Mario Thevis (German Sport University Cologne, Institute of Biochemistry, Center for Preventive Doping Research) is gratefully thanked for the analysis of the blood samples at his facilities.

6.1 Introduction

Pseudoephedrine ($C_{10}H_{15}NO$) is a sympathomimetic drug mainly used as a nasal decongestant to relieve the symptoms of allergies, the common cold and infections such as influenza [347, 348]. Increased blood pressure and heart rate, redistribution of blood, respiratory stimulation, relaxation of digestive tract muscles and vasodilation of skeletal muscles are all additional effects of the drug [349]. Pseudoephedrine is sold over-the-counter in the United Kingdom under brand names such as Sudafed, but legislation in other countries differs from being available on prescription to classification as controlled drug in the misuse of drugs acts [350-352]. Administration is commonly orally by taking tablets containing pseudoephedrine salts such as pseudoephedrine hydrochloride (Figure 6.1).

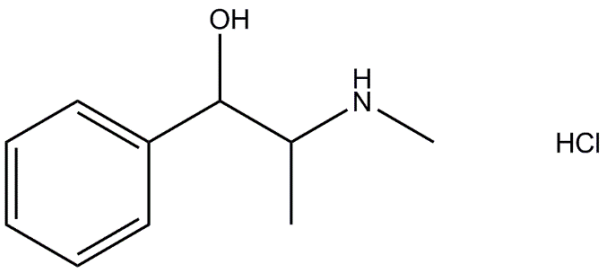

Figure 6.1. Chemical structure of pseudoephedrine hydrochloride (MW 166.12 g/mol).

Pseudoephedrine occurs naturally in certain *Ephedra* plant species [353], but the main production for commercial use is by manufacturing [354, 355]. Aside from its pharmaceutical production, pseudoephedrine has also been reported as a precursor to illicitly produced methamphetamine [355, 356] as shown in Figure 6.2.

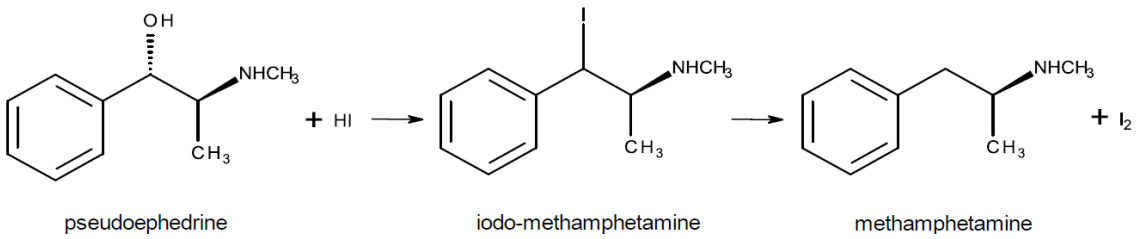

Figure 6.2. Reduction of pseudoephedrine via hydrogen iodide (HI) to produce methamphetamine [356].

In addition to its therapeutic effects, pseudoephedrine has been reported to be abused as a recreational drug [357], as appetite suppressant [358] and to enhance performance in sports [349, 359, 360]. Between 2004 and 2010, pseudoephedrine was temporarily removed from the prohibited list of the World Anti-Doping Agency (WADA). During this period, there was an increase in the number of samples tested positive for pseudoephedrine in sport doping testing [361]. Since 2010, the WADA has set an urine threshold for pseudoephedrine in-competition at 150 µg/mL [289]. However, concentrations exceeding this limit have been found after administration of a therapeutic dose of 240 mg pseudoephedrine by healthy volunteers [361]. Urine concentrations exceeding the WADA limit have also been found in several big sport events such as the Olympic Games [290] and 9 breaches of the limit have been found in athlete's samples tested for pseudoephedrine by the WADA in 2015 [362].

As outlined in Chapter 1, the analysis of analytes from urine samples comes with drawbacks such as the limited possibility of multiple collections from one person, time restrictions for collections e.g. during competitions, and the need for both advanced storage and shipping conditions. Blood samples could be an alternative for doping testing, but trained medical personnel are needed for conventional venous sampling. In addition, venous blood collection is also invasive and both advanced transport and storage requirements need again to be considered. Dried blood spots (DBS) could offer a valuable alternative as its collection is simple, quick, less invasive and potentially cost saving. Additional advantages of DBS are that multiple samples can be collected easily owing to its reduced sample volume and method of collection, regular post can be used for transportation and samples can be stored at room temperature with enhanced stability of many analytes compared to venous blood and/or urine samples. A number of assays have been developed for the measurement of pseudoephedrine from whole blood, plasma and serum [363-370], including three for DBS by liquid chromatography tandem mass spectrometry (LC-MS/MS) [83, 150, 371].

In this study, the suitability of a volumetric absorptive micro-sampling (VAMS) device was investigated for the quantification of pseudoephedrine from micro-volumes of capillary blood. Small adaptations were made to the method published by Tretzel et al. for the quantification of pseudoephedrine from DBS using LC-MS/MS with heated electrospray ionisation (LC-HESI-MS/MS) to analyse pseudoephedrine from blood

sampled onto VAMS devices [83]. The devices have been successfully employed in a similar study for quantitative analysis of cathinone analogues in dried urine, plasma and oral fluid samples [81]. VAMS devices further ease sample collection compared to DBS collection, thereby making them suitable for multiple in- and out-of-competition testing. The volume of blood needed for analysis was reduced from 20 µL DBS used previously to 10.1 µL of capillary blood in this study. This further reduction can be important for the application to (forensic) toxicology cases including those with PM blood, traffic controls for driving under the influence of drugs to avoid the need of medical personnel, cases where repeated sampling is needed such as sport doping testing, but also in paediatric clinical cases where the quantity of blood is a limiting factor [372].

In addition, breath samples were taken in parallel with the micro-volume blood samples from healthy volunteers dosed with pseudoephedrine hydrochloride to investigate if pseudoephedrine hydrochloride and/or its metabolic products such as its main metabolite cathine ($C_9H_{13}NO$) could be detected as volatile organic compounds (VOCs). A clinical trial of Skoglund et al. reported that exhaled breath was the preferred specimen to donate over blood and urine according to interview data [198]. They showed that exhaled breath captured more recent drug administration compared to plasma and urine, which is advantageous for sport doping testing in- and out-of-competition. Breath consists mainly of nitrogen (~74%), oxygen (~15%), water vapour (~6%), carbon dioxide (~5%) and some inert gases, but the mixture also consists of trace volatile metabolites [373]. Endogenous VOCs are released by (patho)psychological processes and transported from blood to the lungs where they are exhaled in breath. VOCs have mainly been studied in breath samples to examine biomarker profiles for disease monitoring [374]. In this discovery study, potential biomarkers for pseudoephedrine intake and breath pharmacodynamics were investigated.

Various techniques are in use for breath analysis, with gas chromatography mass spectrometry (GC-MS) analysis being the gold standard [375]. However, other MS techniques such as proton transfer reaction mass spectrometry (PTR-MS), selected ion flow tube mass spectrometry (SIFT-MS), laser spectrometry and ion mobility spectrometry allow real-time measurements with limited sample preparation and shorter analysis time [376-379]. In this study, a proton transfer reactor combined with

a time-of-flight mass spectrometer (PTR-ToF-MS) was used to analyse breath samples collected by forced incentive exhalation [380, 381]. A trial was also performed with breath samples collected onto sorbent tubes using two-dimensional gas chromatography coupled to a flame ionisation detector and quadrupole mass spectrometer (GCxGC-FID/qMS).

PTR-ToF-MS allows simultaneous non-invasive measurement of multiple mass channels in real-time, which is useful for this non-targeted study. In PTR-ToF-MS, hydronium ions (H_3O^+, *m/z* 19) are produced in the hollow cathode of the PTR compartment by ion-neutral reactions with water vapour (Equation 6.1). Exothermic proton transfer reactions can then occur in the flow drift tube between the H_3O^+ ions and breath sample VOCs (Equation 6.2; neutral volatile compounds having a proton affinity higher than H_2O represented by R, here specifically pseudoephedrine and its metabolic products as the analytes of interest). The entire process results in soft ionisation, which makes the resulting spectra easier to interpret.

Equation 6.1

$$H_2O^+ + H_2O \rightarrow H_3O^+ + OH$$

Equation 6.2

$$H_3O^+ + R \rightarrow RH^+ + H_2O$$

The sorbent tubes used in the GCxGC-FID/qMS trial allow the portability and storage of samples, the possibility for collecting multiple samples at once and they add sensitivity by concentrating larger volume samples. It takes a few minutes longer to collect breath samples onto sorbent tubes than collection with the breath sampler connected to the PTR-ToF-MS, but the method of collection is not forced and therefore less intensive for the person being sampled. Lastly, the GC technique has the advantage of compound separation and of identification over PTR-ToF-MS and two-dimensional GC increases the separation and identification.

As breath and VAMS samples are both unconventional sample types, VAMS results were compared to DBS results from the literature [83]. A few venous blood samples were also collected from one volunteer onto VAMS devices for comparison

with the capillary blood samples collected by VAMS. To further investigate potential biomarkers in breath and a pharmacodynamic profile after pseudoephedrine hydrochloride intake, the PTR-ToF-MS results were compared with the results of the GCxGC-FID/qMS trial. Although previous studies have analysed pseudoephedrine from volunteers using micro-volume blood samples, this is the first time it has been carried out using VAMS and with a higher pseudoephedrine hydrochloride dose. The adapted DBS method was validated according to WADA regulations for urine and plasma [382]. This is also the first time that breath profiles were evaluated in real-time after the administration of pseudoephedrine hydrochloride.

6.2 Experimental design

6.2.1 Chemicals and materials

C_8-C_{20} n-alkanes standard solution, Japanese Indoor Air Mix (JIAM), methanol (MeOH, SupraSolv), phenanthrene-d_{10} certified reference solution and toluene-d_8 certified reference solution were purchased from Sigma Aldrich (Poole, UK). Calibration standard (NJDEP EPH 10/08 Rev.2) was purchased from Thames Restek (Saunderton, UK). K_3-EDTA vacuum tubes were purchased from Vacutest Kima (Arzergrande, Italy). Facemasks with electrostatic filters were purchased from Owlstone Medical (Cambridge, UK). n-octane-d_{18} (99%) was purchased from Cambridge Isotope Laboratories (Leicester, UK). Polypropylene mouth pieces with electrostatic filters and nose clips were purchased from GVS Filter Technology UK Ltd (Morecambe, UK). Safety lancets were purchased from Medscope (Cirencester, UK). Sorbent tubes (Tenax/Ta with Carbograph 1 TD, Hydrophobic), brass caps and Diff-Lok caps were purchased from Markes International Ltd (Llantrisant, UK). Sudafed decongestant tablets containing 60 mg pseudoephedrine hydrochloride (McNeil Products Ltd, Maidenhead, UK) were purchased over-the-counter from a local pharmacy (Leicester, United Kingdom). VAMS devices (brand name Mitra™) were purchased from Neoteryx LLC (Torrance, CA, US).

6.2.2 Administration of pseudoephedrine to healthy volunteers

Twelve healthy volunteers (8 male, 4 females), not part-taking in any doping programme and not taking any other medication, were administered 2 tablets of Sudafed containing

60 mg pseudoephedrine hydrochloride each. Triplicate capillary blood and breath samples were collected in parallel pre-administration and then similarly at 0.5, 1, 1.5, 2, 4, 4.5, 5, 5.5 and 6 hours post Sudafed administration. Two volunteers also donated breath samples at the same sampling time points without administration of pseudoephedrine hydrochloride tablets. Seven volunteers donated additional blood samples 24 hours post-administration. Venous blood was collected additionally from one volunteer pre-administration and at 2 and 6 hours post-administration. Ethical approval was through the University of Leicester – Ethical Application Reference: sm819-6318 and tsev1-9545.

6.2.3 Blood collection

Capillary blood was obtained from fingertips using safety lancets. The first droplet of blood was wiped away and 10.1 µL of blood (calculated average wicking volume as specified on the certificate of performance) was then collected straight onto a VAMS device by allowing the blood to wick up into the tip until it was completely coloured. Three venous blood samples were collected onto VAMS devices by holding the tips just below the surface of the venous blood in the vacuum tubes. All VAMS samples were left to dry for approximately 2 hours before sealing in a polystyrene bag with desiccants and storage in a fridge until shipping.

6.2.4 Preparation and LC-MS/MS analysis of blood samples collected by VAMS

VAMS samples were shipped to the Center for Preventive Doping Research (Cologne, Germany) and further stored in a fridge prior to analysis. An in-house developed method for the analysis of pseudoephedrine and two other compounds from DBS cards was adapted for its application to VAMS devices [83]. The VAMS samples in this study consisted of half the volume of blood and the pseudoephedrine concentration in blood was expected to be 4 times as high compared to the DBS in the study from Tretzel et al. [83]. The method was validated according to WADA regulations for plasma and urine with pseudoephedrine concentrations up to 1000 ng/mL [382]. In summary, VAMS tips were detached and transferred to Eppendorf tubes before extraction by sonication for 60 minutes. The extraction mixture consisted of 100 µL MeOH and 400 µL tert-butyl

methyl ether plus 5 µL ephedrine-d3 as internal-standard. A second extraction was performed by sonicating the organic phase and 400 µL acetone in a new polypropylene tube for 30 minutes. The supernatants were combined and evaporated to dryness using a vacuum centrifuge set at 45 °C. The dry residue was resuspended in 50 µL acetonitrile-water (50:50 v/v) and centrifuged for 5 minutes at 13000x*g*.

5 µL of sample was loaded onto a Hypersil Gold C18 analytical column (50 x 21 mm, with 1.9 µm particle size, Thermo Scientific, Bremen, Germany). Chromatographic separation was achieved by a 16 minutes gradient composed of solvent A (0.2% formic acid in H_2O) and solvent B (0.2% formic acid in acetonitrile). The gradient started with 1% B (0-1 min), followed by an increase to 99% B (2-11 min) and re-equilibration to starting conditions 1% B (12-16 min). LC-HESI-MS/MS analysis was performed using a Thermo Dionex Ultimate 3000 LC interfaced to a Q Exactive Plus MS using a heated electrospray ionisation (HESI-II) source (Thermo Scientific, Bremen, Germany). Ionisation was obtained in positive mode at a spray voltage of 4.0 kV and the collision energy set at 30. The HESI-II source temperature was set to 350 °C and the transfer capillary to 320 °C. Measurements were performed in targeted MS/MS mode with *m/z* 166.1226 being monitored as the precursor ion and *m/z* 117.0701, 133.0887 and 148.116 as product ions, full scans were acquired additionally as in parallel reaction monitoring [383, 384]. The resolution was set to 30,000 full width at half maximum at *m/z* 200 and the precursor isolation window was adjusted to 1.5 *m/z*.

6.2.5 Breath sample collection using PTR-ToF-MS

Breath samples were collected in real-time by breathing through a mouth piece connected to a Loccioni GS/-S single breath sampler (Loccioni Group, Ancona, Italy). Volunteers were asked to exhale with full capacity for 30 seconds after putting on a nose clip. The Loccioni breath sampler was connected to a PTR-ToF-MS (Kore Technology, Ely, UK) as shown separately in Figure 6.3. Mass spectra were acquired over the range *m/z* 0-230 and the sampling flowrate was set to 200 mL/min.

Figure 6.3. Breath sampling setup consisting of the breath sampler with sampling tube (left) and PTR-ToF-MS (right) [385, 386].

Figure 6.4 further shows a schematic of the PTR-ToF-MS instrument. The total ion yield passes to the ToF pulser source, which results in ions being directed perpendicularly through the flight tube to enter the reflectron. Within the reflectron, the ions are separated by their flight time which is directly convertible to their mass to charge ratio (*m/z*). Finally, ion detection occurs by microchannel plate detection in the MS.

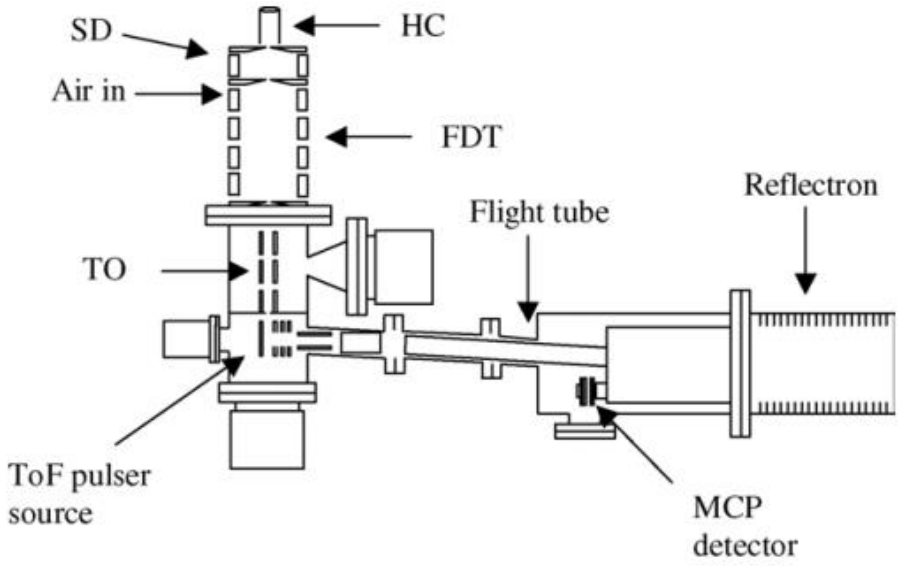

Figure 6.4. PTR-ToF-MS schematic, showing the hollow cathode (HC) ion source, source drift (SD) tube, flow drift tube (FDT), transfer optics (TO), ToF pulser source, field free flight tube, reflectron and microchannel plate (MCP) detector [387].

6.2.6 VOC data analysis of breath samples collected by PTR-ToF-MS

GRAMS software (ThermoFisher Scientific, Waltham, US) was set to extract data for every 0.5 seconds. Spectral data files were extracted and converted to excel files using the GRAMS software. Subsequently, mass channels were binned to nominal masses and normalised to *m/z* 21 representing the H_3O^+ isotope (Equation 6.3).

Equation 6.3

$$\frac{m}{z}\, m/z_{(normalised)} = \frac{m/z_{(unnormalised)}}{\frac{m}{z}21 * 500} * 10^6$$

Line charts of *m/z* 59, putatively representing acetone linked to exhalation [388], were plotted in order to select the abundance values related to exhaled breath for all ions. The abundance values prior to the increase in *m/z* 59 abundance were also selected to determine the background per *m/z* bin, after which background subtraction was performed per sample. Triplicate samples were averaged together and data was pre-processed by removal of low (<15) and high (>180) *m/z* channels which abundances were close to zero as well as removal of ions associated with water vapours (*m/z* 19, 21, 37 and 39) and exclusion of negative values after background subtraction. Exploratory analyses of pseudoephedrine pharmacodynamics were performed by principal component analysis (PCA) using R studio 1.0.143 (64 bits, R version 3.4.3, Vienna, Austria) and mixOmics 6.3.1 package [389]. The effect of logarithm scaling, standardisation and robust scaling was assessed. PCA was also applied to study the difference between the volunteers that donated samples both with and without administration of pseudoephedrine hydrochloride tablets.

6.2.7 Collection and preparation of breath samples onto sorbent tubes

Breath samples were collected from one healthy female volunteer, not part-taking in any doping programme and without medication, on a separate occasion after administration of 2 tablets of Sudafed containing 60 mg pseudoephedrine hydrochloride each. Samples were collected pre-dosing and at 0.5, 1, 1.5, 2, 4, 4.5, 5, 5.5 and 6 hours post Sudafed administration using a ReCIVA breath sampler device

(Owlstone Medical, Cambridge, UK). The device consists of a facemask, air supply and two pumps below four ports for tubes as shown in Figure 6.5. Three multi-bed sorbent tubes were used for triplicate collection and a solid aluminium tube was positioned in the front right port. The ReCIVA was set to collect 1 L of exhaled breath from the lower airways at a flow rate of 250 mL/min. Breath rate, profile and volume were tracked using the operational software (Owlstone Medical, Cambridge, UK). The tubes were capped with brass caps immediately after collection and stored in a fridge for 24 hours prior to sample treatment.

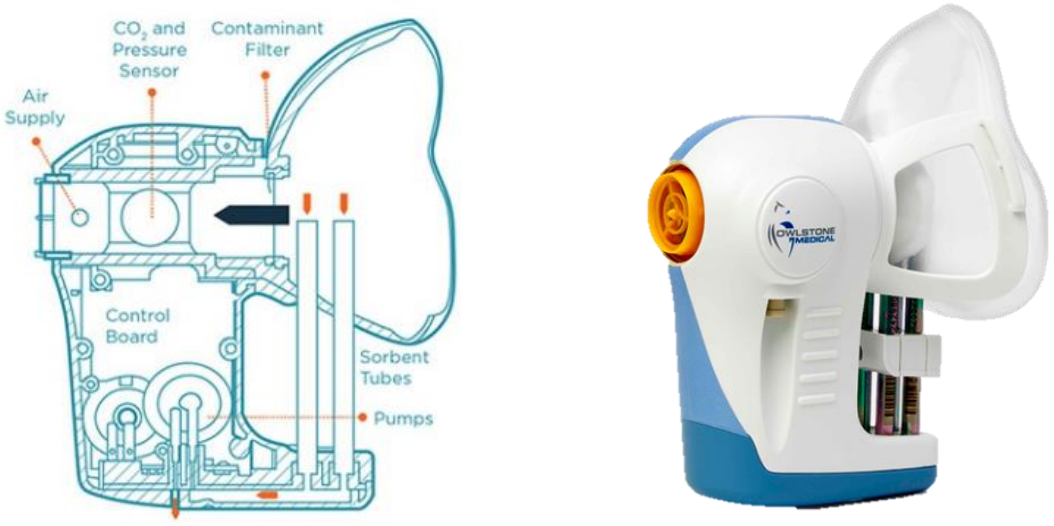

Figure 6.5. Schematic diagram of the ReCIVA breath sampler device showing the location of the air supply, pumps, tubes, sensors and filter relative to the face mask (left) and an image of the sampler device with tubes and face mask (right) [390].

Samples were dry purged for 2 minutes using nitrogen (CP grade, BOC) at a flow rate of 50 mL/min to remove excess water for GCxGC-FID/qMS analysis. A 0.6 µL aliquot of internal standard solution consisting of 20 µg/mL phenanthrene-d_{10} certified reference solution, n-octane-d_{18} and toluene-d_8 certified reference solution in MeOH was loaded onto the tubes using a stream of nitrogen (CP grade, BOC) at a flow rate of 100 mL/min for 2 minutes. A loading rig (CSLR, Markes International Ltd, Llantrisant, UK) was used to hold the samples and also to load 1 µL retention index solution consisting of 10 µL/mL aromatics calibration standard and 20 µg/mL C_8-C_{20} n-alkanes standard solution in MeOH onto five blank tubes using a stream of nitrogen (CP grade, BOC) at a flow rate of 100 mL/min for 1 minute. A 0.6 µL aliquot of internal standard solution was

added afterwards. Additionally, two blank tubes were loaded with 0.6 µL performance mixture consisting of 10 µg/mL multi-component indoor air standard (JIAM) in MeOH using a stream of nitrogen (CP grade, BOC) at a flow rate of 100 mL/min for 1 minute and addition of 0.6 µL internal standard solution afterwards. After spiking the tubes, the brass caps were replaced with Diff-Lok caps.

6.2.8 GCxGC-FID/qMS analysis of breath samples

Tubes were placed in trays and loaded into a TD100-xr automated thermal desorber (Markes International Ltd, Llantrisant, UK). Prior to tube analysis, samples were pre-purged with carrier gas at 50 mL/min for 1 minute and then desorbed at 300 °C for 5 minutes with a flow of 50 mL/min. During desorption, VOCs were trapped and pre-concentrated at -10 °C onto a hydrophobic general trap matching the sorbent in the tubes. The trap was then heated at the maximum heating rate to 300 °C and held for 5 minutes with a split flow rate of 2 mL/min.

GCxGC-FID/qMS analyses were conducted using an Agilent 7890B GC fitted with a forward fill/flush flow modulator and three-way splitter plate coupled to a FID and HES 5977B qMS (Agilent Technologies, Wokingham, UK). A Rtx-5Sil MS column (l = 30 m, I.D. = 0.25 mm, dF = 0.25 µm) was used for the first dimension and a DB-WAX (l = 4 m, I.D. 0.25 mm, dF = 0.25 µm) for the second dimension (Restek Thames, Saunderton, UK). Helium was used as carrier gas with the primary column flow rate starting at 2 mL/min for 3 minutes and ramped with 10 mL/min to 0.6 mL/min, whereas the secondary column was kept constant at 23 mL/min. Between samples, a bake-out method was carried out using an empty tube. The empty tube was pre-purged similarly as samples, but then desorbed at 350 °C for 10 minutes with a flow of 50 mL/min. The trap was held at 30 °C and then desorbed at 320 °C for 5 minutes with a split flowrate of 50 mL/min. The primary column flow was increased to 1.5 mL/min and the oven was held at 250 °C for 30 minutes.

The flow modulator was set to a modulation period of 3 seconds, with a fill and flush time of 2.799 and 0.201 seconds respectively. The restrictor from the first outlet port of the splitter plate to the FID consisted of 1.2 m x 0.25 mm deactivated fused silica and had a constant flow of 23 mL/min, whereas the restrictor from the splitter plate to

the qMS consisted of 0.76 m x 0.1 mm deactivated fused silica giving a split ratio of 1:0.06. The oven was held at 30 °C for 5 minutes, then heated to 80 °C at 3 °C/min, then ramped to 250 °C at 5 °C/min and held for 10 minutes. The FID heater was set to 250 °C. The make-up gas was purified nitrogen set to keep a constant combined restrictor and make-up flow of 25 mL/min, with a purified air flow rate of 400 mL/min and 35 mL/min of hydrogen from a hydrogen generator (Trace hydrogen, Peak Scientific, Inchinnan, UK). The temperature of the transfer line to the qMS was set at 250 °C, the ion source at 230 °C and the quadrupole at 150 °C. The MS was operated in multiple reaction mode with a range set at *m/z* 40 – 300.

Data was acquired with Chemstation B.07.05.2479 (Agilent Technologies, Santa Clara, CA, US) and processed using GC Image™ 2.6 along with GC Project and Image Investigator (JSB Ltd, Horsham, UK). Briefly, the chromatograms were baseline corrected. Alignment of samples from the same batch was then performed using the retention position of the components within the retention index mixture ran at the beginning of each batch. A feature template based on all the chromatographic features across all the aligned chromatograms was auto-generated using an automated tool developed for the non-targeted cross-comparison of samples [391]. The tool produced a template of peak-regions that were found in either 50% or 100% of the samples. The data for each chromatographic feature across all samples was then compared by PCA exploration to evaluate variation between sampling time points.

6.3 Results

6.3.1 Pharmacokinetics of pseudoephedrine by dried blood analysis

A LC-MS/MS method for the analysis of pseudoephedrine from DBS was adapted and validated for its application to VAMS devices [83]. No ion suppression effects nor interfering signals owing to the different sampler matrix were observed at the expected retention time (4.2 minutes). The limit of detection (LOD) was found to be 0.5 ng/mL with a signal to noise (S/N) ratio of >5:1.The lower limit of quantification (LLOQ) was determined to be 1 ng/mL (S/N > 10:1). Signals of pseudoephedrine were found to be linear (linear regression correlation coefficient (R2) of 0.9997) within the range of 1 ng/mL to 1 µg/mL as shown in Figure 6.6.

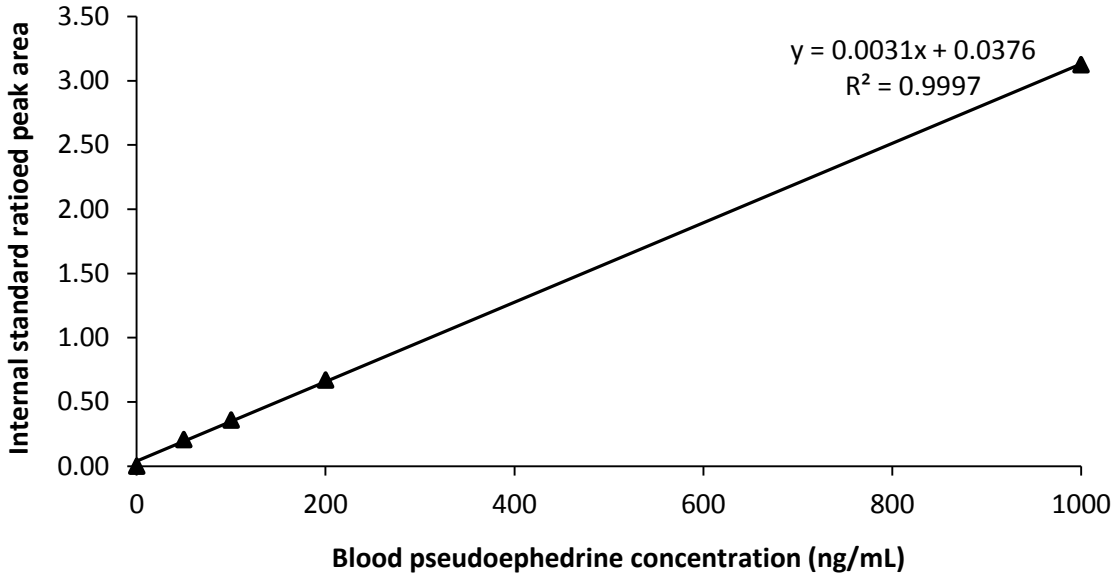

Figure 6.6. Linearity and sensitivity of the LC-HESI-MS/MS method for analysis of pseudoephedrine spiked blood collected onto VAMS devices (n=8).

A wide calibration range of 5 concentrations up to 1000 ng/mL was used to allow for the different pseudoephedrine blood levels anticipated for athletes during competitions, within and above the blood therapeutic range of 500-800 ng/mL [392]. The precision and accuracy of the adapted method were tested at three pseudoephedrine concentrations (5, 50, 150 ng/mL) and the results shown in Table 6.1 fell within WADA limits [382]. The recovery was tested at 500 ng/mL and was found to be 20.9%.

Table 6.1. Precision and accuracy of the LC-HESI-MS/MS method for analysis of dried blood samples containing pseudoephedrine, collected onto VAMS devices (n=6).

Blood pseudoephedrine concentration (ng/mL)	Precision (RSD %)	Accuracy (%)
5	12.4	86.6
50	17.9	84.2
150	6.6	105.9

Pseudoephedrine was successfully measured from the blood of 12 healthy volunteers collected onto VAMS devices. The maximum pseudoephedrine concentrations (C_{max}) detected ranged from 370 ng/mL to 1420 ng/mL for the different volunteers, which was reached between 1 and 5.5 hours (T_{max}). However, the T_{max} for the majority of volunteers (10 out of 12) was between 1 and 2 hours which is slightly quicker but in the range of results from DBS studies [83, 393]. The wide range of both

C_{max} and T_{max} indicates that there was a large inter-person variability, which has also been reported in studies measuring pseudoephedrine in urine [361, 394, 395]. Figure 6.7 shows the results of this study using VAMS and also the average DBS results of the study by Tretzel et al. [83] for comparison (multiplied by 4 because of the lower pseudoephedrine dose administered in the DBS study). The pharmacokinetic profile and pseudoephedrine levels detected for one of the volunteers in this study (number 7) were consistent with the corrected DBS measurements of Tretzel et al. [83]. The C_{max} of two volunteers in this study (number 4 and 6) were lower than the DBS C_{max} values corrected from the literature, whereas the C_{max} of eight volunteers were up to two-fold higher. The profiles of two volunteers (number 11 and 12) were completely different than the other profiles observed, with deferred T_{max} values potentially owing to a slower metabolism. Pseudoephedrine could still be detected 24 hours post-administration in the samples of all seven volunteers that donated additional samples, which was also comparable to the DBS findings of Tretzel et al. [83] as well as with the 24 hour excretion rate reported in the literature [396].

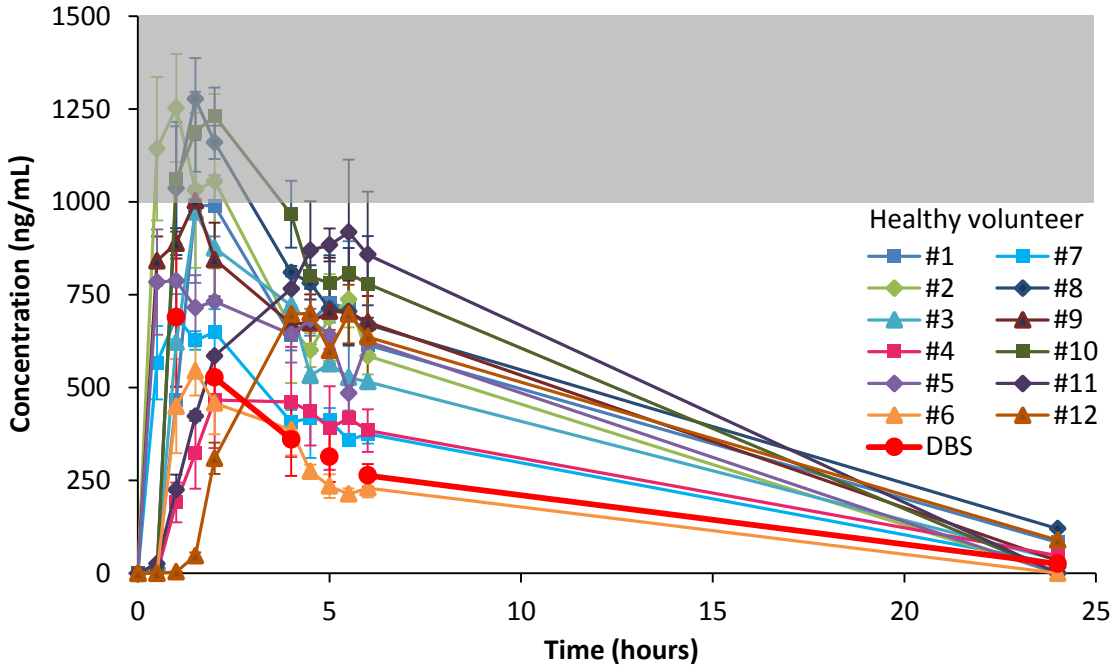

Figure 6.7. Concentration of pseudoephedrine measured from blood collected onto VAMS devices after oral administration of 120 mg pseudoephedrine hydrochloride by twelve healthy volunteers. Corrected DBS literature values are shown in bright red for comparison [83]. The grey area shows estimations of pseudoephedrine concentrations beyond the method's calibration range (>1000ng/mL) for blood samples collected onto VAMS devices.

Pseudoephedrine levels measured in the venous samples collected from one volunteer 2 hours post-administration were slightly lower than their respective levels in the capillary samples (627.2 ± 216.9 ng/mL versus 875.7 ± 357.6 ng/mL respectively), but comparable for the samples collected 6 hours post-administration (480.2 ±124.5 ng/mL versus 516.0 ±61.1 ng/mL). Similar results have also been reported between dried plasma spots and wet plasma samples for cathinone analogues [150].

For 10 volunteers, the half-life ($T_{½}$) of pseudoephedrine was not reached 6 hours post-administration. For two volunteers (number 2 and 6) the $T_{½}$ was around 4.5 hours, although the profile of one of those volunteers showed a spike in concentration after the $T_{½}$ time and reached the $T_{½}$ level again just before 6 hours post-administration. When inspecting the graphs from the 6 hours post-administration sampling point to the 24 hours post-administration sampling point, it seems that $T_{½}$ would be reached within 8 hours post-administration which is in line with reported values of $T_{½}$ between 4 and 8 hours post-administration [396]. Since accurate $T_{½}$ estimations can't be determined here, the concentration difference between T_{max} and 4 hours post-administration was used to calculate clearance (Cl) of which an overview can be found in Table 6.2. Cl represents the volume of blood from which a substance is removed per unit of time, here pseudoephedrine hydrochloride.

Table 6.2. Overview of observed T_{max} and $T_{½}$ as well as the calculated blood Cl per volunteer. Cl could not be calculated for two volunteers (11 and 12) nor for the literature DBS data.

Volunteer	1	2	3	4	5	6	7	8	9	10	11	12	DBS
T_{max} (hours)	1.5	1.0	1.5	2.0	1.0	1.5	1.0	1.5	1.5	2.0	5.5	4.5	1
$T_{½}$ (hours)	>6	4-6	>6	>6	>6	4.5	>6	>6	>6	>6	>6	>6	4-5
Cl (mL/min)	1.2	2.4	1.9	0.3	0.6	1.4	1.2	2.4	1.3	1.9	X	X	X

In terms of application of the VAMS technique to sport doping testing or other cases, the low invasiveness of the sampling technique and the very small blood volume required are beneficial for frequent sampling. Micro-volume blood collection by VAMS would be particularly interesting for application to monitor the relationship between administered doses and blood concentrations of pseudoephedrine as well as its metabolic removal for both in- and out-of-competition scenarios.

6.3.2 Pharmacodynamics of pseudoephedrine by real-time breath analysis

Figure 6.8 shows a pre-processed mass spectrum collected by PTR-ToF-MS of exhaled VOCs 1 hour post-administration of 120 mg pseudoephedrine hydrochloride.

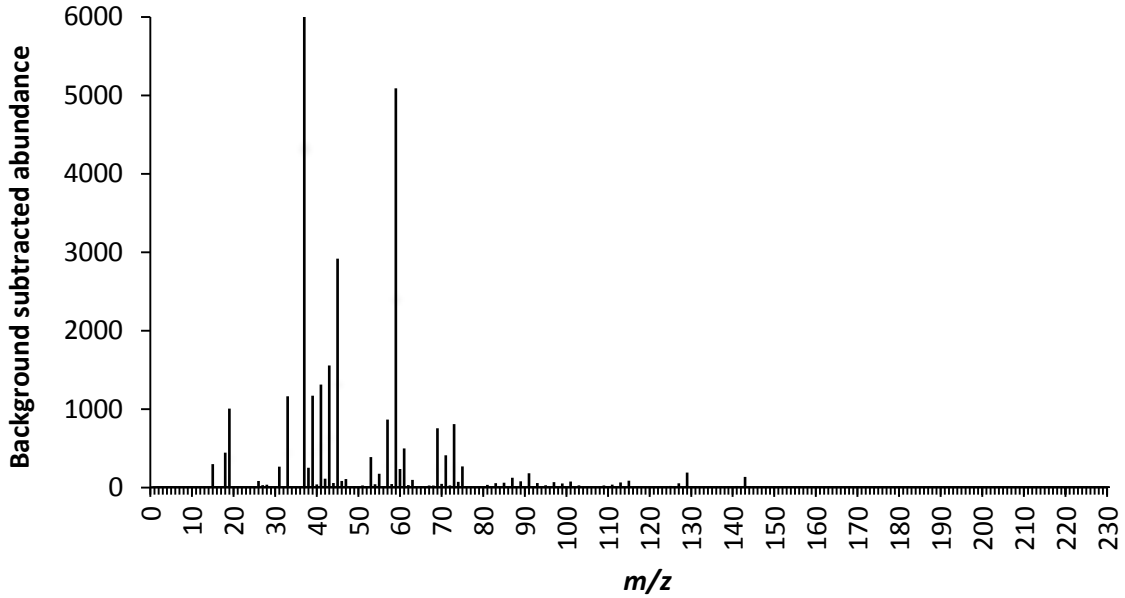

Figure 6.8. PTR-ToF-MS spectrum of breath samples taken in triplicate from one of the volunteers (number 7) 1 hour post-administration of 120 mg pseudoephedrine hydrochloride. Binning to nominal masses, normalisation to *m/z* 21, background subtraction and averaging of triplicates was performed.

After binning to nominal masses and further pre-processing, the mass spectra from all volunteers independent of sampling time point typically showed abundant ions at *m/z* 19, 33, 37, 39, 41, 43, 45, 57, 59, 69 and 73. Time profiles were plotted for the abundant ions individually to investigate if a trend in time similar to the pharmacokinetic profile of pseudoephedrine observed in blood (Figure 6.7) could be found after pseudoephedrine hydrochloride administration, however no such trend was found. Abundances close to zero were detected below *m/z* 15 and above *m/z* 180. The ions of *m/z* 19, 37 and 39 were attributed to the H_3O^+ and hydrated H_3O^+ ions occurring in proton transfer reactions. In PTR-ToF-MS measurements, water vapour within breath samples can react with H_3O^+ ions to form water clusters (Equation 6.4), hence these ions were not considered biomarkers.

Equation 6.4

$$H_3O^+ + H_2O \rightarrow H_3O^+(H_2O)n$$

Exploratory analysis was performed by PCA using the combination of all ions after pre-processing to investigate pseudoephedrine pharmacodynamics per volunteer (Figure 6.7). The most influencing ions for this volunteer appeared to be *m/z* 33, 41, 45, 59 and 69, which are amongst the most abundant ions observed in the pre-processed mass spectra. The first principal component (PC1) showed a variance of 54.9%, separating the data roughly in three clusters. The samples taken at administration of pseudoephedrine hydrochloride and 0.5 hour post-administration are shown at the left of the plot (t0 and t0.5, marked orange and pink respectively). The middle of the plot consists of the samples taken 1 to 2 hours post-administration (t1, t1.5 and t2, marked dark blue, purple and dark green respectively). The right of the plot shows samples taken 4 to 6 hours post-administration (t4, t4.5, t5, t5.5 and t6, marked light green, black, grey, light blue and lilac respectively).

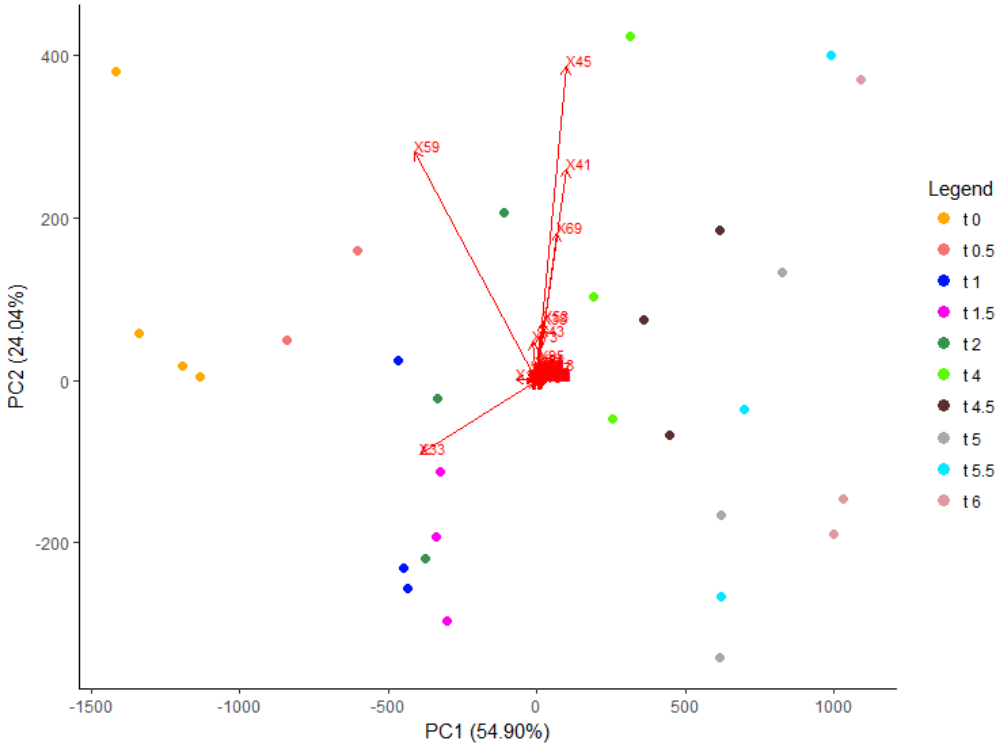

Figure 6.9. PCA plot showing *m/z* 33, 41, 45, 59 and 69 as most influencing for separating the sampling time points (visualised with the different colours) after administration of 120 mg pseudoephedrine hydrochloride by one of the volunteers (number 1).

For most other volunteers, a separation into two clusters was observed. One cluster consisting of the sampling time points up to T_{max} (as derived from blood concentrations of pseudoephedrine, Table 6.2) which coincided roughly with all sampling points before lunch (≤2 post-administration of pseudoephedrine hydrochloride). The other cluster coinciding with the samples taken after lunch (≥4 hours post-administration of pseudoephedrine hydrochloride). The ions of *m/z* 33, 41, 43, 45, 47, 57, 59, 69, 73 and 75 appeared to be the dominating factors for most volunteers. Except for *m/z* 47 and 75, these ions were observed as most abundant in the pre-processed mass spectra and time profiles were plotted as described earlier. Additionally, time profiles of m/z 47 and 75 were plotted individually but no trend in time was found such as the pharmacokinetic profile of pseudoephedrine observed in blood (Figure 6.7).

The PCA plot of Figure 6.9 indicated that a combination of variables might be attributed to pseudoephedrine pharmacodynamics. The most influencing ions found by PCA were reported to be major VOCs present in human breath involved in general metabolic processes such as the metabolism of food and drinks [397], therefore they were not rendered suitable biomarkers for pseudoephedrine intake. Firstly, the ion of *m/z* 33 is linked to methanol production as a result of the breakdown of certain dietary sources [398, 399]. Fasting or dietary specifications were not part of this study's experimental setup, therefore too much variation could occur naturally in the abundance of methanol. The ions of *m/z* 41 and 57 are generally believed to be common metabolic fragments, thus excluded to be specific biomarkers. The ion of *m/z* 43 is putatively linked to propanol, which is converted to acetone by enzymatic conversion [400, 401]. The ion of *m/z* 59 is attributed to acetone (2-propanone), which is an ubiquitous endogenous VOC in breath [388]. Acetone is formed by fatty acid metabolism in the liver and levels are linked to fasting. The ion of *m/z* 45 is putatively linked to acetaldehyde which is a known product of the alcohol dehydrogenase pathway [398, 402]. The ion of *m/z 4*7 has been reported to be linked to instrumental background processes [403]. The ion of *m/z* 69 is often assigned to isoprene (2-methyl-1,3-butadiene) and may be involved in cholesterol metabolism [404, 405]. Isoprene levels have been reported to vary throughout the day linked to circadian rhythm [406] and was therefore also not rendered a useful biomarker for pseudoephedrine intake. Lastly,

m/z 73 and 75 are putatively linked to butanal and butanol respectively, which are again products of general metabolic processes [407].

PCA was also performed using the data of all samples from all volunteers together (Figure 6.10). The ions of *m/z* 45 and 59 were found to be the common variables most influencing the data, but these ions are among the most abundant compounds in breath as described earlier. Therefore, these two variables were removed from the dataset to investigate if sampling time point clusters of less abundant VOCs could be revealed. The ions of *m/z* 18, 33, 42, 43, 57, 69, 71, 73, 75 and 89 became most influential, but still no separation of sampling time points post-administration of pseudoephedrine hydrochloride became evident.

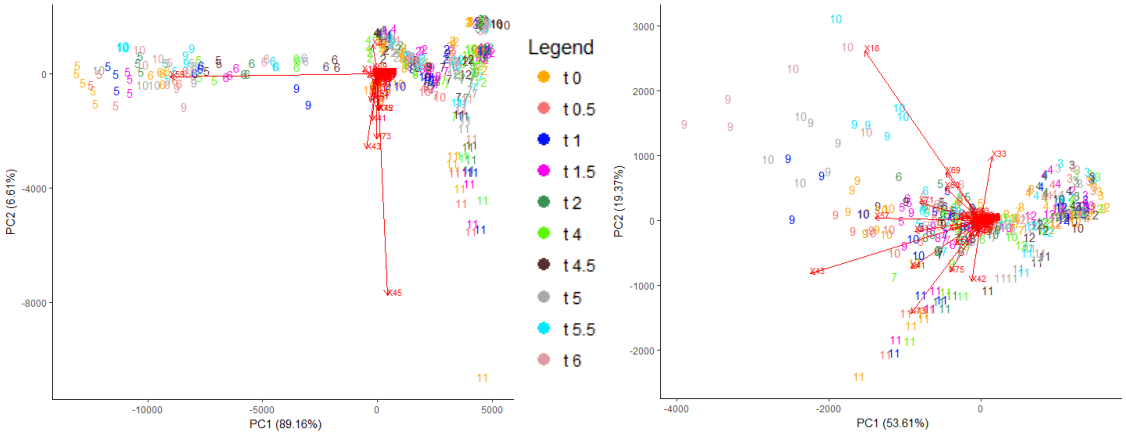

Figure 6.10. PCA plot of breath samples from all volunteers (represented by 1-12) and sampling time points (represented by the different colours). Data was separated by the ions of *m/z* 45 and 59 (left) and by the ions of *m/z* 18, 33, 42, 43, 57, 69, 71, 73, 75 and 89 upon removal of the most abundant ions of *m/z* 45 and 59 (right). No clear separation of sampling time points was observed.

The clustering of sampling time points could be due to inter-person variation of the different volunteers, which was reflected in the varying T_{max} and C_{max} values observed for pseudoephedrine in blood (Table 6.2). To explore inherent inter-person variance, PCA was performed with the breath samples from all volunteers taken at the time of pseudoephedrine hydrochloride administration. Figure 6.11 shows that the inter-person variation was already large (78.4% explained by both PC1 and PC2) at the time of pseudoephedrine hydrochloride administration, thus prior to pseudoephedrine metabolism. PC1 was mostly influenced by the ion of *m/z* 43, which was described to be

putatively linked to propanol and converted to acetone by enzymatic conversion [400, 401]. However, it was found that the variance of both components remained large (72.4%) after removal of the ion of *m/z* 43. PC2 was mostly influenced by the ions of *m/z* 33 and 42. Similar inter-person variances were also found for the later sampling time points, with PC variances ranging from 74.0% to 88.5%.

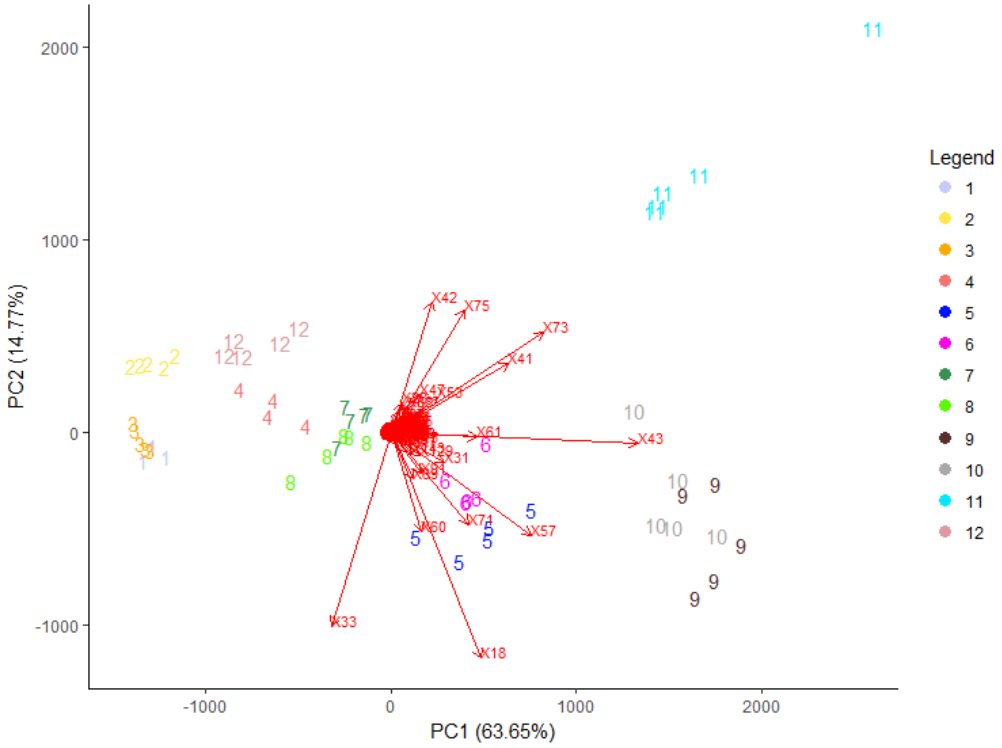

Figure 6.11. PCA plot of breath samples from all volunteers (1-12, represented by the different colours) taken at the time of pseudoephedrine hydrochloride administration. Inter-person variance was large, explained by a variance of 78.4% by PC1 and PC2.

The ratio of the most influential ions of *m/z* 33 and 42 to *m/z* 43 was explored more in-depth. For the breath samples of volunteer 1, 2, 3 and 5, the highest abundances were found for the ion of *m/z* 33 compared to *m/z* 43. Whereas for volunteer 9, 10 and 11, higher abundances were found for the ion of *m/z* 43 compared to *m/z* 33. Comparable abundances were found for the ions of *m/z* 33 and 42 in the breath samples of volunteer 4, 6, 7, 8 and 12. The abundance of the ion of *m/z* 43 was larger than *m/z* 42 for all volunteers but the ratios differed, which is in-line with the separation shown in the PCA of Figure 6.11. Figure 6.12 shows the time profiles of both ratios for one of the volunteers. The ratio of *m/z* 33 to 43 shows a decrease in time, but this trend was not

observed for all volunteers. The opposite trend was even observed for one donor as well as a trend showing a decrease in the samples taken until lunch (≤2 post-administration of pseudoephedrine hydrochloride) and an increase for samples taken after lunch (≥4 hours post-administration of pseudoephedrine hydrochloride). No distinct trends were observed for the ratio of *m/z* 42 to 43.

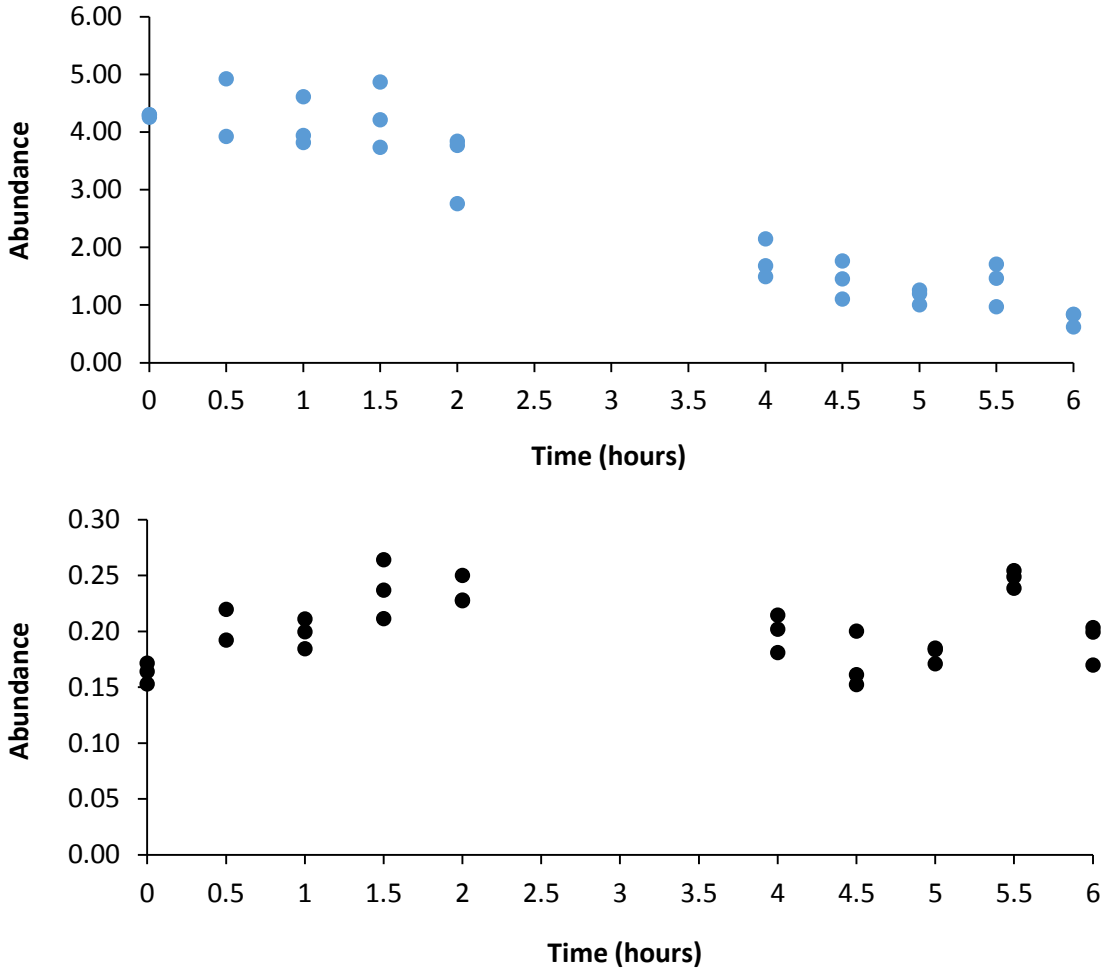

Figure 6.12. Abundance plots of the influential ions *m/z* 33 to 43 (top) and *m/z* 42 to 43 (bottom) detected in the breath of volunteers after administration of 120 mg pseudoephedrine hydrochloride. The ratios are shown for one of the volunteers (number 1) after pre-processing the data by binning to nominal masses, normalisation to *m/z* 21 and background subtraction.

To further investigate VOCs with lower abundances that could be potential biomarkers involved in pseudoephedrine metabolism, scaling could offer a solution for the data analysis. Scaling by standardisation of the data, by subtracting the mean of each abundance and dividing by its standard deviation [408], appeared not to be suitable as all variables became responsible for the variation. Whereas robust scaling,

by replacing the mean with the median and the standard deviation with median absolute deviation from the median [409], appeared to be not appropriate for the opposite reason that the data became compressed. With logarithm scaling [275], PCA showed more factors contributing to the separation but the variance of the PC1 decreased up to 6-fold for the different volunteers. For some volunteers, a separation into the two clusters ≤2 and >2 hours post-administration of pseudoephedrine hydrochloride was still observed but for the majority there was clustering of time points. Additional influencing variables detected after logarithmic scaling of the data were *m/z* 20, 27, 32, 36, 46, 50, 61, 79, 89, 95, 96, 107, 111, 121 and 189. Plots of the individual ions showed no trend in time such as the pharmacokinetic profile of pseudoephedrine observed in blood (Figure 6.7). Therefore, again no VOC was found to be a potential biomarker attributing to pseudoephedrine metabolism.

Finally, it was expected that the samples of two volunteers taken directly at and after pseudoephedrine hydrochloride administration would cluster with the control samples taken at the day without administration (Figure 6.13).

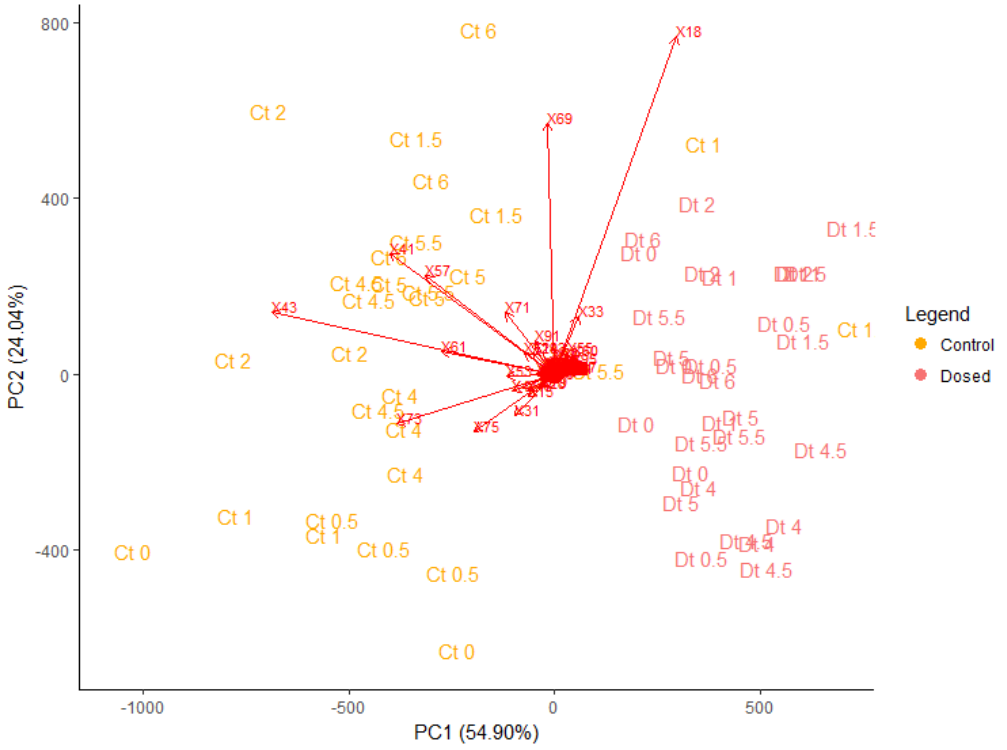

Figure 6.13. PCA plot of breath samples from one of the two volunteers with (red data points; dosed) and without (yellow data points; control) pseudoephedrine hydrochloride administration. Samples of the two sampling days were separated with the exception of three control sample outliers which clustered with the dosed samples.

A clear separation of both sampling days was observed for both volunteers, also after removal of the most abundant ions of *m/z* 45 and 59. Similarly, a separation of volunteer pairs sampled at different days was observed earlier (Figure 6.11). The ratios of the most influential ions of *m/z* 18 and 69 to *m/z* 43 as well as *m/z* 18 to 69 were explored more in-depth and it was found that the ratio *m/z* 69 to 43 was higher for all samples taken at the day of pseudoephedrine hydrochloride administration compared to the control samples. This was also found for the samples taken at the start of the experiments, thus showing a separation of the different sampling days and intra-person variation again.

6.3.3 Linking the pseudoephedrine measurements of dried blood and breath

Figure 6.14 shows the PCA plot of the T_{max} data of each volunteer (as derived from the blood pseudoephedrine concentrations, Table 6.2), to get an indication about influential VOCs detectable upon reaching the C_{max} of pseudoephedrine.

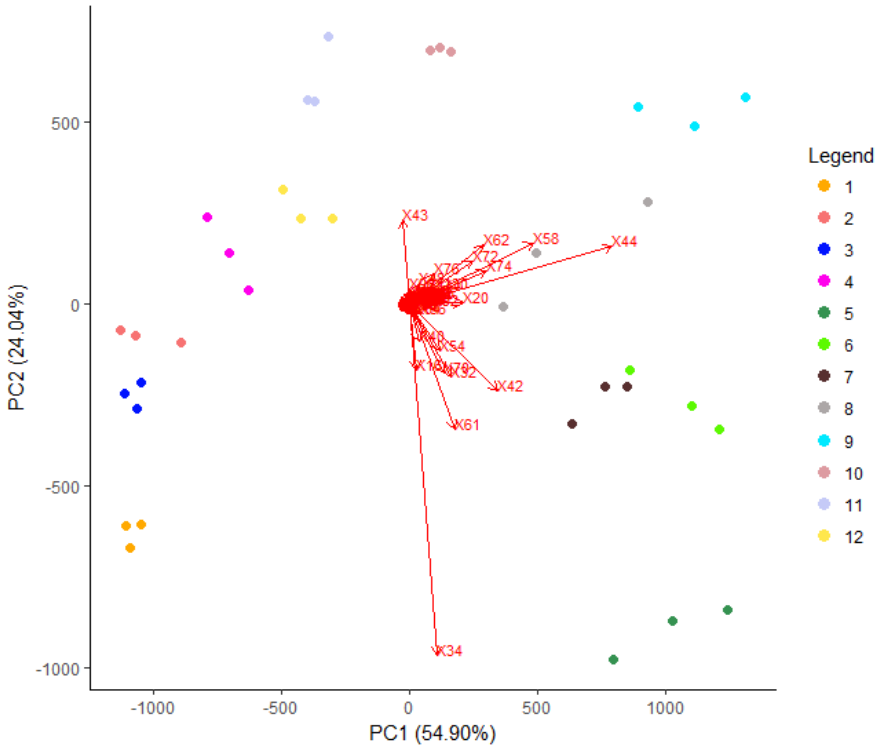

Figure 6.14. PCA plot of the breath samples from all volunteers (1-12, represented by the different colours) sampled in parallel with the blood samples inferred to be taken at the T_{max} of pseudoephedrine hydrochloride in blood. The inter-person variance was large and the ion of *m/z* 34 was most influential.

The inter-person variation was found to be large again (78.9% explained by PC1 and PC2), but interestingly a different ion (*m/z* 34) was found to be the most influential. The ion of *m/z* 34 is putatively linked to methanol as an isotope of the main fragment attributed to *m/z* 33 [407], but again no trend in time was found such as the pharmacokinetic profile of pseudoephedrine observed in blood (Figure 6.7).

6.3.4 Pharmacodynamics of pseudoephedrine by analysis of breath collected onto sorbent tubes

As PTR-ToF-MS analysis of breath samples collected in real-time did not reveal any small molecular weight biomarkers potentially involved in pseudoephedrine metabolism, GCxGC-FID/qMS analysis was performed using breath samples collected onto sorbent tubes from a volunteer after pseudoephedrine hydrochloride administration. The GCxGC chromatogram of the retention index shows the 21 components of the retention index mixture plus the two components of the internal standard solution, which were run to monitor performance and to use for retention comparisons of the compounds detected in the breath samples (Figure 6.15). The first dimension (visualised on the horizontal axis) shows the separation of compounds based on volatility and the second dimension (represented on the vertical axis) shows the separation based on polarity. The GCxGC chromatogram of the breath sample shows the separation of VOCs for a sample collected from the volunteer 1 hour post-administration of pseudoephedrine hydrochloride. The breath sample consisted of many different alkanes (visible at the bottom of the chromatogram) but also of mid polarity components such as carbonyls and aromatics (visible in the middle of the chromatogram) and of high polarity components such as amines and higher aromatics (visible at the top of the chromatogram).

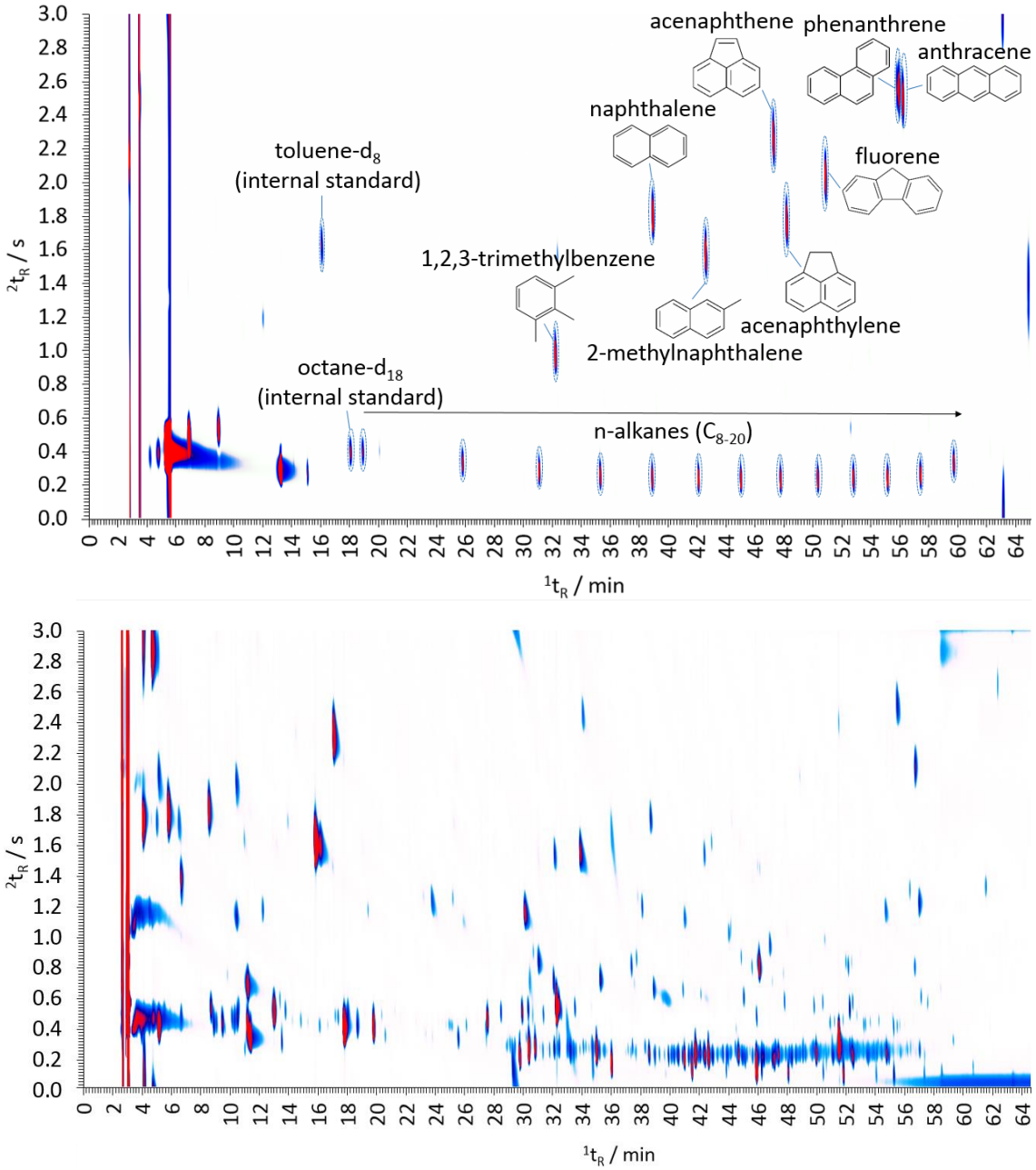

Figure 6.15. FID image of the retention index mixture (top) and a breath sample from a healthy volunteer collected onto sorbent tubes 1 hour post-administration of 120 mg pseudoephedrine hydrochloride (bottom). The retention index mixture was used for baseline correction and alignment of the breath samples. Circles, arrows and names were added to visualise components.

The abundance of each chromatographic feature observed was used to plot time-profiles, but no potential biomarkers were found during this preliminary investigation. The feature template revealed a total of 499 VOCs detected in at least 50% of the samples and 201 VOCs when setting the threshold to 100%. The number of VOCs detected in this study is comparable with VOCs detected in other breath studies, for

example ~200 VOCs were detected on average per breath sample and up to 3481 in the total amount of breath samples from 50 volunteers analysed by GC-MS [410].

PCA was performed with the VOCs detected in 100% of the samples to explore if a combination of VOCs could be marked as potential biomarkers for pseudoephedrine intake and a pharmacodynamic profile be evaluated. Figure 6.16 shows that the samples prior to and at the time of pseudoephedrine hydrochloride administration (tbase and t0, marked with red squares and blue circles in the plot respectively) were separated from the samples collected at later sampling time points (≥t0.5). The features towards t0 and tbase were identified as highly branched C_{12}-C_{14} alkanes alongside two siloxanes and di-octyl-ether. The alkanes identified in the first samples of the day could be attributed to fragments of compounds increased by physical exercise upon travelling to the sampling location [411]. Di-octyl ether might be linked to the use of facial creams in the morning prior to the first measurements. The siloxanes were identified in more samples throughout the day and could be attributed in general to the use of silicone face masks connected to the ReCIVA breath sampler.

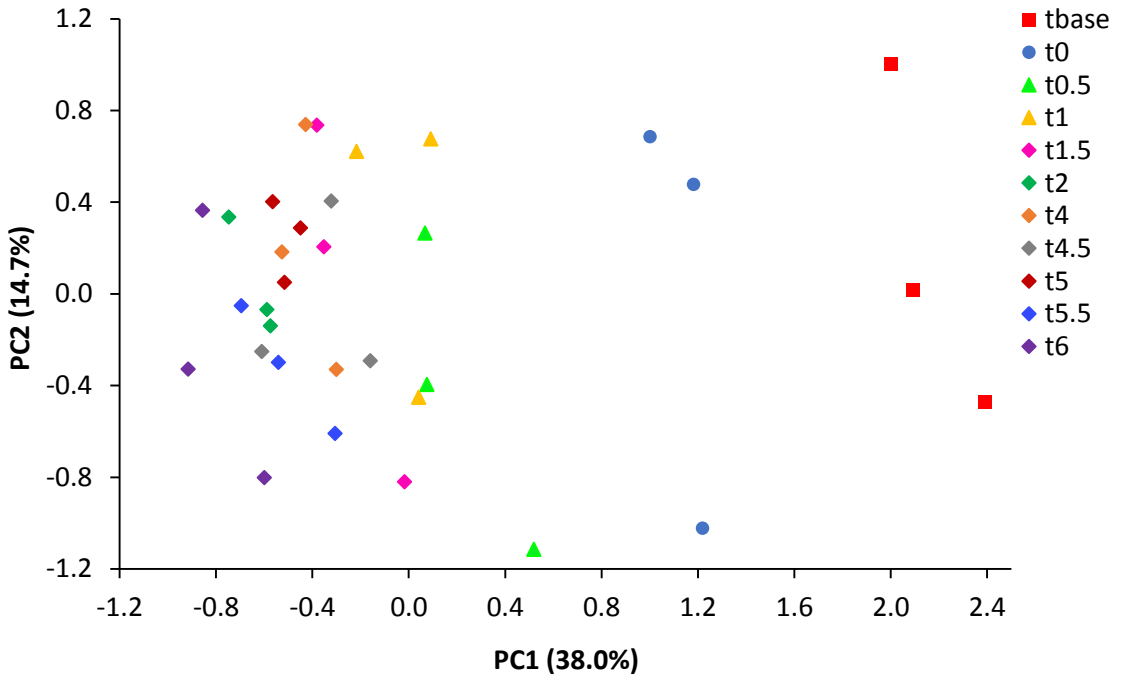

Figure 6.16. PCA of breath samples collected onto sorbent tubes and analysed by GCxGC-FID/qMS. A separation of baseline samples (red squares at the right) and samples collected at the time of pseudoephedrine hydrochloride administration (t0, blue circles in the middle) can be observed compared to the samples collected at later time points (t0.5-t6, at the left).

A slight separation was observed between the samples collected 1 and 1.5 hours post-administration (t1 and t1.5, marked with green and yellow triangles in the plot respectively) and the later sampling time points (>t2), but this separation is minor as the variance of PC1 is small overall (38.0%). Lastly, there was variation between triplicate samples which was unexpected given that the samples were collected under the same conditions at the same time. The variation could be explained by differences in the back pressures of the sorbent tubes and/or pump flow of the ReCIVA breath sampler.

6.3.5 PTR-ToF-MS and GCxGC-FID/qMS for exploring pseudoephedrine pharmacodynamics in breath

The collection of breath samples using PTR-ToF-MS has the advantage of the real-time aspect, but without adaptations to the instrumentation it is unpractical to analyse breath samples at locations of interest such as at sport events. It takes longer to collect breath samples onto sorbent tubes, but they allow the storage and portability of samples, no restriction to location, the possibility of collecting multiple samples at once and they generally add sensitivity by concentrating larger sample volumes.

Currently, breath analysis by PTR-ToF-MS has the potential to give a presumptive indication about the intake of pseudoephedrine. A confirmatory test such as micro-volume blood samples collected by VAMS could be applied to those who test positive, for example to give a quantitative result for inclusion/exclusion of athletes at competitions.

A GCxGC-FID/qMS trial was carried out using breath samples collected onto sorbent tubes to increase separation and to add identification of VOCs. Over 200 VOCs were identified in the breath samples of volunteers, but it was not possible to assess a pharmacodynamic breath profile after pseudoephedrine hydrochloride administration with the current method.

Method development is recommended for the breath analyses by both PTR-ToF-MS and GCxGC-FID/qMS to investigate potential biomarkers for pseudoephedrine intake.

6.4 Concluding remarks and future perspectives

The suitability of VAMS for the quantification of pseudoephedrine from micro-volumes of capillary blood was investigated. Small adaptations were made to the method published by Tretzel et al. for the quantification of pseudoephedrine from DBS using LC-MS to analyse blood of volunteers sampled onto VAMS devices [83]. A reduction in blood volume from 20 µL used previously to 10.1 µL in this study was established. The dose of pseudoephedrine hydrochloride was increased from 30 mg to 120 mg and no ion suppression effects nor interfering signals were observed at the expected retention time for pseudoephedrine by the VAMS sampler matrix. For the first time, pseudoephedrine was successfully measured from the blood of 12 healthy volunteers using VAMS. Similar to previous studies measuring pseudoephedrine from volunteers, large inter-person variation was found. Intra-person variation was not investigated in this study, but it is recommended to always collect multiple samples for a better interpretation of bioanalytical results, e.g. around competitions.

In terms of applying the VAMS technique to sport doping testing or other cases such as traffic controls for driving under the influence of drugs or forensic toxicology cases, the low invasiveness and ease of the sampling technique without the need of medical personnel as well as the very small volume of blood required are beneficial aspects. Micro-volume blood collection by VAMS would be useful for monitoring the relationship between administered doses and blood concentrations of pseudoephedrine as well as its metabolic removal, particularly for frequent sampling both in- and out-of-competition.

Performing a breath test is regarded low invasive and is preferred over blood and urine sampling according to interview data [198]. Exhaled breath is routinely used for alcohol breath tests, but recently more applications have arisen to detect drugs of abuse in breath [196, 197, 199, 412-414]. Here, PTR-ToF-MS was used to analyse breath samples collected in real-time using forced incentive exhalation and a trial was carried out using GCxGC-FID/qMS to analyse breath samples collected onto sorbent tubes. Breath sampling by PTR-ToF-MS has the potential to give a presumptive indication about the presence of pseudoephedrine. A confirmatory test such as micro-volume blood

collection by VAMS could be applied to those who test positive, for example to give a quantitative result for inclusion/exclusion of athletes at competitions.

For future breath studies, it would be interesting to change the design of the volunteer study by having the volunteers exercise instead of sampling them while they are passively sitting still during the experiment to represent sport testing scenarios. Method development is recommended for both the breath analyses by PTR-ToF-MS and GCxGC-FID/qMS. Upon inclusion of more healthy volunteers, the volunteers should donate samples twice; one day with administration of pseudoephedrine hydrochloride and one day without. Further increasing of the pseudoephedrine hydrochloride dose is also recommended to represent higher therapeutic doses and recreational doses. For GCxGC-FID/qMS, an increase in sample volume collected onto sorbent tubes could increase the number and abundance of VOCs detectable useful for identifying potential biomarkers and to assess a pharmacodynamic breath profile after pseudoephedrine intake.

7 Conclusions

7.1 The molecular profile of aged DBS

Blood is among the most frequently encountered evidence types at crime scenes and establishing the time since deposition (TSD) of bloodstains can be critical in certain cases [1, 28, 92, 93]. Whilst there have been advances in determining the age of bloodstains using various techniques over the years, currently no method is accurate enough to be implemented in forensic casework. The influence of environmental variables, the substrate, inter-person variation and sample quantity add to the complexity of developing an accurate method to predict the TSD of bloodstains [96].

Aside from the noticeable visible changes upon drying of bloodstains, there is limited knowledge about the underlying physical and biochemistry changes related to drying and further ageing. Red blood cells dehydrate, become less elastic and lose both cell volume and adhesive force [13-16]. The volatile organic compound (VOC) composition of bloodstains changes with time and both RNA and DNA degradation occurs [17-21]. Blood protein levels are affected; globulins and albumin decompose, creatine kinase and alanine transaminase denature, and alkaline phosphatase, catalase and peroxidase levels decrease [22-25]. Haemoglobin is the most investigated protein with respect to bloodstain ageing and is responsible for the change in colour [26-29].

The hypothesis tested in this thesis was if micro-volume samples of blood can be used to enhance the current forensic practice of blood analysis. To evaluate the TSD of blood it was investigated if a molecular profile of dried blood spot (DBS) ages could be established. A bottom-up proteomics approach was used to digest DBS proteins and the resulting peptides were analysed using nano-liquid chromatography hyphenated to tandem mass spectrometry with electrospray ionisation (nano-LC-ESI-MS/MS), as was presented in Chapter 2. The nano-LC-ESI-MS/MS method showed a repeatability of 89.1% - 96.6%. From single DBS between 929-2595 peptides and 88-206 proteins were identified based on 2946-10,015 spectra. The difference between biological replicates was found to be large (with maxima of 28%, 38%, 36% for spectra, peptide and protein identifications respectively), whereas inter-person variation was found to be lower (with maximum average differences of 12.5%, 12.2%, and 13.5% for spectra, peptide and protein identifications respectively). The extraction of proteins from DBS aged for 398 days posed difficulties, but 13 unique proteins were still identified in those samples

compared to DBS aged for up to 8 days. The number of protein identifications was lower for DBS aged for 0 days compared to DBS aged for up to 8 days, but 8 unique proteins were identified in DBS aged for 0 days. A total of 22 proteins were identified for all DBS ages between ≥1 and ≤8 days, but this was reduced to 4 proteins upon inclusion of DBS aged for 398 days. No distinctive upwards or downwards trend was observed for the number of spectra, peptides or identified proteins over time.

Multiple methods have been developed to quantify and compare protein abundances in label-free bottom-up proteomics studies. Here, the exponentially modified protein abundance index and normalised spectral abundance factor were used to estimate the abundance of common proteins identified from DBS of all ages. Both these label-free spectral counting methods are build-in options of the Scaffold software as well as the non-quantitative options of percentage coverage, percentage of total spectra, peptide count, spectrum count and total ion current. However, none of the approaches resulted in the discovery of a distinctive upwards or downwards trend related to the TSD of DBS. Finally, protein cluster analysis was performed based on estimated precursor intensities but this did also not result in a distinctive upwards or downwards trend useful to predict the TSD of DBS.

In short, for future experiments it is recommended to deplete high abundance proteins (HAPs) or enrich low abundance proteins (LAPs) from DBS as the HAPs could have masked interesting changes of the LAPs. Also, the use of a stable isotope-labelled standard peptide to improve quantification estimations and the deposition of blood onto different forensically relevant substrates not known for their stabilising effects are recommended. To speed up the workflow for future proteomic DBS analyses, an immobilised microfluidic enzyme reactor (IMER) was developed and tested as outlined in Chapter 3. A cyclic-olefin-copolymer based microfluidic reactor was constructed containing trypsin immobilised on a polymer monolithic substrate [233]. The IMER was tested for the rapid offline digestion of both singular protein standards and for the application to a complex protein mixture extracted from DBS. No denaturation or protein pre-treatment was needed prior to IMER-facilitated digestion of proteins. IMER-facilitated digestion of the model protein α-casein resulted in a higher sequence coverage compared to overnight in-solution digestion and a higher concentration of α-casein resulted in a higher number of identified peptides. Various IMER residence times

were tested and a lower limit of 39 seconds was found because of pressure limitations of the syringe pump, syringe and connecting parts. The upper limit was found to be 293 seconds as a longer residence time did not result in increased sequence coverage or a higher number of identified proteins. Good repeatability was demonstrated with an average sequence coverage of 84% and a relative standard deviation (RSD) of 6%. Lastly, IMER-facilitated digestion was found slightly better for proteins in the lower molecular weight (MW) range (≤42.8 kDa), but lower than in-solution digestion for proteins with a higher MW (≥66.5 kDa).

Application of the IMER to digest DBS proteins resulted in a similar distribution in MW, isoelectric point and grand average of hydropathy index for the identified proteins by IMER-facilitated digestion and in-solution digestion. The similarity in distribution of DBS proteins in the higher MW range is worth mentioning as a lower sequence coverage was found for higher MW singular protein standards by IMER-facilitated digestion compared to in-solution digestion. The reusability of the IMER is one of its major advantages compared to in-solution digestion. An associated advantage is that sample pre-treatment steps have to be omitted, which lead to a reduction in overall DBS workflow time from 22.5 hours to 4 hours compared to a workflow with in-solution digestion. The reduction in digestion time itself was the main contributing factor for reducing the total workflow time by a factor of 6, as digestion time was reduced from 16 hours to 5.6 minutes when using the IMER instead of in-solution digestion.

An alternative approach to further explore the molecular profile of aged DBS was described in Chapter 4. The novel ionisation technique surface acoustic wave nebulisation followed by mass spectrometry (SAWN-MS) [263] was applied to the DBS sample set of Chapter 2 analysed using nano-LC-ESI/MS/MS. Similar to other ambient ionisation techniques, the SAWN-MS setup is simple by ionisation of samples in the atmosphere external to the MS, a short acquisition time and both limited sample preparation and a low sample volume are required. When comparing the nano-LC-ESI-MS/MS measurements with the SAWN-MS measurements, the acquisition time was reduced from 90 minutes to 2 minutes per DBS sample. However, the method acquisition precision for the analysis of DBS samples was low with RSDs of approximately 50%. Manual application of the samples onto the SAWN-chip could have

added to the high median RSD values. The manual application of samples to the SAWN-chip is simple and quick, but at present more labour intensive than the nano-LC-ESI-MS/MS analysis by auto-sampling. Less sample pre-treatment is potentially required if the acquisition by SAWN-MS appears suitable for non-digested DBS samples. Preliminary results of non-digested DBS measured by SAWN-MS showed a decreased RSD for method precision compared to the measurement of digested DBS samples. It would be interesting to measure more non-digested samples to see if the entire workflow time for the prediction of DBS age by SAWN-MS can be reduced, but method development would be needed first to increase measurement repeatability.

Principal component analysis (PCA) showed that DBS aged between 1 and 8 days could be separated from the DBS samples not aged (day 0) for 2 out of 6 donors and when pooling samples per DBS age from the donors pre-acquisition. The dataset needed to be pre-treated for the analyses by denoising, peak detection, peak clean-up and outlier removal, which resulted in the removal of ±33% of the initial spectra. Feature selection revealed 13 features as most important to classify DBS age with a relative importance ranging between 10-20%. A support vector machine (SVM) model was developed for the prediction of DBS age. First, a multi-class prediction model was developed which showed a 100% accuracy for the classification of DBS not aged (day 0). However, the number of false positives was high and the classification accuracy for all other DBS ages was low with an overall accuracy of 50.8%. Therefore, a binary class model was adopted with a 98.2% accuracy for classifying DBS age as either day 0 or any other day. However, the SVM was unable to predict age from new batches of DBS.

SAWN-MS is a novel technique with potential for analysing a plethora of sample types quickly, but it may not be compatible with the analysis of DBS for the prediction of the TSD of bloodstains. Extensive method development for DBS analyses would be needed. For future experiments, to be able to quantify molecular changes it is highly recommended to spike the DBS samples with an internal standard as was also recommended for the nano-LC-ESI-MS/MS study.

7.2 VAMS for blood toxicology

For toxicology purposes it was investigated if volumetric absorptive microsampling (VAMS) technology could confer advantages for the detection and quantification of two selected drugs of abuse from micro-volume blood samples [153, 188]. The collection of micro-volumes of blood offers many advantages over conventional blood sampling and other biological sample types. In summary, the collection of capillary blood is simple, quick and less invasive. Samples can be transported by regular post and stored at room temperature. Multiple samples can be collected easily owing to its small sample volume. For many analytes enhanced stability has been demonstrated compared to conventional blood samples and all lead to cost savings. VAMS offers even more simplicity for collection and analysis of micro-volumes of blood by absorption of a fixed sample volume directly onto the device.

For the first time, salbutamol and pseudoephedrine were measured using VAMS from the blood of healthy volunteers administered with either of the drug of abuse. The development of a gas chromatography mass spectrometry (GC-MS) method for the quantification of salbutamol using micro-volume blood samples was presented in Chapter 5 [280]. The quantification of salbutamol from conventional DBS collected onto cards using a fixed volume of blood was compared to blood collected onto VAMS devices. The GC-MS chromatograms showed less interference for blood samples collected onto VAMS devices than for DBS. Improved lower limit of quantification, limit of detection and signal to noise were also found for salbutamol spiked blood samples collected onto VAMS devices compared to DBS samples. The method met accuracy and precision limits for both DBS and VAMS samples according to the bioanalytical validation guidelines of the US Food and Drug Administration [339]. Volumes of 10 µL capillary blood were collected, which is a reduction compared to the 20 µL DBS samples spiked with salbutamol and analysed by UHPLC previously [82]. The sensitivity of the developed GC-MS method was sufficient to allow its application for the measurement of blood salbutamol levels for up to 2 hours post administration of 1 mg of salbutamol to three healthy volunteers. The dose administered in the study was above the normal asthma relieving dose, but below the maximum therapeutic dose of 1600 µg by inhalation over 24 hours set by the World Anti-Doping Agency [289].

The suitability of VAMS for the quantification of pseudoephedrine from micro-volumes of capillary blood was presented in Chapter 6. Small adaptations were made to the method published by Tretzel et al. for the quantification of pseudoephedrine from DBS using LC-MS to analyse blood of volunteers sampled onto VAMS devices [83]. A reduction in blood volume from 20 µL used previously to 10.1 µL in this study was established. The dose of pseudoephedrine hydrochloride was increased from 30 mg to 120 mg and no ion suppression effects nor interfering signals were observed at the expected retention time for pseudoephedrine by the VAMS sampler matrix.

In terms of application of VAMS to sport doping testing, the methods for salbutamol and pseudoephedrine quantification would be applicable to monitor blood concentrations in athletes where reduced invasiveness sampling and a low sample volume are preferable. The methods also facilitate frequent blood sampling in order to quantify blood concentrations of the drugs of abuse both in- and out-of-competition.

7.3 Exhaled breath as another alternative matrix for toxicology

Breath samples were taken in parallel with the micro-volume blood samples from the healthy volunteers dosed with pseudoephedrine hydrochloride to investigate if pseudoephedrine hydrochloride and/or its metabolic products such as the main metabolite cathine could be detected as VOCs. VOCs have mainly been studied in breath samples to examine biomarker profiles for disease monitoring. Chapter 6 described the investigation of potential biomarkers for pseudoephedrine intake and breath pharmacodynamics using two MS methods.

Proton transfer reaction time-of-flight mass spectrometry (PTR-ToF-MS) was used to analyse breath samples collected in real-time using forced incentive exhalation [380, 381]. In addition, a trial was performed using two dimensional gas chromatography coupled to flame ionisation detection and quadrupole mass spectrometry (GCxGC-FID/qMS) to analyse breath samples collected onto sorbent tubes. The collection of breath samples using PTR-ToF-MS has the advantage of the real-time aspect, but without adaptations to the instrumentation it is unpractical to analyse breath samples at locations of interest such as at sport events. It takes a few minutes longer to collect breath samples onto sorbent tubes, but the method of collection is not

forced and the tubes allow the portability and storage of samples, the possibility for collecting multiple samples at once and they generally add sensitivity by concentrating larger sample volumes. GCxGC analysis adds compound separation and identification over PTR-ToF-MS analysis.

Currently, breath analysis by PTR-ToF-MS has the potential to give a presumptive indication about the intake of pseudoephedrine. A confirmatory test such as micro-volume blood samples collected by VAMS could be applied to athletes who test positive in order to give a quantitative result for inclusion/exclusion of athletes at competitions. The GCxGC-FID/qMS trial revealed over 200 VOCs in the breath samples of volunteers, but it was not possible to assess a pharmacodynamic breath profile after pseudoephedrine hydrochloride intake with the current method. Method development is recommended for the breath analyses by both PTR-ToF-MS and GCxGC-FID/qMS to investigate potential biomarkers for pseudoephedrine intake.

7.4 Future perspectives for predicting the past of DBS

To assess a molecular profile of DBS ageing, a few matters of consideration and recommendations were touched upon for future studies. In Chapter 2, depletion of HAPs or enrichment of LAPs from DBS, the deposition of blood onto different substrates not known for their stabilising effects and most importantly the use of stable isotope-labelled standard peptides was recommended. Establishing a molecular profile of ageing DBS would increase the understanding of proteomic changes underlying the ageing of bloodstains and could lead to a method for predicting the TSD of bloodstains. The developed IMER presented in Chapter 3 was found suitable to speed up proteomic DBS workflows by reducing digestion time and omitting pre-treatment steps. For future applications, the implementation of flow-through IMERs in-line with LC-MS is worth investigation for high-throughput sample analysis. Long-term stability tests of the IMER are also advised. Lastly, SAWN-MS was explored as an alternative approach for assessing a molecular profile of aged DBS in Chapter 4. The technique has the potential for analysing a plethora of sample types quickly, but this might not coincide with the analysis of DBS for TSD predictions. Extensive method development would be needed including spiking of samples with an internal standard for quantification.

The establishment of a molecular profile of DBS aged under lab conditions and the development of a model for evaluating the TSD of DBS would be the first step towards predicting the past of bloodstains in forensic scenarios. The effects of unknown quantities of blood present at crime scenes, the influence of surface texture and environmental conditions such as temperature, humidity, light, changing weather conditions and even micro-organisms need to be assessed. In addition, the current sample preparation and complex instrumentation limit the possibility of performing molecular DBS analyses directly at a crime scene.

VAMS technology was found successful for the quantification of two selected drugs of abuse from micro-volume blood samples. VAMS offered improved micro-volume blood collection over DBS and conventional blood samples by absorption of a fixed sample volume onto the device without the need of other specialist equipment. Chapter 5 and Chapter 6 showed the successful application of VAMS to quantify salbutamol and pseudoephedrine from micro-volume blood samples of healthy volunteers dosed with one of the two drugs of abuse in the lab. As the pharmacokinetics of blood could change with exercise, it would be interesting to change the design of future studies by having the volunteers exercise instead of sampling them while they are passively sitting still during the experiments to represent sport testing scenarios.

In order to apply and extend toxicological assays to bloodstains at crime scenes [85], the volume of blood samples to be collected would need to be determined if quantification of drugs is desired. VAMS devices could be used if there is still liquid blood present and DBS cards were recently found applicable to recover blood evidence from crime scenes [415]. Blood was recovered from a concrete substrate for DNA recovery, but the method has the potential for toxicology. Furthermore, methods for estimating the volume of bloodstains by fractal analysis of digital images [416], stain diameter and number of spines for bloodstains onto four different surfaces [417], blood area estimation on knit fabrics [418] and optical coherence tomography [419] were published. The issue of haematocrit (HCT) effect does not have to be a restraining factor as HCT can also be measured, even from post-mortem blood [420, 421]. However, the current sample preparation and complex instrumentation restrict toxicology analyses of micro-volumes of blood directly at crime scenes.

References

[1] James S.H., Kish P.E., Sutton T.P., Principles of bloodstain pattern analysis: theory and practice, CRC Press, 2005.

[2] Virkler K., Lednev I.K., Analysis of body fluids for forensic purposes: from laboratory testing to non-destructive rapid confirmatory identification at a crime scene, Forensic Science International, 188 (2009) 1-17.

[3] Doi Y., Yamamoto Y., Inagaki S., Shigeta Y., Miyaishi S., Ishizu H., A new method for ABO genotyping using a multiplex single-base primer extension reaction and its application to forensic casework samples, Legal Medicine, 6 (2004) 213-223.

[4] Boron W.F., Boulpaep E.L., Medical Physiology, Chapter 18 (Blood), Saunders, Philadelphia, 2009, pp. 448-481.

[5] Skopp G., Postmortem toxicology, Forensic Science, Medicine, and Pathology, 6 (2010) 314-325.

[6] Donaldson A., Lamont I., Metabolomics of post-mortem blood: identifying potential markers of post-mortem interval, Metabolomics, 11 (2015) 237-245.

[7] Drummer O.H., Postmortem toxicology of drugs of abuse, Forensic Science International, 142 (2004) 101-113.

[8] Janko M., Stark R.W., Zink A., Preservation of 5300 year old red blood cells in the Iceman, Journal of the Royal Society Interface, 9 (2012) 2581-2590.

[9] Tomellini L., De l'emploi d'une table chromatique pour les taches du sang, Archives d'Antropologie Criminelle de Criminologie, 14 (1907).

[10] Brutin D., Sobac B., Loquet B., Sampol J., Pattern formation in drying drops of blood, Journal of Fluid Mechanics, 667 (2011) 85-95.

[11] Zimmerman M.R., Blood cells preserved in a mummy 2000 years old, Science, 180 (1973) 303-304.

[12] Loy T.H., Prehistoric blood residues: detection on tool surfaces and identification of species of origin, Science, 220 (1983) 1269-1271.

[13] Cizdziel J.V., Determination of lead in blood by laser ablation ICP-TOF-MS analysis of blood spotted and dried on filter paper: a feasibility study, Analytical and Bioanalytical Chemistry, 388 (2007) 603-611.

[14] Hortolà P., SEM analysis of red blood cells in aged human bloodstains, Forensic Science International, 55 (1992) 139-159.

[15] Strasser S., Zink A., Kada G., Hinterdorfer P., Peschel O., Heckl W.M., Nerlich A.G., Thalhammer S., Age determination of blood spots in forensic medicine by force spectroscopy, Forensic Science International, 170 (2007) 8-14.

[16] Wu Y., Hu Y., Cai J., Ma S., Wang X., Chen Y., Pan Y., Time-dependent surface adhesive force and morphology of RBC measured by AFM, Micron, 40 (2009) 359-364.

[17] Chilcote B., Rust L., Nizio K.D., Forbes S.L., Profiling the scent of weathered training aids for blood-detection dogs, Science & Justice, 58 (2017) 98-102.

[18] Rust L., Nizio K.D., Forbes S.L., The influence of ageing and surface type on the odour profile of blood-detection dog training aids, Analytical and Bioanalytical Chemistry, 408 (2016) 6349-6360.

[19] Bauer M., Polzin S., Patzelt D., Quantification of RNA degradation by semi-quantitative duplex and competitive RT-PCR: a possible indicator of the age of bloodstains?, Forensic Science International, 138 (2003) 94-103.

[20] Anderson S., Howard B., Hobbs G.R., Bishop C.P., A method for determining the age of a bloodstain, Forensic Science International, 148 (2005) 37-45.

[21] Morta W., A study on nucleic acid degradation in drying and dried bloodstains as a means to determine the time since deposition, PhD Thesis, University of Auckland, 2012.
[22] Rajamannar K., Determination of the age of bloodstains using immunoelectrophoresis, Journal of Forensic Science, 22 (1977) 159-164.
[23] Agudelo J., Huynh C., Halámek J., Forensic determination of blood sample age using a bioaffinity-based assay, Analyst, 140 (2015) 1411-1415.
[24] Agudelo J., Halámková L., Brunelle E., Rodrigues R., Huynh C., Halámek J., Ages at a crime scene: Simultaneous estimation of the time since deposition and age of its originator, Analytical Chemistry, 88 (2016) 6479-6484.
[25] Schwarz F., Quantitative untersuchungen der katalase und peroxydase im blutfleck, International Journal of Legal Medicine, 27 (1937) 1-34.
[26] Kumagai R., Analysis of hemoglobin in bloodstains using high-performance liquid chromatography, Nihon Hoigaku Zasshi (The Japanese Journal of Legal Medicine), 47 (1993) 213-219.
[27] Matsuoka T., Taguchi T., Okuda J., Estimation of bloodstain age by rapid determinations of oxyhemoglobin by use of oxygen electrode and total hemoglobin, Biological and Pharmaceutical Bulletin, 18 (1995) 1031-1035.
[28] Edelman G.L., van Leeuwen T.G., Aalders M.C., Hyperspectral imaging for the age estimation of blood stains at the crime scene, Forensic Science International, 223 (2012) 72-77.
[29] Bremmer R.H., Nadort A., Van Leeuwen T.G., Van Gemert M.J., Aalders M.C., Age estimation of blood stains by hemoglobin derivative determination using reflectance spectroscopy, Forensic Science International, 206 (2011) 166-171.
[30] Keevil B.G., The analysis of dried blood spot samples using liquid chromatography tandem mass spectrometry, Clinical Biochemistry, 44 (2011) 110-118.
[31] Bang J., Der blutzucker, Wiesbaden, (1913).
[32] Guthrie R., Susi A., A simple phenylalanine method for detecting phenylketonuria in large populations of newborn infants, Pediatrics, 32 (1963) 338-343.
[33] Alfazil A.A., Anderson R.A., Stability of benzodiazepines and cocaine in blood spots stored on filter paper, Journal of Analytical Toxicology, 32 (2008) 511-515.
[34] Boy R.G., Henseler J., Mattern R., Skopp G., Determination of morphine and 6-acetylmorphine in blood with use of dried blood spots, Therapeutic Drug Monitoring, 30 (2008) 733-739.
[35] Faller A., Richter B., Kluge M., Koenig P., Seitz H.K., Thierauf A., Gnann H., Winkler M., Mattern R., Skopp G., LC-MS/MS analysis of phosphatidylethanol in dried blood spots versus conventional blood specimens, Analytical and Bioanalytical Chemistry, 401 (2011) 1163.
[36] Jantos R., Skopp G., Comparison of drug analysis in whole blood and dried blood spots, Toxichem Krimtech, 78 (2011) 268-275.
[37] Jantos R., Veldstra J.L., Mattern R., Brookhuis K.A., Skopp G., Analysis of 3, 4-methylenedioxymetamphetamine: whole blood versus dried blood spots, Journal of Analytical Toxicology, 35 (2011) 269-273.
[38] Burnett J.E., Dried blood spot sampling: practical considerations and recommendation for use with preclinical studies, Bioanalysis, 3 (2011) 1099-1107.
[39] Mei J.V., Alexander J.R., Adam B.W., Hannon W.H., Use of filter paper for the collection and analysis of human whole blood specimens, The Journal of Nutrition, 131 (2001) 1631S-1636S.
[40] Denniff P., Spooner N., Effect of storage conditions on the weight and appearance of dried blood spot samples on various cellulose-based substrates, Bioanalysis, 2 (2010) 1817-1822.

[41] Denniff P., Woodford L., Spooner N., Effect of ambient humidity on the rate at which blood spots dry and the size of the spot produced, Bioanalysis, 5 (2013) 1863-1871.
[42] Bowen C.L., Dopson W., Kemp D.C., Lewis M., Lad R., Overvold C., Investigations into the environmental conditions experienced during ambient sample transport: impact to dried blood spot sample shipments, Bioanalysis, 3 (2011) 1625-1633.
[43] Adam B., Hall E., Sternberg M., Lim T., Flores S., O'Brien S., Simms D., Li L., De Jesus V., Hannon W., The stability of markers in dried-blood spots for recommended newborn screening disorders in the United States, Clinical Biochemistry, 44 (2011) 1445-1450.
[44] Stove C.P., Ingels A.-S.M.E., De Kesel P.M.M., Lambert W.E., Dried blood spots in toxicology: from the cradle to the grave?, Critical Reviews in Toxicology, 42 (2012) 230-243.
[45] Denniff P., Spooner N., The effect of hematocrit on assay bias when using DBS samples for the quantitative bioanalysis of drugs, Bioanalysis, 2 (2010) 1385-1395.
[46] de Vries R., Barfield M., van de Merbel N., Schmid B., Siethoff C., Ortiz J., Verheij E., van Baar B., Cobb Z., White S., The effect of hematocrit on bioanalysis of DBS: results from the EBF DBS-microsampling consortium, Bioanalysis, 5 (2013) 2147-2160.
[47] Patel P., Mulla H., Tanna S., Pandya H., Facilitating pharmacokinetic studies in children: a new use of dried blood spots, Archives of Disease in Childhood, 95 (2010) 484-487.
[48] Adam B.W., Alexander J.R., Smith S.J., Chace D.H., Loeber J.G., Elvers L., Hannon W.H., Recoveries of phenylalanine from two sets of dried-blood-spot reference materials: prediction from hematocrit, spot volume, and paper matrix, Clinical Chemistry, 46 (2000) 126-128.
[49] Wilhelm A., Den Burger J., Vos R., Chahbouni A., Sinjewel A., Analysis of cyclosporin A in dried blood spots using liquid chromatography tandem mass spectrometry, Journal of Chromatography B, 877 (2009) 1595-1598.
[50] O'Broin S., Influence of hematocrit on quantitative analysis of "blood spots" on filter paper, Clinical Chemistry, 39 (1993) 1354-1355.
[51] Holub M., Tuschl K., Ratschmann R., Strnadová K.A., Mühl A., Heinze G., Sperl W., Bodamer O.A., Influence of hematocrit and localisation of punch in dried blood spots on levels of amino acids and acylcarnitines measured by tandem mass spectrometry, Clinica Chimica Acta, 373 (2006) 27-31.
[52] O'Mara M., Hudson-Curtis B., Olson K., Yueh Y., Dunn J., Spooner N., The effect of hematocrit and punch location on assay bias during quantitative bioanalysis of dried blood spot samples, Bioanalysis, 3 (2011) 2335-2347.
[53] Lawson A., Bernstone L., Hall S., Newborn screening blood spot analysis in the UK: influence of spot size, punch location and haematocrit, Journal of Medical Screening, 23 (2016) 7-16.
[54] Li F., Ploch S., Fast D., Michael S., Perforated dried blood spot accurate microsampling: the concept and its applications in toxicokinetic sample collection, Journal of Mass Spectrometry, 47 (2012) 655-667.
[55] Capiau S., Stove V.V., Lambert W.E., Stove C.P., Prediction of the hematocrit of dried blood spots via potassium measurement on a routine clinical chemistry analyzer, Analytical Chemistry, 85 (2012) 404-410.
[56] Capiau S., Wilk L.S., De Kesel P.M., Aalders M.C., Stove C.P., Correction for the hematocrit bias in dried blood spot snalysis using a non-destructive, single-wavelength reflectance-based hematocrit prediction method, Analytical Chemistry, (2017).
[57] Wagner M., Tonoli D., Varesio E., Hopfgartner G., The use of mass spectrometry to analyze dried blood spots, Mass Spectrometry Reviews, 35 (2016) 361-438.
[58] van Baar B.L., Verhaeghe T., Heudi O., Rohde M., Wood S., Wieling J., De Vries R., White S., Cobb Z., Timmerman P., IS addition in bioanalysis of DBS: results from the EBF DBS-microsampling consortium, Bioanalysis, 5 (2013) 2137-2145.

[59] Kolocouri F., Dotsikas Y., Loukas Y.L., Dried plasma spots as an alternative sample collection technique for the quantitative LC-MS/MS determination of gabapentin, Analytical and Bioanalytical Chemistry, 398 (2010) 1339-1347.
[60] Li Y., Henion J., Abbott R., Wang P., The use of a membrane filtration device to form dried plasma spots for the quantitative determination of guanfacine in whole blood, Rapid Communications in Mass Spectrometry, 26 (2012) 1208-1212.
[61] Kim J.-H., Woenker T., Adamec J., Regnier F.E., Simple, miniaturized blood plasma extraction method, Analytical Chemistry, 85 (2013) 11501-11508.
[62] Ryona I., Henion J., A book-type dried plasma spot card for automated flow-through elution coupled with online SPE-LC-MS/MS bioanalysis of opioids and stimulants in blood, Analytical Chemistry, 88 (2016) 11229-11237.
[63] Chambers A.G., Percy A.J., Hardie D.B., Borchers C.H., Comparison of proteins in whole blood and dried blood spot samples by LC/MS/MS, Journal of The American Society for Mass Spectrometry, 24 (2013) 1338-1345.
[64] Redondo A.H., Körber C., König S., Längin A., Al-Ahmad A., Weinmann W., Inhibition of bacterial degradation of EtG by collection as dried urine spots (DUS), Analytical and Bioanalytical Chemistry, 402 (2012) 2417-2424.
[65] Otero-Fernández M., Cocho J.Á., Tabernero M.J., Bermejo A.M., Bermejo-Barrera P., Moreda-Piñeiro A., Direct tandem mass spectrometry for the simultaneous assay of opioids, cocaine and metabolites in dried urine spots, Analytica Chimica Acta, 784 (2013) 25-32.
[66] DuBey I., Caplan Y., The storage of forensic urine drug specimens as dry stains: recovery and stability, Journal of Forensic Science, 41 (1996) 845-850.
[67] Christianson C.D., Laine D.F., Zimmer J.S., Johnson C.J., Sheaff C.N., Carpenter A., Needham S.R., Development and validation of an HPLC–MS/MS method for the analysis of dexamethasone from pig synovial fluid using dried matrix spotting, Bioanalysis, 2 (2010) 1829-1837.
[68] Chace D.H., Kalas T.A., Naylor E.W., Use of tandem mass spectrometry for multianalyte screening of dried blood specimens from newborns, Clinical Chemistry, 49 (2003) 1797-1817.
[69] De Jesús V.R., Mei J.V., Bell C.J., Hannon W.H., Improving and assuring newborn screening laboratory quality worldwide: 30-year experience at the Centers for Disease Control and Prevention, Seminars in Perinatology, Elsevier, 2010, pp. 125-133.
[70] Koal T., Burhenne H., Roemling R., Svoboda M., Resch K., Kaever V., Quantification of antiretroviral drugs in dried blood spot samples by means of liquid chromatography/tandem mass spectrometry, Rapid Communications in Mass Spectrometry, 19 (2005) 2995-3001.
[71] Cheung C.Y., Van Der Heijden J., Hoogtanders K., Christiaans M., Liu Y.L., Chan Y.H., Choi K.S., Van De Plas A., Shek C.C., Chau K.F., Dried blood spot measurement: application in tacrolimus monitoring using limited sampling strategy and abbreviated AUC estimation, Transplant International, 21 (2008) 140-145.
[72] Leichtle A.B., Ceglarek U., Witzigmann H., Gäbel G., Thiery J., Fiedler G.M., Potential of dried blood self-sampling for Cyclosporine C Journal of Transplantation, 2010 (2010).
[73] Merton G., Jones K., Lee M., Johnston A., Holt D.W., Accuracy of cyclosporin measurements made in capillary blood samples obtained by skin puncture, Therapeutic Drug Monitoring, 22 (2000) 594-598.
[74] Li W., Tse F.L., Dried blood spot sampling in combination with LC-MS/MS for quantitative analysis of small molecules, Biomedical Chromatography, 24 (2010) 49-65.

[75] Sosnoff C.S., Ann Q., Bernert Jr J.T., Powell M.K., Miller B.B., Henderson L.O., Hannon W.H., Fernhoff P., Sampson E.J., Analysis of benzoylecgonine in dried blood spots by liquid chromatography-atmospheric pressure chemical ionization tandem mass spectrometry, Journal of Analytical Toxicology, 20 (1996) 179-184.
[76] Parker S., Cubitt W., The use of the dried blood spot sample in epidemiological studies, Journal of Clinical Pathology, 52 (1999) 633.
[77] Versace F., Déglon J., Lauer E., Mangin P., Staub C., Automated DBS extraction prior to HILIC/RPLC–MS/MS target screening of drugs, Chromatographia, 76 (2013) 1281-1293.
[78] Mercolini L., Mandrioli R., Gerra G., Raggi M.A., Analysis of cocaine and two metabolites in dried blood spots by liquid chromatography with fluorescence detection: a novel test for cocaine and alcohol intake, Journal of Chromatography A, 1217 (2010) 7242-7248.
[79] Saussereau E., Lacroix C., Gaulier J., Goulle J., On-line liquid chromatography/tandem mass spectrometry simultaneous determination of opiates, cocainics and amphetamines in dried blood spots, Journal of Chromatography B, 885 (2012) 1-7.
[80] Wood D.M., Nicolaou M., Dargan P.I., Epidemiology of recreational drug toxicity in a nightclub environment, Substance Use & Misuse, 44 (2009) 1495-1502.
[81] Mercolini L., Protti M., Catapano M.C., Rudge J., Sberna A.E., LC–MS/MS and volumetric absorptive microsampling for quantitative bioanalysis of cathinone analogues in dried urine, plasma and oral fluid samples, Journal of Pharmaceutical and Biomedical Analysis, 123 (2016) 186-194.
[82] Thomas A., Geyer H., Schänzer W., Crone C., Kellmann M., Moehring T., Thevis M., Sensitive determination of prohibited drugs in dried blood spots (DBS) for doping controls by means of a benchtop quadrupole/Orbitrap mass spectrometer, Analytical and Bioanalytical Chemistry, 403 (2012) 1279-1289.
[83] Tretzel L., Thomas A., Geyer H., Pop V., Schänzer W., Thevis M., Dried blood spots (DBS) in doping controls: a complementary matrix for improved in-and out-of-competition sports drug testing strategies, Analytical Methods, 7 (2015) 7596-7605.
[84] Tretzel L., Thomas A., Geyer H., Gmeiner G., Forsdahl G., Pop V., Schänzer W., Thevis M., Use of dried blood spots in doping control analysis of anabolic steroid esters, Journal of Pharmaceutical and Biomedical Analysis, 96 (2014) 21-30.
[85] Schütz H., Gotta J.C., Erdmann F., Rißе M., Weiler G., Simultaneous screening and detection of drugs in small blood samples and bloodstains, Forensic Science International, 126 (2002) 191-196.
[86] Demirev P.A., Dried blood spots: Analysis and applications, Analytical Chemistry, 85 (2013) 779-789.
[87] Spooner N., Lad R., Barfield M., Dried blood spots as a sample collection technique for the determination of pharmacokinetics in clinical studies: considerations for the validation of a quantitative bioanalytical method, Analytical Chemistry, 81 (2009) 1557-1563.
[88] Mohammed B.S., Cameron G.A., Cameron L., Hawksworth G.H., Helms P.J., McLay J.S., Can finger-prick sampling replace venous sampling to determine the pharmacokinetic profile of oral paracetamol?, British Journal of Clinical Pharmacology, 70 (2010) 52-56.
[89] Barfield M., Spooner N., Lad R., Parry S., Fowles S., Application of dried blood spots combined with HPLC-MS/MS for the quantification of acetaminophen in toxicokinetic studies, Journal of Chromatography B, 870 (2008) 32-37.
[90] Anderson L., Candidate-based proteomics in the search for biomarkers of cardiovascular disease, The Journal of Physiology, 563 (2005) 23-60.
[91] Sharma A., Jaiswal S., Shukla M., Lal J., Dried blood spots: concepts, present status, and future perspectives in bioanalysis, Drug Testing and Analysis, 6 (2014) 399-414.
[92] Nuorteva P., Age determination of a blood stain in a decaying shirt by entomological means, Forensic Science, 3 (1974) 89-94.

[93] Guo K., Achilefu S., Berezin M.Y., Dating bloodstains with fluorescence lifetime measurements, Chemistry-A European Journal, 18 (2012) 1303-1305.
[94] Leers O., Die forensische blutuntersuchung, Berlin, 1910.
[95] Schwarzacher, Determination of the age of bloodstains, American Journal of Police Science, 1 (1930) 374-380.
[96] Bremmer R.H., de Bruin K.G., van Gemert M.J., van Leeuwen T.G., Aalders M.C., Forensic quest for age determination of bloodstains, Forensic Science International, 216 (2012) 1-11.
[97] Arany S., Ohtani S., Age estimation of bloodstains: A preliminary report based on aspartic acid racemization rate, Forensic Science International, 212 (2011) e36-e39.
[98] Chen Y., Cai J., Membrane deformation of unfixed erythrocytes in air with time lapse investigated by tapping mode atomic force microscopy, Micron, 37 (2006) 339-346.
[99] McCutcheon J.N., Forensic discrimination, age estimation, and spectral optimization for trace detection of blood on textile substrates using infrared spectroscopy and chemometrics, PhD Thesis, University of South Carolina, 2010.
[100] Orphanou C.M.R., A bioanalytical approach to forensic body fluid identification & age determination, PhD Thesis, Staffordshire University, 2015.
[101] Zhang Y., Wang Q., Li B., Wang Z., Li C., Yao Y., Huang P., Wang Z., Changes in attenuated total reflection Fourier transform infrared spectra as blood dries out, Journal of Forensic Sciences, 62 (2017) 761-767.
[102] Thanakiatkrai P., Yaodam A., Kitpipit T., Age estimation of bloodstains using smartphones and digital image analysis, Forensic Science International, 233 (2013) 288-297.
[103] Miki T., Kai A., Ikeya M., Electron spin resonance of bloodstains and its application to the estimation of time after bleeding, Forensic Science International, 35 (1987) 149-158.
[104] Sakurai H., Tsuchiya K., Fujita Y., Okada K., Dating of human blood by electron spin resonance spectroscopy, Naturwissenschaften, 76 (1989) 24-25.
[105] Fujita Y., Tsuchiya K., Abe S., Takiguchi Y., Kubo S.-i., Sakurai H., Estimation of the age of human bloodstains by electron paramagnetic resonance spectroscopy: long-term controlled experiment on the effects of environmental factors, Forensic Science International, 152 (2005) 39-43.
[106] Ackermann K., Ballantyne K.N., Kayser M., Estimating trace deposition time with circadian biomarkers: a prospective and versatile tool for crime scene reconstruction, International Journal of Legal Medicine, 124 (2010) 387-395.
[107] Inoue H., Takabe F., Iwasa M., Maeno Y., Seko Y., A new marker for estimation of bloodstain age by high performance liquid chromatography, Forensic Science International, 57 (1992) 17-27.
[108] Inoue H., Takabe F., Iwasa M., Maeno Y., Identification of fetal hemoglobin and simultaneous estimation of bloodstain age by high-performance liquid chromatography, International Journal of Legal Medicine, 104 (1991) 127-131.
[109] Andrasko J., The estimation of age of bloodstains by HPLC analysis, Journal of Forensic Science, 42 (1997) 601-607.
[110] Li B., Beveridge P., O'Hare W.T., Islam M., The age estimation of blood stains up to 30days old using visible wavelength hyperspectral image analysis and linear discriminant analysis, Science & Justice, 53 (2013) 270-277.
[111] Botonjic-Sehic E., Brown C.W., Lamontagne M., Tsaparikos M., Forensic application of near-infrared spectroscopy: aging of bloodstains, Spectroscopy, 24 (2009) 42-48.
[112] Edelman G., Manti V., van Ruth S.M., van Leeuwen T., Aalders M., Identification and age estimation of blood stains on colored backgrounds by near infrared spectroscopy, Forensic Science International, 220 (2012) 239-244.

[113] Rauschke J., Beitrag zur frage der altersbestimmung von blutspuren, International Journal of Legal Medicine, 40 (1951) 578-584.
[114] Anderson S.E., Hobbs G.R., Bishop C.P., Multivariate analysis for estimating the age of a bloodstain, Journal of Forensic Sciences, 56 (2011) 186-193.
[115] Alrowaithi M.A., McCallum N.A., Watson N.D., A method for determining the age of a bloodstain, Forensic Science International, 234 (2014) e30-e31.
[116] Boyd S., Bertino M.F., Seashols S.J., Raman spectroscopy of blood samples for forensic applications, Forensic Science International, 208 (2011) 124-128.
[117] Li B., Beveridge P., O'Hare W.T., Islam M., The estimation of the age of a blood stain using reflectance spectroscopy with a microspectrophotometer, spectral pre-processing and linear discriminant analysis, Forensic Science International, 212 (2011) 198-204.
[118] Sun H., Dong Y., Zhang P., Meng Y., Wen W., Li N., Guo Z., Accurate age estimation of bloodstains based on visible reflectance spectroscopy and chemometrics methods, Insitute of Electrical and Electronic Engineers - Photonics Journal, 9 (2017) 1-14.
[119] Fiori A., Detection and identification of bloodstains, Methods of Forensic Science, 1 (1962) 243-290.
[120] Forbes S.L., Rust L., Trebilcock K., Perrault K.A., McGrath L.T., Effect of age and storage conditions on the volatile organic compound profile of blood, Forensic science, Medicine, and Pathology, 10 (2014) 570-582.
[121] Mc Shine S., Suhling K., Beavil A., Daniel B., Frascione N., The applicability of fluorescence lifetime to determine the time since the deposition of biological stains, Analytical Methods, 9 (2017) 2007-2013.
[122] Patterson D., Use of reflectance measurements in assessing the colour changes of ageing bloodstains, Nature, 187 (1960) 688-689.
[123] Kleihauer E., Stein G., Schmidt G., Beitrag zur altersbestimmung von blutflecken, Archiv fur Kriminologie, 140 (1967) 84-94.
[124] Kind S., Patterson D., Owen G., Estimation of the age of dried blood stains by a spectrophotometric method, Forensic Science, 1 (1972) 27-54.
[125] Köhler U., Oepen I., On the suitability of spectrophotometric analyses for the estimation of blood stain age (author's transl), Zeitschrift fur Rechtsmedizin (Journal of Legal Medicine), 79 (1977) 183-187.
[126] Blazek V., Lins G., Spectroscopic age determination of blood stains: new technical aspects, Acta Medicinae Legalis et Socialis, 32 (1982) 613.
[127] Bergmann T., Heinke F., Labudde D., Towards substrate-independent age estimation of blood stains based on dimensionality reduction and k-nearest neighbor classification of absorbance spectroscopic data, Forensic Science International, 278 (2017) 1-8.
[128] Tsutsumi A., Yamamoto Y., Ishizu H., Determination of the age of bloodstains by enzyme activities in blood cells, Japanese Journal of Legal Medicine, 37 (1983) 770-776.
[129] Hanson E.K., Ballantyne J., A blue spectral shift of the hemoglobin soret band correlates with the age (time since deposition) of dried bloodstains, PLoS One, 5 (2010) 12830-12840.
[130] Thevis M., Schänzer W., Examples of doping control analysis by liquid chromatography-tandem mass spectrometry: Ephedrines, β-receptor blocking agents, diuretics, sympathomimetics, and cross-linked hemoglobins, Journal of Chromatographic Science, 43 (2005) 22-31.
[131] Remane D., Wissenbach D.K., Peters F.T., Recent advances of liquid chromatography–(tandem) mass spectrometry in clinical and forensic toxicology—an update, Clinical Biochemistry, 49 (2016) 1051-1071.

[132] Jebrail M.J., Yang H., Mudrik J.M., Lafreniere N.M., McRoberts C., Al-Dirbashi O.Y., Fisher L., Chakraborty P., Wheeler A.R., A digital microfluidic method for dried blood spot analysis, Lab on a Chip, 11 (2011) 3218-3224.
[133] Shih S.C., Yang H., Jebrail M.J., Fobel R., McIntosh N., Al-Dirbashi O.Y., Chakraborty P., Wheeler A.R., Dried blood spot analysis by digital microfluidics coupled to nanoelectrospray ionization mass spectrometry, Analytical Chemistry, 84 (2012) 3731-3738.
[134] Lafrenière N.M., Shih S.C., Abu-Rabie P., Jebrail M.J., Spooner N., Wheeler A.R., Multiplexed extraction and quantitative analysis of pharmaceuticals from DBS samples using digital microfluidics, Bioanalysis, 6 (2014) 307-318.
[135] Meesters R.J., van Kampen J.J., Reedijk M.L., Scheuer R.D., Dekker L.J., Burger D.M., Hartwig N.G., Osterhaus A.D., Luider T.M., Gruters R.A., Ultrafast and high-throughput mass spectrometric assay for therapeutic drug monitoring of antiretroviral drugs in pediatric HIV-1 infection applying dried blood spots, Analytical and Bioanalytical Chemistry, 398 (2010) 319-328.
[136] Swales J.G., Gallagher R.T., Denn M., Peter R.M., Simultaneous quantitation of metformin and sitagliptin from mouse and human dried blood spots using laser diode thermal desorption tandem mass spectrometry, Journal of Pharmaceutical and Biomedical Analysis, 55 (2011) 544-551.
[137] Rashed M.S., Bucknall M.P., Little D., Awad A., Jacob M., Alamoudi M., Alwattar M., Ozand P.T., Screening blood spots for inborn errors of metabolism by electrospray tandem mass spectrometry with a microplate batch process and a computer algorithm for automated flagging of abnormal profiles, Clinical Chemistry, 43 (1997) 1129-1141.
[138] Abu-Rabie P., Direct analysis of DBS: emerging and desirable technologies, Bioanalysis, 3 (2011) 1675-1678.
[139] Van Berkel G.J., Kertesz V., Application of a liquid extraction based sealing surface sampling probe for mass spectrometric analysis of dried blood spots and mouse whole-body thin tissue sections, Analytical Chemistry, 81 (2009) 9146-9152.
[140] Kertesz V., Van Berkel G.J., Fully automated liquid extraction-based surface sampling and ionization using a chip-based robotic nanoelectrospray platform, Journal of Mass Spectrometry, 45 (2010) 252-260.
[141] Abu-Rabie P., Spooner N., Direct quantitative bioanalysis of drugs in dried blood spot samples using a thin-layer chromatography mass spectrometer interface, Analytical Chemistry, 81 (2009) 10275-10284.
[142] Ooms J.A., Knegt L., Koster E.H.M., Exploration of a new concept for automated dried blood spot analysis using flow-through desorption and online SPE–MS/MS, Bioanalysis, 3 (2011) 2311-2320.
[143] Verplaetse R., Henion J., Quantitative determination of opioids in whole blood using fully automated dried blood spot desorption coupled to on-line SPE-LC-MS/MS, Drug Testing and Analysis, 8 (2016) 30-38.
[144] Déglon J., Thomas A., Cataldo A., Mangin P., Staub C., On-line desorption of dried blood spot: a novel approach for the direct LC/MS analysis of µ-whole blood samples, Journal of Pharmaceutical and Biomedical Analysis, 49 (2009) 1034-1039.
[145] Wiseman J.M., Evans C.A., Bowen C.L., Kennedy J.H., Direct analysis of dried blood spots utilizing desorption electrospray ionization (DESI) mass spectrometry, Analyst, 135 (2010) 720-725.
[146] Crawford E., Gordon J., Wu J.-T., Musselman B., Liu R., Yu S., Direct analysis in real time coupled with dried spot sampling for bioanalysis in a drug-discovery setting, Bioanalysis, 3 (2011) 1217-1226.
[147] Wang H., Liu J., Cooks R.G., Ouyang Z., Paper spray for direct analysis of complex mixtures using mass spectrometry, Angewandte Chemie, 122 (2010) 889-892.

[148] Edelbroek P.M., van der Heijden J., Stolk L.M., Dried blood spot methods in therapeutic drug monitoring: methods, assays, and pitfalls, Therapeutic Drug Monitoring, 31 (2009) 327-336.
[149] Quraishi R., Jain R., Ambekar A., The use of dried blood spot samples in screening drugs of abuse, Pharmacology & Pharmacy, 4 (2013) 152.
[150] Ambach L., Hernández Redondo A., König S., Weinmann W., Rapid and simple LC-MS/MS screening of 64 novel psychoactive substances using dried blood spots, Drug Testing and Analysis, 6 (2014) 367-375.
[151] Fokkema M.R., Bakker A.J., de Boer F., Kooistra J., de Vries S., Wolthuis A., HbA1c measurements from dried blood spots: validation and patient satisfaction, Clinical Chemistry and Laboratory Medicine, 47 (2009) 1259-1264.
[152] Woods K., Douketis J.D., Schnurr T., Kinnon K., Powers P., Crowther M.A., Patient preferences for capillary vs. venous INR determination in an anticoagulation clinic: a randomized controlled trial, Thrombosis Research, 114 (2004) 161-165.
[153] Denniff P., Spooner N., Volumetric absorptive microsampling: A dried sample collection technique for quantitative bioanalysis, Analytical Chemistry, 86 (2014) 8489-8495.
[154] Amsterdam P.v., Waldrop C., The application of dried blood spot sampling in global clinical trials, Bioanalysis, 2 (2010) 1783-1786.
[155] Martial L.C., Aarnoutse R.E., Schreuder M.F., Henriet S.S., Brüggemann R.J., Joore M.A., Cost evaluation of dried blood spot home sampling as compared to conventional sampling for therapeutic drug monitoring in children, PloS One, 11 (2016) e0167433.
[156] World Health Organization. Guidance on regulations for the transport of infectious substances 2017-2018: applicable as from 1 January 2017, (2017).
[157] Knudsen R.C., Slazyk W.E., Richmond J.Y., Hannon W.H., Guidelines for the shipment of dried blood spot specimens, Infant Screening, 16 (1993).
[158] Evengard B., Von Sydow M., Ehrnst A., Pehrson P., Lundbergh P., Linder E., Filter paper sampling of blood infected with HIV: effect of heat on antibody activity and viral infectivity, BMJ: British Medical Journal, 297 (1988) 1178.
[159] Bowen C.L., Hemberger M.D., Kehler J.R., Evans C.A., Utility of dried blood spot sampling and storage for increased stability of photosensitive compounds, Bioanalysis, 2 (2010) 1823-1828.
[160] Verplaetse R., Henion J., Hematocrit-independent quantitation of stimulants in dried blood spots: pipet versus microfluidic-based volumetric sampling coupled with automated flow-through desorption and online solid phase extraction-LC-MS/MS bioanalysis, Analytical Chemistry, 88 (2016) 6789-6796.
[161] Chace D.H., Adam B.W., Smith S.J., Alexander J.R., Hillman S.L., Hannon W.H., Validation of accuracy-based amino acid reference materials in dried-blood spots by tandem mass spectrometry for newborn screening assays, Clinical Chemistry, 45 (1999) 1269-1277.
[162] Chambers A.G., Percy A.J., Yang J., Borchers C.H., Multiple reaction monitoring enables precise quantification of 97 proteins in dried blood spots, Molecular & Cellular Proteomics, 14 (2015) 3094-3104.
[163] Li L., Zhou Y., Bell C.J., Earley M.C., Hannon W.H., Mei J.V., Development and characterization of dried blood spot materials for the measurement of immunoreactive trypsinogen, Journal of Medical Screening, 13 (2006) 79-84.
[164] Lundsjö A., Hagelberg S., Palmer K., Lindblad B.S., Amino acid profiles by HPLC after filter paper sampling: 'appropriate technology' for monitoring of nutritional status, Clinica Chimica Acta, 191 (1990) 201-209.
[165] Odoardi S., Anzillotti L., Strano-Rossi S., Simplifying sample pretreatment: Application of dried blood spot (DBS) method to blood samples, including postmortem, for UHPLC–MS/MS analysis of drugs of abuse, Forensic Science International, 243 (2014) 61-67.

[166] Chace D.H., DiPerna J.C., Mitchell B.L., Sgroi B., Hofman L.F., Naylor E.W., Electrospray tandem mass spectrometry for analysis of acylcarnitines in dried postmortem blood specimens collected at autopsy from infants with unexplained cause of death, Clinical Chemistry, 47 (2001) 1166-1182.
[167] Kupke I., Kather B., Zeugner S., On the composition of capillary and venous blood serum, Clinica Chimica Acta, 112 (1981) 177-185.
[168] Yang Z.W., Yang S.H., Chen L., Qu J., Zhu J., Tang Z., Comparison of blood counts in venous, fingertip and arterial blood and their measurement variation, Clinical & Laboratory Haematology, 23 (2001) 155-159.
[169] Cox H.D., Rampton J., Eichner D., Quantification of insulin-like growth factor-1 in dried blood spots for detection of growth hormone abuse in sport, Analytical and Bioanalytical Chemistry, 405 (2013) 1949-1958.
[170] Vu D., Koster R., Alffenaar J., Brouwers J., Uges D., Determination of moxifloxacin in dried blood spots using LC–MS/MS and the impact of the hematocrit and blood volume, Journal of Chromatography B, 879 (2011) 1063-1070.
[171] Emmons G., Rowland M., Pharmacokinetic considerations as to when to use dried blood spot sampling, Bioanalysis, 2 (2010) 1791-1796.
[172] Turpin P.E., Burnett J.E., Goodwin L., Foster A., Barfield M., Application of the DBS methodology to a toxicokinetic study in rats and transferability of analysis between bioanalytical laboratories, Bioanalysis, 2 (2010) 1489-1499.
[173] D'Arienzo C.J., Ji Q.C., Discenza L., Cornelius G., Hynes J., Cornelius L., Santella J.B., Olah T., DBS sampling can be used to stabilize prodrugs in drug discovery rodent studies without the addition of esterase inhibitors, Bioanalysis, 2 (2010) 1415-1422.
[174] Denery J.R., Nunes A.A., Dickerson T.J., Characterization of differences between blood sample matrices in untargeted metabolomics, Analytical Chemistry, 83 (2010) 1040-1047.
[175] Alsaif M., Guest P.C., Schwarz E., Reif A., Kittel-Schneider S., Spain M., Rahmoune H., Bahn S., Analysis of serum and plasma identifies differences in molecular coverage, measurement variability, and candidate biomarker selection, Proteomics-Clinical Applications, 6 (2012) 297-303.
[176] McDade T.W., Williams S., Snodgrass J.J., What a drop can do: dried blood spots as a minimally invasive method for integrating biomarkers into population-based research, Demography, 44 (2007) 899-925.
[177] Luckwell J., Denniff P., Capper S., Michael P., Spooner N., Mallender P., Johnson B., Clegg S., Green M., Ahmad S., Woodford L., Assessment of the within- and between-lot variability of Whatman™ FTA® DMPK and 903® DBS papers and their suitability for the quantitative bioanalysis of small molecules, Bioanalysis, 5 (2013) 2613-2630.
[178] Liu G., Ji Q.C., Jemal M., Tymiak A.A., Arnold M.E., Approach to evaluating dried blood spot sample stability during drying process and discovery of a treated card to maintain analyte stability by rapid on-card pH modification, Analytical Chemistry, 83 (2011) 9033-9038.
[179] Leuthold L.A., Heudi O., Déglon J., Raccuglia M., Augsburger M., Picard F., Kretz O., Thomas A.l., New microfluidic-based sampling procedure for overcoming the hematocrit problem associated with dried blood spot analysis, Analytical Chemistry, 87 (2015) 2068-2071.
[180] Lenk G., Pohanka A., Stemme G., Beck O., Roxhed N., A disposable chip enabling metering in dried blood spot sampling, Micro TAS 2013, 2013, pp. 281-283.
[181] Li F., Zulkoski J., Fast D., Michael S., Perforated dried blood spots: a novel format for accurate microsampling, Bioanalysis, 3 (2011) 2321-2333.

[182] Youhnovski N., Bergeron A., Furtado M., Garofolo F., Pre-cut dried blood spot (PCDBS): an alternative to dried blood spot (DBS) technique to overcome hematocrit impact, Rapid Communications in Mass Spectrometry, 25 (2011) 2951-2958.
[183] Fan L., Lee J.A., Managing the effect of hematocrit on DBS analysis in a regulated environment, Bioanalysis, 4 (2012) 345-347.
[184] Neto R., Gooley A., Breadmore M.C., Hilder E.F., Lapierre F., Precise, accurate and user-independent blood collection system for dried blood spot sample preparation, Analytical and Bioanalytical Chemistry, 410 (2018) 3315-3323.
[185] Wong P., Pham R., Bruenner B.A., James C.A., Increasing efficiency for dried blood spot analysis: prospects for automation and simplified sample analysis, Bioanalysis, 2 (2010) 1787-1789.
[186] Clark G., Giddens G., Burrows L., Strand C., Utilization of dried blood spots within drug discovery: modification of a standard DiLab® AccuSampler® to facilitate automatic dried blood spot sampling, Laboratory Animals, 45 (2011) 124-126.
[187] Gunaratna P.C., Kissinger P.T., Kissinger C.B., Gitzen J.F., An automated blood sampler for simultaneous sampling of systemic blood and brain microdialysates for drug absorption, distribution, metabolism, and elimination studies, Journal of Pharmacological and Toxicological Methods, 49 (2004) 57-64.
[188] Spooner N., Denniff P., Michielsen L., De Vries R., Ji Q.C., Arnold M.E., Woods K., Woolf E.J., Xu Y., Boutet V., A device for dried blood microsampling in quantitative bioanalysis: overcoming the issues associated blood hematocrit, Bioanalysis, 7 (2015) 653-659.
[189] VAMS™ publications 2014-2018, https://app.hubspot.com/documents/1806452/view/7151312?accessId=8cb916, pp. 1-9, (Accessed 10/09/2018).
[190] Banfi G., Salvagno G.L., Lippi G., The role of ethylenediamine tetraacetic acid (EDTA) as in vitro anticoagulant for diagnostic purposes, Clinical Chemical Laboratory Medicine, 45 (2007) 565-576.
[191] Luque-Garcia J.L., Neubert T.A., Sample preparation for serum/plasma profiling and biomarker identification by mass spectrometry, Journal of Chromatography A, 1153 (2007) 259-276.
[192] Laan N., Impact of blood droplets, PhD Thesis, University of Amsterdam, 2015.
[193] Hsieh S.Y., Chen R.K., Pan Y.H., Lee H.L., Systematical evaluation of the effects of sample collection procedures on low-molecular-weight serum/plasma proteome profiling, Proteomics, 6 (2006) 3189-3198.
[194] Thevis M., Geyer H., Tretzel L., Schänzer W., Sports drug testing using complementary matrices: Advantages and limitations, Journal of Pharmaceutical and Biomedical Analysis, 130 (2016) 220-230.
[195] Bosker W.M., Huestis M.A., Oral fluid testing for drugs of abuse, Clinical Chemistry, 55 (2009) 1910-1931.
[196] Beck O., Stephanson N., Sandqvist S., Franck J., Detection of drugs of abuse in exhaled breath from users following recovery from intoxication, Journal of Analytical Toxicology, 36 (2012) 638-646.
[197] Beck O., Leine K., Palmskog G., Franck J., Amphetamines detected in exhaled breath from drug addicts: a new possible method for drugs-of-abuse testing, Journal of Analytical Toxicology, 34 (2010) 233-237.
[198] Skoglund C., Hermansson U., Beck O., Clinical trial of a new technique for drugs of abuse testing: A new possible sampling technique, Journal of Substance Abuse Treatment, 48 (2015) 132-136.
[199] Beck O., Stephanson N., Sandqvist S., Franck J., Detection of drugs of abuse in exhaled breath using a device for rapid collection: comparison with plasma, urine and self-reporting in 47 drug users, Journal of Breath Research, 7 (2013) 026006.

[200] Thevis M., Thomas A., Schänzer W., Targeting prohibited substances in doping control blood samples by means of chromatographic–mass spectrometric methods, Analytical and Bioanalytical Chemistry, 405 (2013) 9655-9667.
[201] Nanjappa V., Thomas J.K., Marimuthu A., Muthusamy B., Radhakrishnan A., Sharma R., Ahmad Khan A., Balakrishnan L., Sahasrabuddhe N.A., Kumar S., Plasma proteome database as a resource for proteomics research: 2014 update, Nucleic Acids Research, 42 (2013) D959-D965.
[202] Kramer G., Woolerton Y., van Straalen J.P., Vissers J.P., Dekker N., Langridge J.I., Beynon R.J., Speijer D., Sturk A., Aerts J.M., Accuracy and reproducibility in quantification of plasma protein concentrations by mass spectrometry without the use of isotopic standards, PloS One, 10 (2015) e0140097.
[203] Keshishian H., Burgess M.W., Gillette M.A., Mertins P., Clauser K.R., Mani D., Kuhn E.W., Farrell L.A., Gerszten R.E., Carr S.A., Multiplexed, quantitative workflow for sensitive biomarker discovery in plasma yields novel candidates for early myocardial injury, Molecular & Cellular Proteomics, (2015) mcp. M114. 046813.
[204] Geyer P.E., Kulak N.A., Pichler G., Holdt L.M., Teupser D., Mann M., Plasma proteome profiling to assess human health and disease, Cell Systems, 2 (2016) 185-195.
[205] Farrah T., Deutsch E.W., Omenn G.S., Campbell D.S., Sun Z., Bletz J.A., Mallick P., Katz J.E., Malmström J., Ossola R., A high-confidence human plasma proteome reference set with estimated concentrations in PeptideAtlas, Molecular & Cellular Poteomics, 10 (2011) M110. 006353.
[206] Martin N.J., Bunch J., Cooper H.J., Dried blood spot proteomics: surface extraction of endogenous proteins coupled with automated sample preparation and mass spectrometry analysis, Journal of the American Society for Mass Spectrometry, 24 (2013) 1242-1249.
[207] van den Broek I., van Dongen W.D., LC–MS-based quantification of intact proteins: perspective for clinical and bioanalytical applications, Bioanalysis, 7 (2015) 1943-1958.
[208] Zhang Y., Fonslow B.R., Shan B., Baek M.-C., Yates III J.R., Protein analysis by shotgun/bottom-up proteomics, Chemical Reviews, 113 (2013) 2343-2394.
[209] Chambers A.G., Percy A.J., Yang J., Camenzind A.G., Borchers C.H., Multiplexed quantitation of endogenous proteins in dried blood spots by multiple reaction monitoring-mass spectrometry, Molecular & Cellular Proteomics, 12 (2013) 781-791.
[210] Szykuła K., Age determination of body fluids by mass spectrometry, MSc Thesis, University of Amsterdam, 2016.
[211] Gillet L.C., Navarro P., Tate S., Röst H., Selevsek N., Reiter L., Bonner R., Aebersold R., Targeted data extraction of the MS/MS spectra generated by data-independent acquisition: a new concept for consistent and accurate proteome analysis, Molecular & Cellular Proteomics, 11 (2012) O111. 016717.
[212] Deutsch E.W., Mendoza L., Shteynberg D., Farrah T., Lam H., Tasman N., Sun Z., Nilsson E., Pratt B., Prazen B., A guided tour of the Trans-Proteomic Pipeline, Proteomics, 10 (2010) 1150-1159.
[213] Anderson N.L., Anderson N.G., The human plasma proteome history, character, and diagnostic prospects, Molecular & Cellular Proteomics, 1 (2002) 845-867.
[214] Bragulla H.H., Homberger D.G., Structure and functions of keratin proteins in simple, stratified, keratinized and cornified epithelia, Journal of Anatomy, 214 (2009) 516-559.
[215] Blein-Nicolas M., Zivy M., Thousand and one ways to quantify and compare protein abundances in label-free bottom-up proteomics, Biochimica et Biophysica Acta - Proteins and Proteomics, 1864 (2016) 883-895.
[216] Rappsilber J., Ryder U., Lamond A.I., Mann M., Large-scale proteomic analysis of the human spliceosome, Genome Research, 12 (2002) 1231-1245.

[217] Ishihama Y., Oda Y., Tabata T., Sato T., Nagasu T., Rappsilber J., Mann M., Exponentially modified protein abundance index (emPAI) for estimation of absolute protein amount in proteomics by the number of sequenced peptides per protein, Molecular & Cellular Proteomics, 4 (2005) 1265-1272.
[218] Trudgian D.C., Ridlova G., Fischer R., Mackeen M.M., Ternette N., Acuto O., Kessler B.M., Thomas B., Comparative evaluation of label-free SINQ normalized spectral index quantitation in the central proteomics facilities pipeline, Proteomics, 11 (2011) 2790-2797.
[219] Colaert N., Vandekerckhove J., Gevaert K., Martens L., A comparison of MS2-based label-free quantitative proteomic techniques with regards to accuracy and precision, Proteomics, 11 (2011) 1110-1113.
[220] McIlwain S., Mathews M., Bereman M.S., Rubel E.W., MacCoss M.J., Noble W.S., Estimating relative abundances of proteins from shotgun proteomics data, BMC bioinformatics, 13 (2012) 308.
[221] Zhang Y., Wen Z., Washburn M.P., Florens L., Refinements to label free proteome quantitation: how to deal with peptides shared by multiple proteins, Analytical Chemistry, 82 (2010) 2272-2281.
[222] Zybailov B., Mosley A.L., Sardiu M.E., Coleman M.K., Florens L., Washburn M.P., Statistical analysis of membrane proteome expression changes in Saccharomyces cerevisiae, Journal of Proteome Research, 5 (2006) 2339-2347.
[223] Ning K., Fermin D., Nesvizhskii A.I., Comparative analysis of different label-free mass spectrometry based protein abundance estimates and their correlation with RNA-Seq gene expression data, Journal of Proteome Research, 11 (2012) 2261-2271.
[224] Jmeian Y., El Rassi Z., Liquid-phase-based separation systems for depletion, prefractionation and enrichment of proteins in biological fluids for in-depth proteomics analysis, Electrophoresis, 30 (2009) 249-261.
[225] Selvaraju S., El Rassi Z., Liquid-phase-based separation systems for depletion, prefractionation and enrichment of proteins in biological fluids and matrices for in-depth proteomics analysis–An update covering the period 2008–2011, Electrophoresis, 33 (2012) 74-88.
[226] Puangpila C., Mayadunne E., El Rassi Z., Liquid phase based separation systems for depletion, prefractionation, and enrichment of proteins in biological fluids and matrices for in-depth proteomics analysis—An update covering the period 2011–2014, Electrophoresis, 36 (2015) 238-252.
[227] El Rassi Z., Puangpila C., Liquid-phase based separation systems for depletion, prefractionation, and enrichment of proteins in biological fluids and matrices for in-depth proteomics analysis—An update covering the period 2014–2016, Electrophoresis, 38 (2017) 150-161.
[228] Colantonio D.A., Dunkinson C., Bovenkamp D.E., Van Eyk J.E., Effective removal of albumin from serum, Proteomics, 5 (2005) 3831-3835.
[229] Funk W.E., Li H., Iavarone A.T., Williams E.R., Riby J., Rappaport S.M., Enrichment of cysteinyl adducts of human serum albumin, Analytical biochemistry, 400 (2010) 61-68.
[230] Fang X., Zhang W.-W., Affinity separation and enrichment methods in proteomic analysis, Journal of Proteomics, 71 (2008) 284-303.
[231] Polaskova V., Kapur A., Khan A., Molloy M.P., Baker M.S., High-abundance protein depletion: Comparison of methods for human plasma biomarker discovery, Electrophoresis, 31 (2010) 471-482.
[232] Mrozinski P., Zolotarjova N., Chen H., Human serum and plasma protein depletion – novel high-capacity affinity column for the removal of the “top 14” abundant proteins application, Agilent Technologies Inc documents, (2008).

[233] Wouters B., Dapic I., Valkenburg T.S., Wouters S., Niezen L., Eeltink S., Corthals G.L., Schoenmakers P.J., A cyclic-olefin-copolymer microfluidic immobilized-enzyme reactor for rapid digestion of proteins from dried blood spots, Journal of Chromatography A, 1491 (2017) 36-42.
[234] Corthals G., Gygi S., Aebersold R., Patterson S., Identification of proteins by mass spectrometry, Proteome Research: Two-dimensional Gel Electrophoresis and Identification Methods, Springer2000, pp. 197-231.
[235] Ma J., Zhang L., Liang Z., Shan Y., Zhang Y., Immobilized enzyme reactors in proteomics, TrAC Trends in Analytical Chemistry, 30 (2011) 691-702.
[236] Slysz G.W., Schriemer D.C., Blending protein separation and peptide analysis through real-time proteolytic digestion, Analytical Chemistry, 77 (2005) 1572-1579.
[237] Yates III J.R., Mass spectrometry and the age of the proteome, Journal of Mass Spectrometry, 33 (1998) 1-19.
[238] Santos H.M., Kouvonen P., Capelo J.L., Corthals G.L., On-target ultrasonic digestion of proteins, Proteomics, 13 (2013) 1423-1427.
[239] Switzar L., Giera M., Niessen W.M., Protein digestion: an overview of the available techniques and recent developments, Journal of Proteome Research, 12 (2013) 1067-1077.
[240] Capelo J., Carreira R., Diniz M., Fernandes L., Galesio M., Lodeiro C., Santos H., Vale G., Overview on modern approaches to speed up protein identification workflows relying on enzymatic cleavage and mass spectrometry-based techniques, Analytica Chimica Acta, 650 (2009) 151-159.
[241] Lazar I.M., Ramsey R.S., Ramsey J.M., On-chip proteolytic digestion and analysis using “wrong-way-round” electrospray time-of-flight mass spectrometry, Analytical Chemistry, 73 (2001) 1733-1739.
[242] Krenkova J., Lacher N.A., Svec F., Highly efficient enzyme reactors containing trypsin and endoproteinase LysC immobilized on porous polymer monolith coupled to MS suitable for analysis of antibodies, Analytical Chemistry, 81 (2009) 2004-2012.
[243] Wu S., Sun L., Ma J., Yang K., Liang Z., Zhang L., Zhang Y., High throughput tryptic digestion via poly (acrylamide-co-methylenebisacrylamide) monolith based immobilized enzyme reactor, Talanta, 83 (2011) 1748-1753.
[244] Jiang B., Yang K., Zhao Q., Wu Q., Liang Z., Zhang L., Peng X., Zhang Y., Hydrophilic immobilized trypsin reactor with magnetic graphene oxide as support for high efficient proteome digestion, Journal of Chromatography A, 1254 (2012) 8-13.
[245] Mateo C., Palomo J.M., Fernandez-Lorente G., Guisan J.M., Fernandez-Lafuente R., Improvement of enzyme activity, stability and selectivity via immobilization techniques, Enzyme and Microbial Technology, 40 (2007) 1451-1463.
[246] Pereira-Medrano A.G., Forster S., Fowler G.J., McArthur S.L., Wright P.C., Rapid fabrication of glass/PDMS hybrid µIMER for high throughput membrane proteomics, Lab on a Chip, 10 (2010) 3397-3406.
[247] Amankwa L.N., Kuhr W.G., Trypsin-modified-fused-silica capillary microreactor for peptide mapping by capillary zone electrophoresis, Analytical Chemistry, 64 (1992) 1610-1613.
[248] Cooper J.W., Chen J., Li Y., Lee C.S., Membrane-based nanoscale proteolytic reactor enabling protein digestion, peptide separation, and protein identification using mass spectrometry, Analytical Chemistry, 75 (2003) 1067-1074.
[249] Xu F., Wang W.-H., Tan Y.-J., Bruening M.L., Facile trypsin immobilization in polymeric membranes for rapid, efficient protein digestion, Analytical Chemistry, 82 (2010) 10045-10051.

[250] Le Nel A., Minc N., Smadja C., Slovakova M., Bilkova Z., Peyrin J.-M., Viovy J.-L., Taverna M., Controlled proteolysis of normal and pathological prion protein in a microfluidic chip, Lab on a Chip, 8 (2008) 294-301.
[251] Cingöz A., Hugon-Chapuis F., Pichon V., Total on-line analysis of a target protein from plasma by immunoextraction, digestion and liquid chromatography–mass spectrometry, Journal of Chromatography B, 878 (2010) 213-221.
[252] Duan J., Liang Z., Yang C., Zhang J., Zhang L., Zhang W., Zhang Y., Rapid protein identification using monolithic enzymatic microreactor and LC-ESI-MS/MS, Proteomics, 6 (2006) 412-419.
[253] Nunes P.S., Ohlsson P.D., Ordeig O., Kutter J.P., Cyclic olefin polymers: emerging materials for lab-on-a-chip applications, Microfluidics and Nanofluidics, 9 (2010) 145-161.
[254] Wouters B., Davydova E., Wouters S., Vivo-Truyols G., Schoenmakers P.J., Eeltink S., Towards ultra-high peak capacities and peak-production rates using spatial three-dimensional liquid chromatography, Lab on a Chip, 15 (2015) 4415-4422.
[255] Logan T.C., Clark D.S., Stachowiak T.B., Svec F., Frechet J.M., Photopatterning enzymes on polymer monoliths in microfluidic devices for steady-state kinetic analysis and spatially separated multi-enzyme reactions, Analytical Chemistry, 79 (2007) 6592-6598.
[256] Gasteiger E., Hoogland C., Gattiker A., Duvaud S.e., Wilkins M.R., Appel R.D., Bairoch A., Protein identification and analysis tools on the ExPASy server, The proteomics protocols handbook, Humana press, pp. 571-6072005.
[257] Kyte J., Doolittle R.F., A simple method for displaying the hydropathic character of a protein, Journal of Molecular Biology, 157 (1982) 105-132.
[258] Takats Z., Wiseman J.M., Gologan B., Cooks R.G., Mass spectrometry sampling under ambient conditions with desorption electrospray ionization, Science, 306 (2004) 471-473.
[259] Cody R.B., Laramée J.A., Durst H.D., Versatile new ion source for the analysis of materials in open air under ambient conditions, Analytical Chemistry, 77 (2005) 2297-2302.
[260] Ifa D.R., Wu C., Ouyang Z., Cooks R.G., Desorption electrospray ionization and other ambient ionization methods: current progress and preview, Analyst, 135 (2010) 669-681.
[261] Gross J.H., Ambient mass spectrometry, Mass Spectrometry, (2011) 621-649.
[262] Ifa D.R., Jackson A.U., Paglia G., Cooks R.G., Forensic applications of ambient ionization mass spectrometry, Analytical and Bioanalytical Chemistry, 394 (2009) 1995-2008.
[263] Goodlett D.R., Heron S.R., Cooper J., Methods and systems for mass spectrometry, Google Patents, 2014.
[264] Qi A., Yeo L.Y., Friend J.R., Interfacial destabilization and atomization driven by surface acoustic waves, Physics of Fluids, 20 (2008) 074103.
[265] Heron S.R., Wilson R., Shaffer S.A., Goodlett D.R., Cooper J.M., Surface acoustic wave nebulization of peptides as a microfluidic interface for mass spectrometry, Analytical Chemistry, 82 (2010) 3985-3989.
[266] Ho J., Tan M.K., Go D.B., Yeo L.Y., Friend J.R., Chang H.-C., Paper-based microfluidic surface acoustic wave sample delivery and ionization source for rapid and sensitive ambient mass spectrometry, Analytical Chemistry, 83 (2011) 3260-3266.
[267] Huang Y., Yoon S.H., Heron S.R., Masselon C.D., Edgar J.S., Tureček F., Goodlett D.R., Surface acoustic wave nebulization produces ions with lower internal energy than electrospray ionization, Journal of the American Society for Mass Spectrometry, 23 (2012) 1062-1070.

[268] Astefanei A., van Bommel M., Corthals G.L., Surface acoustic wave nebulisation mass spectrometry for the fast and highly sensitive characterisation of synthetic dyes in textile samples, Journal of The American Society for Mass Spectrometry, 28 (2017) 2108-2116.
[269] Groothuis S.F., Development of a data processing pipeline for SAWN-MS for the prediction of dried blood spot age, Master Thesis, University of Amsterdam, 2017.
[270] Hoang V.D., Wavelet-based spectral analysis, TRAC Trends in Analytical Chemistry, 62 (2014) 144-153.
[271] Yang C., He Z., Yu W., Comparison of public peak detection algorithms for MALDI mass spectrometry data analysis, BioMed Central - Bioinformatics, 10 (2009) 4.
[272] Cook R.D., Detection of influential observation in linear regression, Technometrics, 19 (1977) 15-18.
[273] Hothorn T., Lausen B., Double-bagging: Combining classifiers by bootstrap aggregation, Pattern Recognition, 36 (2003) 1303-1309.
[274] Chandrashekar G., Sahin F., A survey on feature selection methods, Computers & Electrical Engineering, 40 (2014) 16-28.
[275] van den Berg R.A., Hoefsloot H.C., Westerhuis J.A., Smilde A.K., van der Werf M.J., Centering, scaling, and transformations: improving the biological information content of metabolomics data, BioMed Central - Genomics, 7 (2006) 142.
[276] Wold S., Esbensen K., Geladi P., Principal component analysis, Chemometrics and Intelligent Laboratory Systems, 2 (1987) 37-52.
[277] Noble W.S., What is a support vector machine?, Nature Biotechnology, 24 (2006) 1565-1567.
[278] Smola A.J., Schölkopf B., A tutorial on support vector regression, Statistics and Computing, 14 (2004) 199-222.
[279] Scholkopf B., Sung K.-K., Burges C.J., Girosi F., Niyogi P., Poggio T., Vapnik V., Comparing support vector machines with Gaussian kernels to radial basis function classifiers, Insitute of Electrical and Electronic Engineers - Transactions on Signal Processing, 45 (1997) 2758-2765.
[280] Cordell R.L., Valkenburg T.S.E., Pandya H.C., Hawcutt D.B., Semple M.G., Monks P.S., Quantitation of salbutamol using micro-volume blood sampling – applications to exacerbations of pediatric asthma, Journal of Asthma, (2017) 1-9.
[281] Morton A.R., Papalia S.M., Fitch K.D., Is salbutamol ergogenic?: The effects of salbutamol on physical performance in high-performance nonasthmatic athletes, Clinical Journal of Sport Medicine, 2 (1992) 93-97.
[282] British Thoracic Society and Scottish Intercollegiate Guidelines Network. British guideline on the management of asthma. A national clinical guideline (Guideline 101), (2012).
[283] Tobin A., Intravenous salbutamol: too much of a good thing?, Critical Care and Resuscitation, 7 (2005) 119.
[284] Saleh M., Koh Y., Tan S., Aishah A., Clean-up, detection and determination of salbutamol in human urine and serum, Analyst, 125 (2000) 1569-1572.
[285] Schweizer C., Saugy M., Kamber M., Doping test reveals high concentrations of salbutamol in a Swiss track and field athlete, Clinical Journal of Sport Medicine, 14 (2004) 312-315.
[286] Dumasia M., Houghton E., Screening and confirmatory analysis of β-agonists, β-antagonists and their metabolites in horse urine by capillary gas chromatography—mass spectrometry, Journal of Chromatography B: Biomedical Sciences and Applications, 564 (1991) 503-513.
[287] Warriss P., Kestin S., Rolph T., Brown S., The effects of the beta-adrenergic agonist salbutamol on meat quality in pigs, Journal of Animal Science, 68 (1990) 128-136.

[288] Sporer B.C., Sheel A.W., Taunton J., Rupert J.L., McKenzie D.C., Inhaled salbutamol and doping control: effects of dose on urine concentrations, Clinical Journal of Sport Medicine, 18 (2008) 282-285.
[289] World Anti-Doping Agency. World anti-doping code, International standard, Prohibited list, (2016).
[290] Spyridaki M.-H., Kiousi P., Vonaparti A., Valavani P., Zonaras V., Zahariou M., Sianos E., Tsoupras G., Georgakopoulos C., Doping control analysis in human urine by liquid chromatography–electrospray ionization ion trap mass spectrometry for the Olympic Games Athens 2004: Determination of corticosteroids and quantification of ephedrines, salbutamol and morphine, Analytica Chimica Acta, 573 (2006) 242-249.
[291] Fitch K.D., β2-agonists at the Olympic Games, Clinical Reviews in Allergy & Immunology, 31 (2006) 259-268.
[292] Pichon A., Venisse N., Krupka E., Perault-Pochat M.-C., Denjean A., Urinary and blood concentrations of β2-agonists in trained subjects: comparison between routes of use, International Journal of Sports Medicine, 27 (2006) 187-192.
[293] Elers J., Pedersen L., Henninge J., Hemmersbach P., Dalhoff K., Backer V., Urine concentrations of repetitive doses of inhaled salbutamol, International Journal of Sports Medicine, 32 (2011) 574-579.
[294] Goyal R.N., Oyama M., Singh S.P., Fast determination of salbutamol, abused by athletes for doping, in pharmaceuticals and human biological fluids by square wave voltammetry, Journal of Electroanalytical Chemistry, 611 (2007) 140-148.
[295] Martin L.-E., Rees J., Tanner R.J.N., Quantitative determination of salbutamol in plasma, as either its trimethylsilyl or t-butyldimethylsilyl ether, using a stable isotope multiple ion recording technique, Biological Mass Spectrometry, 3 (1976) 184-190.
[296] Fairfax A., McNabb W., Davies H., Spiro S., Slow-release oral salbutamol and aminophylline in nocturnal asthma: relation of overnight changes in lung function and plasma drug levels, Thorax, 35 (1980) 526-530.
[297] Leferink J.-G., Dankers J., Maes R., A time-saving method for the determination of the β2 sympathomimetics terbutaline, salbutamol and fenoterol. Preliminary results, Journal of Chromatography B: Biomedical Sciences and Applications, 229 (1982) 217-221.
[298] Oosterhuis B., Van Boxtel C., Determination of salbutamol in human plasma with bimodal high-performance liquid chromatography and a rotated disc amperometric detector, Journal of Chromatography B: Biomedical Sciences and Applications, 232 (1982) 327-334.
[299] Hutchings M.J., Paull J.D., Morgan D.J., Determination of salbutamol in plasma by high-performance liquid chromatography with fluorescence detection, Journal of Chromatography B: Biomedical Sciences and Applications, 277 (1983) 423-426.
[300] Powell M.L., Weisberger M., Gural R., Chung M., Patrick J.E., Radwanski E., Symchowicz S.S., Comparative bioavailability and pharmacokinetics of three formulations of albuterol, Journal of Pharmaceutical Sciences, 74 (1985) 217-219.
[301] Tan Y.K., Soldin S.J., Determination of salbutamol in human serum by reversed-phase high-performance liquid chromatography with amperometric detection, Journal of Chromatography B: Biomedical Sciences and Applications, 311 (1984) 311-317.
[302] Colthup P., Dallas F., Saynor D., Carey P., Skidmore L., Martin L., Wilson K., Determination of salbutamol in human plasma and urine by high-performance thin-layer chromatography, Journal of Chromatography B: Biomedical Sciences and Applications, 345 (1985) 111-118.
[303] Haukkamaa M., Gummerus M., Kleimola T., Serum salbutamol concentrations during oral and intravenous treatment in pregnant women, International Journal of Obstetrics & Gynaecology, 92 (1985) 1230-1233.

[304] Miller L.G., Greenblatt D.J., Determination of albuterol in human plasma by high-performance liquid chromatography with fluorescence detection, Journal of Chromatography B: Biomedical Sciences and Applications, 381 (1986) 205-208.
[305] Morgan D., Paull J., Richmond B., Wilson-Evered E., Ziccone S., Pharmacokinetics of intravenous and oral salbutamol and its sulphate conjugate, British Journal of Clinical Pharmacology, 22 (1986) 587-593.
[306] Goldstein D., Tan Y., Soldin S., Pharmacokinetics and absolute bioavailability of salbutamol in healthy adult volunteers, European Journal of Clinical Pharmacology, 32 (1987) 631-634.
[307] Emm T., Lesko L., Leslie J., Perkal M., Determination of albuterol in human serum by reversed-phase high-performance liquid chromatography with electrochemical detection, Journal of Chromatography B: Biomedical Sciences and Applications, 427 (1988) 188-194.
[308] Lipworth B., Clark R., Dhillon D., Charter M., Palmer J., McDevitt D., Single dose and steady-state pharmacokinetics of 4 mg and 8 mg oral salbutamol controlled-release in patients with bronchial asthma, European Journal of Clinical Pharmacology, 37 (1989) 49-52.
[309] Ong H., Adam A., Perreault S., Marleau S., Bellemare M., Du Souich P., Beaulieu N., Analysis of albuterol in human plasma based on immunoaffinity chromatograhic clean-up combined with high-performance liquid chromatography with fluorimetric detection, Journal of Chromatography B: Biomedical Sciences and Applications, 497 (1989) 213-221.
[310] Bland R., Tanner R., Chern W., Lang J., Powell J., Determination of albuterol concentrations in human plasma using solid-phase extraction and high-performance liquid chromatography with fluorescence detection, Journal of Pharmaceutical and Biomedical Analysis, 8 (1990) 591-596.
[311] Hindle M., Chrystyn H., Determination of the relative bioavailability of salbutamol to the lung following inhalation [see comments], British Journal of Clinical Pharmacology, 34 (1992) 311-315.
[312] Le Roux A., Wium C., Joubert J., Van Jaarsveld P., Evaluation of a high-performance thin-layer chromatographic technique for the determination of salbutamol serum levels in clinical trials, Journal of Chromatography B: Biomedical Sciences and Applications, 581 (1992) 306-309.
[313] Gupta R.N., Fuller H.D., Dolovich M.B., Optimization of a column liquid chromatographic procedure for the determination of plasma salbutamol concentration, Journal of Chromatography B: Biomedical Sciences and Applications, 654 (1994) 205-211.
[314] Boulton D., Fawcett J., Enantioselective disposition of salbutamol in man following oral and intravenous administration, British Journal of Clinical Pharmacology, 41 (1996) 35-40.
[315] Boulton D.W., Fawcett J.P., Determination of salbutamol enantiomers in human plasma and urine by chiral high-performance liquid chromatography, Journal of Chromatography B: Biomedical Sciences and Applications, 672 (1995) 103-109.
[316] Duarte A.G., Dhand R., Reid R., Fink J.B., Fahey P.J., Tobin M.J., Jenne J.W., Serum albuterol levels in mechanically ventilated patients and healthy subjects after metered-dose inhaler administration, American Journal of Respiratory and Critical Care Medicine, 154 (1996) 1658-1663.
[317] Couper F.J., Drummer O.H., Gas chromatographic-mass spectrometric determination of ß2-agonists in postmortem blood: application in forensic medicine, Journal of Chromatography B: Biomedical Sciences and Applications, 685 (1996) 265-272.

[318] Logsdon T.W., Zhou X., Breen P., Anderson P., Gann L., Hiller C., Compadre C.M., Determination of albuterol in plasma after aerosol inhalation by gas chromatography-mass spectrometry with selected-ion monitoring, Journal of Chromatography B: Biomedical Sciences and Applications, 692 (1997) 472-477.
[319] Ventura R., González G., Smeyers M., De la Torre R., Segura J., Screening procedure for β-adrenergic drugs in sports drug testing by immunological methods, Journal of Analytical Toxicology, 22 (1998) 127-134.
[320] Anderson P.J., Zhou X., Breen P., Gann L., Logsdon T.W., Compadre C.M., Charles Hiller F., Pharmacokinetics of (R, S)-Albuterol after aerosol inhalation in healthy adult volunteers, Journal of Pharmaceutical Sciences, 87 (1998) 841-844.
[321] Black S., Hansson R., Determination of salbutamol and detection of other β-agonists in human postmortem whole blood and urine by GC-MS-SIM, Journal of Analytical Toxicology, 23 (1999) 113-118.
[322] Schmekel B., Rydberg I., Norlander B., Sjöswärd K., Ahlner J., Andersson R., Stereoselective pharmacokinetics of S-salbutamol after administration of the racemate in healthy volunteers, European Respiratory Journal, 13 (1999) 1230-1235.
[323] Koh Y.M., Saleh M., Tan S., Aishah A., Development in the clean-up and detection method to determine salbutamol level in human serum/urine, Social Science Research Network, 2000 (2000) 104-121.
[324] Bergés R., Segura J., Ventura R., Fitch K.D., Morton A.R., Farré M., Mas M., de la Torre X., Discrimination of prohibited oral use of salbutamol from authorized inhaled asthma treatment, Clinical Chemistry, 46 (2000) 1365-1375.
[325] Bergés R., Segura J., de la Torre X., Ventura R., Analytical methodology for enantiomers of salbutamol in human urine for application in doping control, Journal of Chromatography B: Biomedical Sciences and Applications, 723 (1999) 173-184.
[326] Damasceno L., Ventura R., Cardoso J., Segura J., Diagnostic evidence for the presence of β-agonists using two consecutive derivatization procedures and gas chromatography–mass spectrometric analysis, Journal of Chromatography B, 780 (2002) 61-71.
[327] Forsdahl G., Gmeiner G., Quantification and stability of salbutamol in human urine, Journal of Separation Science, 27 (2004) 110-114.
[328] Sporer B.C., Sheel A.W., Mckenzie D.C., Dose response of inhaled salbutamol on exercise performance and urine concentrations, Medicine and Science in Sports and Exercise, 40 (2008) 149-157.
[329] Elers J., Pedersen L., Henninge J., Lund T.K., Hemmersbach P., Dalhoff K., Backer V., Blood and urinary concentrations of salbutamol in asthmatic subjects, Medicine and Science in Sports and Exercise, 42 (2010) 244-249.
[330] Rotta E.T., Amantéa S.L., Froehlich P.E., Becker A., Plasma concentrations of salbutamol in the treatment of acute asthma in a pediatric emergency. Could age be a parameter of influence?, European Journal of Clinical Pharmacology, 66 (2010) 605-610.
[331] Van Eenoo P., Van Gansbeke W., De Brabanter N., Deventer K., Delbeke F.T., A fast, comprehensive screening method for doping agents in urine by gas chromatography–triple quadrupole mass spectrometry, Journal of Chromatography A, 1218 (2011) 3306-3316.
[332] Caban M., Stepnowski P., Kwiatkowski M., Migowska N., Kumirska J., Determination of β-blockers and β-agonists using gas chromatography and gas chromatography–mass spectrometry–A comparative study of the derivatization step, Journal of Chromatography A, 1218 (2011) 8110-8122.
[333] Sidler-Moix A.L., Mercier T., Decosterd L.A., Di Paolo E.R., Berger-Gryllaki M., Cotting J., Pannatier A., A highly sensitive LC–tandem MS assay for the measurement in plasma and in urine of salbutamol administered by nebulization during mechanical ventilation in healthy volunteers, Biomedical Chromatography, 26 (2012) 672-680.

[334] Lee K.M., Kim H.J., Jeong E.S., Yoo H.H., Kwon O.S., Jin C., Kim D.H., Lee J., Simple and accurate quantitative analysis of seven prohibited threshold substances in human urine by liquid chromatography/tandem mass spectrometry in doping control, Rapid Communications in Mass Spectrometry, 25 (2011) 2261-2267.
[335] De Brabanter N., Van Gansbeke W., Geldof L., Van Eenoo P., An improved gas chromatography screening method for doping substances using triple quadrupole mass spectrometry, with an emphasis on quality assurance, Biomedical Chromatography, 26 (2012) 1416-1435.
[336] Elers J., Pedersen L., Henninge J., Hemmersbach P., Dalhoff K., Backer V., The pharmacokinetic profile of inhaled and oral salbutamol in elite athletes with asthma and nonasthmatic subjects, Clinical Journal of Sport Medicine, 22 (2012) 140-145.
[337] Hostrup M., Kalsen A., Auchenberg M., Rzeppa S., Hemmersbach P., Bangsbo J., Backer V., Urine concentrations of oral salbutamol in samples collected after intense exercise in endurance athletes, Drug Testing and Analysis, 6 (2014) 528-532.
[338] Janson C., Boe J., Boman G., Mossberg B., Svedmyr N., Bronchodilator intake and plasma levels on admission for severe acute asthma, European Respiratory Journal, 5 (1992) 80-85.
[339] US Department of Health and Human Services. Food and Drug Administration. Center for Drug Evaluation and Research. Guidance for industry: Bioanalytical method validation, (2001) pp. 1-25.
[340] Ventura R., Segura J., Bergés R., Fitch K.D., Morton A.R., Berruezo S., Jiménez C., Distinction of inhaled and oral salbutamol by urine analysis using conventional screening procedures for doping control, Therapeutic Drug Monitoring, 22 (2000) 277-282.
[341] De Kesel P.M., Lambert W.E., Stove C.P., Does volumetric absorptive microsampling eliminate the hematocrit bias for caffeine and paraxanthine in dried blood samples? A comparative study, Analytica Chimica Acta, 881 (2015) 65-73.
[342] US Department of Health and Human Services. Food and Drug Administration. Center for Drug Evaluation and Research. Guidance for industry: Bioanalytical method validation, (2013).
[343] US Department of Health and Human Services. Food and Drug Administration. Center for Drug Evaluation and Research. Guidance for industry: Bioanalytical method validation, (2018) pp. 1-44.
[344] Starkey E., Mulla H., Sammons H., Pandya H., Intravenous salbutamol for childhood asthma: evidence-based medicine?, Archives of Disease in Childhood, 99 (2014) 873-877.
[345] Koster R.A., Botma R., Greijdanus B., Uges D.R., Kosterink J.G., Alffenaar J.-W.C., Touw D.J., The influence of the dried blood spot drying time on the recoveries of six immunosuppressants, Journal of Applied Bioanalysis, 1 (2015) 116-122.
[346] Rhee J., Erickson T., Barceloux D.G., Clenbuterol and salbutamol (albuterol), Medical Toxicology of Drug Abuse: Synthesized Chemicals and Psychoactive Plants, (2012) 295.
[347] Hikino H., Konno C., Takata H., Tamada M., Antiinflammatory principle of Ephedra herbs, Chemical and Pharmaceutical Bulletin, 28 (1980) 2900-2904.
[348] Horak F., Zieglmayer P., Zieglmayer R., Lemell P., Yao R., Staudinger H., Danzig M., A placebo-controlled study of the nasal decongestant effect of phenylephrine and pseudoephedrine in the Vienna Challenge Chamber, Annals of Allergy, Asthma & Immunology, 102 (2009) 116-120.
[349] Gill N.D., Shield A., Blazevich A.J., Zhou S., Weatherby R.P., Muscular and cardiorespiratory effects of pseudoephedrine in human athletes, British Journal of Clinical Pharmacology, 50 (2000) 205-213.

[350] UK Medicines and Healthcare products Regulatory Agency, Commission on Human Medicines, Drug safety update, (2008).
[351] Food and Drug Administration. Legal requirements for the sale and purchase of drug products containing pseudoephedrine, ephedrine, and phenylpropanolamine, (2017).
[352] New Zealand Legislation, Misuse of Drug Act 1975, Schedule 2, Class B controlled drugs, (2018).
[353] Caveney S., Charlet D.A., Freitag H., Maier-Stolte M., Starratt A.N., New observations on the secondary chemistry of world Ephedra (Ephedraceae), American Journal of Botany, 88 (2001) 1199-1208.
[354] Andrews K., Ephedra's role as a precursor in the clandestine manufacture of methamphetamine, Journal of Forensic Science, 40 (1995) 551-560.
[355] Barker W., Antia U., A study of the use of Ephedra in the manufacture of methamphetamine, Forensic Science International, 166 (2007) 102-109.
[356] McKenzie E., Chemical contamination in former clandestine methamphetamine laboratories, PhD Thesis, University of Auckland, 2014.
[357] Deluca P., Davey Z., Corazza O., Di Furia L., Farre M., Flesland L.H., Mannonen M., Majava A., Peltoniemi T., Pasinetti M., Identifying emerging trends in recreational drug use; outcomes from the Psychonaut Web Mapping Project, Progress in Neuro-Psychopharmacology and Biological Psychiatry, 39 (2012) 221-226.
[358] Enevoldson T., Recreational drugs and their neurological consequences, Journal of Neurology, Neurosurgery & Psychiatry, 75 (2004) iii9-iii15.
[359] Hodges K., Hancock S., Currell K., Hamilton B., Jeukendrup A.E., Pseudoephedrine enhances performance in 1500-m runners, Medicine and Science in Sports and Exercise, 38 (2006) 329-333.
[360] Bents R.T., Marsh E., Patterns of ephedra and other stimulant use in collegiate hockey athletes, International Journal of Sport Nutrition and Exercise Metabolism, 16 (2006) 636-643.
[361] Deventer K., Van Eenoo P., Baele G., Pozo O., Van Thuyne W., Delbeke F., Interpretation of urinary concentrations of pseudoephedrine and its metabolite cathine in relation to doping control, Drug Testing and Analysis, 1 (2009) 209-213.
[362] World Anti-Doping Agency. International Standard for Laboratories, Anti-Doping Testing Figures, (2015).
[363] Odoardi S., Fisichella M., Romolo F.S., Strano-Rossi S., High-throughput screening for new psychoactive substances (NPS) in whole blood by DLLME extraction and UHPLC–MS/MS analysis, Journal of Chromatography B, 1000 (2015) 57-68.
[364] Shakya A.K., Arafat T.A., Abuawwad A.N., Melhim M., Al-Ghani J., Yacoub M.J., Simultaneous determination of triprolidine and pseudoephedrine in human plasma by liquid chromatography–ion trap mass spectrometry, Journal of Chromatography B, 877 (2009) 4071-4078.
[365] Nirogi R.V., Kandikere V.N., Shukla M., Mudigonda K., Maurya S., Komarneni P., Quantification of pseudoephedrine in human plasma by LC-MS/MS using mosapride as internal standard, Biomedical Chromatography, 21 (2007) 241-248.
[366] Shen J.X., Xu Y., Tama C.I., Merka E.A., Clement R.P., Hayes R.N., Simultaneous determination of desloratadine and pseudoephedrine in human plasma using micro solid-phase extraction tips and aqueous normal-phase liquid chromatography/tandem mass spectrometry, Rapid Communications in Mass Spectrometry, 21 (2007) 3145-3155.
[367] Ma M., Feng F., Sheng Y., Cui S., Liu H., Development and evaluation of an efficient HPLC/MS/MS method for the simultaneous determination of pseudoephedrine and cetirizine in human plasma: Application to Phase-I pharmacokinetic study, Journal of Chromatography B, 846 (2007) 105-111.

[368] Gunn J., Kriger S., Terrell A.R., Identification and quantitation of amphetamine, methamphetamine, MDMA, pseudoephedrine, and ephedrine in blood, plasma, and serum using gas chromatography-mass spectrometry (GC/MS), Clinical Applications of Mass Spectrometry, Humana Press(2010), pp. 37-43.
[369] Bye C., Hill H., Hughes D., Peck A., A comparison of plasma levels of L(+)pseudoephedrine following different formulations, and their relation to cardiovascular and subjective effects in man, European Journal of Clinical Pharmacology, 8 (1975) 47-53.
[370] Sørensen L.K., Determination of cathinones and related ephedrines in forensic whole-blood samples by liquid-chromatography–electrospray tandem mass spectrometry, Journal of Chromatography B, 879 (2011) 727-736.
[371] Chepyala D., Tsai I.-L., Liao H.-W., Chen G.-Y., Chao H.-C., Kuo C.-H., Sensitive screening of abused drugs in dried blood samples using ultra-high-performance liquid chromatography-ion booster-quadrupole time-of-flight mass spectrometry, Journal of Chromatography A, 1491 (2017) 57-66.
[372] Wingert W.E., Mundy L.A., Collins G.L., Chmara E.S., Possible role of pseudoephedrine and other over-the-counter cold medications in the deaths of very young children, Journal of Forensic Sciences, 52 (2007) 487-490.
[373] Smith D., Turner C., Španěl P., Volatile metabolites in the exhaled breath of healthy volunteers: their levels and distributions, Journal of Breath Research, 1 (2007) 014004.
[374] Boots A.W., van Berkel J.J., Dallinga J.W., Smolinska A., Wouters E.F., van Schooten F.J., The versatile use of exhaled volatile organic compounds in human health and disease, Journal of Breath Research, 6 (2012) 027108.
[375] Phillips M., Method for the collection and assay of volatile organic compounds in breath, Analytical Biochemistry, 247 (1997) 272-278.
[376] Lindinger W., Hansel A., Jordan A., On-line monitoring of volatile organic compounds at pptv levels by means of proton-transfer-reaction mass spectrometry (PTR-MS) medical applications, food control and environmental research, International Journal of Mass Spectrometry and Ion Processes, 173 (1998) 191-241.
[377] Smith D., Španěl P., Selected ion flow tube mass spectrometry, SIFT-MS, for on-line trace gas analysis of breath, Mass Spectrometry Reviews 24 (2005) 661-700.
[378] Von Basum G., Halmer D., Hering P., Mürtz M., Laser spectroscopic on-line monitoring of exhaled trace gases, Breath Analysis for Clinical Diagnosis and Therapeutic Monitoring, World Scientific (2005), pp. 67-74.
[379] Ruzsanyi V., Baumbach J.I., Sielemann S., Litterst P., Westhoff M., Freitag L., Detection of human metabolites using multi-capillary columns coupled to ion mobility spectrometers, Journal of Chromatography A, 1084 (2005) 145-151.
[380] White I.R., Willis K.A., Whyte C., Cordell R., Blake R.S., Wardlaw A.J., Rao S., Grigg J., Ellis A.M., Monks P.S., Real-time multi-marker measurement of organic compounds in human breath: towards fingerprinting breath, Journal of Breath Research, 7 (2013) 017112.
[381] Blake R.S., Whyte C., Hughes C.O., Ellis A.M., Monks P.S., Demonstration of proton-transfer reaction time-of-flight mass spectrometry for real-time analysis of trace volatile organic compounds, Analytical Chemistry, 76 (2004) 3841-3845.
[382] World Anti-Doping Agency. Technical Document, TD2018DL, https://www.wada-ama.org/sites/default/files/resources/files/td2018dl_v1_en.pdf, pp. 1-18, (Accessed 21/09/2018).
[383] Peterson A.C., Russell J.D., Bailey D.J., Westphall M.S., Coon J.J., Parallel reaction monitoring for high resolution and high mass accuracy quantitative, targeted proteomics, Molecular & Cellular Proteomics, 11 (2012) 1475-1488.

[384] Gallien S., Duriez E., Crone C., Kellmann M., Moehring T., Domon B., Targeted proteomic quantification on quadrupole-orbitrap mass spectrometer, Molecular & Cellular Proteomics, 11 (2012) 1709-1723.
[385] Loccioni. Humancare, http://humancare.loccioni.com/.
[386] Kore Technology. Proton Transfer Reactor Time-of-Flight Mass Spectrometry (PTR-TOF-MS), https://www.kore.co.uk/ptrtof.htm.
[387] Ennis C., Reynolds J., Keely B., Carpenter L., A hollow cathode proton transfer reaction time of flight mass spectrometer, International Journal of Mass Spectrometry, 247 (2005) 72-80.
[388] Schwarz K., Pizzini A., Arendacka B., Zerlauth K., Filipiak W., Schmid A., Dzien A., Neuner S., Lechleitner M., Scholl-Bürgi S., Breath acetone—aspects of normal physiology related to age and gender as determined in a PTR-MS study, Journal of Breath Research, 3 (2009) 027003.
[389] Rohart F., Gautier B., Singh A., Le Cao K.-A., mixOmics: An R package for 'omics feature selection and multiple data integration, PLoS Computational Biology, 13 (2017) e1005752.
[390] Owlstone Medical. ReCIVA breath sampler, https://www.owlstonemedical.com/products/reciva/.
[391] Reichenbach S.E., Tian X., Tao Q., Ledford Jr E.B., Wu Z., Fiehn O., Informatics for cross-sample analysis with comprehensive two-dimensional gas chromatography and high-resolution mass spectrometry (GCxGC–HRMS), Talanta, 83 (2011) 1279-1288.
[392] Schulz M., Iwersen-Bergmann S., Andresen H., Schmoldt A., Therapeutic and toxic blood concentrations of nearly 1,000 drugs and other xenobiotics, Critical Care, 16 (2012) R136.
[393] Thomas A., Geyer H., Guddat S., Schänzer W., Thevis M., Dried blood spots (DBS) for doping control analysis, Drug Testing and Analysis, 3 (2011) 806-813.
[394] Chester N., Mottram D.R., Reilly T., Powell M., Elimination of ephedrines in urine following multiple dosing: The consequences for athletes, in relation to doping control, British Journal of Clinical Pharmacology, 57 (2004) 62-67.
[395] Strano-Rossi S., Leone D., De La Torre X., Botrè F., The relevance of the urinary concentration of ephedrines in anti-doping analysis: Determination of pseudoephedrine, cathine, and ephedrine after administration of over-the-counter medicaments, Therapeutic Drug Monitoring, 31 (2009) 520-526.
[396] Bouchard R., Weber A.R., Geiger J.D., Informed decision-making on sympathomimetic use in sport and health, Clinical Journal of Sport Medicine, 12 (2002) 209-224.
[397] Libardoni M., Stevens P., Waite J.H., Sacks R., Analysis of human breath samples with a multi-bed sorption trap and comprehensive two-dimensional gas chromatography (GC× GC), Journal of Chromatography B, 842 (2006) 13-21.
[398] Lindinger W., Taucher J., Jordan A., Hansel A., Vogel W., Endogenous production of methanol after the consumption of fruit, Alcoholism: Clinical and Experimental Research, 21 (1997) 939-943.
[399] Garriga M.M., Metcalfe D., Aspartame intolerance, Annals of Allergy, 61 (1988) 63-69.
[400] Turner C., Španěl P., Smith D., A longitudinal study of ammonia, acetone and propanol in the exhaled breath of 30 subjects using selected ion flow tube mass spectrometry, SIFT-MS, Physiological Measurement, 27 (2006) 321.
[401] Warneke C., Kuczynski J., Hansel A., Jordan A., Vogel W., Lindinger W., Proton transfer reaction mass spectrometry (PTR-MS): propanol in human breath, International Journal of Mass Spectrometry and Ion Processes, 154 (1996) 61-70.
[402] Swift R., Direct measurement of alcohol and its metabolites, Addiction, 98 (2003) 73-80.
[403] Herbig J., Müller M., Schallhart S., Titzmann T., Graus M., Hansel A., On-line breath analysis with PTR-TOF, Journal of Breath Research, 3 (2009) 027004.

[404] Stone B.G., Besse T.J., Duane W.C., Evans C.D., DeMaster E.G., Effect of regulating cholesterol biosynthesis on breath isoprene excretion in men, Lipids, 28 (1993) 705-708.
[405] Taucher J., Hansel A., Jordan A., Fall R., Futrell J.H., Lindinger W., Detection of isoprene in expired air from human subjects using proton-transfer-reaction mass spectrometry, Rapid Communications in Mass Spectrometry, 11 (1997) 1230-1234.
[406] DeMaster E.G., Nagasawa H.T., Isoprene, an endogenous constituent of human alveolar air with a diurnal pattern of excretion, Life Sciences, 22 (1978) 91-97.
[407] Kushch I., Schwarz K., Schwentner L., Baumann B., Dzien A., Schmid A., Unterkofler K., Gastl G., Španěl P., Smith D., Compounds enhanced in a mass spectrometric profile of smokers' exhaled breath versus non-smokers as determined in a pilot study using PTR-MS, Journal of Breath Research, 2 (2008) 026002.
[408] Gelman A., Scaling regression inputs by dividing by two standard deviations, Statistics in Medicine, 27 (2008) 2865-2873.
[409] Chiang L.H., Pell R.J., Seasholtz M.B., Exploring process data with the use of robust outlier detection algorithms, Journal of Process Control, 13 (2003) 437-449.
[410] Phillips M., Herrera J., Krishnan S., Zain M., Greenberg J., Cataneo R.N., Variation in volatile organic compounds in the breath of normal humans, Journal of Chromatography B: Biomedical Sciences and Applications, 729 (1999) 75-88.
[411] Senthilmohan S.T., Milligan D.B., McEwan M.J., Freeman C.G., Wilson P.F., Quantitative analysis of trace gases of breath during exercise using the new SIFT–MS technique, Redox Report, 5 (2000) 151-153.
[412] Thevis M., Krug O., Geyer H., Schänzer W., Expanding analytical options in sports drug testing: Mass spectrometric detection of prohibited substances in exhaled breath, Rapid Communications in Mass Spectrometry, 31 (2017) 1290-1296.
[413] Himes S.K., Scheidweiler K.B., Beck O., Gorelick D.A., Desrosiers N.A., Huestis M.A., Cannabinoids in exhaled breath following controlled administration of smoked cannabis, Clinical Chemistry, 59 (2013) 1780-1789.
[414] Beck O., Sandqvist S., Dubbelboer I., Franck J., Detection of Δ9-tetrahydrocannabinol in exhaled breath collected from cannabis users, Journal of Analytical Toxicology, 35 (2011) 541-544.
[415] Lipic S.G., Giordullo L.M., Fredericks J.D., A novel FTA™ elute card collection method that improves direct DNA amplification from bloodstained concrete, Science & Justice, (2018).
[416] Sant S.P., Fairgrieve S.I., Exsanguinated blood volume estimation using fractal analysis of digital images, Journal of Forensic Sciences, 57 (2012) 610-617.
[417] Hulse-Smith L., Mehdizadeh N.Z., Chandra S., Deducing drop size and impact velocity from circular bloodstains, Journal of Forensic Science, 50 (2005) JFS2003224-2003210.
[418] Li J., Li X., Michielsen S., Alternative method for determining the original drop volume of bloodstains on knit fabrics, Forensic Science International, 263 (2016) 194-203.
[419] Laan N., Bremmer R.H., Aalders M.C., de Bruin K.G., Volume determination of fresh and dried bloodstains by means of optical coherence tomography, Journal of Forensic Sciences, 59 (2014) 34-41.
[420] Skopp G., Ganßmann B., Mattern R., Aderjan R., Postmortem distribution pattern of morphine and morphine glucuronides in heroin overdose, International Journal of Legal Medicine, 109 (1996) 118-124.
[421] Baandrup J.D., Markvardsen L.H., Peters C.D., Schou U.K., Jensen J.L., Magnusson N.E., Ørntoft T.F., Kruhøffer M., Simonsen U., Pressure load: the main factor for altered gene expression in right ventricular hypertrophy in chronic hypoxic rats, PLoS One, 6 (2011) e15859.